

ANALYTICAL AND EXPERIMENTAL DETERMINATION OF NONLINEAR WHEEL/RAIL GEOMETRIC CONSTRAINTS

**N.K. COOPERRIDER, E.H. LAW, R. HULL
P.S. KADALA, J.M. TUTEN**

**DECEMBER 1975
INTERIM REPORT**

Document is available to the public through the National
Technical Information Service; Springfield, Virginia, 22161

Prepared for:

**U.S. DEPARTMENT OF TRANSPORTATION
Federal Railroad Administration
Office of Research and Development
Washington, D.C. 20590**

NOTICE

This document is disseminated under the sponsorship of the Department of Transportation in the interest of information exchange. The United States Government assumes no liability for its contents or use thereof.

1. Report No.	2. Government Accession No.	3. Recipient's Catalog No.	
4. Title and Subtitle ANALYTICAL AND EXPERIMENTAL DETERMINATION OF WHEEL-RAIL CONSTRAINT RELATIONSHIPS		5. Report Date December 30, 1975	
		6. Performing Organization Code	
7. Authors N. K. Cooperrider, E. H. Law, R. Hull, P. S. Kadala, J. M. Tuten		8. Performing Organization Report No.	
9. Performing Organization Name and Address Clemson University Arizona State University Dept. of Mechanical Engineering Dept. of Mech. Engineering Clemson, S. C. 29631 Tempe, Arizona 85281		10. Work Unit No. (TRAIS)	
		11. Contract or Grant No. DOT-OS-40018	
12. Sponsoring Agency Name and Address U. S. Department of Transportation Federal Railroad Administration Washington, D. C.		13. Type of Report and Period Covered Interim	
		14. Sponsoring Agency Code	
15. Supplementary Notes Prepared in cooperation with Association of American Railroads Research Center, Chicago, Illinois			
16. Abstract Wheel/rail geometric constraint relationships, such as the effective conicity and gravitational stiffness, strongly influence the lateral dynamics of railway vehicles. In general, these geometric constraints are nonlinear functions of the wheelset lateral displacement. This report describes the development and validation of an analytical procedure to determine these nonlinear functions for arbitrary wheel and rail profiles. Data for validation of this analysis was obtained experimentally. Experimental and analytical data for three validation cases is presented. Results of a limited parametric study are also reported. The computer program for the analytical procedure is described and documented.			
17. Key Words wheel/rail kinematics wheel/rail geometry railroads conicity, gravitational stiffness wheelset wheel profile, rail profile		18. Distribution Statement Document is available to the public through the National Technical Information Service, Springfield, Virginia 22151	
19. Security Classif. (of this report) UNCLASSIFIED	20. Security Classif. (of this report) UNCLASSIFIED	21. No. of Pages 182	22. Price

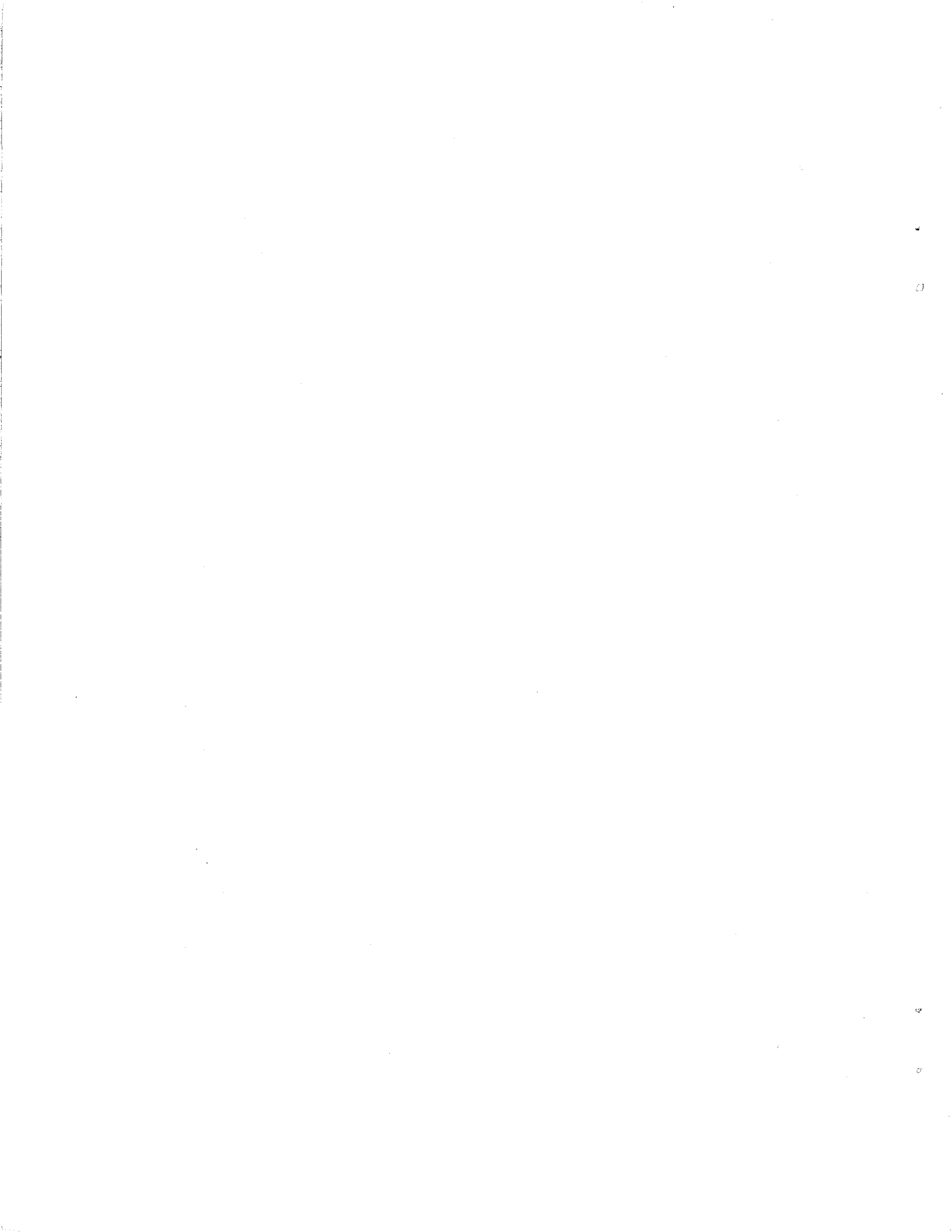


TABLE OF CONTENTS

	PAGE
1. INTRODUCTION	
Motivation	1
Previous Work	1
Objectives	6
Summary of Work	7
2. WHEEL/RAIL GEOMETRIC CONSTRAINTS	
Introduction	9
Wheel and Rail Profiles	11
Constraint Relationships	17
Quasi-Linearization	23
Approach	25
3. EXPERIMENTAL RESEARCH	
Introduction	27
Experimental Apparatus	27
Profilometer Experimental Procedure	32
Profilometer Experimental Results	39
Graphical to Digital Profile Conversion	51
Wheel/Rail Geometric Constraints	56
Conclusions.	58
4. ANALYTICAL RESEARCH	
Introduction	61
Approach	62
Computational Procedure.	63
Validation	69
Conclusions.	80

	PAGE
5. PARAMETRIC STUDY	
Introduction	81
Wheel Wear Effects	81
Rail Gauge Effects	102
Rail Wear Effects	115
Conclusions	127
6. CONCLUSIONS	
Status and Accomplishments	129
Future Work	132
REFERENCES.	136
APPENDIX -- WHEEL/RAIL CONTACT CHARACTERIZATION PROGRAM	
A. Purpose	139
B. Program Description	139
C. Method	143
D. Test Problem	149
E. Program Listing with Example I/O	149

LIST OF ILLUSTRATIONS

FIGURE NO.		PAGE
2-1	Example Wheel Profiles for Wheels with 85,000 Miles of Wear.	10
2-2	Wheel Profiles from a 70 Ton Hopper Car	12
2-3	Modified Heumann Wheel Profile	13
2-4	Rail Head Profiles	15
2-5	Rail Head Profiles	16
2-6	Wheel/Rail Parameters, Rear View	19
2-7	Wheel/Rail Coordinate Systems	20
3-1	Wheel/Rail Profilometer	28
3-2	Close-up, Wheel/Rail Profilometer	30
3-3	Resistance Wire on Wheel Tread, Wheel/Rail Profilometer	31
3-4	Operation of Wheel/Rail Profilometer	33
3-5	Wiring Schematic, Wheel/Rail Contact Circuit	35
3-6	Experimental Wheel Contact Point Location vs. Wheelset Displacement, New Wheel/New Rail	41
3-7	Experimental Rail Contact Point vs. Wheelset Displacement, New Wheel/New Rail	42
3-8	Experimental Wheelset Roll Angle vs. Wheelset Displacement, New Wheel/New Rail	43
3-9	Experimental Wheel Contact Point vs. Wheelset Displacement, Worn Wheel/Worn Rail.	45
3-10	Experimental Rail Contact Point vs. Wheelset Displacement, Worn Wheel/Worn Rail.	46
3-11	Experimental Wheelset Roll Angle vs. Wheelset Displacement, Worn Wheel/Worn Rail.	47
3-12	Experimental Wheel Contact Point vs. Wheelset Displacement, Worn Wheel/Worn Rail.	48
3-13	Experimental Rail Contact Point vs. Wheelset Displacement, Worn Wheel/Worn Rail.	49
3-14	Experimental Wheelset Roll Angle vs. Wheelset Displacement, Worn Wheel/Worn Rail.	50
3-15	Wheel Profile Measurement Procedure Using Sonic Digitizer.	53
3-16	Flow Chart of Profile Measurement Procedure.	54
3-17	Flow Chart for Computing Wheel/Rail Constraint Relationships	57

FIGURE NO.		PAGE
4-1	Wheel/Rail Characterization Program (Flow Chart)	64
4-2	Experimental and Analytical Results for New Wheels on New Rails at Nominal Gauge	70
4-3	Experimental and Analytical Results for Severely Worn Wheels on Worn Rails at Nominal Gauge	73
4-4	Experimental and Analytical Results for Severely Worn Wheels on Worn Rails at Wide Gauge	76
5-1	New Wheels, Worn Rails at Nominal Gauge	84
5-2	Slightly Worn Wheels, Worn Rails, at Nominal Gauge .	87
5-3	Moderately Worn Wheels, Worn Rails at Nominal Gauge.	90
5-4	Severely Worn Wheels, Worn Rails at Nominal Gauge. .	93
5-5	Modified Heumann Wheels, Worn Rails at Nominal Gauge.	96
5-6	Describing Function for Rolling Radii Difference vs. Nondimensional Wheelset Lateral Displacement . .	98
5-7	Contact Angle Difference Describing Function vs. Nondimensional Wheelset Lateral Displacement	100
5-8	Describing Function for Wheelset Roll vs. Nondimensional Wheelset Lateral Displacement	101
5-9	New Wheels, Worn Rails at Tight Gauge.	103
5-10	New Wheels, Worn Rails at Wide Gauge	105
5-11	Severely Worn Wheels, Worn Rails at Tight Gauge . .	108
5-12	Severely Worn Wheels, Worn Rails at Wide Gauge . . .	110
5-13	Describing Function for Rolling Radii Difference vs. Nondimensional Wheelset Lateral Displacement	112
5-14	Contact Angle Difference Describing Function vs. Nondimensional Wheelset Lateral Displacement	113
5-15	Describing Function for Wheelset Roll vs. Nondimensional Wheelset Lateral Displacement	114
5-16	New Wheels, New Rails at Nominal Gauge	116
5-17	Worn Wheels, New Rails at Nominal Gauge	119
5-18	Modified Heumann Wheels, New Rails at Nominal Gauge.	121
5-19	Describing Function for Rolling Radii Difference vs. Nondimensional Wheelset Lateral Displacement . .	124
5-20	Contact Angle Difference Describing Function vs. Nondimensional Wheelset Lateral Displacement	125
5-21	Describing Function for Wheelset Roll vs. Nondimensional Wheelset Lateral Displacement	126

CHAPTER 1

INTRODUCTION

MOTIVATION

The parameters that characterize the geometry or kinematics of wheel and rail contact have a dominant influence on rail vehicle dynamic behavior. The most important of these parameters, or wheel/rail geometric constraint relationships, are those describing the wheel rolling radii and the wheel/rail contact angles as functions of the wheelset lateral position. Combinations of these functions enter the rail vehicle equations of motion in the terms that are referred to as effective conicity and gravitational stiffness.

The wheel/rail constraint functions can be estimated or computed for idealized wheel and rail profiles such as simple conical sections, cylinders, or profiles with constant transverse radii of curvature. These estimates have been used extensively to study the small motions of vehicles with new or slightly worn wheels.

In developing mathematical models for the prediction and evaluation of freight car dynamic behavior, it became apparent that idealized wheel and rail profiles and associated wheel/rail constraint relationships could not be used in most cases. The worn wheel profiles observed on many of the freight cars in service appear to exhibit severely nonlinear characteristics that we expect to have a dominant influence on the vehicle stability and motion. Consequently, we undertook development of a method for obtaining accurately and rapidly the desired wheel/rail constraint relationships for arbitrary wheel and rail head profiles.

PREVIOUS WORK

The linear estimates of the wheel/rail geometric constraint functions that can be easily obtained by observation for small motions of a wheelset with new, conical wheels were used in most early studies of the lateral dynamics of railway vehicles. However, the dominant influence of worn or

profiled wheels on the lateral dynamics of railway vehicles was well known. Efforts were soon begun to determine the various wheel/rail geometric constraint relationships for profiled wheels. As most of the initial investigations of the lateral dynamics of railway vehicles were linearized analyses, early efforts focused on obtaining equivalent linear estimates of the difference in rolling radii and the difference in contact angles of the two wheels of a wheelset. After it became evident that the kinematic, or geometric constraint relationships were, in general, strongly nonlinear functions of wheelset lateral displacement for given wheel and rail profiles, efforts were undertaken to obtain the geometric constraint relationships for actual wheel and rail profiles.

Investigators at the British Railways Technical Centre have made major contributions to developing methods for determining the wheel/rail geometric constraint relationships. In their initial work, linear estimates of the constraint relationships were expressed as functions of the wheel and rail profile radii of curvature and the slope of the wheel/rail contact plane at the equilibrium or centered position [1-1]. As discussed in reference [1-2], it was soon realized that the kinematic or geometric constraint relationships were, in general, strongly nonlinear functions of wheelset lateral displacement for given wheel and rail profiles. Attention was then directed toward determining these nonlinear functions.

The British Railway Technical Centre's efforts to obtain the geometric constraint relationships for actual wheel and rail profiles are reported in

-
- 1-1. Wickens, A. H., "The Dynamic Stability of Railway Vehicle Wheelsets and Bogies Having Profiled Wheels," International Journal of Solids and Structures, Vol. 1, 1965, p. 319-341.
 - 1-2. Wickens, A. H., "General Aspects of the Lateral Dynamics of Railway Vehicles," ASME Journal of Engineering for Industry, Vol. 91, Series B. No. 3, August, 1969, p. 869-878.

references [1-3], [1-4], and [1-5]. In [1-3], the variation of the contact point locations with wheelset lateral displacement were determined for given wheel and rail profiles by traversing optically enlarged profiles across each other and inspecting for the point of contact. Once the contact points were found, the desired constraint relationships could be calculated with knowledge of the wheel and rail profiles. The wheel profiles were obtained using a mechanical wheel profile recorder. Although the discussion in [1-3] is not sufficiently detailed to draw a firm conclusion, it does not appear that two wheel profiles comprising a wheelset were traversed over two rail profiles separated by gauge distance. Thus, effects of wheelset roll angle may not have been considered. This is an important effect which should be simulated, especially for worn wheels and flange contact conditions. Nevertheless, the work in [1-3] was an important first step.

Shortly afterward, as reported in [1-4], the finding that critical speeds of certain vehicles were lower on lengths of new track than on adjacent worn rails provided impetus for further investigations into the wheel/rail geometric constraint relationships. In [1-4] it was reported that a new instrument had been developed to record digital profile data. A new method of determining

-
- 1-3. King, B. L., "An Evaluation of the Contact Conditions Between a Pair of Worn Wheels and Worn Rails in Straight Track", DYN/37, September, 1966, British Railways Research Department, Derby, England.
 - 1-4. King, B. L., "An Assessment of the Contact Conditions between Worn Tyres and New Rails in Straight Track," DYN/42, December 1966, British Railways Research Department, Derby, England.
 - 1-5. Gilchrist, A. O., "Variation Along the Track of Conicity and Rolling Line Offset," DYN/62, July 1967, British Railways Research Department, Derby, England.

wheel/rail contact points had apparently replaced the optical method described in [1-3]. The method used in [1-4] depended on matching the slopes of the wheel and rail profiles at the contact position. Apparently this was still done by hand after calculating and plotting the slopes of the wheel and rail profiles relative to distance along the axle centerline and rail base, respectively. It also appears that this technique was applied to a single wheel on a single rail as opposed to considering a complete wheelset on a pair of rails. Thus, the roll angle of the wheelset was neglected.

A computer technique was soon developed [1-5] to calculate automatically the variation with wheelset lateral displacement of the contact points and the difference in rolling radii. This technique required tabular input data for the wheel and rail profiles. This approach evidently considered a complete wheelset on two rails and thus accounted for wheelset roll. Details of the computational procedure or algorithm used were not discussed. From data presented, it appears that the procedure could be used for asymmetrical wheel and rail profiles. Various procedures for obtaining linear estimates for the wheel/rail geometric constraint relationships are discussed. These included the following: (a) fitting a straight line by eye through a central, nearly linear portion of the graph; (b) obtaining a least squares fit for a specific wheelset lateral amplitude; and (c) applying, for a given probability distribution of wheelset lateral amplitude, the statistical linearization procedure described by Booton in [1-6]. Experimental validation of the computational procedure used in [1-5] was not discussed or presented. Machines for measuring wheel and rail head profiles are shown and discussed in [1-5].

More recently [1-7], devices for recording wheel and rail profiles and analytical methods for evaluating the wheel/rail geometric constraint relationships have been developed by British Railways (BR), the French National

1-6. Booton, R. C., "Nonlinear Control Systems with Random Inputs," Inst. of Radio Engineers, Trans. on Circuit Theory, Vol. CT-1, No. 1, 1954.

1-7. Anon., "Geometry of the Contact Between Wheelset and Track Part 1: Methods of measurement and Analysis," Question C116, Interaction Between Vehicles and Track, Report No. 3, October, 1973, Office for Research and Experiments of the International Union of Railways (ORE), Utrecht, the Netherlands.

Railways (SNCF), and the German Federal Railways (DB). A very much abbreviated discussion of topics discussed in [1-7] is presented in [1-8]. The devices developed by the BR and SNCF record the wheel and rail profile coordinates on dial indicators. Those developed by the DB record the profile in analog form on a waxed paper chart. These devices are evidently designed to be located with respect to the opposite wheel or rail and record the distance between flange backs or rail gauge. A separate device is used to measure wheel diameter at a specified distance from the flange back.

The analytical method for determination of the wheel/rail contact points developed by the SNCF as reported in [1-7] does not consider wheelset roll relative to the track. However, it does consider a complete wheelset on a pair of rails. The algorithm or logic used to determine contact is not discussed. However, it may be based on finding points of equal and minimum separation between the right and left wheels and rails.*

The first step of the analytical procedure developed by the DB is to digitize the analog profiles recorded by the measuring machines. High order polynomials are then fitted to the wheel tread and rail head in each of about three or four sections. The polynomial approximations are obtained by ensuring that the sum of the squares of the errors between polynomial and profile data points are minimized. The algorithm for finding contact points depends on assuring equality of the slopes of wheel and rail surfaces at contact. If several points fulfill the slope equality condition, the point of contact is considered to be that where the minimum separation distance occurs. The algorithm is also capable of detecting two-point contact. It appears that wheelset roll angle is considered.

1-8. Anon., "Geometry of the Contact Between Wheelset and Track," Communications of the ORE, Rail International, March 1974, p. 252-256.

* This assumption is based on the statement that "...point contact is assumed both on the right and on the left, this being a direct result of the separation of wheelset and rails" [1-7].

The first step of the method developed by BR is to fit circular arcs over a number of zones (typically about thirty) to both the wheel and rail tabular profile data. Prior to calculating contact points the wheel and rail profile data are smoothed. It is not apparent from the discussion in [1-7] whether this is done to the data before or after the circular arc approximations are fitted. However, the discussion seems to imply that the raw data are smoothed before fitting the circular arcs. The algorithm for determining the contact points calculates the minimum distance between wheel and rail profiles for each zone. The minimum of these minima gives the contact points provided equal minima are calculated for left and right wheels. If the minima for left and right wheels are not equal, the program iterates on wheelset roll angle until equality is obtained. This process is repeated over a range of wheelset lateral displacement. The effective conicity is obtained via the statistical linearization procedure of Booton [1-6]. The linearization procedure is carried out for a range of standard deviations of lateral wheelset motion.

The three methods (SNCF, DB, and BR) of obtaining the variation of the difference in rolling radii with wheelset lateral displacement are compared in [1-7]. Profile data were obtained from the same wheels and rails by the measuring devices of each organization and then processed by each of the three methods. The methods gave fairly similar results although differences are apparent.

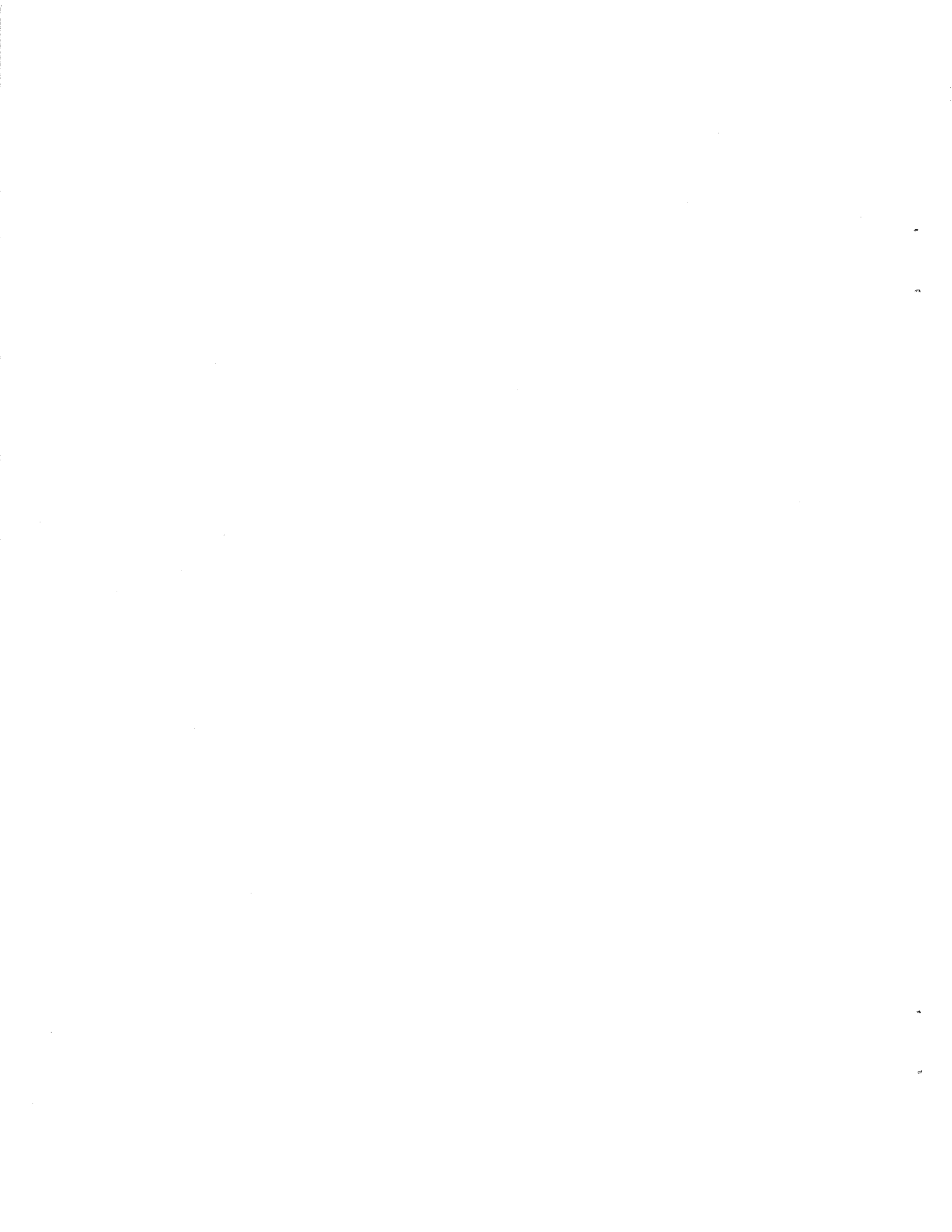
OBJECTIVES

The objectives of the work described in this report were (a) to develop an analytical procedure to calculate the nonlinear wheel/rail geometric constraint relationships for any given wheel and rail head profiles; (b) to develop experimental equipment and a procedure to obtain experimental data that could be used to validate the analytical procedure; (c) to use the validated analysis to calculate wheel/rail geometric constraint relationships for several wheel and rail head profiles; (d) to examine effects of wheel and rail

wear and gauge on the wheel/rail geometric constraint relationships; and, (e) to develop and use an accurate and fast procedure to obtain tabular wheel and rail head profile data from graphical data.

SUMMARY OF REPORT

The work performed in achieving the objectives outlined above is discussed in the following chapters. We discuss the general subject of the wheel/rail geometric constraints in Chapter 2, focusing on (a) the physical bases for the effective conicity and gravitational stiffness effects, (b) the specific wheel and rail profiles used in this study, and (c) the quasi-linearization procedures used in obtaining equivalent linear values. The experimental work is described in Chapter 3. The apparatus developed during the study and the experimental procedures developed to determine the contact points are discussed together with the interactive computing procedure developed to obtain tabular data from graphical profile data. In Chapter 4 we discuss the computational algorithm developed to predict analytically the contact point variation with wheelset lateral displacement. The results of the analytical process are then compared at two levels with those determined experimentally. Experimental and analytical data are compared for contact points and constraint relationships (such as difference in rolling radii and contact angles). In Chapter 5, we present a limited parametric study for several combinations of wheel and rail profiles in various states of wear. We also present an evaluation of the effects of gauge for a particular combination of wheel and rail profiles. Finally, in Chapter 6 we present our conclusions and recommendations for future work. A Users' Manual and listing for the digital computer program to determine analytically the wheel/rail geometric constraint parameters is included in the Appendix.



CHAPTER 2

WHEEL/RAIL GEOMETRIC CONSTRAINTS

INTRODUCTION

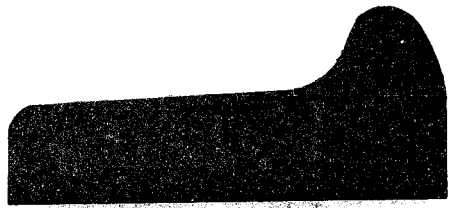
Although nearly all railroad wheels start out with identical wheel tread profiles, these profiles wear with service, assuming a wide variety of shapes as they wear. Rails, too, begin with nearly identical head profiles that are altered by the traffic over them. The distance between rails, or rail gauge, will also vary due to initial construction tolerances and the effects of the loads imposed on them. This report presents the results of our first efforts to understand how these variations in wheel and rail geometry affect the parameters that influence the lateral motions of railway vehicles.

This effort should be regarded as an initial investigation to determine the sensitivity of the wheel/rail geometric constraints to wide variations in wheel and rail conditions rather than a comprehensive survey of wheel and rail conditions on American railroads. The results of this work revealed a strong sensitivity of the wheel/rail constraints to wheel/rail geometry. Consequently, we expect a wide variation of the wheel/rail parameters from wheelset to wheelset and track section to track section. The comprehensive survey mentioned above should be undertaken to establish the ranges of wheel and rail wear that can be expected, and to define nominal cases for wheel and rail profiles in various states of wear.

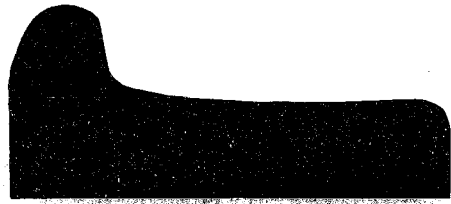
The five wheel profiles and two rail profiles used in this study are discussed in the following section. In subsequent sections we discuss (1) the wheel/rail constraint relationships and their influence on vehicle dynamics, and (2) methods for approximating these relationships in dynamic analyses. In the final section of this chapter we outline the approach taken to obtain the desired information about the wheel/rail geometric constraints for arbitrary wheel and rail profiles.

LEFT

RIGHT



AXLE 1



AXLE 2



AXLE 3



AXLE 4

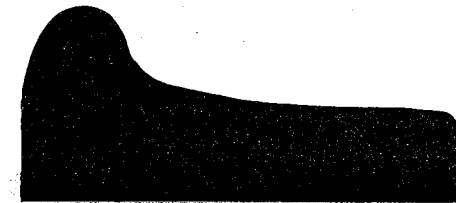


FIGURE 2-1. EXAMPLE WHEEL PROFILES FOR WHEELS WITH 85,000 MILES OF WEAR.

WHEEL AND RAIL PROFILES

The changes in wheel profile that occur during the service life of the wheel are due to both material wear and cold working of the wheel material. The rate of change and the nature of the change depend on a variety of factors including the vehicle condition, the vehicle suspension system, the vehicle loading, the operating speed, and the track condition.

The wheel tread profiles for all eight wheels of a railcar with 85,000 miles of service are presented in figure 2-1. Interestingly, the wheels on this car show a wide variety of wear patterns. Wheel wear begins by a hollowing of the tread from the flange throat toward the field side on the tread, and from the flange throat up the flange. This initial wear may be seen by comparing the nearly new tread on the left wheel of axle 1 with the light wear seen on the right wheel of axle 3. As the wheels continue to wear, hollowing of the tread continues and the flange wears to increase the flange slope, as seen in the extreme case on the left wheel of axle 4.

Unequal wear patterns such as those seen in figure 2-1 are common on American freight cars. Several theories for this unequal wear have been advanced, including unequal forces in the brake rigging, variations in wheel diameters on the same axle, friction at the centerplate, and misalignment of the axles. Once unequal wear begins, it appears that continued wear will reinforce the unequal pattern. This is probably due to a tendency of the wheelset with unequal wheel profiles to align itself on the rail in an off-set position. When this happens the points of wear will differ on the left and right wheel. Consequently, unequal wear will continue. Severe examples of this behavior may be seen on axles 3 and 4 of figure 2-1.

In this study, five wheel profiles were investigated including a new wheel, a worn wheel in three different states of wear, and a modified Heumann profile. These profiles are shown in figure 2-2 and 2-3. The new wheel has a standard, 1/20 tapered profile. The worn profiles, supplied by the Association of American Railroads, depict three wear conditions for a wheel in service on a 70 ton hopper car. The downward slope on the outer portion of the

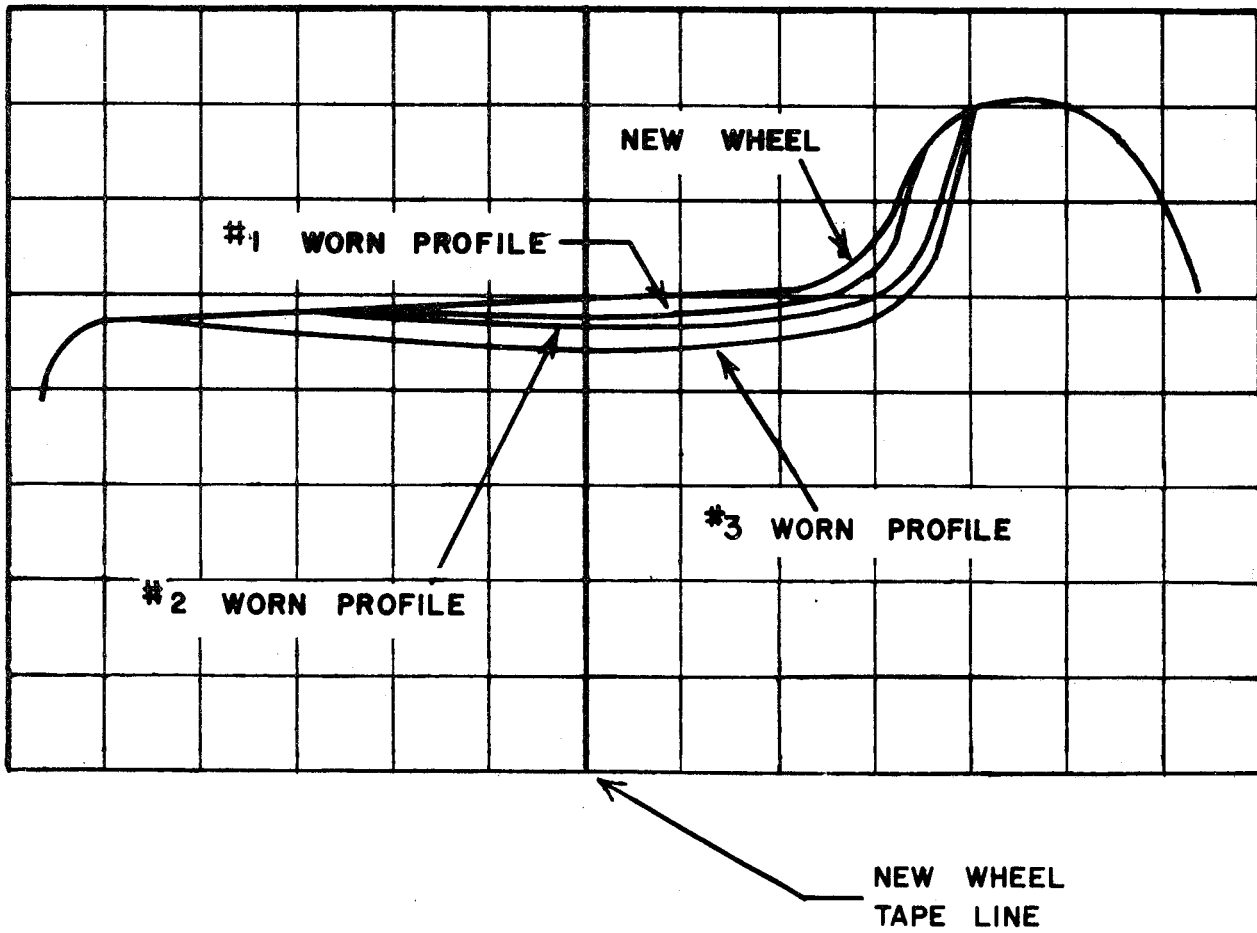


FIGURE 2-2 WHEEL PROFILES FROM A 70 TON HOPPER CAR

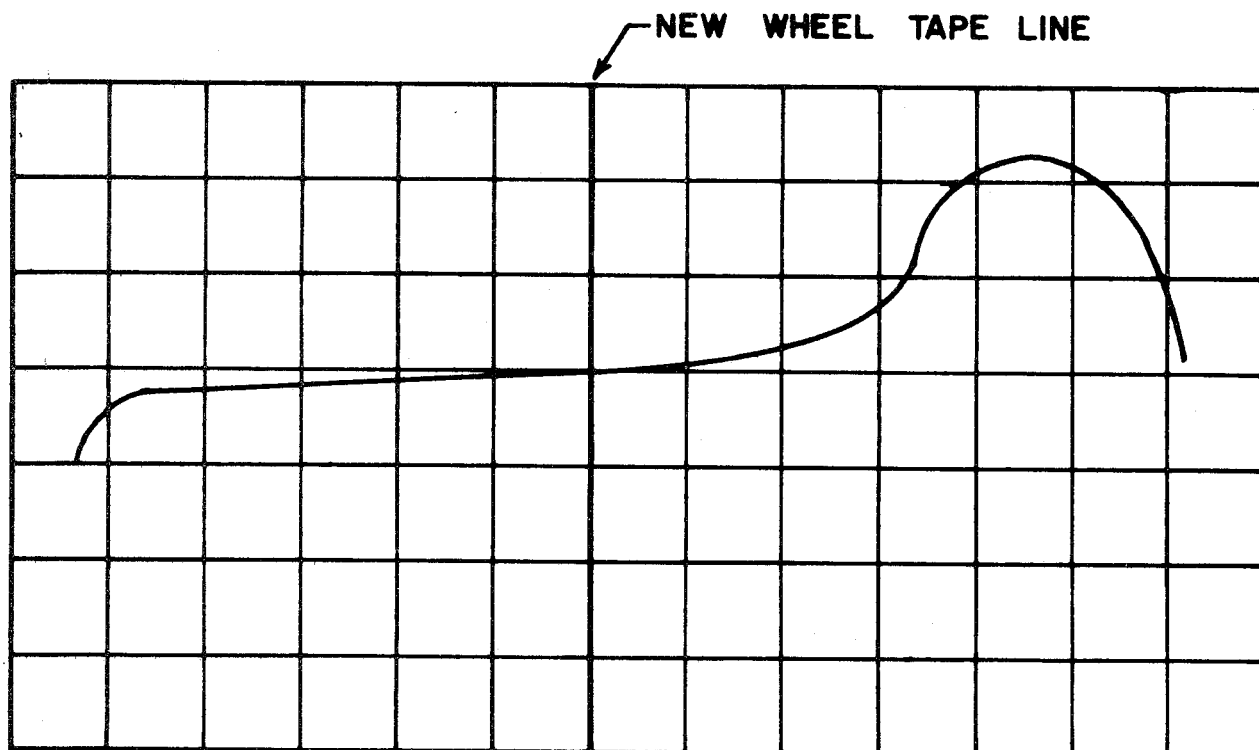


FIGURE 2-3 MODIFIED HEUMANN WHEEL PROFILE

concave profile of the two most worn profiles should be noted. This "down-turned" characteristic* influences the wheel/rail parameters in an important way, as discussed at length in Chapter 5.

Increasing wheel mileage also leads to flange wear, as easily seen in figure 2-2. Because the wheel gauge is determined by a flange back to flange back measurement and does not change after the wheels are mounted on the axle, worn wheels have a great deal more clearance between the flange and the rail than do new wheels. The most severely worn wheel profile shown in figure 2-2 has 0.20 inches more clearance before climbing the flange than does the new wheel.

The fifth wheel profile studied in this project, the modified Heumann profile was originally developed in the 1930's by H. Heumann, a German engineer [2-1]. This profile was designed to provide a single point of contact between wheel and rail at all wheelset lateral positions. Several years ago, this contour was modified by J. L. Koffmann of the British Railways Board for use on the British Railways [2-2]. This modified Heumann profile may provide better wear characteristics than the standard, tapered profile. The modified Heumann profile shown in figure 2-3 is a slight modification of Koffman's profile, designed by Eck and Berg [2-3] to meet U.S. rail conditions.

In this initial study, only the geometric constraints between symmetrical wheelsets and rails were investigated. Although the analytical techniques and programs are capable, with minor modifications, of handling unequally worn or asymmetrical wheels and rails, a thorough study of such situations was left for a future project.

The changes in rail profile under the influence of traffic are not as dramatic as the wheel profile changes. New and worn rail head profiles are shown in figure 2-4 and 2-5. The worn rail profile C shown in figure 2-4 has

*We do not know, at this time, whether this "downturn" is representative of the worn railroad wheel population. Such an investigation should be made.

2-1. Heumann, H. "The Problem of the Tyre Profile," Organ. f.d. Fortschritte des Eisenbahnwesens, vol. 89, no. 18, Sept. 15, 1934, p. 336-342.

2-2. Koffmann, J. L., "Heumann Tyre Profile Tests on British Railways," Railway Gazette, 1965, p. 279.

2-3. Eck, B.J. and N.A. Berg, "Looking for Tomorrow's Wheel Profile," ASME Winter Annual Meeting, Detroit, Nov. 1973.

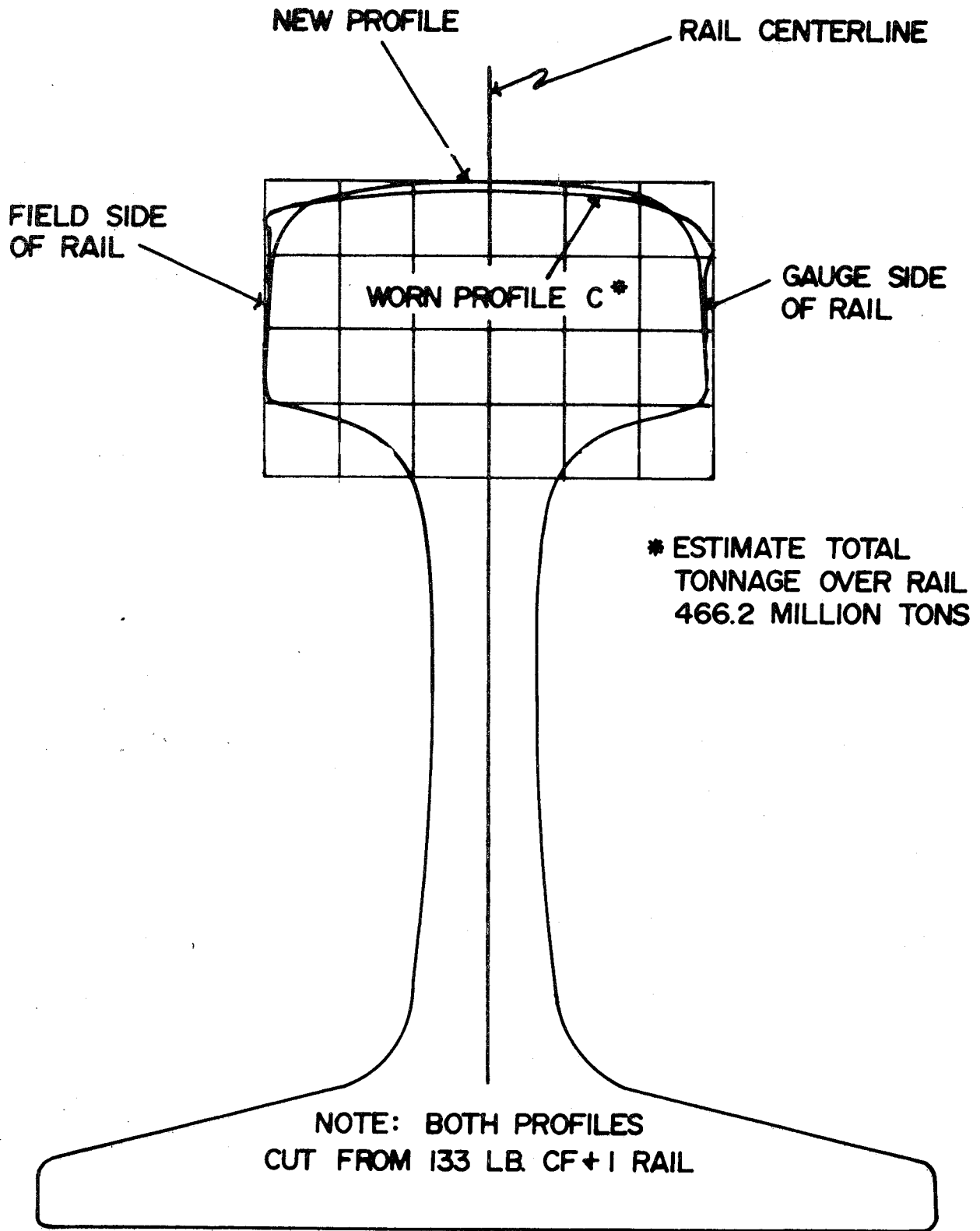


FIGURE 2-4 RAIL HEAD PROFILES

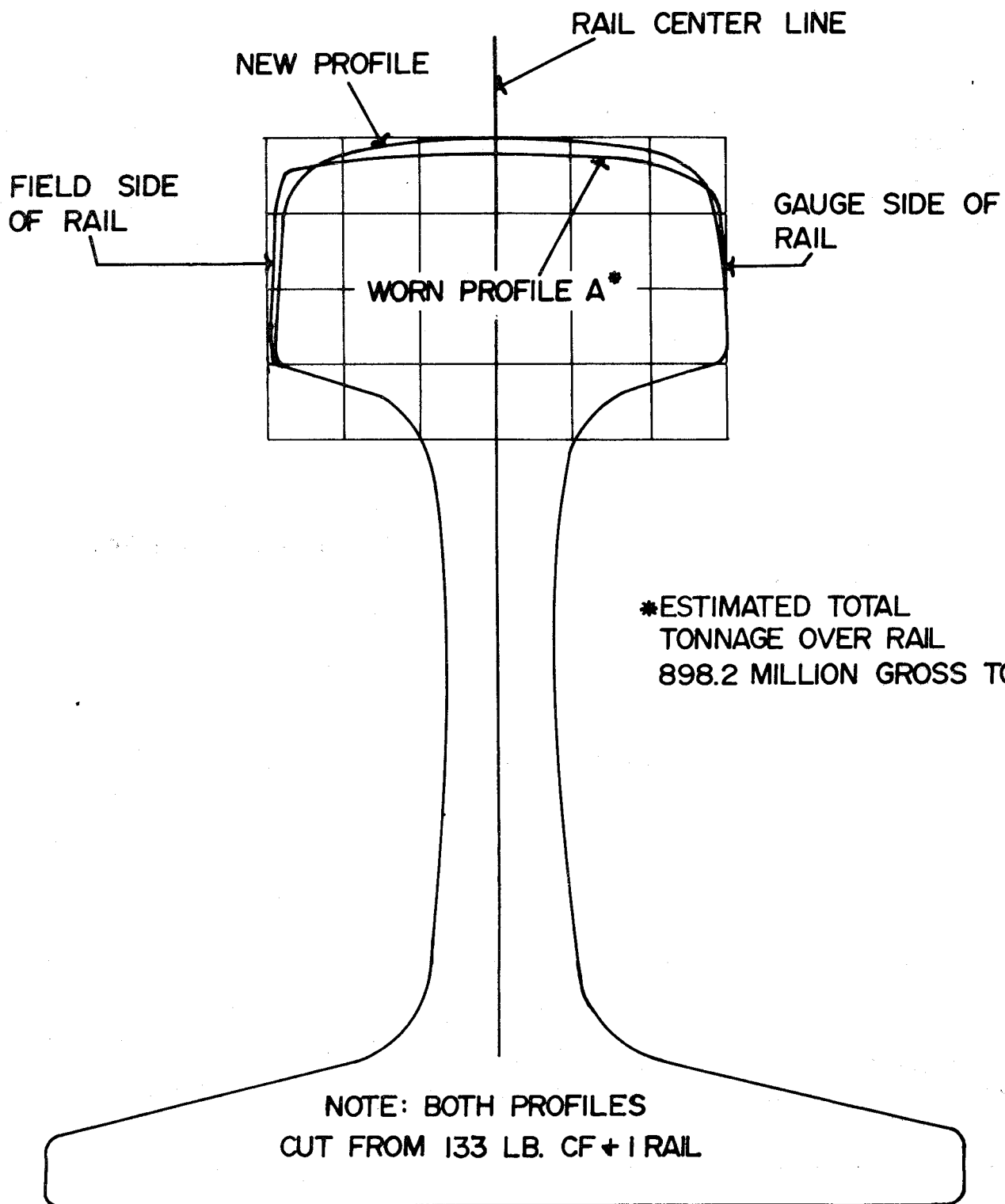


FIGURE 2-5 RAIL HEAD PROFILES

seen 466 million gross tons of service while the worn profile A of figure 2-5 has been subjected to nearly 900 million gross tons. Wheel/rail contact on new rail occurs over the gauge or inner half of the rail profile, causing wear and cold working of the rail head. This initial wear skews the rail head profile, often wearing the gauge more than the field or outer side, as seen in profile C of figure 2-4. However, many worn wheels will contact a rail profile such as profile C on the field side of the rail. This contact position is more likely to occur when the wheels have the concave profile with negative slope seen in profiles 2 and 3 of figure 2-2. Contact on the field side of the rail is also more frequent on wide gauge track for worn wheels. When contact occurs on the field side of the rail head this side wears and material is cold worked to the inside. The result is a worn rail profile such as that shown in profile A of figure 2-5.

The rail profiles shown in figure 2-5 were used in the parametric study described in Chapter 5.

WHEEL RAIL CONSTRAINT RELATIONSHIPS

Railway wheelsets, as they roll along the track, are constrained to move laterally and vertically in a prescribed space determined by the geometry of the wheels, rails and track structure. The characteristics of these geometric constraints determine, to a large extent, the nature of the lateral motions of the wheelsets. The wheelset position may be described by two independent variables, the lateral position of its geometric center relative to the track centerline, x_w , and the angular rotation of the wheelset about a vertical axis, θ_w . The remaining motions of the wheelset such as roll or vertical movement, are determined by the geometric constraints.

For our purposes in studying the lateral dynamics of rail vehicles, we must know the following information as a function of the independent variables, x_w and θ_w :

- r_L -- instantaneous rolling radius of the left wheel
- r_R -- instantaneous rolling radius of the right wheel

- y_L -- instantaneous height of contact point on the left rail
- y_R -- instantaneous height of contact point on the right rail
- δ_L -- angle between the contact plane on the left wheel and the axle centerline
- δ_R -- angle between the contact plane on the right wheel and the axle centerline
- ϕ_w -- roll angle of the wheelset with respect to the plane of the rails.

These constrained variables, corresponding coordinate systems, and contact point definitions, are illustrated in figures 2-6 and 2-7.

The dependence of these constrained variables on the yaw angle of the wheelset is a second order effect. Consequently, for our purposes it is sufficient to determine the functional relationships between the wheelset lateral displacement and each of the constrained variables.

The rolling radii constraints enter the wheelset equations of motion as the difference between the rolling radii at the two wheels of the wheelset. When the wheelset is displaced from a centered position between the rails the difference between the rolling radii at the left and right wheels requires that the velocity of the wheel at the contact point on the wheel with a larger rolling radius be greater than the velocity at the contact point on the other wheel. The result is partial slip, or creep, at the wheel/rail interface giving rise to a moment which results from the tangential or creep forces at the wheel/rail interfaces. This moment tends, in most cases, to steer the wheelset towards the centered position of the rails.

The nature of the relationship between rolling radii difference and wheelset lateral position varies widely. For a new wheel with a conical taper, the difference in rolling radii depends linearly on the wheelset lateral displacement, x_w , until flange contact is made. The constant of proportionality, called the wheelset conicity, is the wheel profile taper (usually 1/20 or 0.05). As the wheels wear, the change in rolling radii difference with wheelset lateral displacement becomes more nonlinear, and, over certain ranges, is much greater than the change with new wheels. Thus, the "effective"*

*The meaning of "effective" in this context is discussed in the section on quasi-linearization.

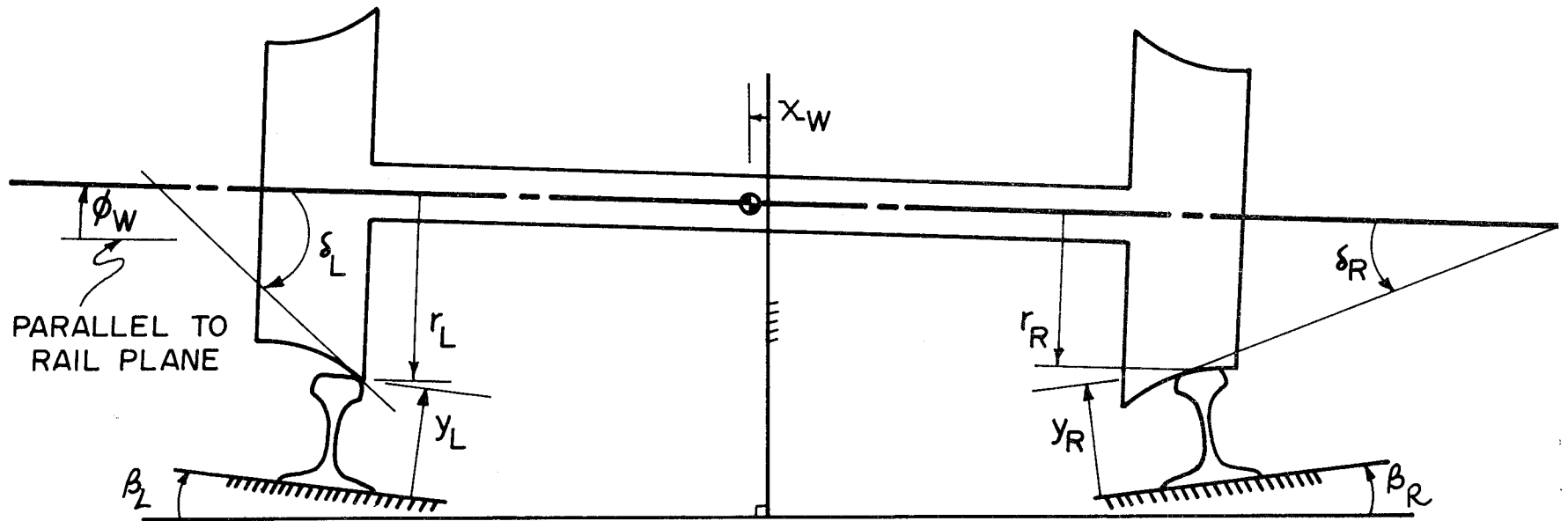
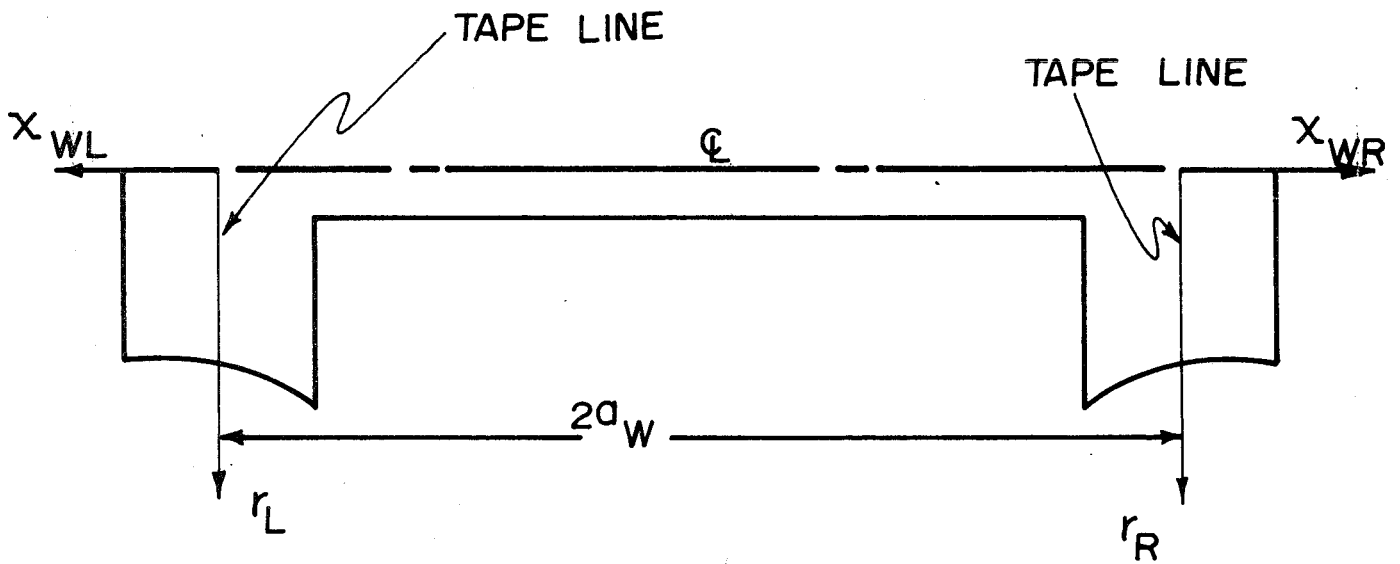
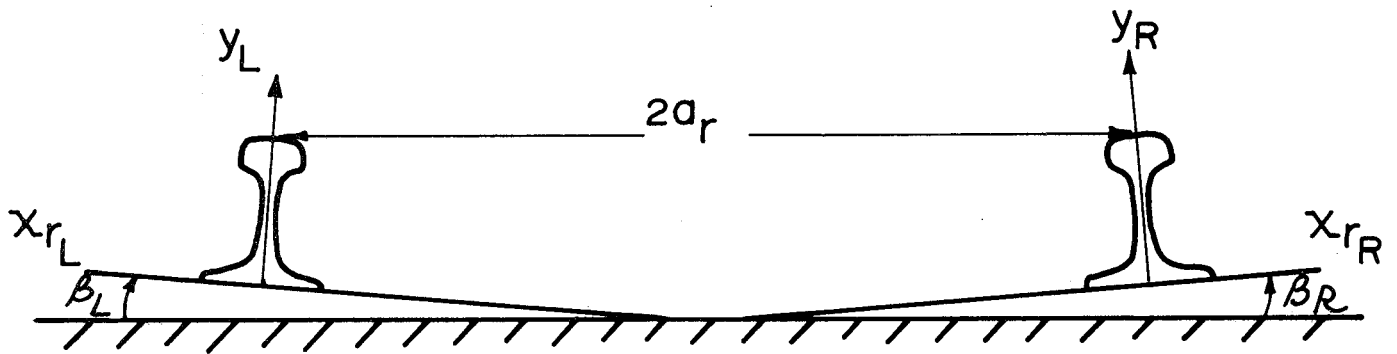


FIGURE 2-6 WHEEL / RAIL PARAMETERS, REAR VIEW



A - WHEEL COORDINATE SYSTEMS
REAR VIEW



B - RAIL COORDINATE SYSTEMS
REAR VIEW

FIGURE 2-7 WHEEL/RAIL COORDINATE SYSTEMS

conicity with worn wheels is often much greater than for new wheels. The nature of this relationship between the difference in rolling radii and wheelset lateral position is discussed at greater length in Chapter 5.

The important influence of the difference in rolling radii on rail vehicle dynamics has been recognized for quite some time. The difference in rolling radii with wheelset lateral displacement has a dominant effect on the nature and stability of the rail vehicle motion. If the conicity is zero, as it is for cylindrical wheel tread profiles, then the vehicle will never experience hunting, but must rely on the wheel flanges for guidance. In general, increasing the "effective" conicity is a destabilizing effect, meaning that the critical speed for onset of hunting is lower with larger values of conicity.

The contact angle constraints enter the rail vehicle equations of motion in the description of the magnitude and direction of the contact forces between the wheel and rail. Of particular importance is the difference in lateral components of the normal forces between wheels and rails. This difference, often referred to as the gravitational stiffness effect, is approximately equal to the axle load multiplied by half the difference in contact angles plus the roll angle, for small contact angles, i.e.,

$$\text{gravitational stiffness force} = \text{axle load} \times \left(\frac{\delta_L - \delta_R}{2} + \phi_w \right)$$

At larger contact angles trigonometric functions of the contact angles enter the expressions for these terms.

In most cases, this gravitational stiffness force acts in a direction to move the wheelset towards the centered position. If the gravitational stiffness is large, due to a large change in contact angle difference with lateral displacement, significant lateral restoring forces will be produced. Thus, gravitational stiffness can be termed a stabilizing effect.

The contact angles for new wheels when centered are, of course, the angles of the wheel tread taper. The angle of contact with respect to the axle remains at this value until the wheelset is shifted laterally far enough for the contact point to move to the flange. For either new or worn wheels,

the contribution of the roll angle to the gravitational stiffness effect is about the same. However, when contact occurs in the tread region, the contribution of the difference in contact angles to the gravitational stiffness is potentially very large for worn wheels but is always zero for new wheels.

This gravitational stiffness effect can provide more restoring force than the vehicle suspension for a heavily loaded wheelset. The stabilizing benefit of this effect, however, is far less important for light vehicles. In general, as the wheels wear, both the wheelset conicity and the wheelset contact angle difference increase. Because one change is stabilizing and the other destabilizing, the resultant effect on vehicle stability depends on the relative magnitudes of the terms. The dependence of the gravitational stiffness effect on wheel load means that wheel wear will be more destabilizing for light vehicles than for loaded or heavy vehicles.

The assumption is often made, in setting up the lateral equations of motion for rail vehicles, that the gravitational stiffness terms are approximately equal in magnitude and opposite in sign to terms in the tangential wheel/rail force expression that describe the lateral/spin creep* contribution to these forces. This assumption permits one to omit both the gravitational stiffness and the lateral/spin creep terms from the equations of motion. This assumption appears reasonable for passenger vehicles, or European freight vehicles where the wheel loads are smaller than those carried by North American freight cars. However, this equivalence assumption does not hold for the large wheel loads carried by North American freight cars.

The third geometric constraint to enter the equations of motion describes the roll of the wheelset about a longitudinal axis as the wheelset moves laterally. Although the roll inertia of the wheelset only enters as a second order effect, the roll dependence also appears in terms describing the "gyroscopic" effects, certain aspects of the creep forces, and the

*The lateral force due to lateral/spin creep arises from an asymmetric distribution of shear stresses in the contact region due to a relative angular velocity, or spin, about the normal to the contact plane.

gravitational stiffness as previously discussed. These gyroscopic effects are normally small, but can be important at high speeds.

The roll constraint relationship, like the other wheel/rail geometric constraints, may vary considerably from one wheel profile to the next. The roll displacement of a wheelset with new wheels as it moves laterally is quite small. As the wheels wear, variation of the angle of roll with lateral displacement may or may not change significantly from the new wheel case. There is rarely a dramatic change in this relationship as the wheels wear. In most cases, these wheel/rail constraint relationships are not well behaved functions of the wheelset lateral position. When the contact point between wheel and rail jumps, the rolling radii and contact angle constraints also change discontinuously, and only the wheelset roll angle remains a continuous function of lateral position. The most obvious of these jump discontinuities occurs when the flange comes into contact. Worn wheels may, and usually do, have several lateral positions where the contact point jumps across the wheel and rail.

QUASI-LINEARIZATION

The dynamics of rail vehicles can be studied most easily when the vehicle behavior is described by linearized equations of motion. Techniques for determining stability and forced response of linear systems are widely available and offer great computational advantages over nonlinear analysis methods. The rail freight car, however, has several nonlinear characteristics that can not be ignored, including suspension friction, clearances between components, and the wheel/rail geometric constraints under discussion here. We shall refer to such an equivalent linear representation as a quasi-linearization.

The describing function approach to quasi-linearization is particularly convenient for investigating the stability of nonlinear systems such as the rail vehicle. Quasi-linearization of a nonlinear system involves replacing the nonlinear functions,

$$\underline{y} = f(\underline{x}) \quad (2-1)$$

where: \underline{x} , \underline{y} , are vector quantities

with quasi-linear functions of the form,

$$\underline{y}_q = N(\underline{\alpha}) \underline{x} \quad (2-2)$$

where: $\underline{\alpha}$ is a vector that depends on the properties of \underline{x} .

The describing function approach [2-4], [2-5], selects the matrix, $N(\underline{\alpha})$, to minimize the mean square error between the nonlinear and the quasi-linear response, i.e.

$$\min_N \overline{\varepsilon(t)^2} = \min_N (\underline{f} - N\underline{x})^T (\underline{f} - N\underline{x}) \quad (2-3)$$

To carry out the minimization suggested in equation 2-3, the input signal, $\underline{x}(t)$, must be specified. In general [2-4], $\underline{x}(t)$, can be composed of sinusoidal, constant bias, and random input signals. In this discussion, only sinusoidal input signals are considered.

The describing function defined by equation 2-3 for a nonlinear element, $y = f(x)$, reduces to the following equation* when $x(t)$ is $A \sin(\theta)$,

$$y_q = N(A) = \frac{1}{2\pi A} \int_0^{2\pi/\omega} f(A \sin \theta) \sin \theta d\theta \quad (2-4)$$

Using this equation, the describing function for any single-valued, nonlinear relationship can be computed either analytically or numerically. In general, the resulting describing function will be a function of both the frequency and amplitude of the input signal. However, when $f(x)$ is single-valued and does not depend on derivatives of x , the describing function will only depend on the input amplitude. If $f(x)$ is linear, then the describing function determined by equation 2-4 will be merely the coefficient of x , a constant.

If the nonlinear wheel/rail geometric relationships are known, describing functions for these relationships can be computed numerically using equation 2-4. The computation of such describing functions for the contact angle difference, the rolling radii difference and the roll angle relationships is discussed in Chapter 4, and the results of the computations presented in Chapters 4 and 5.

These describing functions can be used in a linear analysis in several ways. If one is only interested in a qualitative understanding of the expected

2-4. Gelb, A., and W. Vander Velde, Multiple-Input Describing Functions and Nonlinear System Design, McGraw-Hill, 1968.

2-5. Siljak, D., Nonlinear Systems: The Parameter Analysis and Design, J. Wiley & Sons, 1969.

*This equation is only valid for single valued functions.

vehicle behavior, one might select an equivalent linear value for each of the wheel/rail constraints by choosing the describing function value at one particular amplitude, the flange clearance perhaps. A more complex analysis to determine the existence and stability of limit cycles entails an iterative solution that searches out the amplitude and corresponding describing function values that meet the conditions for limit cycle existence. This process is described in reference [2-6].

APPROACH

The specific objective of the study discussed in this report was to develop the capability of determining the wheel/rail geometric constraints for arbitrary wheel, rail, and track structure conditions, and to put these relationships in a form that could be easily incorporated into rail vehicle dynamic analyses. We felt that achievement of this objective required development of analytical techniques to determine numerically the desired relationships, conduct of experiments to determine the relationships for several representative wheel and rail conditions, validation of the analytical technique with the experimental results, and computation of the constraint relationships for a limited sample of cases.

The results of our efforts on each of these tasks are discussed in the following chapters. Completion of this effort has brought us a great deal closer to our goal of modeling dynamic behavior of American rail freight cars. Extensive application of the techniques described here, however, requires effort beyond the scope of this study. Of particular importance is the development of a data bank of wheel and rail profiles in a wide variety of conditions.

2-6. Cooperrider, N.K., Hedrick, J.K., Law, E.H. and C. W. Malstrom, "The Application of Quasi-Linearization to the Prediction of Nonlinear Railway Vehicle Response," presented at the IUTAM Symposium on Vehicle Mechanics, Delft, August 1975.

CHAPTER 3

EXPERIMENTAL RESEARCH

INTRODUCTION

The equipment and procedures that we developed and used to determine wheel/rail contact points, to obtain tabular wheel/rail profile data, and to compute the wheel/rail geometric constraint relationships are discussed in this chapter. One objective of this experimental research was to provide the data needed for validation of the analytical procedure described in Chapter 4. An additional objective of this work was to develop a fast and accurate method of obtaining tabular data from graphical profiles of wheels and rails for subsequent use in providing input data to the analytical procedure.

The experimental apparatus used in this research effort is described in the first section below, followed in the second section by a description of the experimental procedure used with this equipment to determine the wheel and rail contact points. The experimental results are presented and discussed in the third section. The interactive computing procedure developed to obtain wheel and rail profiles is discussed in the fourth section. The fifth section of this chapter deals with the computational procedures used to find the wheel/rail geometric constraints from the experimental profile and contact position data. We summarize our conclusions on the experimental research in the final section.

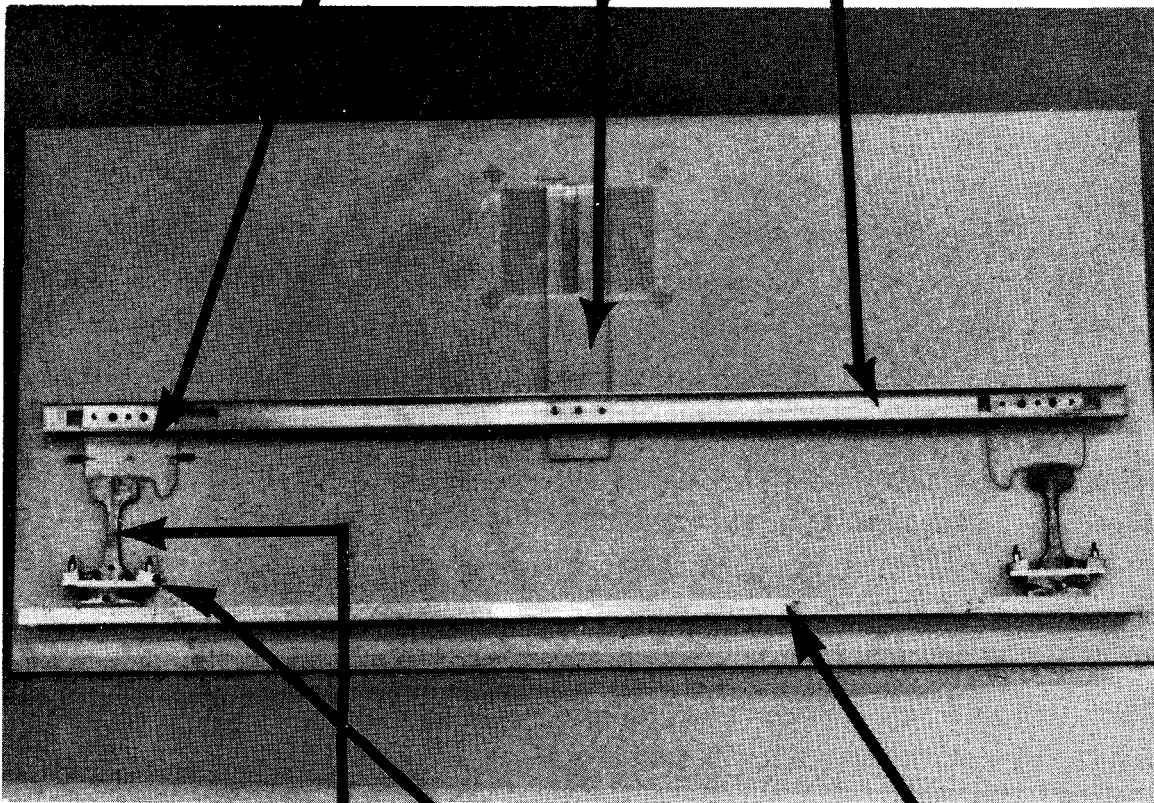
EXPERIMENTAL APPARATUS

The experimental apparatus that we developed and used to measure the wheel/rail geometric parameters is a full scale model of the wheel and rail surfaces. We call this device a profilometer. The profilometer, shown in figure 3-1, consists of two main assemblies (1) a track assembly, and (2) a wheelset assembly. The track assembly comprises two rail sub-assemblies, each holding a one half inch thick rail section mounted on an aluminum bar that is rigidly bolted to a flat surface. The rail sub-assemblies are constructed to allow adjustment of the rail cant angle and gauge. The wheelset assembly consists of two, one half inch thick, plexiglass wheel profiles and a wheelset centroid locating bar mounted on another aluminum bar. The distance between wheels on this assembly can be adjusted.

WHEELSET ASSEMBLY

CENTROID LOCATING BAR

WHEEL PROFILE



RAIL SECTION

RAIL SUBASSEMBLY

TRACK ASSEMBLY (horizontal)

FIGURE 3-1

WHEEL / RAIL PROFILOMETER

Wheel profiles supplied by the Association of American Railroads (AAR) in full scale graphical form were used for these experiments. The first step in making the plexiglass profiles was to paste a paper copy of the profile on the plexiglass. The plexiglass profile was then cut carefully with a jig saw, smoothed and polished. The accuracy of the plexiglass profile produced by this process depended on the skill and care of the machinist who cut and polished the wheel profile.

Wheel tape lines were defined and marked on each profile for later use in establishing the separation between the two wheels. For the new wheel, the line was located by the standard procedure shown in figure 5.11 of reference [3-1]. The tape line location for worn wheel profiles was defined by transferring the tape line for a new wheel of the same type to the worn profile. Thus, the tape line position remained unchanged by wheel wear.

As shown in figure 3-2, a small hole was drilled in each wheel profile. This hole is used to plot the vertical displacement of each wheel profile as the wheelset is shifted laterally. The roll angle of the wheelset at each lateral position is computed from these vertical displacement measurements.

The contact position between the wheel and rail at each lateral position is measured by means of a resistance wire mounted on the wheel tread. The resistance wire is bonded in a shallow groove on the wheel tread, and is extended up both sides of the wheel profile to connections at terminals mounted on the wheel profile. Figures 3-2 and 3-3 illustrate the resistance wire and its connections.

The one half inch thick sections of actual rails used in the profilometer were supplied by the AAR. The rail sections are mounted on sub-assemblies that can be moved with respect to the track center line, and can be adjusted to different values of rail cant angle. A center line, perpendicular to the base of the rail and passing through the center of the base, was scribed on the face of each rail section. The lateral locations of the contact points on the rail head were referred to this line.

The lateral position of the wheelset assembly is measured with the wheelset centroid locating bar. This locating bar is mounted at the center of the wheelset assembly in a position perpendicular to the wheelset centerline.

3-1. Anon., "Wheel and Axle Manual," Tenth Edition, Oct. 1972, Association of American Railroads, Washington, DC.

PLOTTING HOLE

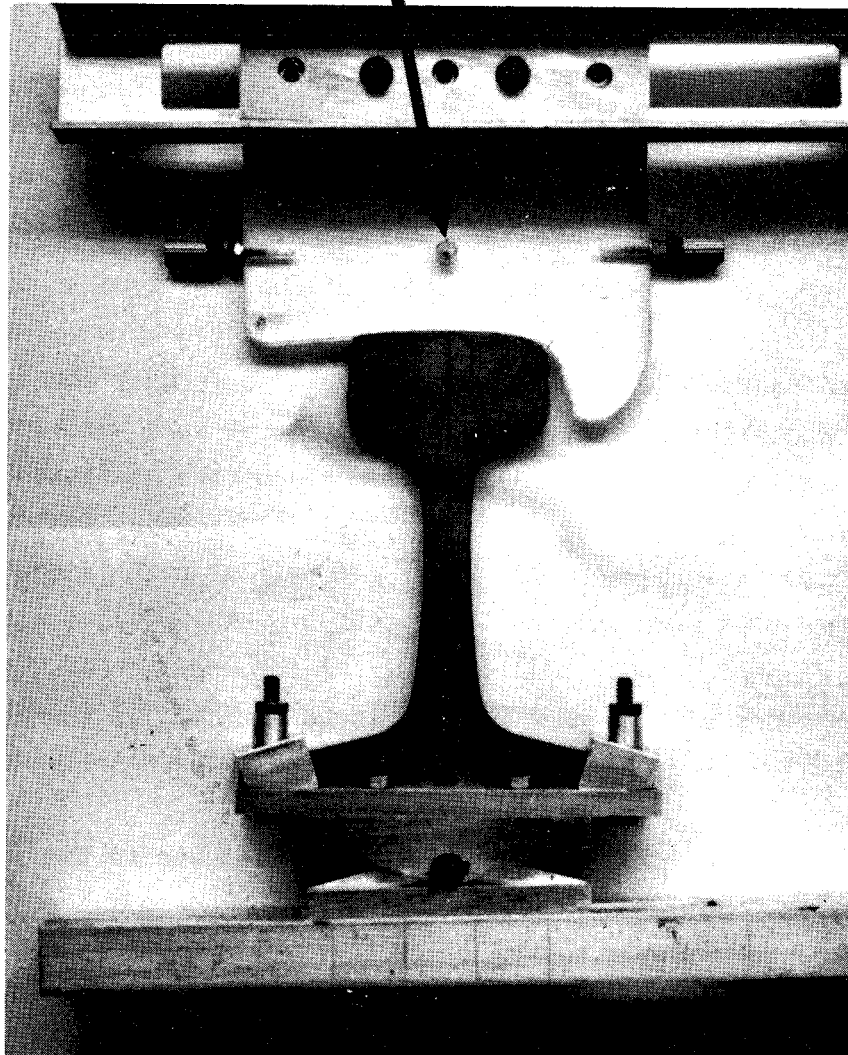


FIGURE 3-2

CLOSE-UP , WHEEL / RAIL PROFILOMETER

TERMINAL # 2

RESISTANCE WIRE

TERMINAL # 1

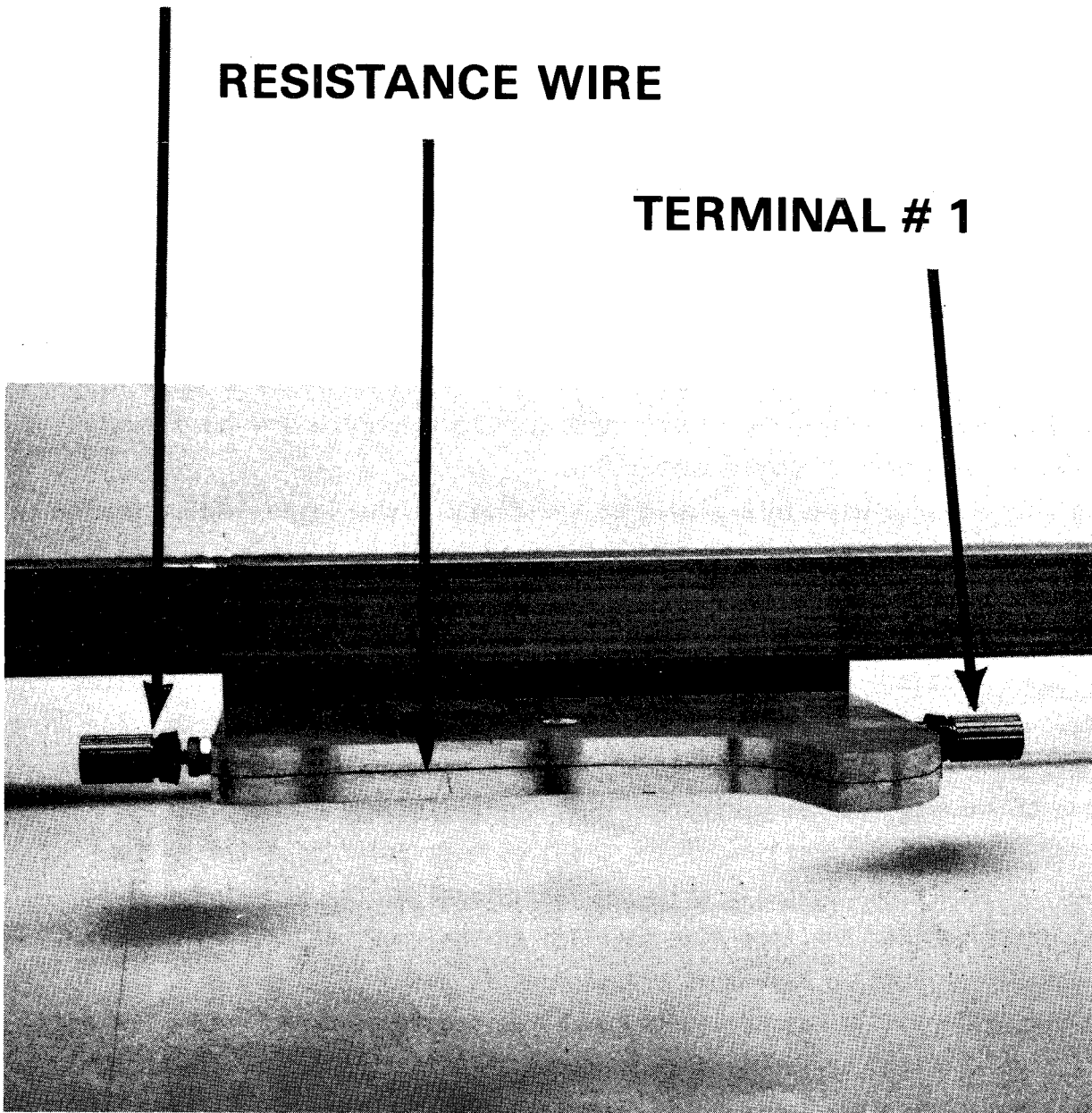


FIGURE 3- 3
RESISTANCE WIRE ON WHEEL TREAD,
WHEEL / RAIL PROFILOMETER

PROFILOMETER EXPERIMENTAL PROCEDURE

The experimental procedure used to obtain data with the profilometer was developed over a period of time to that described below. Initially, we tried to locate the rail/wheel contact points by sliding thin shims towards the contact point from either side. The midpoint of the contact length defined by the maximum penetrations of the shims was considered to be the contact point. However, that procedure was not sufficiently accurate. We then attempted to develop a discrete means of defining the contact point by using for the wheel a "sandwich" constructed alternately of thin conducting and insulating materials. We intended to place this "sandwiched" wheel on the rail, impose a voltage across wheel and rail, and check each conductor to see which one was actually conducting. This method proved cumbersome. We then developed the method of placing a resistance wire in a groove on the tread. This latter method was suggested by Mr. I. Gitlin of the Association of American Railroads.

Calibration of Wheel Profiles

The contact position on the wheel profile is located by measuring the electrical resistance of the high resistance wire* mounted on the wheel tread surface. This measurement yields the resistance from either one of the terminals on the plexiglass wheel to the rail. Because the electrical resistance of the rail can be neglected, only the resistance of the wire is measured. The lateral position of the wheel contact point relative to the wheelset is determined by calibrating the resistance of the wire in terms of lateral distance from the tape line parallel to the wheelset centerline. The equipment set-up used to make this measurement is shown in figure 3-4.

Each wheel profile was calibrated by a two step procedure. First, points along the wheel tread surface, equally spaced at 0.05 inch intervals, were located. The resistance of the wire from each terminal to each of these equally spaced points on the wheel surface was measured using a digital VOM** capable of reading to 10^{-2} ohms. This step was done twice for each wheel profile calibrated. Excellent repeatability was obtained in all cases. The second step involved locating the points on the wheel surface relative to the wheel tape line.

*The wire used was made of nickel-chromium alloy (Nichrome V) and was 32 gauge, 0.008 in. diameter, and had a nominal resistance of 10.16 ohm/ft.

**A Data Precision digital VOM, Model 2540, was used.

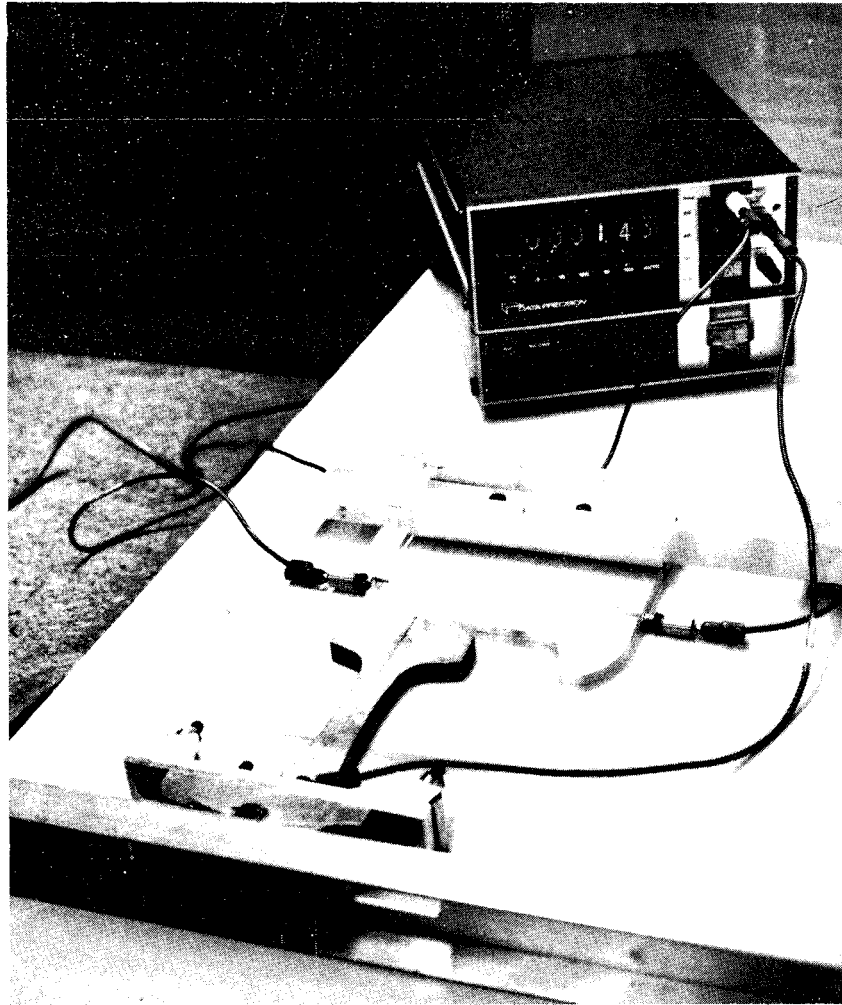


FIGURE 3-4
OPERATION OF WHEEL /RAIL PROFILOMETER

The calibration results were recorded in a table listing the resistance in ohms and distance from the tape line at each of the equally spaced points along the wheel surface. The sign convention used in this work assigned positive values to distances from the tape line to points on the field side of the wheel and negative values to distances to points on the gauge or flange side of the wheel.

Profilometer Set-Up and Alignment

The profilometer must be aligned and adjusted before beginning the contact point measurements. The rail gauge is established by setting the distance between points located on the gauge sides of the left and right rails at a distance of 5/8 inch vertically below the top of the rail. Lines were scribed accurately on an aluminum gauge bar to define the position of each rail for three rail gauges corresponding to tight, nominal, and wide gauge. The track centerline position was scribed on the bar as were the positions of the wheelset centroid and the wheel tape lines for a nominal wheel gauge. This bar was then used to set and check wheel and rail gauge and the locations of the wheelset centroid and track centerline in all cases. The rail cant was adjusted to the desired angle between the base of the rail and the horizontal reference. This angle was checked by measuring the height of each side of the rail base above the horizontal reference with calipers and then calculating the angle.

Contact Point Measurement/Wheel

Wheel contact position measurements were taken at a series of lateral positions of the wheelset. The displacement of the wheelset centroid from the track center line was established by aligning the centroid locating bar with lines on a sheet of graph paper fixed to the board holding the track assembly. Graph paper with twenty divisions to the inch provided convenient intervals of wheelset lateral displacement for these contact point measurements.

The location of the contact point on the wheel at each value of wheelset lateral displacement was determined by measuring the resistance from each terminal to the rail via the tread resistance wire, and finding the distance from the tape line to the contact position in the calibration table. The wiring diagram for this measurement is shown in figure 3-5. Measurements were made for each wheelset lateral position using both terminals. This allowed us to determine the length of the contact between the wire and the rail.

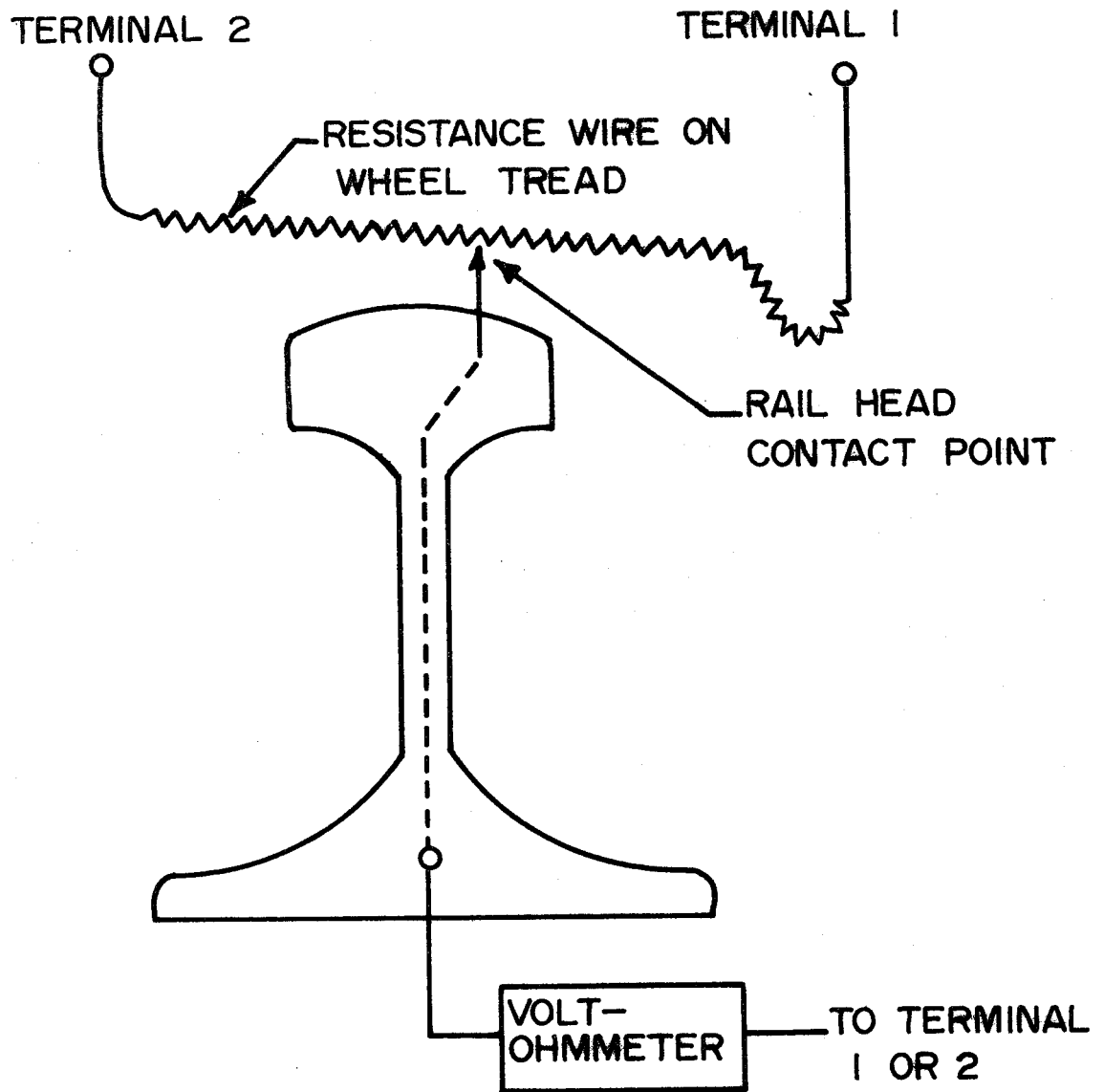


FIGURE 3-5 WIRING SCHEMATIC, WHEEL / RAIL CONTACT CIRCUIT.

Occasionally the wheel and rail contacted simultaneously at two separate points. In such a case one reading located the end point of one contact segment, and the other reading established the end point of the other contact segment. We observed that the length of each contact segment when two point contact occurs is usually very small. Therefore, the points of contact obtained from the two resistance readings should be very close to the midpoints of the contact segments.

Contact Point Measurement/Rail

The contact point on the rail head at each value of wheelset lateral displacement was determined after the contact point on the wheel was found. A square was laid against the aluminum bar of the wheelset assembly (figure 3-1) such that the edge normal to the bar was directly over the midpoint of the wheel contact "point" (the middle of the length of wheel in contact with the rail). The point of intersection of the edge of the square with the rail head surface was assumed to be the contact point on the rail. The lateral distance of this point from the rail centerline was measured with the calipers. In places of two point contact, this procedure was used to locate each point of contact on the rail.

Roll Angle Measurement

The wheelset roll angle was determined by plotting the vertical position of each wheel on a sheet of graph paper taped on the board below each wheel profile. The plotting hole provided in each wheel profile was used for this process. Initially, the wheelset was located in its centered position, and a point was plotted for the left and right wheels. If everything is properly adjusted, a straight line drawn through these points will be parallel to the horizontal reference. As the wheelset was displaced laterally, the vertical positions of each wheel were plotted on the two sheets of graph paper. The wheelset roll angle was computed from these vertical displacement records.

Experimental Error

Errors in experimental measurements made with the profilometer can be attributed to two major sources: (1) tolerances or errors in manufacturing and setting up the experimental apparatus, and (2) tolerances or errors in the measurement processes involved in using the device. The possible manufacturing and set up errors are due to the following operations:

1. Calibration of the resistance wire. This is accomplished by placing the ohmmeter probe at points along a piece of graph paper

that has been attached to the plexiglass wheel profile. The error in this calibration is due to two independent sources; location of the probe relative to the graph paper, and reading the ohmmeter. We estimate that the maximum error in each of these processes is ± 0.01 inches.*

2. Locating the wheel tape line relative to the graph paper used for the resistance wire calibration. The distance between the tape line scribed on the wheel during the manufacturing process and each of the major grid lines on the graph paper was measured and used to set up the calibration table for the resistance wire. We estimate that the possible error in this process is ± 0.01 inch.
3. Setting the wheel gauge and locating the wheelset centerline. This process requires aligning the scribed tapelines on the wheels and the scribed line on the centroid locating bar with lines scribed on a gauge bar. The gauge bar was accurately machined to tolerances of about ± 0.001 inches. The processes of locating the tape lines and centerline relative to the gauge bar are independent with maximum errors of ± 0.01 inch.
4. Setting up the rail gauge and locating the rail centerline. This process employs a gauge bar similar to that used to set rail gauge in the field. The errors in manufacturing the bar are minimal. The processes of locating each rail and placing a piece of graph paper at the centerline between the rails are independent, with estimated error bounds of ± 0.01 inch.

The errors that may be incurred during the process of using the profilometer arise in the following operations:

1. Locating the wheelset centroid relative to the rail centerline. This process involves aligning the scribed line on the centroid locating bar with grid lines on the graph paper that is attached to the table holding the rails. We estimate that the possible errors in the step are ± 0.02 inches.

*The ohmmeter specifications state that the meter accuracy is ± 0.01 ohms. The wire used has a linear resistance of about one ohm per inch. Consequently the meter reading has an error range of ± 0.01 inches.

2. Measuring the contact position. The most significant source of error in this step is due to the ohmmeter. As stated above, the possible error here is ± 0.01 inch.

In interpreting and using the data obtained with the profilometer we are interested in the uncertainty in the values of the measured contact positions, and the uncertainty in the wheelset lateral position where certain events occur, such as a jump from tread to flange contact. To obtain estimates for these two values certain assumptions must be made. We will assume that the operations that contribute to the experimental uncertainty are stochastic processes with Gaussian statistics. We will also assume that the error bounds discussed above represent 99.7% of the possible variation, and consequently can be equated to $\pm 3\sigma$, where σ is the standard deviation of the Gaussian process. The assumption will also be made that the various operations are statistically independent. With these assumptions, the following result for the sum of independent, normally distributed, random variables [3-2] will be used:

$$\sigma_s^2 = \sum_{i=1}^N \sigma_i^2 \quad (3-1)$$

where N -- number of random variables

σ_i -- standard deviation of the i th variable

σ_s -- standard deviation of the sum of n variables

The cumulative uncertainty in locating the wheelset centroid at the desired position relative to the centerline of the rails is due to uncertainties in establishing the wheelset centroid, establishing the rail centerline, and setting the wheelset centroid at the desired position relative to the graph paper that measures distances from the rail centerline. The first two operations have error bounds of ± 0.01 inches while the bound on the third operation is ± 0.02 inches. If we equate these error bounds with $\pm 3\sigma$, and employ equation 3-1 we find that the standard deviation for the combined operations is 0.0082 inches. Thus we expect that the uncertainty in locating the wheelset centroid at the desired location relative to the rails is ± 0.0246 inches.

3-2 Siddall, J. N., Analytical Decision Making in Engineering Design, Prentice-Hall, 1972, p. 43.

The uncertainty in the measurement of the wheel contact position relative to the wheelset is due to uncertainties in calibrating the resistance wire, locating the wheel tape line relative to the graph paper pasted on the wheel tread, locating the tape line of the wheel relative to the gauge bar, and measuring the contact position. Each of these operations has an error bound of ± 0.01 inches. The uncertainty of the sum of the operations, under the assumptions discussed above, is ± 0.020 inches.

These experimental error estimates should be applied to the experimental data for wheel contact positions as a function of wheelset lateral position. At a given wheelset lateral position, the estimated error in the wheel contact position measurement is ± 0.020 inches, as discussed above.

Another situation of particular interest in validating the analytical technique with the experimental results is the uncertainty in the measured wheelset lateral position where a particular event occurs, such as a jump in contact position from the wheel tread to the wheel flange. The uncertainty in the measurement of lateral position where such an event takes place is due to all the uncertainties in the operations that enter the wheelset centroid measurement, the wheel contact measurement, plus the additional ± 0.01 inch uncertainty in locating the rail at the desired position. The uncertainty for the sum of these operations, obtained using equation 3-1, is ± 0.033 inches.

PROFILOMETER EXPERIMENTAL RESULTS

Three wheel/rail configurations were investigated experimentally with the profilometer:

- (1) New wheels (figure 2-2) on New Rails (figure 2-5), nominal gauge (56 1/2 inches)
- (2) Worn wheels (profile #3, figure 2-2) on worn rails (profile A, figure 2-5), nominal gauge (56 1/2 inches)
- (3) Worn wheels (profile #3, figure 2-2) on worn rails (profile A, figure 2-5), wide gauge (57 1/2 inches)

Two data collection runs were made for each configuration over ranges of wheelset lateral displacement sufficient to reach contact positions high on the flange with corresponding large contact angles. During each run the contact point locations relative to wheel and rail were determined by the techniques described previously. The vertical position of each wheel was also determined to calculate subsequently the wheelset roll angle. The first

of each pair of runs was made with increments of 0.05 inch in lateral displacement. The second or "back up" run for each configuration was made with increments of 0.1 inches. In all cases, excellent agreement was obtained between the two runs. Plots of the experimental data together with results of the analytical procedure are presented and discussed in the section entitled "Validation" in Chapter 4.

Case 1, New Wheels/New Rails, Nominal Gauge

Results for the contact point location measurements on the right wheel relative to the wheel and rail are shown in figures 3-6 and 3-7. The values of wheelset roll angle calculated from the vertical displacement data for each wheel are shown in figure 3-8.

For this case, the contact point location on the wheel as indicated by terminal 1 was, for all practical purposes, identical to that indicated by terminal 2.

As seen on figures 3-6 and 3-7, two point contact (or a jump in the contact point from tread to flange) occurs at a wheelset lateral displacement of about 0.3 to 0.35 inches. The maximum difference in the location of the point of contact on the wheel for the two data runs was about 0.025 inches, while the maximum difference between the two runs for the location of the contact point relative to the rail was also about 0.025 inches. The average of the differences for the two data runs for the wheel contact point was +0.0046 inches while the average for the rail was -0.0029 inches.

The values of wheelset roll angle calculated from the vertical displacement data for each wheel are shown in figure 3-8. The maximum difference in calculated roll angle between the two data runs is about +0.00070 radians and the average difference is about +0.00019 radians.

The profilometer set-up for this case was checked after the data collection process. The averages of three measurements for the cant angles for the right and left rails of the profilometer were 0.026 and 0.025 radians, respectively. The cant angle for the right rail was 4% greater than the nominal of 0.025 radians. The slopes of the straight tapered sections of the wheel profile relative to the axle centerline on the profilometer were also checked. These were 0.049 and 0.047 for the right and left wheels, respectively. Thus, the actual values of the taper ratios of the right and left wheels were 2% and 6% less than the nominal value of 0.05. Wheel gauge and rail gauge were at nominal values as checked with the gauge bar.

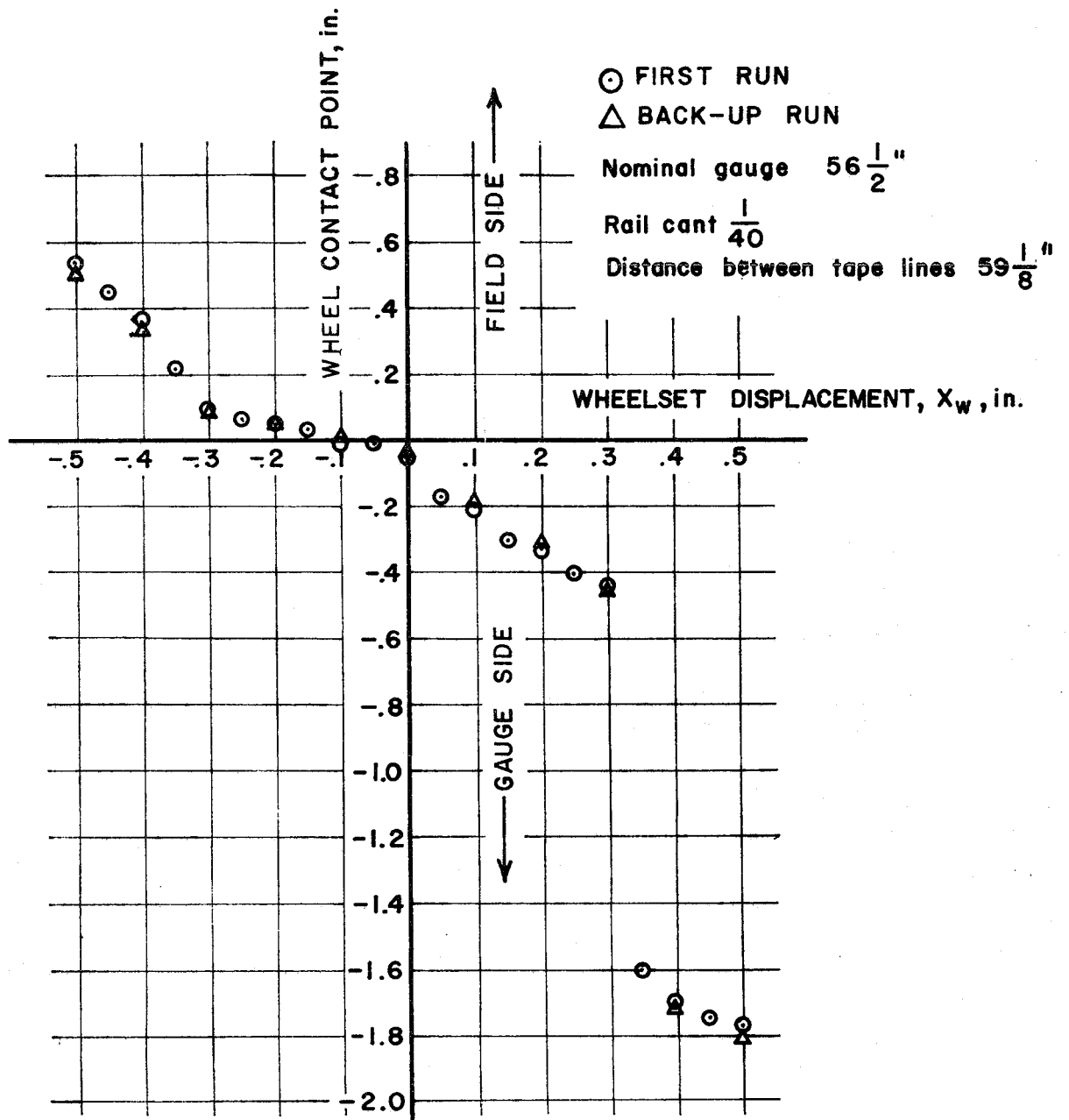


FIGURE 3 - 6 , EXPERIMENTAL WHEEL CONTACT POINT LOCATION vs. WHEELSET DISPLACEMENT
 NEW WHEEL / NEW RAIL

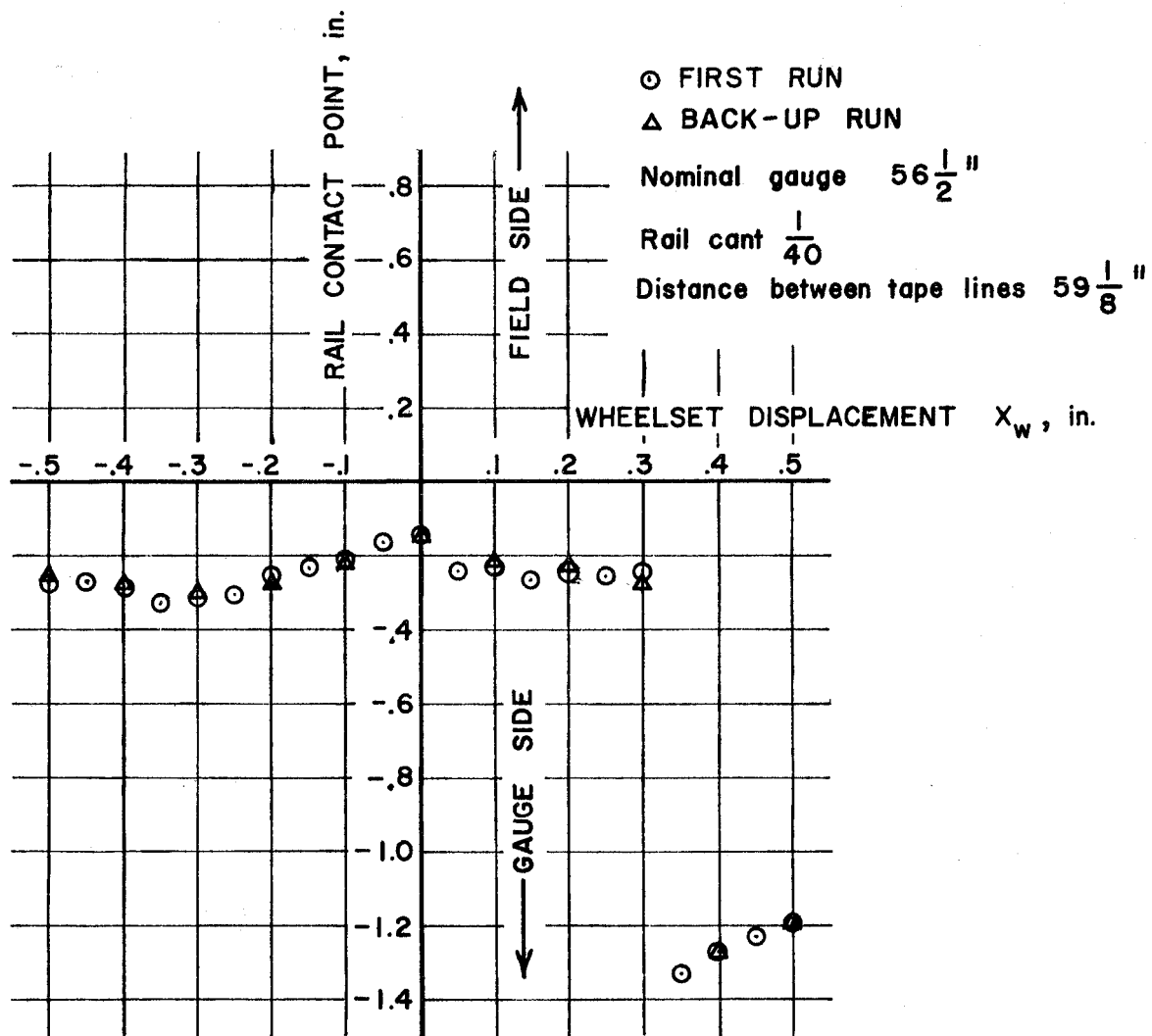


FIGURE 3 - 7 , EXPERIMENTAL RAIL CONTACT POINT
 vs. WHEELSET DISPLACEMENT
 NEW WHEEL / NEW RAIL

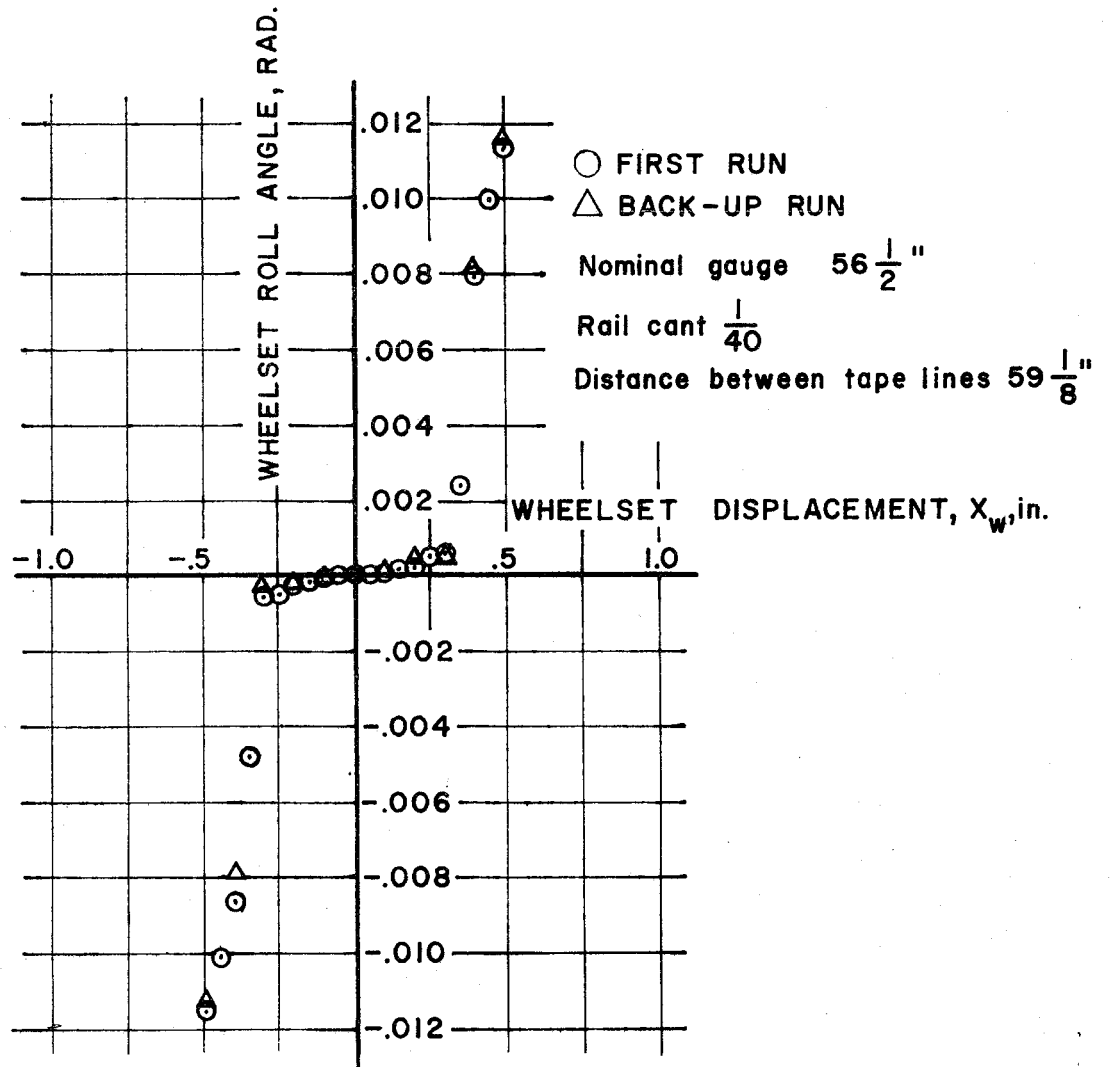


FIGURE 3 - 8 , EXPERIMENTAL WHEELSET ROLL ANGLE vs. WHEELSET DISPLACEMENT NEW WHEEL / NEW RAIL

Case 2, Worn Wheels/Worn Rails, Nominal Gauge

The experimental results for contact point locations relative to wheel and rail (for the left wheel) and wheelset roll angle are shown in figures 3-9, 3-10, and 3-11 for this case.

In this case (and for the wide gauge case) there was usually a non-zero length of wire over which contact was indicated. The maximum value of this length was on the order of 0.1 to 0.2 inches. There was a jump in the contact point location across the middle of the tread region at a wheelset lateral displacement of about -0.35 to -0.40 inches. Subsequently, there was a jump from tread to flange contact at a wheelset displacement of about -0.45 to -0.50 inches. During the back-up data run, the resistance wire separated from the wheel tread over a small region. Consequently, data for values of wheelset lateral displacement of -0.1 and -0.2 inches are considered invalid*.

Averages of the terminal readings were calculated to give a "mid-point" for the contact region on the wheel. The maximum difference in this value for the wheel contact region "mid-point" for the two data runs was -0.010 inches while the average difference was about -0.0036 inches. The maximum difference in the rail contact point location for the two runs was 0.013 inches while the average difference was 0.005 inches. For the calculated wheelset roll angle, the maximum difference for the two data runs was 0.0007 radians; the average difference was -0.00014 radians.

We checked the profilometer set-up after the data runs. Wheel and rail gauge were at nominal values as measured by the gauge bar. The average of two measurements for the cant angle of right and left rails indicated that the cant angle was the nominal 0.025 for each rail. The difference in the angle of inclination of the right and left wheels relative to the axle centerline was 0.0024 radians (or 0.1375 degrees).

Case 3, Worn Wheels/Worn Rails, Wide Gauge

The experimental results for contact point locations relative to wheel and rail (for the left wheel) and wheelset roll angle are shown in figures 3-12, 3-13 and 3-14.

*The separation of the wire from the tread occurred occasionally if the wheelset was not handled carefully. In all previous instances, we had to re-do the entire calibration procedure as well as the actual data collections after re-fastening the wire to the tread.

FIRST RUN

○ Terminal 1

△ Terminal 2

BACK-UP RUN

□ Terminal 1

◇ Terminal 2

Nominal gauge $56 \frac{1}{2}$ "

Rail cant $\frac{1}{40}$

Distance between tape lines $59 \frac{1}{8}$ "

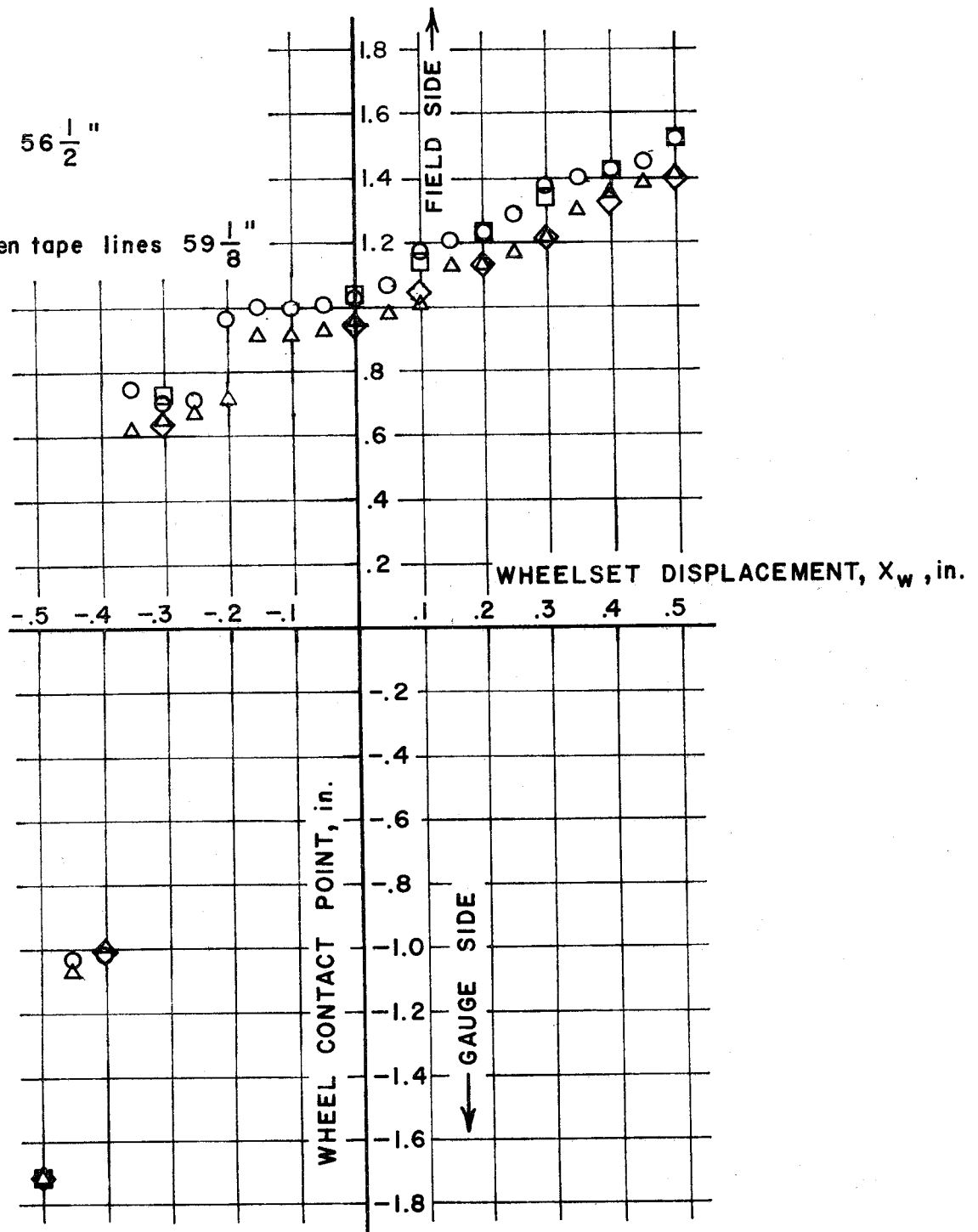


FIGURE 3-9 , EXPERIMENTAL WHEEL CONTACT POINT vs. WHEELSET DISPLACEMENT WORN WHEEL / WORN RAIL

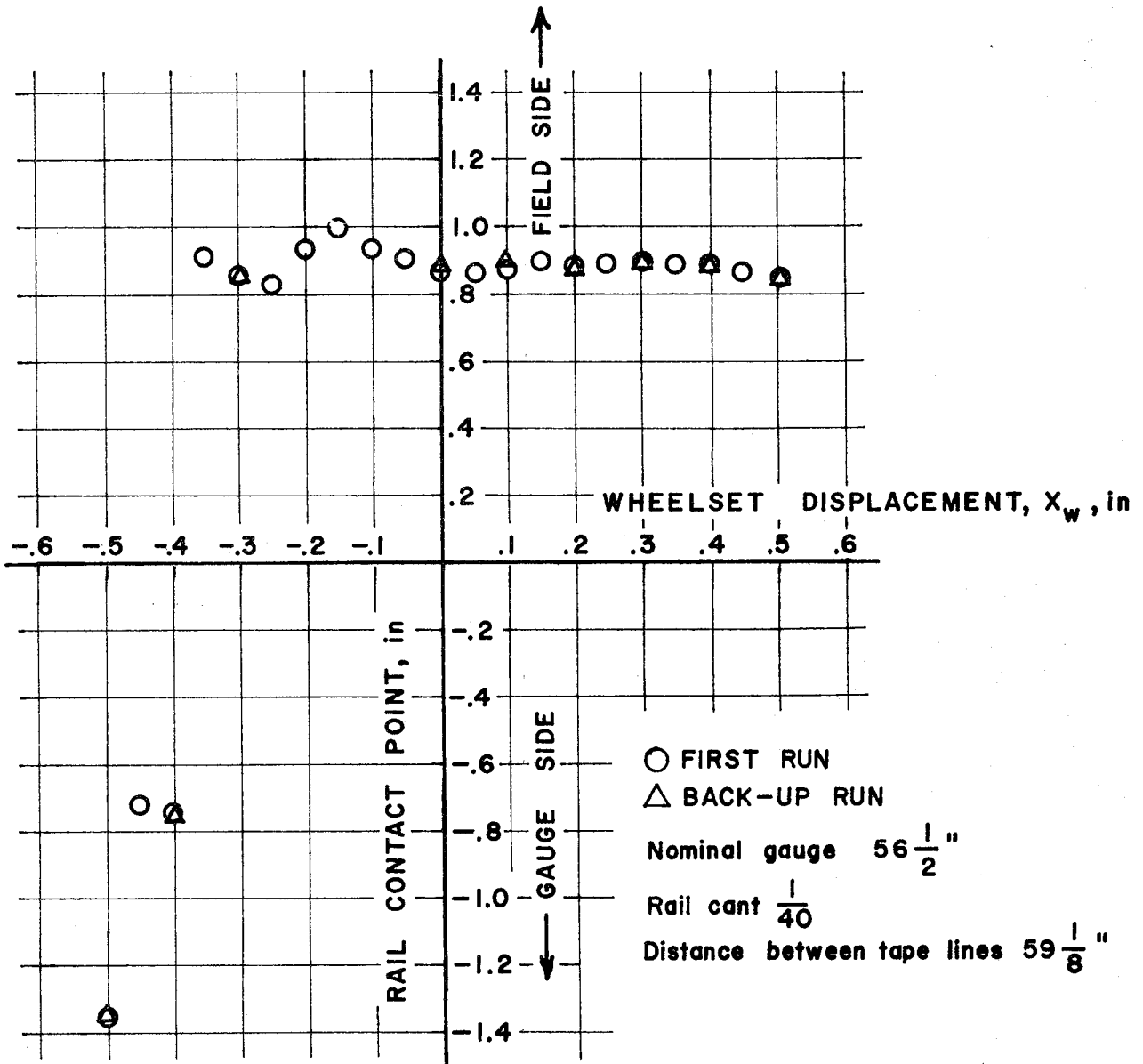


FIGURE 3-10, EXPERIMENTAL RAIL CONTACT POINT
 vs. WHEELSET DISPLACEMENT
 WORN WHEEL / WORN RAIL

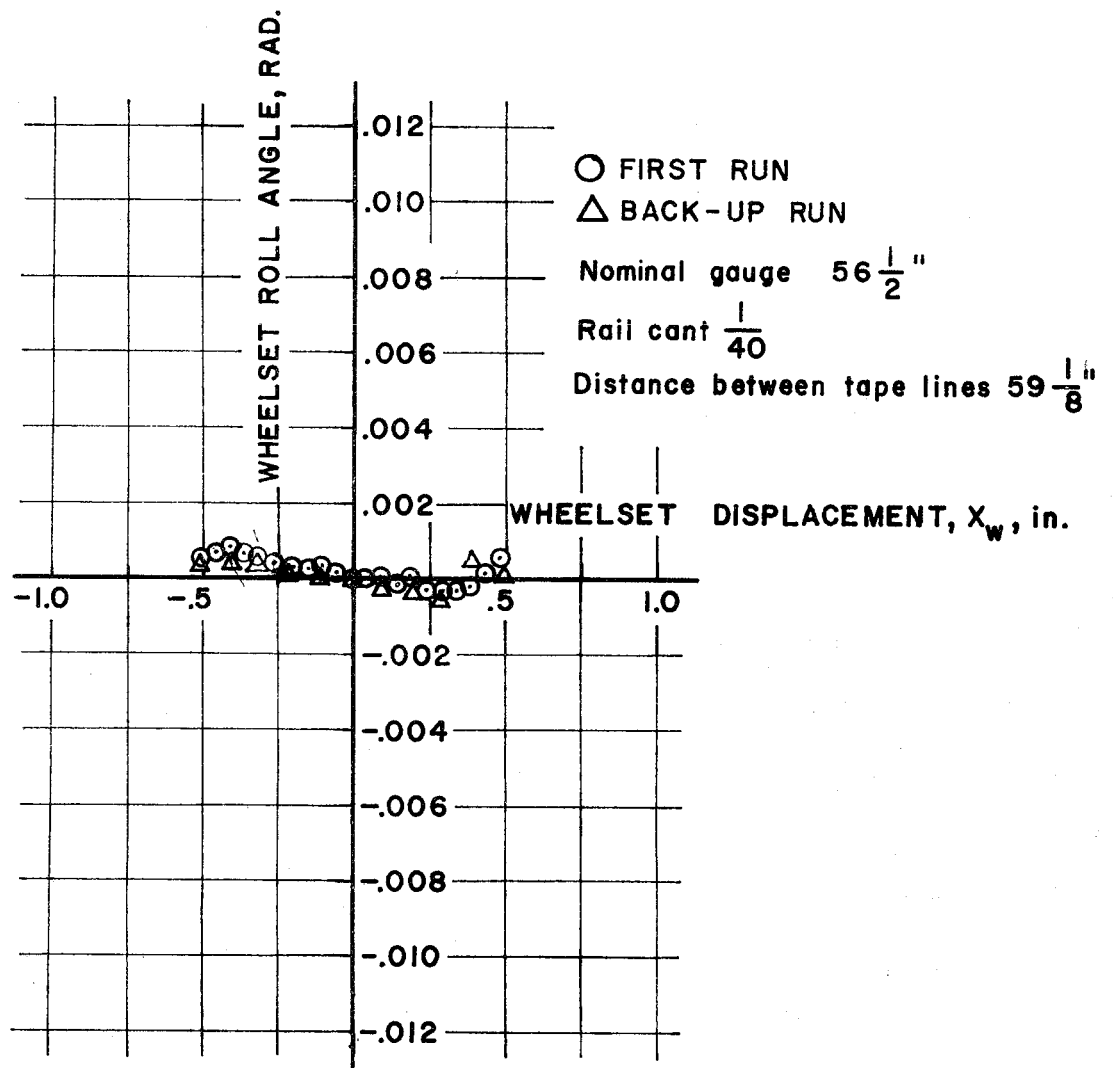


FIGURE 3-11 , EXPERIMENTAL WHEELSET ROLL
 ANGLE vs. WHEELSET DISPLACEMENT
 WORN WHEEL / WORN RAIL

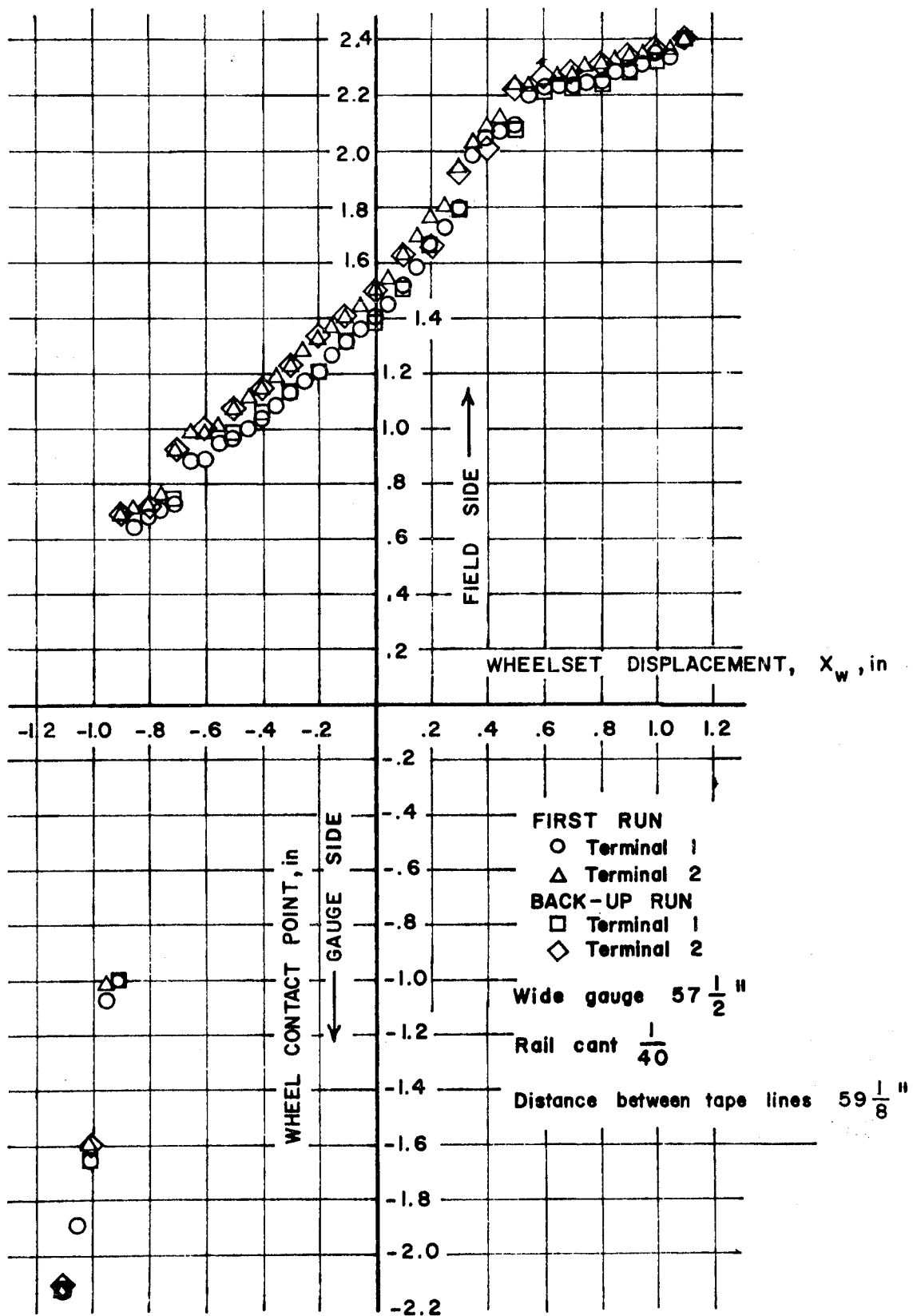


FIGURE 3-12 , EXPERIMENTAL WHEEL CONTACT POINT vs. WHEELSET DISPLACEMENT WORN WHEEL / WORN RAIL

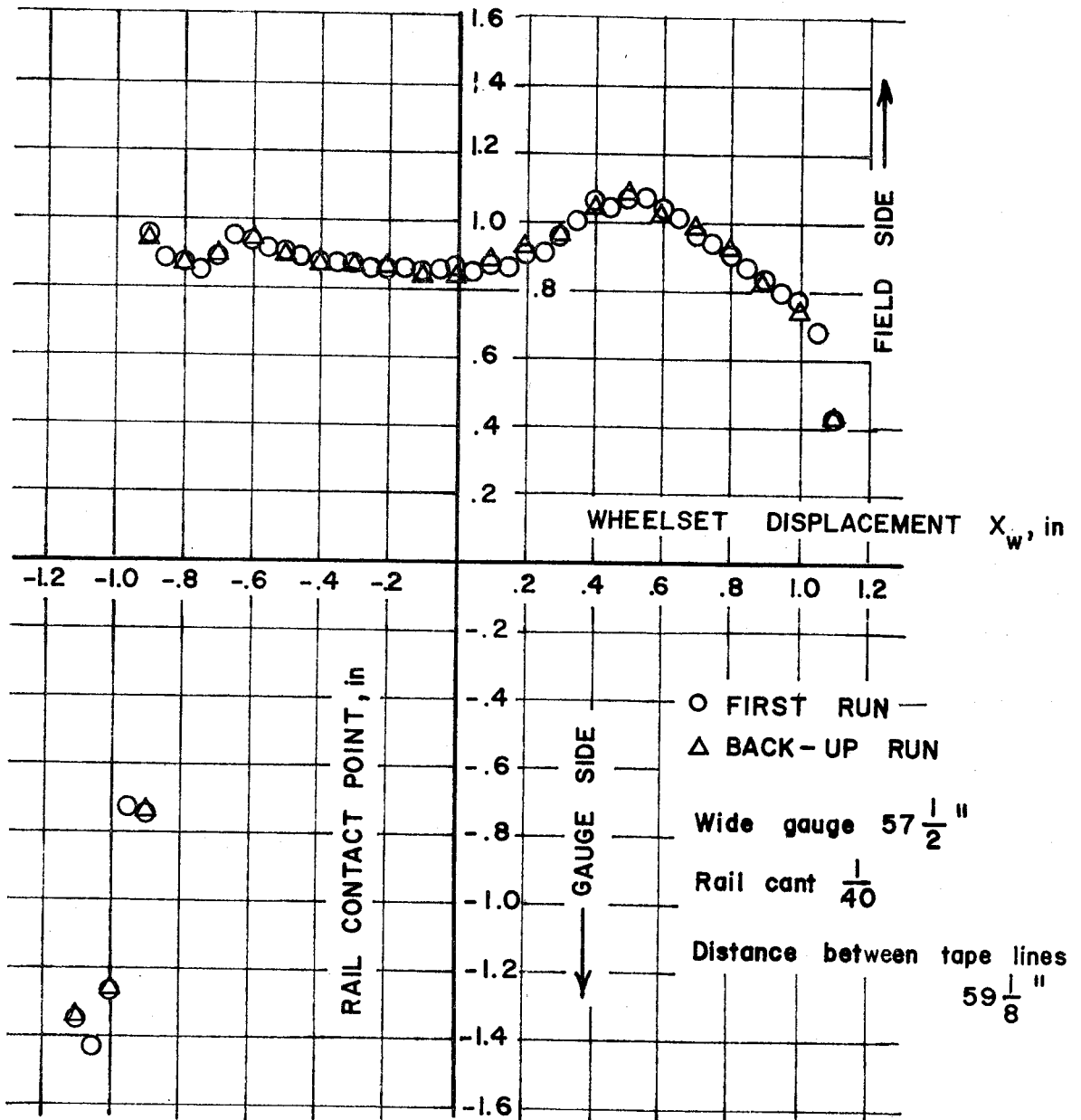


FIGURE 3-13 , EXPERIMENTAL RAIL CONTACT POINT vs. WHEELSET DISPLACEMENT WORN WHEEL / WORN RAIL

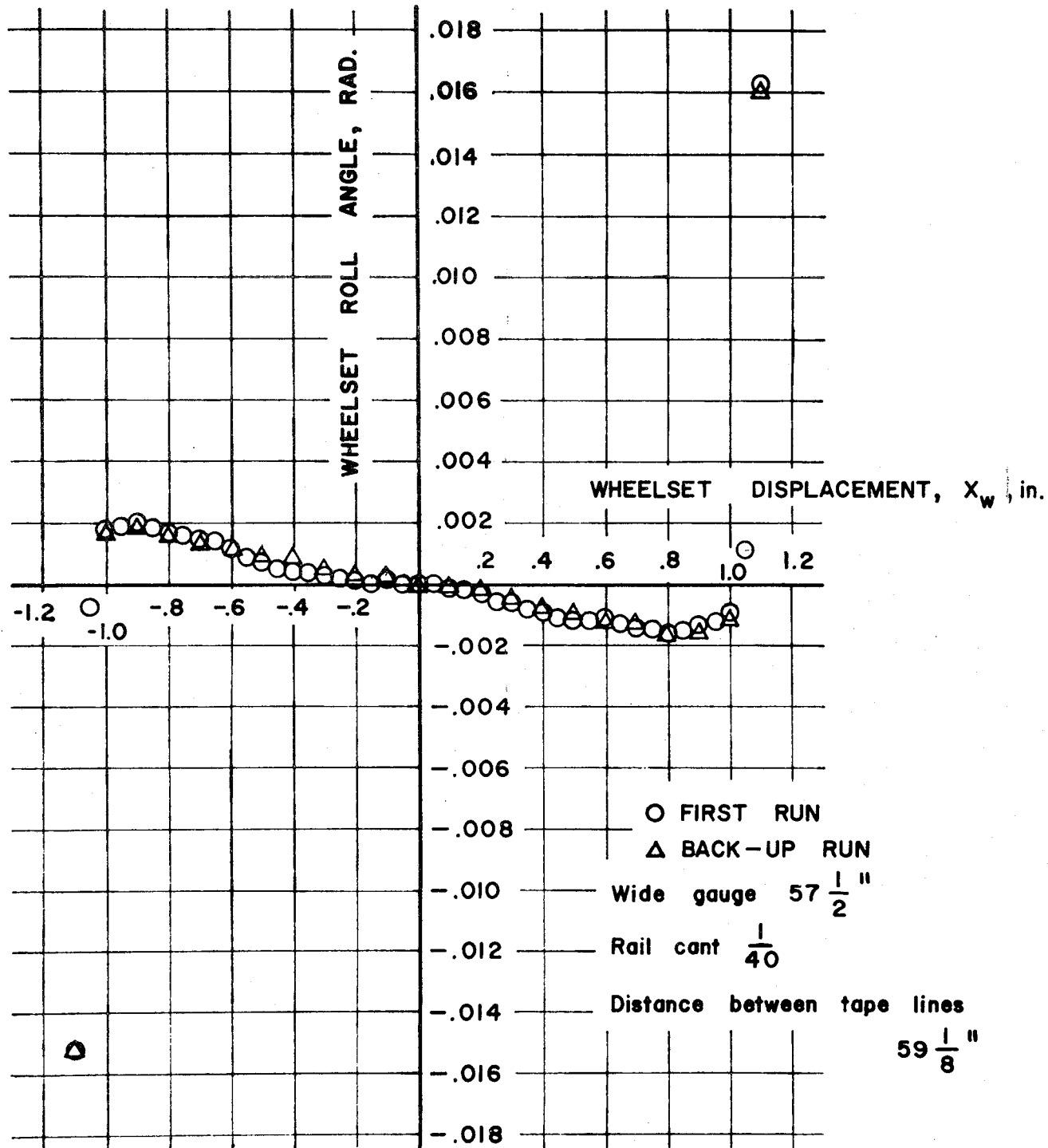


FIGURE 3-14, EXPERIMENTAL WHEELSET ROLL ANGLE vs. WHEELSET DISPLACEMENT WORN WHEEL / WORN RAIL

Again, contact usually occurred over a short length (0.1 to 0.2 inches) of wire. A jump in contact point location across the middle of the tread occurred at a wheelset lateral displacement of about -0.9 to -0.95 inches. As might be expected, the locations of the contact points on the wheel and rail for this jump were the same for the nominal and the wide gauge cases. With a larger displacement of the wheelset from the track centerline (-0.95 to -1.0 inches), there is a jump in contact from the tread to the throat of the flange.

As for the previous case, averages of the terminal readings were calculated to give a "mid-point" of the contact region on the wheel for each data run. The maximum difference in this value for the two data runs was 0.016 inches while the average difference in this value for the two runs was 0.001 inches. The maximum difference in the rail contact point location for the two runs was +0.02 inches while the average difference was -0.004 inches. The maximum difference between the two runs in the values for calculated wheelset roll angle was -0.0005 radians while the average difference was -0.00002 radians.

GRAPHICAL TO DIGITAL PROFILE DATA CONVERSION

We anticipated evaluating many combinations of wheel and rail profiles in this study as well as future studies. To facilitate these evaluations, we needed a fast and accurate method for obtaining tabular data for the wheel and rail profile coordinates. To our knowledge, the only methods currently used by the railroad industry to measure wheel and rail profiles record these data in graphical form. The interactive computing process described below converts these data from graphical to digital form. The slopes of the wheel and rail profiles are also determined in this process.

After making the plexiglass models of the wheel profiles to be used in the experimental procedure, the profiles of the plexiglass models were traced carefully as were the actual rail sections. A pair of reference points were drawn on each traced profile and the profile was photographed and enlarged about two or three times. Care was taken to minimize distortion during the photographic process.

To obtain tabular data from the enlarged profiles, the DEC VWO1 Sonic Digitizer/Writing Tablet of the Clemson Engineering Computer Laboratory was used. The sonic digitizer consists of an 11 inch square "tablet" and a pen. When the pen tip is pressed on the tablet, a microswitch is closed triggering

a spark that jumps a gap at the tip of the pen. A picture of this process is shown in figure 3-15. The tablet is equipped with a row of microphones along both the horizontal and vertical edges. The position of the pen on the tablet is determined by measuring the time required for the sound of the spark to reach the microphones. Data are recorded by moving the pen along the profile and pressing down the pen at each desired point. The software incorporated with the digitizer associates integer pairs between 0 and 1024 with the x and y coordinates of the data points. The advantage of using the sonic digitizer for obtaining tabular data for the wheel and rail profiles is that it is quick, reliable, and accurate. However, the accuracy depends on (a) the accuracy with which the operator places the pen, and (b) the degree of enlargement of the profile to be traced on the digitizer.

An interactive computing procedure was developed to minimize the error in the digitizing process. The flow chart describing this interactive computing procedure is shown in figure 3-16. This procedure is implemented on the EAI-680/PDP-15 hybrid computer of the Clemson Engineering Computer Laboratory. The program MAIN controls the digitizing process. The first of the three loops comprising MAIN calls the subroutine POINTS. Using digitizer software, POINTS takes the x and y coordinates of the profile as they are fed in by the operator. These coordinates are then displayed on the cathode ray tube video display of the VT-15. If there are gross errors between the displayed points and the enlarged profile, the operator has the option of repeating the data collection process. This is a visual check which allows the correction of gross errors in the placement of the pen.

The second loop in MAIN scales the profile data back to the original dimensions of the profile. The first two points that are fed in by the operator are the two reference points marked on the original profile. This information is used to obtain the scale factor between true (unenlarged) distance and the measured (enlarged) distance between the points. The integer pairs of x and y profile coordinates are then converted to true coordinates in inches and transferred back to MAIN. MAIN then calls ACTREF to transfer these coordinate pairs to a standard coordinate system.

The second loop in MAIN also converts the profile data to a standard coordinate system. The axes of the standard coordinate system for the wheel profile are parallel and normal to the axle centerline with the origin at the

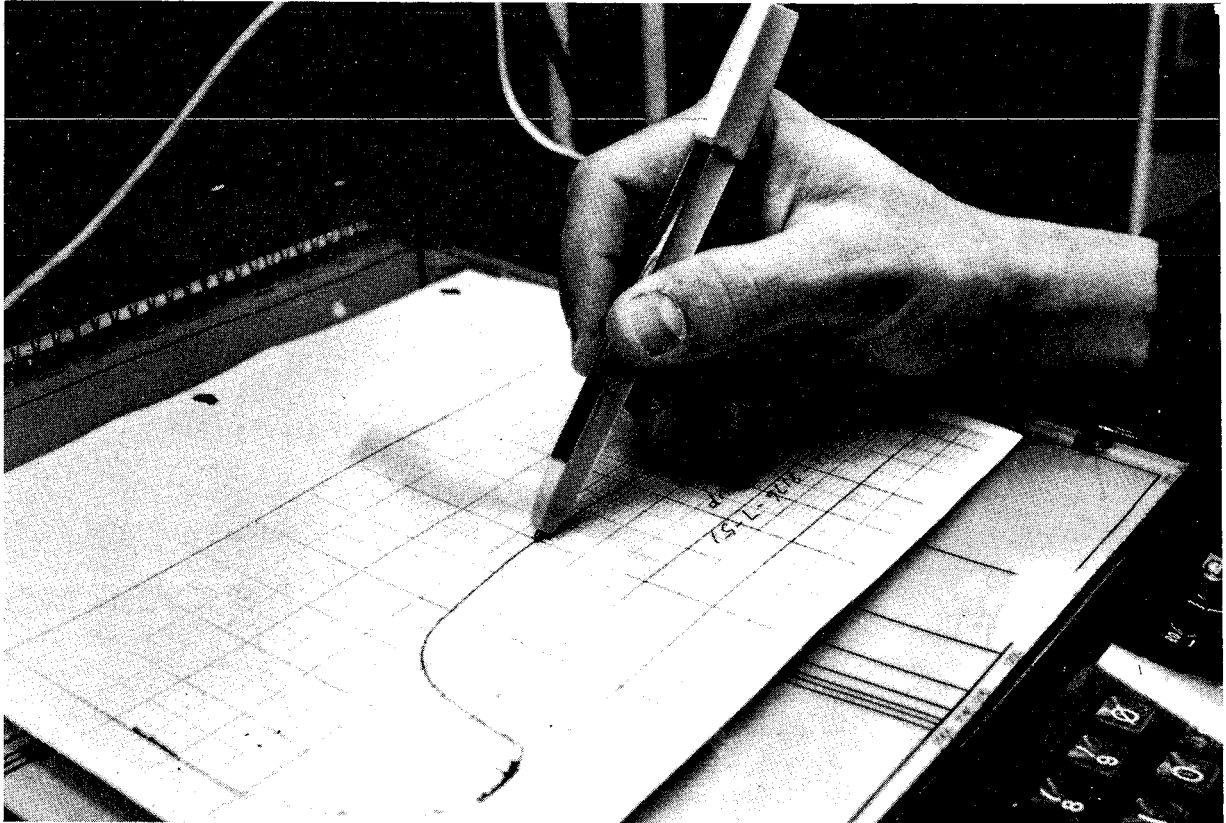


FIGURE 3-15
WHEEL PROFILE MEASUREMENT PROCEDURE
USING SONIC DIGITIZER

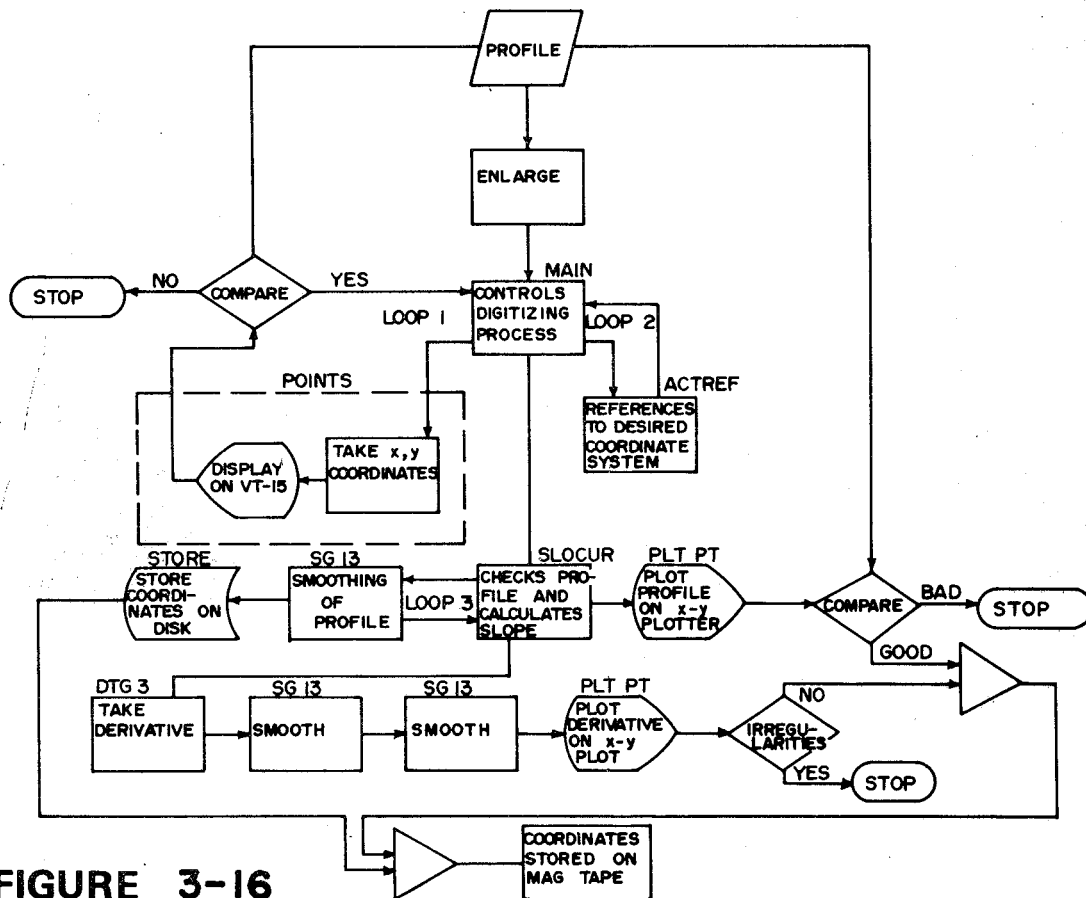


FIGURE 3-16
FLOW CHART OF PROFILE MEASUREMENT PROCEDURE

intersection of the axle centerline and the wheel tape line. For the rail profile, the axes of the standard system are parallel and normal to the base of the rail with the origin at the intersection of the base with the rail section centerline. After obtaining the coordinate pairs referenced to the standard system, the coordinates are transferred back to MAIN.

The third loop in MAIN checks the profile coordinates and stores them on disk. This subroutine, SLOCUR, initially smooths the profile using the subroutine SG13 from the IBM Scientific Subroutine Package. SG13 fits a least squares linear approximation to three points at a time, and evaluates the function at the center point. The process is repeated after shifting down the input array one point until the entire input array is traversed. SLOCUR stores the array of smoothed coordinates in a named file on disk using the subroutine STORE.

The second step of SLOCUR is to plot the smoothed profile on the xy plotter using the hybrid interface and PLTPT. This plot is actual size and may be compared visually with the original profile to check for accuracy. If the operator finds that the plot does not match the original profile sufficiently well, the job is started over and a new data set is taken.

In the third step of SLOCUR, the smoothed profile is re-checked for smoothness by calculating and plotting the slope of the smoothed profile. This is done using the subroutine DGT3 from the IBM Scientific Subroutine Package. DGT3 fits the Lagrangian interpolation polynomial of degree two to three successive points in the input array and evaluates the derivative at the middle point. It repeats this operation after shifting down the input array point by point until the entire array is traversed. The resulting array of derivative values is then smoothed twice using SG13. The smoothed array of derivative values is plotted on the xy plotter using PLTPT. This plot is examined visually to check for major irregularities such as abrupt changes in slope on a smooth section of the profile. If none are found, the array of profile coordinates is considered acceptable and is transferred from disk to magnetic tape for later use.

A potential source of error that was noticed during this procedure was associated with the recording of the reference points on the wheel profile. The first two points recorded by the Sonic digitizer were the two reference points. Slight errors in the placement of the sparking pen could result in a rotated and displaced reference axis system, and hence a rotated and displaced set of wheel profile data points. We will refine this procedure to minimize this

possible source of error. A proposed approach is to record each reference point several times with the sparking pen and take the average x and y coordinates of the recorded points as the reference point.

WHEEL/RAIL GEOMETRIC CONSTRAINTS

We wished to compute the wheel/rail geometric constraint relations for the differences in rolling radii and contact angles using the experimentally determined contact point data and the data for rolling radius versus distance from the tape line obtained by the graphical to digital profile data conversion procedure. The process for computing these constraint relations, which is described in this section, is similar to that used in the analytical procedure described in Chapter 4 once the contact points are found by analytical means. Having calculated the differences in rolling radii and contact angles using experimental contact point data, and having measured wheelset roll angle, we could compare experimental and analytical results. This comparison or validation process will be discussed in Chapter 4.

The determination of the wheel/rail geometric constraint relations is performed using a program written in FORTRAN for the IBM 370 Computer. The flow chart for this program is shown in figure 3-17. The program MAIN controls the process. The input data to MAIN are comprised of tabular data for (a) the wheel rolling radius versus distance from the tape line, and (b) the wheel contact point distance relative to the tape line versus wheelset lateral displacement. The former data are those obtained during the process described in the section, "Graphical to Digital Profile Data Conversion". The latter are those obtained in the process described in the section, "Contact Point Measurement/Wheel".

MAIN is comprised of three loops. The first loop is the subroutine CONANG. In CONANG the wheel profile radius array is first smoothed using the subroutine SG13, a subroutine from the IBM Scientific Subroutine Package. This is the second time the profile data are smoothed as they are also smoothed during the process of profile measurement. The slope at each point on the profile is calculated using the subroutine DGT3 from the IBM Scientific Subroutine Package. The array of slope data is then smoothed twice using SG13. The resultant data arrays for rolling radius and slope (or contact angle) as functions of distance from the tape line are transferred back to MAIN.

The experimental data for the lateral position relative to the tape line of the wheel contact points versus wheelset lateral displacement are related to the wheel profile and slope data to obtain the desired kinematic parameters.

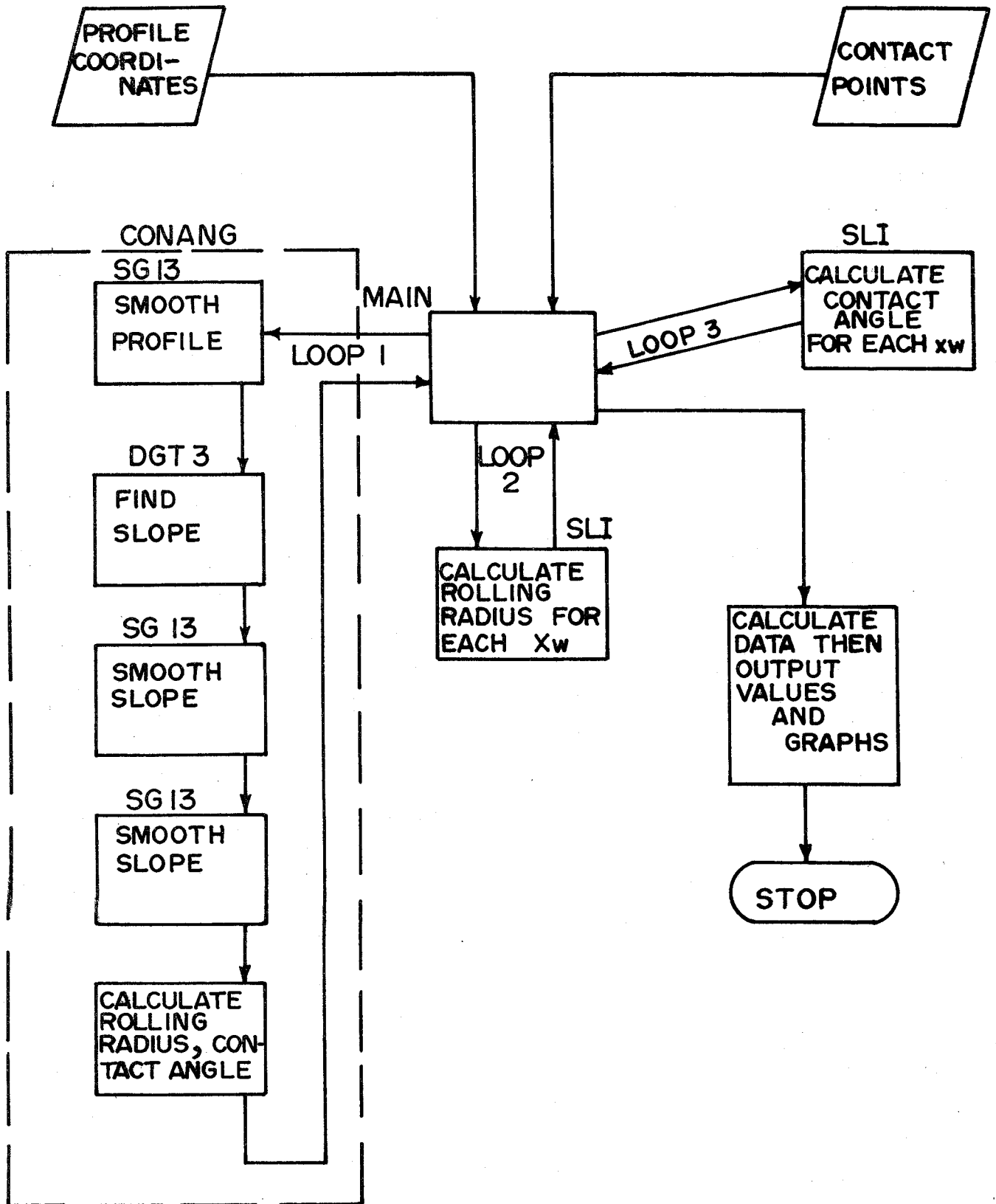


FIGURE 3-17 FLOW CHART FOR COMPUTING WHEEL/RAIL CONSTRAINT RELATIONSHIPS.

This process is performed in loops 2 and 3 of MAIN. In loops 2 and 3, at each lateral wheelset displacement the distance of the wheel contact point from the tape line is used as the input argument of the linear interpolation routine SLI to obtain the corresponding wheel rolling radius and slope from the appropriate data arrays. The end results are tables of wheel rolling radius and contact angle versus wheelset lateral displacement. The desired kinematic parameters involving the differences of rolling radii and the sums and differences of the contact angles of left and right wheels versus wheelset lateral displacement are obtained as follows. For the symmetrical wheel and rail profiles used in the experimental procedure,

$$r_L(x_w) = r_R(-x_w) \quad (3-2)$$

and,

$$\delta_L(x_w) = \delta_R(-x_w) \quad (3-3)$$

Thus,

$$r_L(x_w) - r_R(x_w) = r_L(x_w) - r_L(-x_w) \quad (3-4)$$

$$\delta_L(x_w) - \delta_R(x_w) = \delta_L(x_w) - \delta_R(-x_w) \quad (3-5)$$

$$\delta_L(x_w) + \delta_R(x_w) = \delta_L(x_w) + \delta_L(-x_w) \quad (3-6)$$

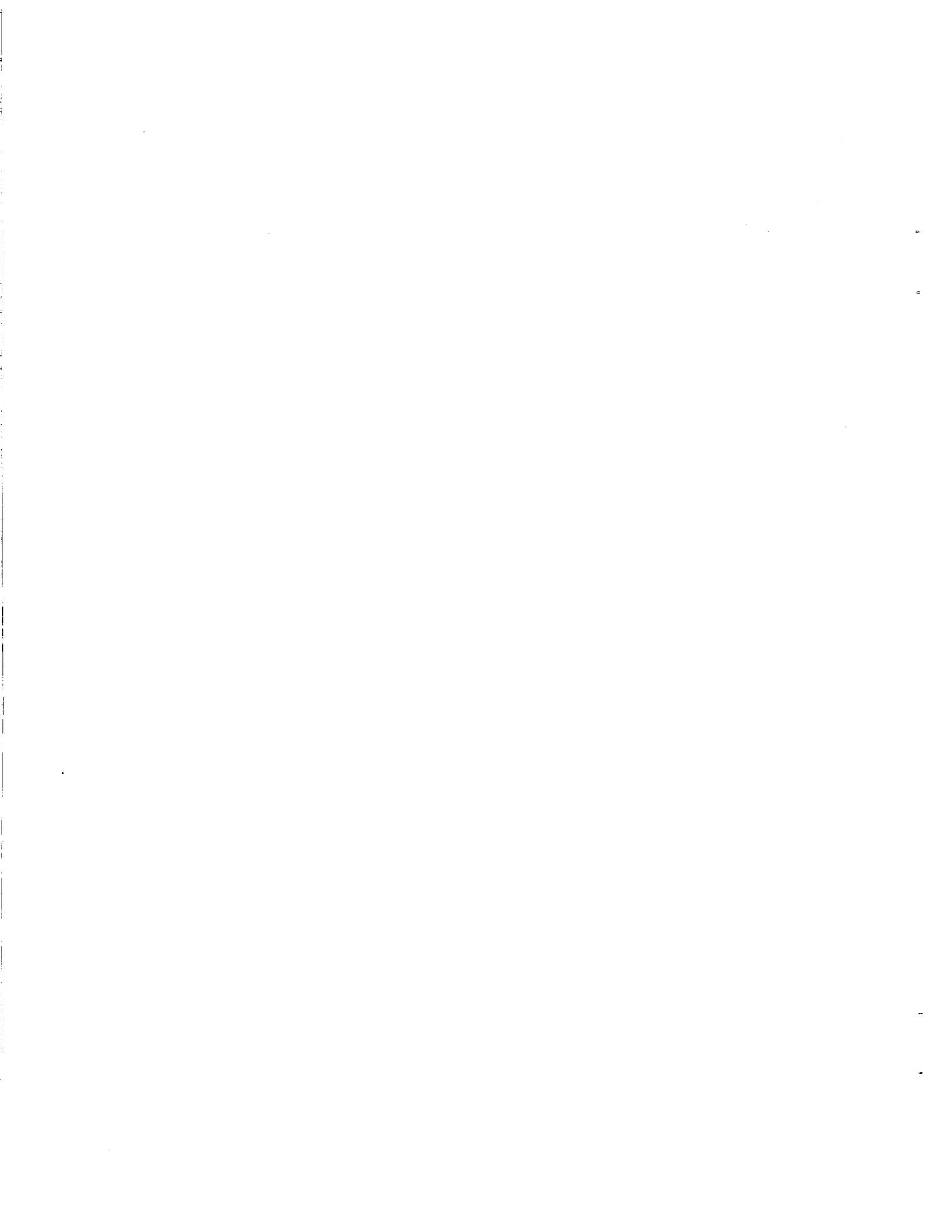
CONCLUSIONS

A full-scale, experimental apparatus consisting of a two-dimensional model of a wheelset on a pair of rails was developed to determine wheel and rail contact points versus wheelset lateral displacement. Measurement techniques were developed that gave repeatable and accurate contact point data.

The experimental determination of the wheel/rail contact points was a successful process. However, it was also a very time-consuming process that required the operator to use a very careful measurement technique for best results. Consequently, we feel that the primary utility of the experimental apparatus and associated procedures is as a validation for analytical processes. As will be described in Chapter 4, the experimental data we developed was used to validate the analytical techniques.

An interactive computing procedure was developed and used to obtain digital profile data from graphical representations of these profiles. This digital profile data may then be used in digital computer programs to determine the wheel/rail geometric constraint relationships. The full efficiency of this conversion procedure is realized when many (rather than one or two)

profiles are to be analyzed. We will make improvements in the accuracy of this procedure. However, in order for these results to be meaningful, the graphical profile data must be accurate. This is not always the case. Thus, we see a need for an accurate wheel and rail head profile recorder that can also accurately reference the profile being measured to the opposite wheel or rail. This is required because the resulting wheel/rail constraint relationships are the result of two wheels moving together over two rails. The diameter of each wheel, the wheel gauges and the inclination of each profile to the axle centerline must be measured at the same time the wheel profiles are recorded. Similarly, the cant angle of each rail and the gauge must be recorded at the same time that the rail profiles are recorded. Devices that perform such measurements have been developed in Europe. These are described briefly in Chapter 1.



CHAPTER 4
ANALYTICAL RESEARCH

INTRODUCTION

This chapter deals with the analytical aspects of our wheel/rail research effort. The procedures developed to determine the desired wheel/rail geometric constraint relationships for arbitrary wheel and rail head profiles and the validation of these procedures are discussed here.

The objective of this analytical effort was to develop a mathematical means of determining the wheel/rail geometric constraint relationships. Such an analytical model provides a means of calculating the relationships listed below for a variety of wheel and rail profiles without the limitations imposed by the experimental approach such as model construction costs, time consuming measurement processes, etc.

The analysis was implemented in the form of a digital computer program. The program is documented in Appendix A. This program accepts tabular data for the wheel and rail profiles, and computes the contact points and wheel/rail constraint relationships as functions of wheelset lateral position. Describing functions or quasi-linearizations of the resulting relationships are calculated within the computer program.

The variables desired as functions of wheelset lateral displacement are the following:

- (1) Rolling radii of the wheels
- (2) Contact angles between contact plane and axle centerline
- (3) Roll angle of the wheelset with respect to the rail plane
- (4) Difference in rolling radii
- (5) Difference in contact angles

The functional dependence of the contact positions and the constraints described above on the wheelset yaw position was not computed because wheelset yaw has a very weak influence on these variables.

APPROACH

The approach we took to modeling the rail/wheel geometry can be broken down into the following steps:

- (1) Formulation of mathematical descriptions of the rail and wheel profiles using a series of fourth order polynomials over sub-intervals of the profile.
- (2) Calculation of the locations of the contact points.
- (3) Calculation of the desired parameters using the contact point locations and the polynomial descriptions of the wheel and rail profiles.
- (4) Computation of describing functions, or quasi-linearizations of the resulting relationships.

Our approach to describing mathematically the wheel and rail profiles involved fitting a series of fourth order polynomials to the tabular wheel and rail data. Curve-fitting was used rather than interpolation between the data points because it provided some numerical smoothing of irregularities in the input data. The polynomials also allowed easy calculation of the slopes of the profiles. A series of fourth order curves was used rather than fewer higher order curves or a different function because of the reduced complexity of calculations necessary to manipulate polynomials of only fourth order.

We calculated the contact point locations by applying a numerical search procedure to find the points that satisfied the following definition of a contact point:

- (1) Position equation -- a contact point on the wheel occupies the same point in space as the corresponding contact point on the rail.
- (2) Rigid body constraint -- the wheel profile cannot penetrate into the rail profile and,
- (3) Slope constraint -- the profiles are tangent at the contact points.

These requirements, when combined, identify the location of the contact points at any wheelset lateral position as those points where the difference between the wheel profile height above a datum and the rail profile height above the

same datum is at a minimum. An iterative search process was used to find the points where this minimum occurred, and thus satisfied the contact point definition at each wheelset lateral position.

Another method of solution for the contact point locations was tried and used successfully. This consisted of writing the equations requiring the profiles to be tangent at the contact and for the contact points on the wheel and rail to occupy the same point in space. These nonlinear algebraic equations were solved numerically using a Newton-Raphson scheme. The scheme, however, was later discarded due to problems associated with the requirement for a "sufficiently close" initial approximation to the contact point locations. If the initial approximation was not sufficiently close, the numerical procedure would converge to a false solution or yield no solution at all. This problem was encountered every time the contact point location jumped. The search procedure described above does not encounter problems of this type because it is based on approximating the wheelset roll angle, which is a continuous function.

The geometric constraint relationships were computed by substituting the profile equations and the computed contact point locations into the defining equations for the constraint relationships on a point-by-point basis. For example, the rolling radius of a wheel at a specified wheelset lateral displacement was found by substituting the contact point location into the corresponding wheel profile equation, a fourth order polynomial in the appropriate interval, to obtain the rolling radius at the given contact location.

Quasi-linear descriptions were needed for some of the wheel/rail geometric constraint relationships. The describing function technique with a sinusoidal input was used to compute quasi-linear functions for the difference in rolling radii, the difference in contact angles, and the wheelset roll constraints.

COMPUTATIONAL PROCEDURE

The computational procedures for this wheel/rail contact analysis were programmed in FORTRAN. This discussion summarizes the computational steps of that computer program. A detailed description of the program logic and a Users' Manual are provided in Appendix A.

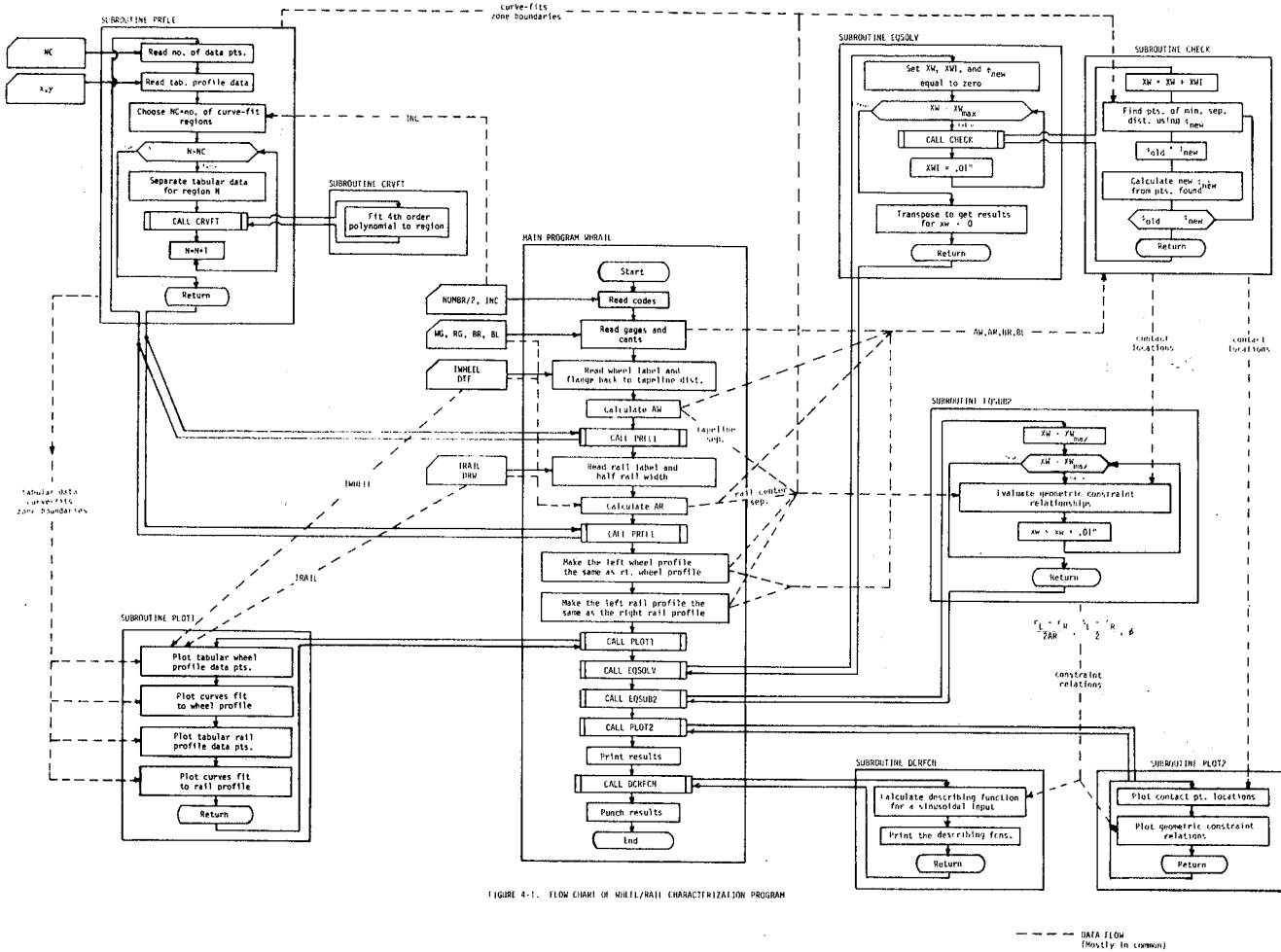


FIGURE 4-1. FLOW CHART OF WHEEL/RAIL CHARACTERIZATION PROGRAM

Fig. 4-1 WHEEL/RAIL CHARACTERIZATION PROGRAM
(FLOW CHART)

The computer program is written to analyze the contact geometry for a symmetric wheelset on symmetric rails, i.e., identical wheel and rail profiles on the left and right, and equal rail cant angles on both rails. The program, however, will be modified in the near future to analyze asymmetric wheelsets and rails.

A flow chart of the program logic and information flow is shown in Figure 4-1. The main program, WHRAIL, controls data input and output and calls the subroutines that carry out the computational steps of the procedure. Subroutine PRFLE reads the digital wheel or rail profile data and fits a series of fourth order polynomials to the profile data. Subroutines EQSOLV and CHECK perform the iterative computations to determine the wheel and rail contact points at each wheelset lateral position. Subroutine EQSUB2 computes the geometric constraint functions with the curve fit and contact position data. Describing functions for the geometric constraint functions are computed in Subroutine DCRCFN. Plotting of input, curve fit, contact position and geometric constraint data is done by subroutines PLOT1 and PLOT2.

The first step in the program involves fitting fourth order polynomials to the data points for the wheel and rail profiles. In addition to the tabular wheel and rail profile data, codes specifying the size of regions to be curve-fitted and the amplitude of wheelset lateral displacement allowed, wheel and rail gauge, and the rail cant are inputs to the program.

The main program calls Subroutine PRFLE to carry out this step. PRFLE reads the profile data and separates the data into sets of data points, where the number of data points per set is a specified input. A "canned" curve-fitting subroutine, CRVFT [4-1], is used to fit a fourth order polynomial to each of the sets of data points plus three points overlap on either side to insure some continuity and smoothness between curve fits.* The profile subroutine is called twice, once for the wheel profile and once for the rail profile.

* Continuity and smoothness between curve fits could be ensured by requiring equality of the slopes at the ends of each fit as well as the points themselves. However, the curve-fitting routine used here did not provide this option.

4-1 MATH-PACK, UP-7542 Rev. 1, Univac Large-Scale Systems, Sperry-Rand Corp., Sec. 13, pp. 24-44.

Thus, for each profile there is a set of fourth order polynomials with each polynomial fitting a certain zone of the profile, and a set of limits defining the curve-fit zones.

The numerical procedure to find the contact point locations involves an iterative search. At each iteration step the orientation and position of the wheels and rails are specified and the potential contact points between them are searched to find the point that meets the definition of a contact point. The wheelset orientation is computed from the resultant contact point, and compared with the values specified at the beginning of the iteration step. If the difference in orientation is within a specified error range, the contact point computed in the final iteration is stored and a new wheelset lateral position is selected. Otherwise, the computed orientation is used in the next iteration step.

In computing the contact points, the rail profile points are specified in a coordinate system with axes parallel and perpendicular to the track plane with the origin at the midpoint of the track. The two rails are located at the correct cant angle on either side of the origin, half the gauge distance from the midpoint.

To position the wheel profile, the wheelset lateral displacement from the track midpoint, the wheelset roll angle, and the vertical position of the wheelset c.g. must be known. The lateral displacement of the wheelset is specified by the program, but the roll angle and vertical displacement are functions of the contact point locations, and are not known initially. However, only the roll angle is needed to find the contact point. When the coordinates of the rail profile points and the wheel profile points only differ by a vertical distance, the contact point definition given in the preceding section can be redefined as follows: a point where the difference formed by subtracting the height of a point on the rail from the height of the corresponding point on the wheel, is a minimum. Thus, the vertical displacement of the wheelset is not needed in the contact point computation.

In the computer program, subroutine EQSOLV is called to choose the wheelset lateral positions and guess a wheelset roll angle. EQSOLV calls CHECK to search for the corresponding contact points, compute a new roll angle, and compare the new roll angle with the "guessed" roll angle. If the difference in the two roll angles is outside a specified error range, the calculated

roll angle is used as a guess and new contact point locations are found. CHECK continues the iteration process until the "guessed" and calculated roll angles converge within the given tolerance. After finding the contact position for one lateral wheelset position, EQSOLV increments the wheelset lateral position and calls CHECK to repeat the process.

EQSOLV begins the procedure just described by setting the wheelset lateral displacement to zero where, due to symmetry, the wheelset roll angle is known to be zero. Thus, there is no problem in choosing a "sufficiently close" initial approximation for the roll angle. The procedure is repeated with the wheelset lateral displacement incremented until the wheelset is displaced as far as desired in one direction. At each new wheelset lateral position, the roll angle at the previous lateral position is used as the first guess in CHECK. Due to symmetry, the locations of the contact points for the wheelset displaced laterally in the opposite direction can be found by transposing the results.

In subroutine CHECK, the wheels and rails are checked every 0.01 inches along their profiles to find the contact points. The iteration procedure is repeated until the difference in the assumed roll angle and the calculated roll angle is less than or equal to 10^{-5} radians, or 8 iterations have been exceeded. In most cases, convergence to this value takes two iterations. The full eight iterations are needed only when contact occurs on one of the wheel flanges, where a slight change in contact position can cause a large change in roll angle. The contact points are found for 0.01 inch increments of the wheelset lateral position.

After computing the wheel and rail contact positions, subroutine EQSUB2 is called to calculate the desired wheel/rail geometric constraint functions. The equations for the desired variables are given below. These constrained variables are illustrated in Figure 2-6 and Figure 2-7.

$r_L(x_w)$, $r_R(x_w)$ -- the left and right rolling radii evaluated by substituting the contact point locations on the left and right wheel, x_{WR} & x_{WL} , at specific values of wheelset lateral, x_w into the wheel profile polynomial for the appropriate interval.

$Y_L(x_W), Y_R(x_W)$ - the height of the left and right rail contact point evaluated by substitution into the railhead profile equations.

$\delta_L(x_W), \delta_R(x_W)$ - the left and right contact angles evaluated by substitution into the derivative of the wheel profile equations and using the arc tangent function.

$\phi_W(x_W)$ - wheelset roll angle, evaluated in an iterative process using the contact positions, rolling radii, rail contact heights and wheelset roll angle along with the rail and wheel gauges and the rail cant angles.

$\frac{\delta_L - \delta_R}{2}$ - normalized difference in contact angles

$\frac{r_L - r_R}{2a_r}$ - normalized difference in rolling radii

Describing functions are computed by subroutine DCRFCN for the normalized rolling radii difference, normalized contact angle difference and wheelset roll angle functions. This computation entails numerical integration of equation 2-4 by the trapezoid rule. This integration is repeated for amplitudes of the sinusoidal input ranging from 0.05 inches to 1.0 inch in 0.05 inch increments.

The computer program prints and punches cards for most of the output data. In addition, subroutines PLOT1 and PLOT2 generate CALCOMP plots of the contact positions, constraint functions, and curve fits to the input profile data. Examples of these plots may be seen in Figures 4-2, 3,4 and the figures of Chapter 5. A detailed list of output variables, and a sample output listing is given in Appendix A.

VALIDATION

Validation of the analytical model was made by comparing analytical and experimental results for the following three cases:

1. New wheel on new rail at nominal gauge.
2. Severely worn wheel on worn rail at nominal gauge.

The worn wheel and rail profiles were supplied by the Association of American Railroads as described in Chapter 2. The profile data used as input to the modeling routine for the validation was obtained directly from the plexiglass wheel and actual rail cross-sections of the experimental apparatus using the conversion procedure described in Chapter 3.

Analytical and experimental results were compared at two levels: (1) location of contact points on wheel and rail as functions of lateral wheelset displacement and (2) wheel/rail constraint relations such as roll angle and rolling radii difference as functions of lateral wheelset displacement. With a few exceptions, good agreement was obtained between experimental and analytical results.

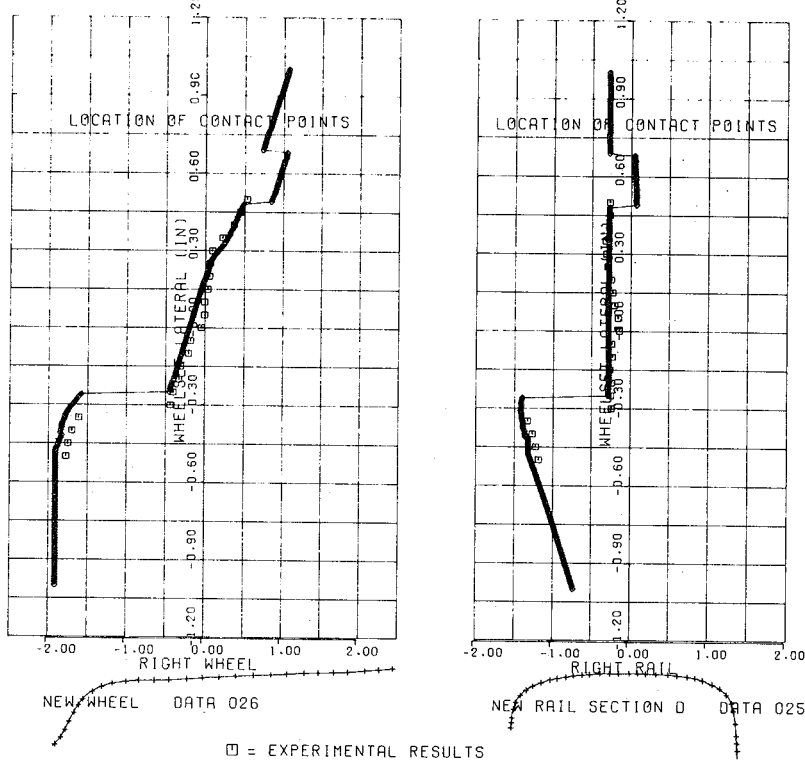
Contact Point Validation

The analytical and experimental values for the contact point locations of the new wheel on new rail at nominal gauge, shown in figures 4-2a, and 4-2b, correlate well at most wheelset lateral positions. The experimental points shown on these figures are averages of the points shown in figures 3-6 and 3-7. At contact positions on the wheel tread* the agreement between measured and computed values is within the ± 0.020 inches accuracy of the experimental process.**

* The input wheel and rail profile data and curve fits to this data are plotted directly below the contact position graphs in all the figures represented in this report. The input data points are indicated by "+" and the solid curves represent the functions fitted to this data. Note that the profiles are aligned with the graphs above, so that one may drop directly down from a point on the graph to the actual profile. This helps visualize the wheel and rail contact configurations.

** The experimental uncertainties of the procedure are discussed in Chapter 3.

a. WHEEL CONTACT POSITION b. RAIL CONTACT POSITION



□ = EXPERIMENTAL RESULTS

WHEEL GAGE 53.000 IN. RAIL CANT .0250
 RAIL GAGE 56.500 IN.

c. WHEELSET ROLL

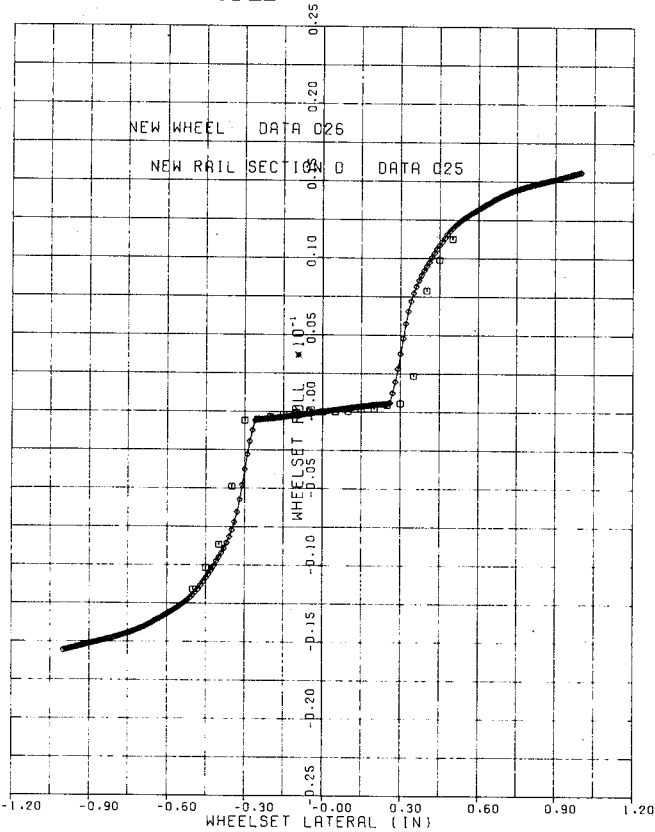
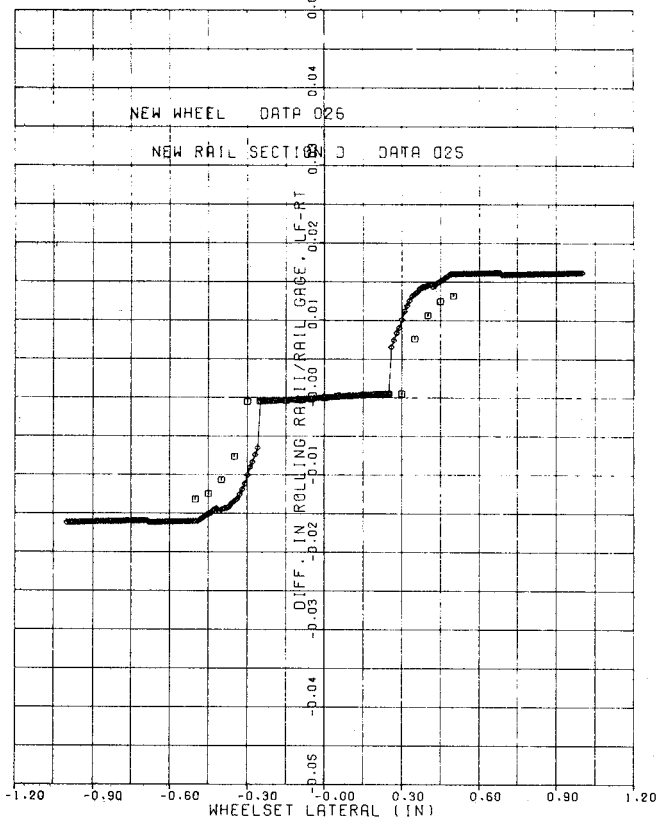
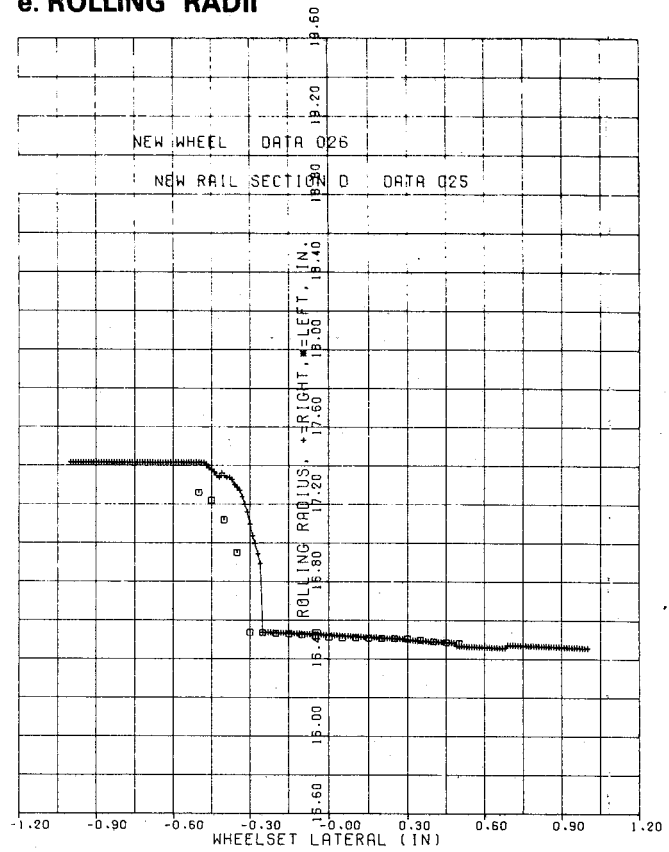


FIGURE 4-2 EXPERIMENTAL AND ANALYTICAL RESULTS FOR NEW WHEELS ON NEW RAILS AT NOMINAL GAUGE

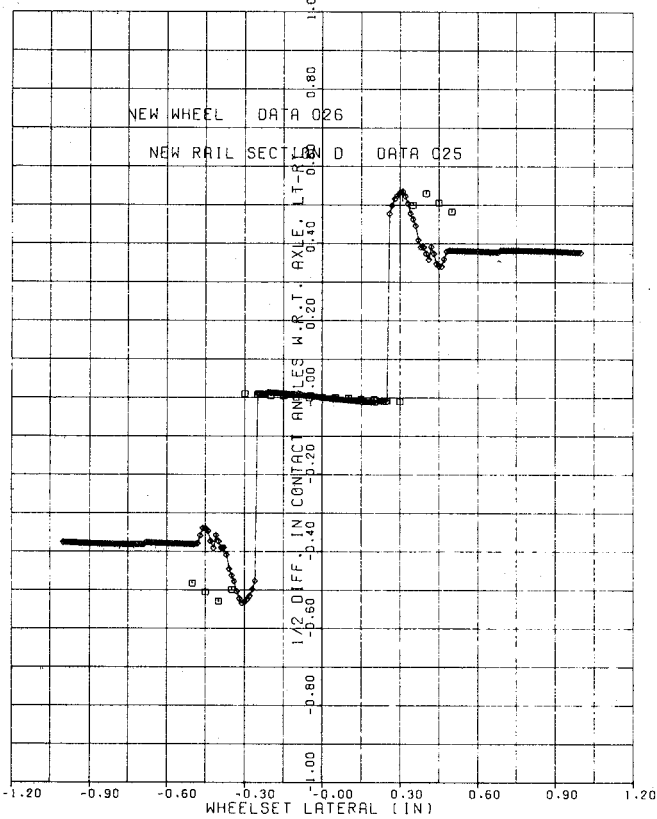
d. NORMALIZED ROLLING RADII DIFFERENCE



e. ROLLING RADII



f. ONE HALF CONTACT ANGLE DIFFERENCE



g. CONTACT ANGLES

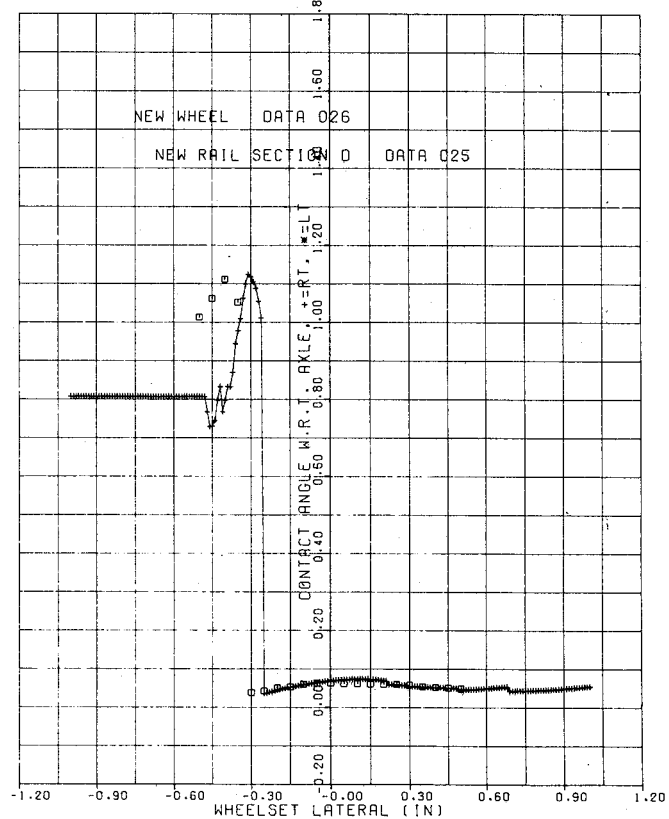


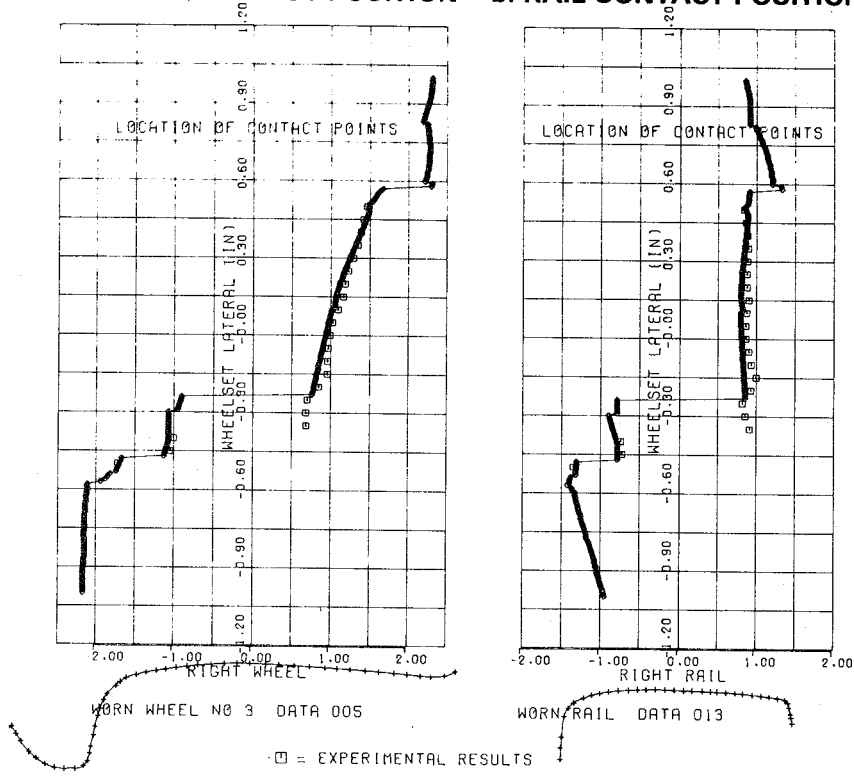
FIGURE 4-2 EXPERIMENTAL AND ANALYTICAL RESULTS FOR NEW WHEELS ON NEW RAILS AT NOMINAL GAUGE

However the value of the wheelset lateral displacement at the jump to wheel flange contact differed from that predicted by the experimental procedure by approximately 0.06 inches. This difference exceeds the ± 0.033 inch uncertainty in the experimental determination of this value. An explanation of this discrepancy was found by comparing the wheel and rail profiles of figures 4-2a and 4-2b with the plexiglass wheel and actual rail profiles used in the experimental measurements. The flange of the actual plexiglass wheel profile was about 0.03 inches closer to the tape-line than the flange on the profile data input to the analysis, while the gauge side edge of the actual rail profile was about 0.06 inches closer to the rail centerline than was the input rail profile. The overall effect of these two discrepancies caused the jump of the measured wheel contact point from the tread to the flange to occur at a wheelset lateral position about 0.03 inches larger than the computed position. The wheel profile discrepancy can be attributed to a slight error in orienting the wheel profile during the digital conversion process, while the rail profile discrepancy probably occurred because the rail data was obtained from a drawing of the rail profile, rather than the actual profile used in the experiments. We believe that the results presented here, in light of the discussion above, validate the analytical procedure for the new wheel, new rail case.

The analytical results shown in figure 4-2 are smoother than those found experimentally. This is due to the smoothing accomplished by the digital conversion of the profile data and the curve fitting carried out within the analytical procedure. For example, any slight ridge or rough spot that might exist on the machined wheel profile would be smoothed out in the digital conversion and curve-fitting procedures. Such ridges or rough spots on the wheel profile would cause some irregularity in the measured contact position values as the contact point jumps from one ridge to another.

The measured and computed contact positions shown in figures 4-3a and 4-3b for the severely worn wheel on worn rail at nominal gauge also correlated well at all but one region of lateral wheelset position. The agreement between experimental and analytical points at contact positions along

a. WHEEL CONTACT POSITION b. RAIL CONTACT POSITION



□ = EXPERIMENTAL RESULTS
 WHEEL GAGE 53.000 IN. RAIL CANT .0250
 RAIL GAGE 56.500 IN.

c. WHEELSET ROLL

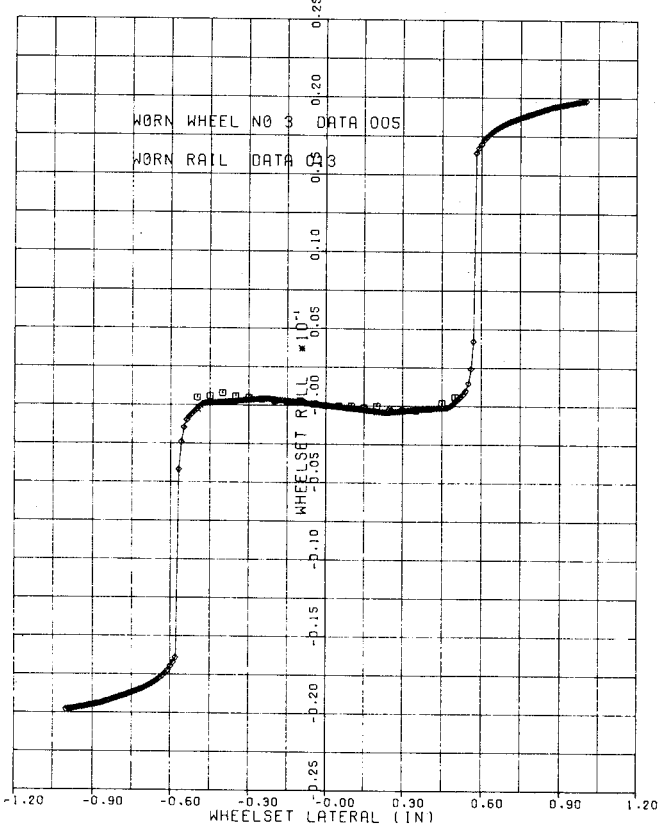
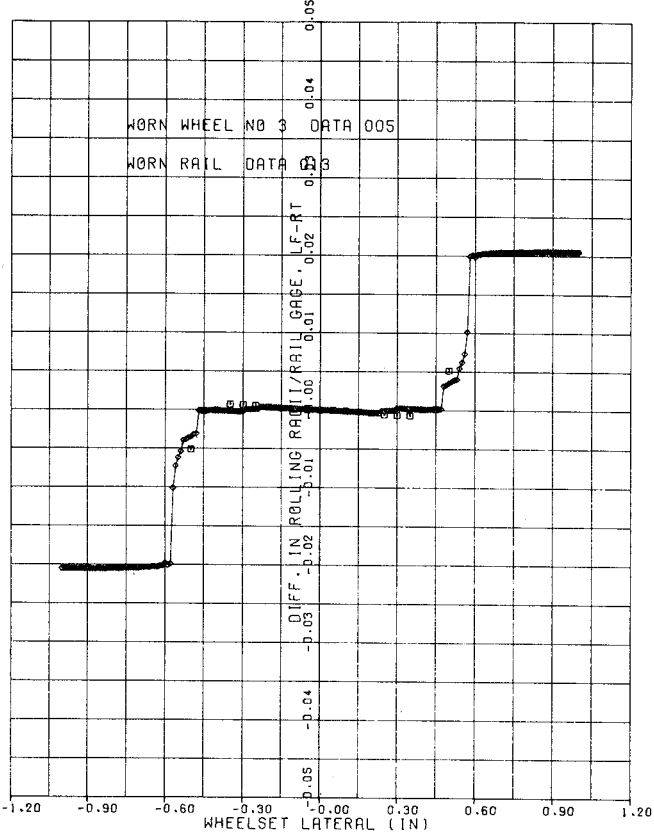
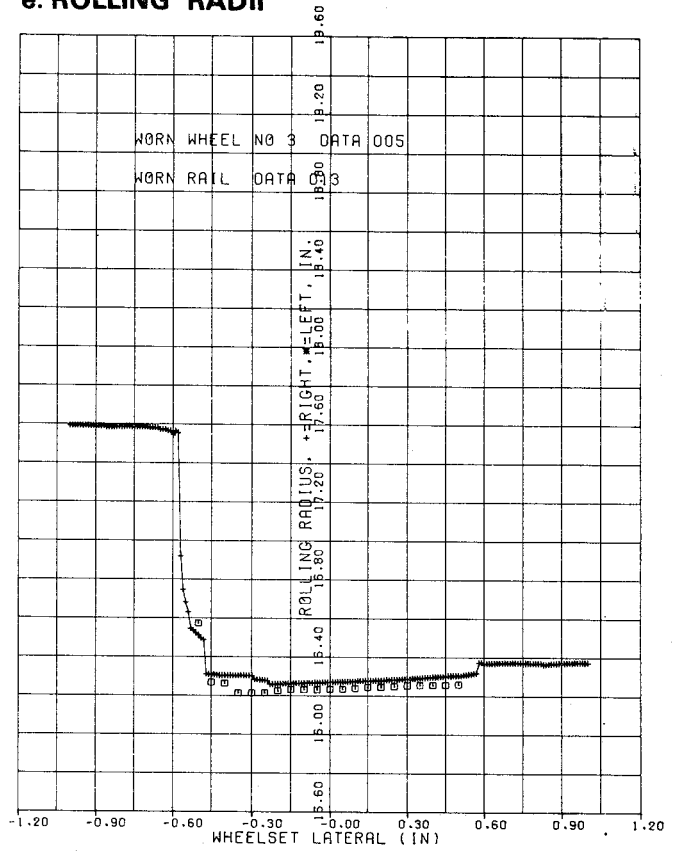


FIGURE 4-3 EXPERIMENTAL AND ANALYTICAL RESULTS FOR SEVERELY WORN WHEELS ON WORN RAILS AT NOMINAL GAUGE

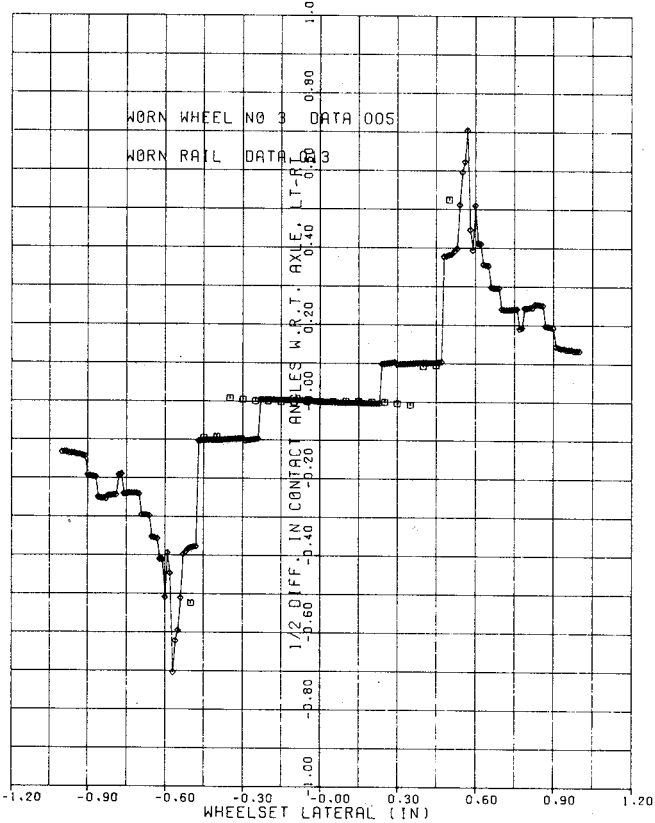
d. NORMALIZED ROLLING RADII DIFFERENCE



e. ROLLING RADII



f. ONE HALF CONTACT ANGLE DIFFERENCE



g. CONTACT ANGLES

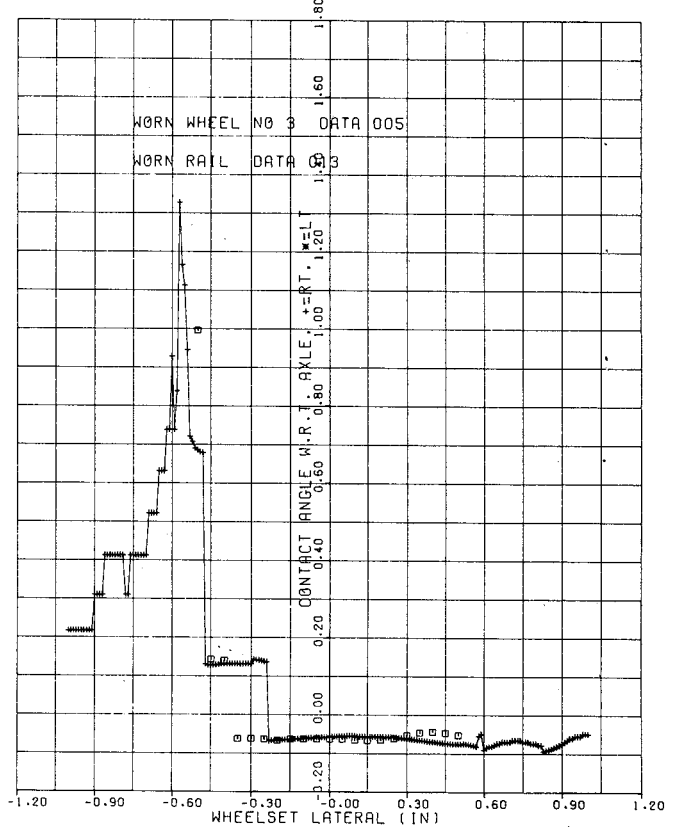


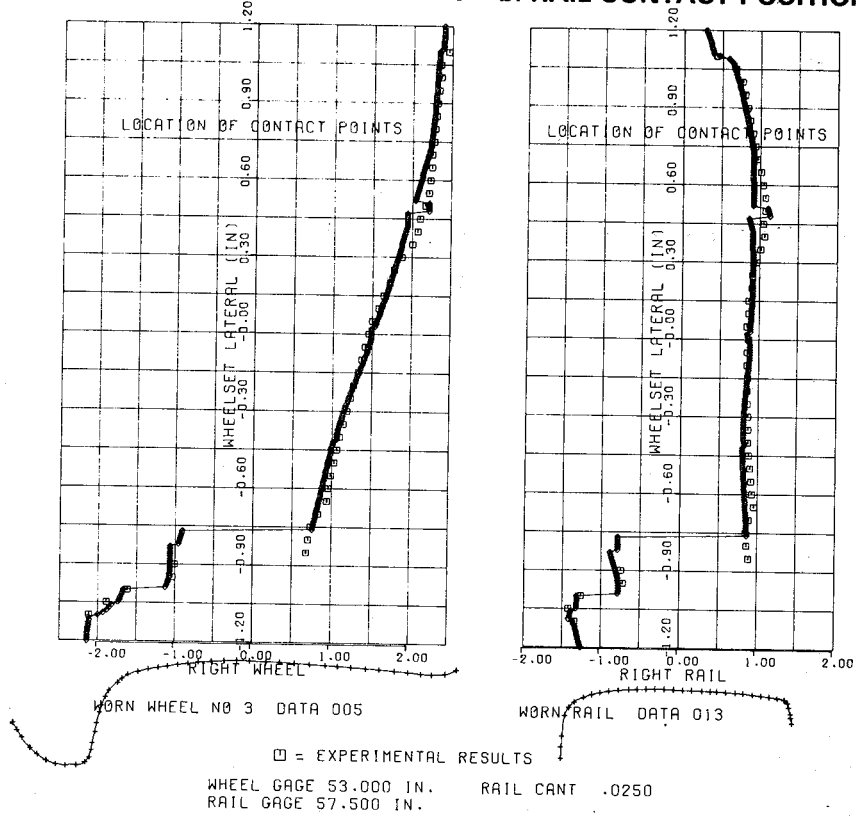
FIGURE 4-3 EXPERIMENTAL AND ANALYTICAL RESULTS FOR SEVERELY WORN WHEELS ON WORN RAILS AT NOMINAL GAUGE

the wheel tread is well within the errors inherent in the two processes. However, the wheelset lateral position where the contact point jumps from tread to flange contact differs by 0.12 inches in the two processes. The measured contact position remained on the wheel tread until a wheelset lateral position of -0.35 inches was reached, while the computed contact position jumped to the wheel tread at a wheelset lateral position of -0.23 inches. This discrepancy can also be explained by a difference between the actual plexiglass wheel profile and the profile data input to the analytical procedure. In this case, the plexiglass profile was slightly more hollow than the wheel profile data in the region of the profile between 0.80 and 0.71 inches inside the tapeline. This additional concavity causes the measured jump on the plexiglass profile to occur at a larger amplitude of wheelset lateral displacement. It should be noted that the difference between the two profiles was quite small, indicating that the results of this wheel/rail contact analysis are very sensitive to small differences in wheel profiles.

The measured and computed contact point locations for the severely worn wheel on worn rail at wide gauge are shown in figures 4-4a and 4-4b. Again, the correlation between analysis and experiment was within the experimental uncertainty in all but two regions. As in the nominal gauge case, the computed and measured contact point jumps from wheel tread to wheel flange did not occur at the same wheelset lateral position. However, the computed and measured flange jumps occurred at the same positions on the wheel profile in both the nominal and wide gauge cases, indicating that this discrepancy is also due to the difference in wheel profiles discussed above. The other discrepancy between analysis and experiment occurred at a contact position far to the outside (field side) of the wheel and rail. Here there was a short jump in the computed contact locations that was not observed experimentally. There is no readily observable explanation for this jump, because the profile curves appear to fit the tabular profile data quite well in this region. However, this jump occurs at the same position on the wheel profile in both the nominal and wide gauge cases that were calculated,* indicating that the problem lies with the wheel profile.

* This discrepancy was not noted in the nominal gauge case because experimental data was not obtained in this region.

a. WHEEL CONTACT POSITION b. RAIL CONTACT POSITION



c. WHEELSET ROLL

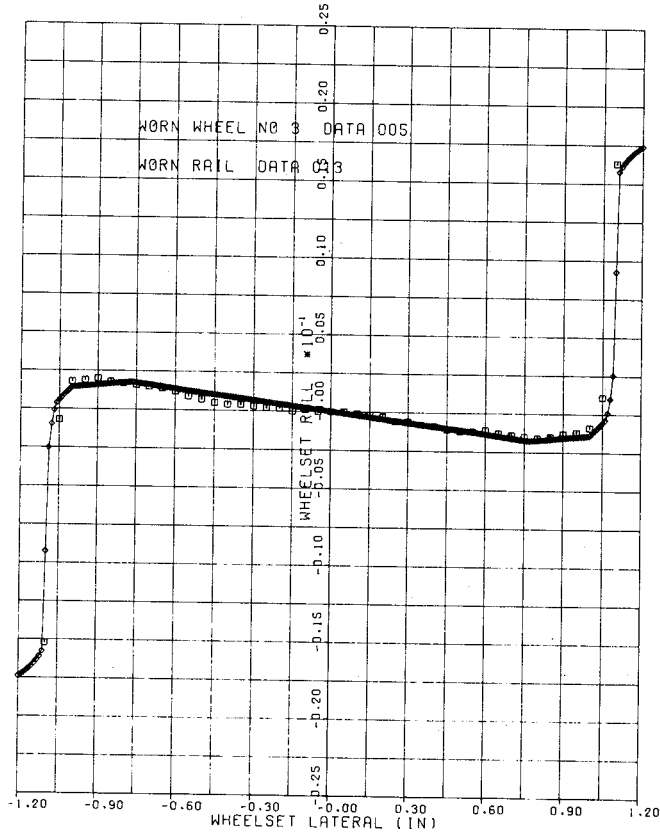
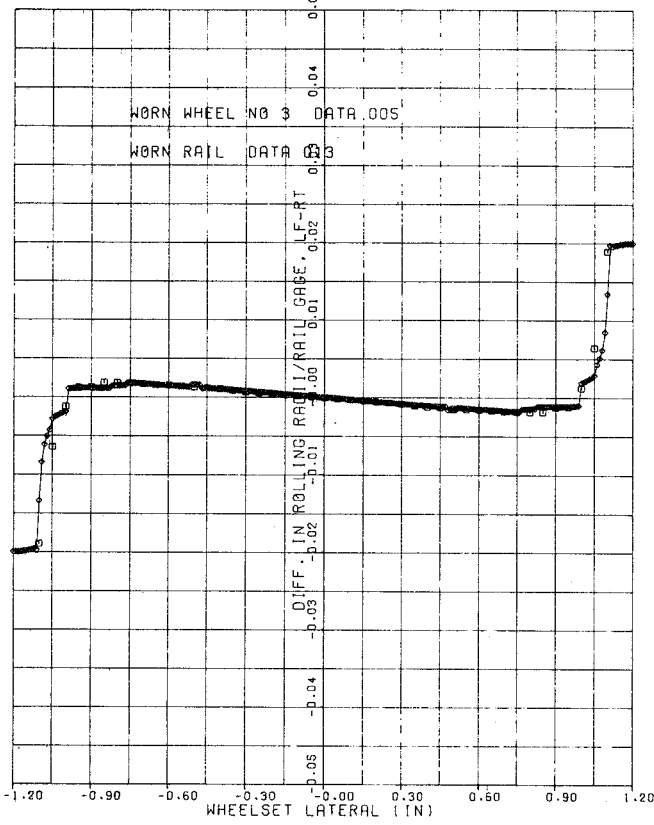
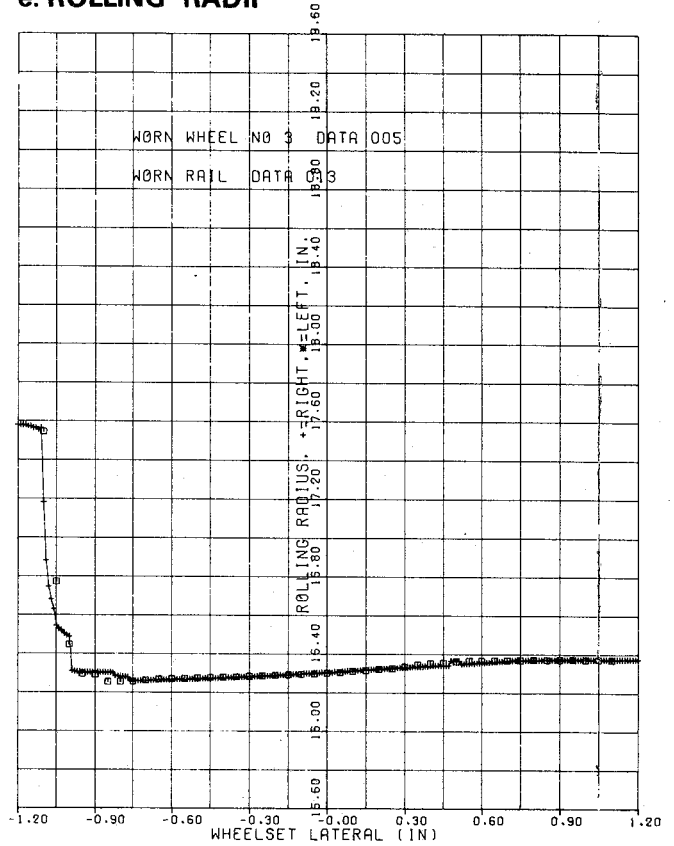


FIGURE 4-4 EXPERIMENTAL AND ANALYTICAL RESULTS FOR SEVERELY WORN WHEELS ON WORN RAILS AT WIDE GAUGE

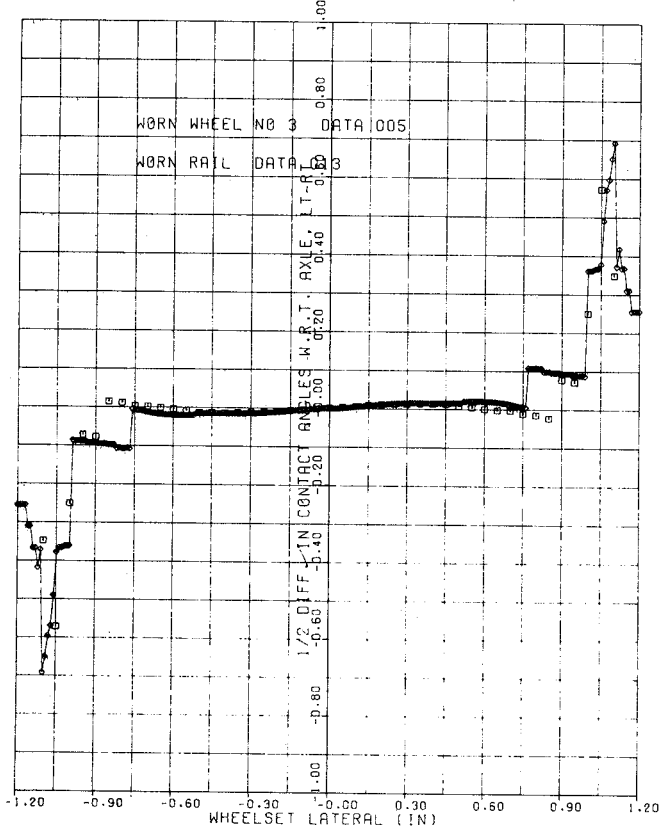
d. NORMALIZED ROLLING RADII DIFFERENCE



e. ROLLING RADII



f. ONE HALF CONTACT ANGLE DIFFERENCE



g. CONTACT ANGLES

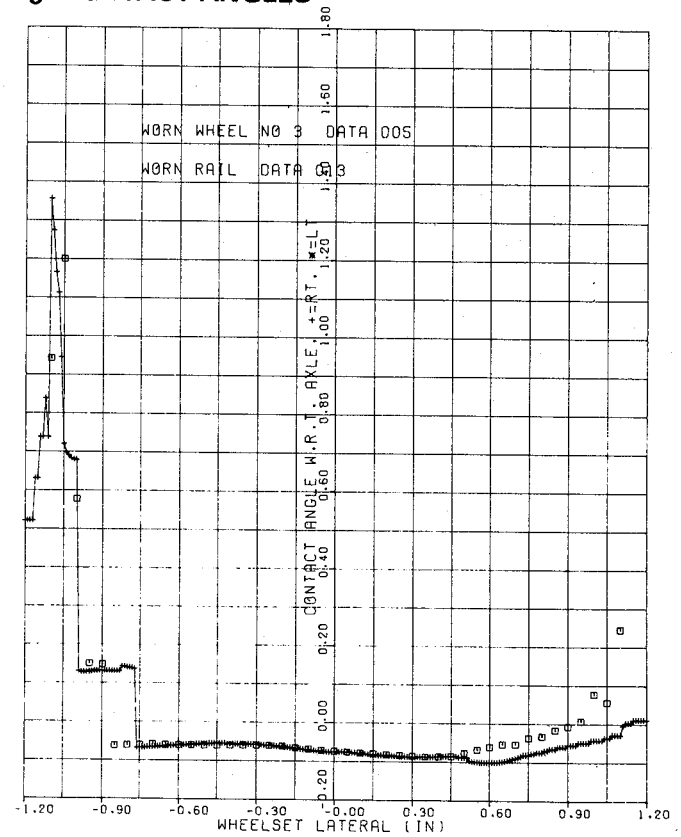


FIGURE 4-4 EXPERIMENTAL AND ANALYTICAL RESULTS FOR SEVERELY WORN WHEELS ON WORN RAILS AT WIDE GAUGE

This behavior can probably be attributed to the change from one curve fit to another that occurs in this region. One curve must be slightly lower at this point, causing the contact to momentarily jump to this low point. This discrepancy, although not serious because of its small magnitude and because it is centered about the experimental results, suggests that the curve fitting process should receive attention in future refinements of the analytical process.

We believe that the results presented in figures 4-2, 4-3 and 4-4 validate the wheel and rail contact point analytical procedure described in this chapter. The major discrepancies between analytical and experimental results are due to differences between the profile data supplied to the analytical procedure and the actual profiles used in the measurement, and are not due to errors in the analytical procedure.

Wheel/Rail Constraint Validation

The agreement between the values of the wheel/rail geometric constraints determined from the analytical and experimental procedures was as good as that found for the contact point positions. This is not surprising in view of the fact that the wheel/rail constraints, such as roll angle, rolling radii and contact angles, are computed by the same procedure from the data for contact positions on the wheel and rail as functions of lateral wheelset displacement. Consequently, the inconsistencies in the contact position results discussed above can be seen in each of the constraint functions.

There was very good correlation between the rolling radii, difference in rolling radii, contact slopes, difference in contact slopes and wheelset roll for the case of the new wheel on new rail at nominal gauge. These constraint functions are shown in Figures 4-2c, 4-2d, 4-2e, 4-2f, and 4-2g. As explained in Chapter 3, the experimental values for all but the wheelset roll relationship were obtained by a computational procedure using the measured contact positions and the measured wheel and rail profile data. The only significant difference between the experimental and analytical results seen

in figure 4-2 is due to the difference in wheelset lateral position when the contact jump to the flange occurs. This difference, due to slight differences in the wheel and rail profiles used in the two procedures, causes the jumps in rolling radii and contact angle that accompany a jump to flange contact to occur at different wheelset lateral positions in the experimental and analytical results.

The wheel/rail geometric constraint functions found experimentally and analytically for the severely worn wheel on worn rail at nominal gauge are shown in figures 4-3c, d, e, f and g. These figures show good correlation between measured and computed values with two exceptions. One exception, a difference in position where the contact slope jumps, is due to the difference in the wheelset lateral position when the contact position jumps across the wheel tread to begin flange contact. As discussed above, this difference between measured and computed values is due to slight differences in wheel and rail profiles. Note that this did not cause any discrepancies in the rolling radii results because both the rolling radii and the height of the rail at the two positions, before and after the jump, are nearly equal. The second exception is the constant offset seen between the measured and computed rolling radii results in figures 4-3e. This offset is due to a slight difference between the rolling radii in the data used for the experimental results and the data used for the analytical investigation. This offset cancels in the rolling radii difference function, as seen in figure 4-3c. The jaggedness observed in the analytical curve for the plot of contact slopes is due to the discontinuity in slope that occurs at the junctions between curve fit zones. This discontinuity is significant only when contact occurs on the wheel flange, where the slope of the profile is very large, because differences in slope in this region are proportionately larger. However, the mean value of the contact slopes on the two overlapping curves is much smoother, and perhaps should be used in future analyses.

Experimental and analytical wheel/rail constraint functions for the severely worn wheel on worn rail at wide gauge are shown in figures 4-4c, d, e, f and g. Good correlation between the two results also was achieved in this case, as seen in these figures. Again, the only significant discrepancy, the premature jump in the computed contact slopes, is due to the difference in the predicted wheelset lateral position where the wheel contact point jumps across the wheel

tread. The offset between rolling radii results seen in the nominal gauge results was not present here because the same data sets were used in both processes.

CONCLUSIONS

The analytical procedure developed in this project and described in this chapter is capable of determining the contact positions between wheel and rail and the wheel/rail geometric constraint relationships as functions of wheelset lateral position for arbitrary combinations of wheel and rail profile, rail gauge, and rail cant angle. Excellent correlation was obtained between the experimental results described in Chapter 3 and analytical results for the same cases. We believe that the high level of agreement between results of the two procedures establishes the validity of the analytical process.

The validation process demonstrated that the fidelity of the constraint relationship calculations depends on the accuracy of the contact position results. The accuracy of the contact positions, in turn, depends on the accuracy of the wheel and rail profile data, and the fidelity of the curves fitted to the profile data. The sensitivity of the results to these factors demonstrates the importance of carefully recording and transcribing the wheel and rail profile data.

The extraneous jumps in the computed contact positions and contact angles could be eliminated by improving the process of fitting curves to the wheel and rail profile data. Possible changes that should receive attention in future development of this process include using slope constraints to insure better continuity between curve fit zones, the use of functions other than polynomials to represent the profiles, and using the average between the two curves in the overlap region at the ends of each curve fit zone.

CHAPTER 5

PARAMETRIC STUDY

INTRODUCTION

The results of our limited investigation of the influence of variations in wheel and rail head profiles and track gauge on the wheel/rail geometric constraint relationships are presented in this chapter. The analytical procedure described in the preceding chapter was used to determine the contact positions, contact angles, difference in contact angles, rolling radii, difference in rolling radii and wheelset roll as functions of the wheelset lateral position.

The various wheel and rail combinations that were investigated for this study are summarized in Table 5-1. The wheel and rail profiles used here were described in Chapter 2 and are shown in figures 2-2, 2-3 and 2-5. Tabular data for these profiles were prepared by the interactive computational procedure described in Chapter 3. Figures illustrating the various constraint relationships are presented in the course of the discussion below.

The effects of wheel wear, the effects of rail wear and the influence of track gauge on the wheel/rail constraint relationships are discussed in the following sections.

WHEEL WEAR EFFECTS

The wheel/rail analysis results for five different wheel profiles are presented and discussed in this section. These cases consist of a new wheel, a wheel in three stages of wear and the modified Heumann wheel profile.

New Wheels

The contact positions and wheel/rail constraint relationships for new wheels on a worn rail at nominal (56.5 inch) track gauge are shown in figure 5-1. The contact positions on the wheel and rail shown in figures 5-1a and 5-1b illustrate that the contact position on the rail remains

TABLE 5-1

WHEEL/RAIL CONSTRAINT PARAMETRIC STUDY CASES

CASE	1	2	3	4	5	6	7	8	9	10	11
WHEELS											
New	x	x							x	x	
Worn #1 (least wear)							x				
Worn #2 (moderate wear)								x			
Worn #3 (heavy wear)			x	x	x	x					
Heumann											x
RAILS											
New	x		x								
Worn (Profile A)		x		x	x	x	x	x	x	x	x
TRACK GAUGE											
Narrow (4'8")					x				x		
Nominal (4'8 1/2")	x	x	x	x			x	x			x
Wide (4'9 1/2")						x				x	

nearly stationary at a position just to the inside of the rail center until the flange contacts. Consequently, over this range the wheel contact point moves in a direction opposite that of the wheelset lateral displacement and nearly equal in magnitude. The one slight jump in contact point at a lateral displacement of about 0.27 inches is probably due to a spurious dip in one of the profiles introduced either in the data generation process or during the curve fit procedure. This slight dip has very little effect on the resulting constraint relationships, as the curves in figures 5-1c,d,e,f, and g illustrate.

As expected, all the constraint relationships are nearly linear over the range before the flange contacts the rails. If we represent the three constraints that directly enter the equations of motion with the following equations,

Rolling Radii Difference:

$$\frac{r_L - r_R}{2a_w} = \lambda_e \left(\frac{X_w}{a_w} \right) \quad (5-1)$$

Contact Angle Difference:

$$\frac{\Delta_L - \Delta_R}{2} = \Delta_e \left(\frac{X_w}{a_w} \right) \quad (5-2)$$

Wheelset Roll:

$$\phi_w = a_e \left(\frac{X_w}{a_w} \right) \quad (5-3)$$

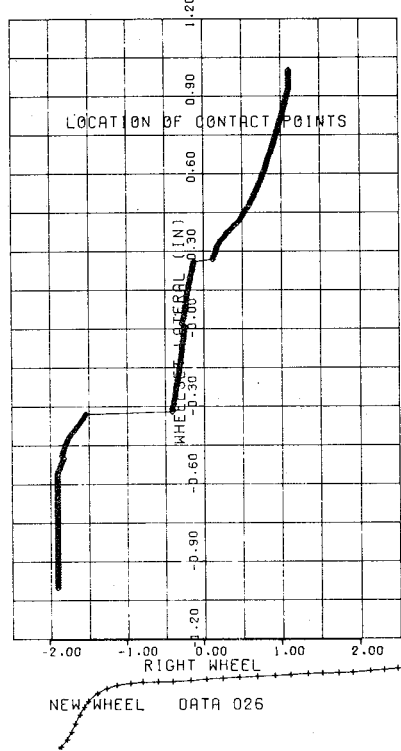
then the linear coefficients may be represented by values of the describing functions at an amplitude of wheelset lateral motion within this range: For example, at $\frac{X_w}{a_w} = 0.30$ the describing functions provide the following values:

$$\lambda_e = 0.0446$$

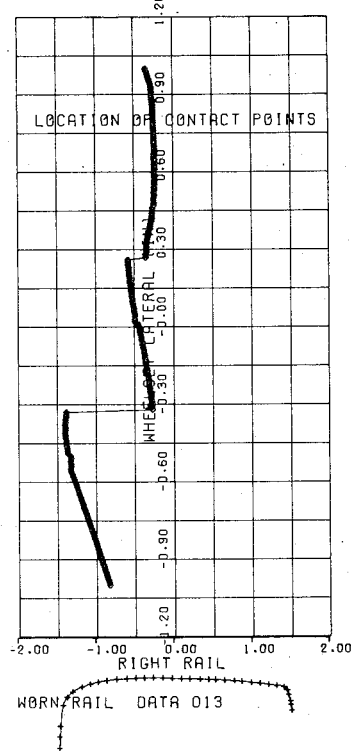
$$\Delta_e = -0.921$$

$$a_e = 0.0643$$

a. WHEEL CONTACT POSITION



b. RAIL CONTACT POSITION



WHEEL GAGE 53.000 IN.
RAIL GAGE 56.500 IN.

RAIL CANT .0250

c. WHEELSET ROLL

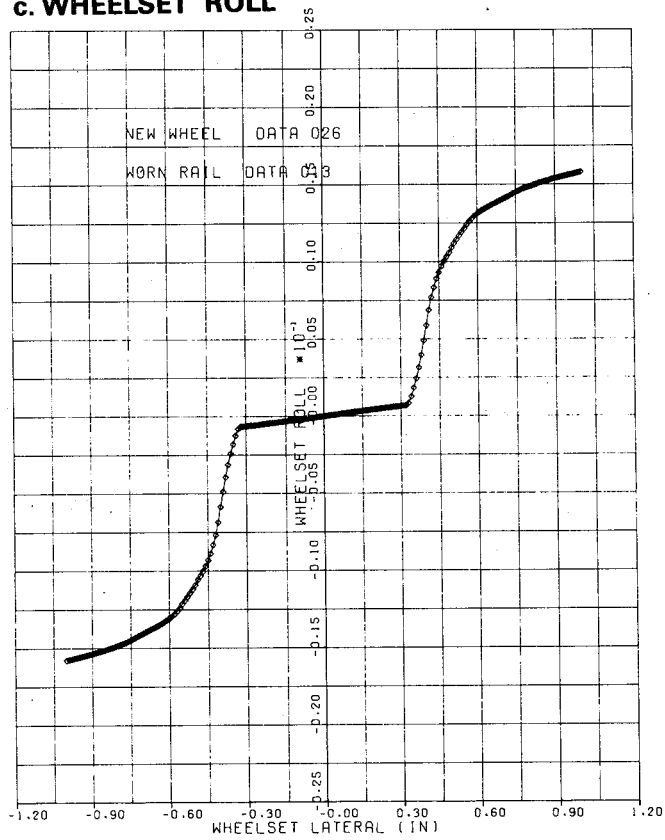
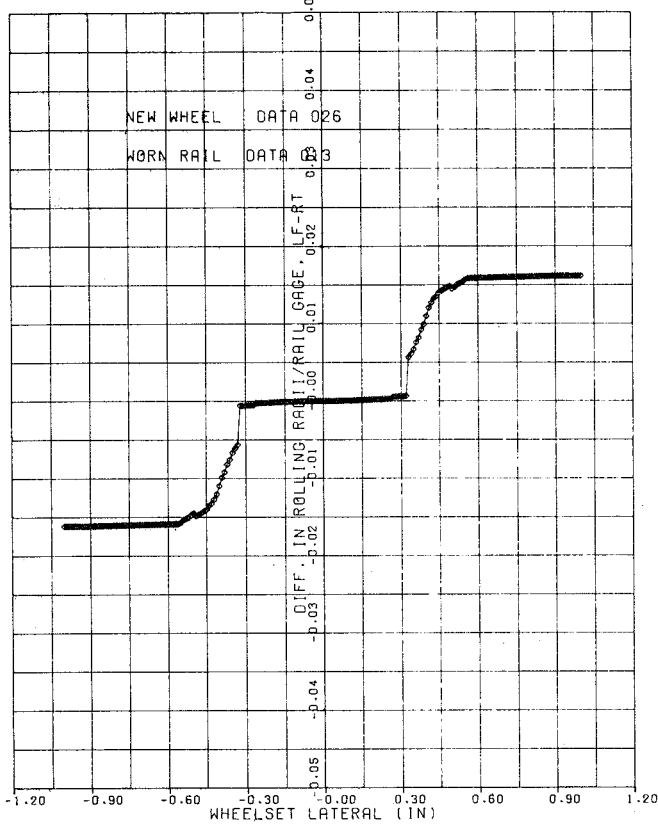
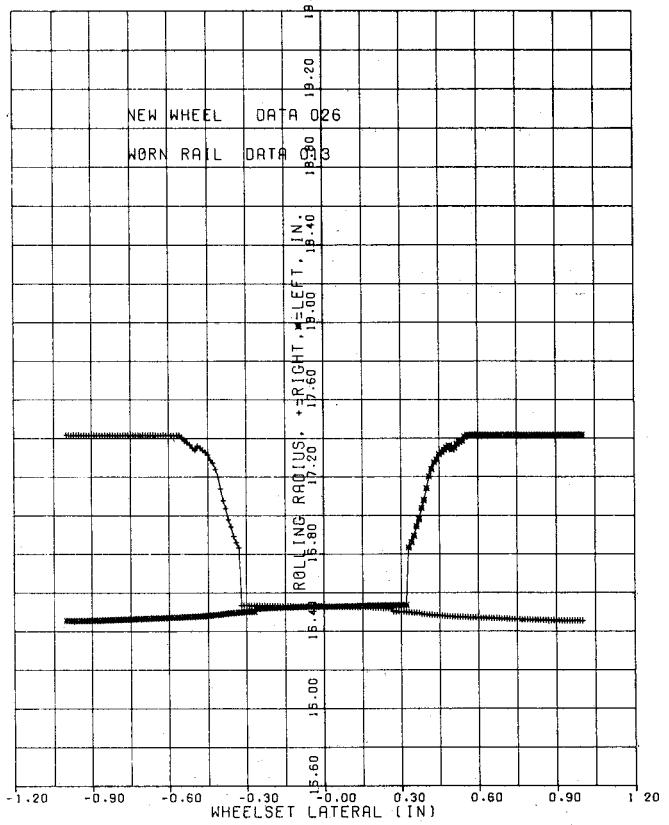


FIGURE 5-1 NEW WHEELS, WORN RAILS AT NOMINAL GAUGE

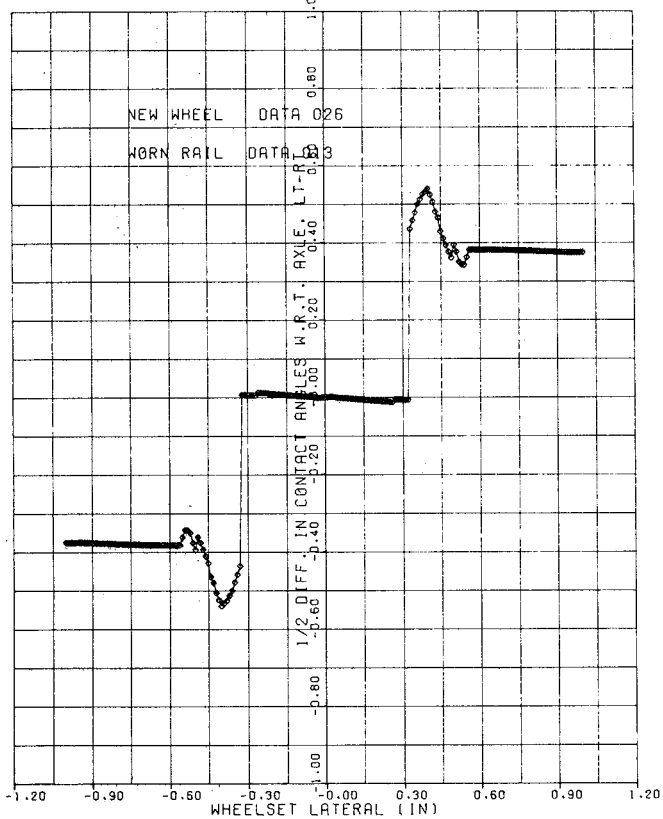
d. NORMALIZED ROLLING RADII DIFFERENCE



e. ROLLING RADII



f. ONE HALF CONTACT ANGLE DIFFERENCE



g. CONTACT ANGLES

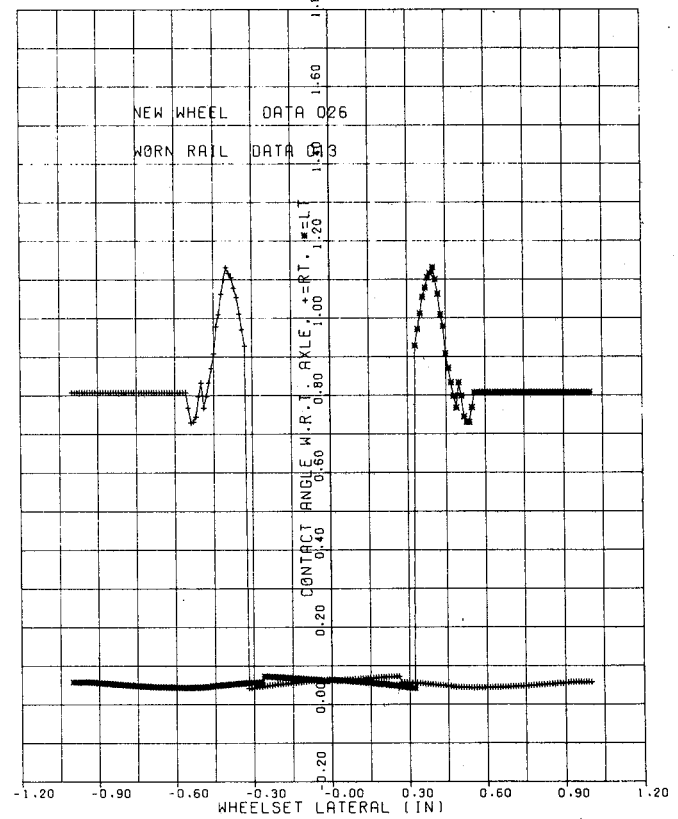


FIGURE 5-1 NEW WHEELS, WORN RAILS AT NOMINAL GAUGE

These values should be compared with $\lambda_e = a_e = .05$ and $\Delta_e = 0$ for an ideal new wheel on a new rail. The deviation from these "ideal" values is due primarily to the effect of the worn rail. However, the experimental error in the data measurement and computational procedures may also contribute to the difference. The wheel conicity, λ_e , in particular, is smaller than we might expect because the contact point shifts on the worn rail.

When the flange contacts the rail, the contact point moves to the inside edge of the rail, and remains there. The contact point on the wheel also jumps from the tread to the flange. This contact jump is reflected in jump discontinuities in the rolling radii difference and contact angle difference. Further lateral displacement of the wheelset moves the contact point on up the flange and eventually down the other side when the displacement exceeds 0.70 inches.

Slightly Worn Wheel

The contact positions and constraint relationships for the least worn wheel, profile #1 in figure 2-2, on a worn rail, profile A in figure 2-5, at nominal rail gauge are illustrated in figure 5-2. In this case, the contact points on the wheel and rail move in a series of small jumps across a wide band of the wheel and rail profile, as seen in figures 5-2a and 5-2b. By contrast with the new wheel, the contact covers a wider band of the wheel and rail, and moves to the outside half of the rail over a moderate range of wheelset lateral movement.

Because the slope at the contact point with the wheelset centered is nearly zero, both the rolling radii difference and contact angle difference are nearly zero in a narrow ± 0.05 inch band about this centered position. The rolling radii difference and wheelset roll relationships appear to be nearly linear over the full ± 0.3 inch range before flange contact occurs. Approximate values for the linear coefficients in equations 5-1, 5-2, and 5-3 obtained from the describing functions for the appropriate functions at $\frac{X_w}{a_w} = 0.30$ follow:

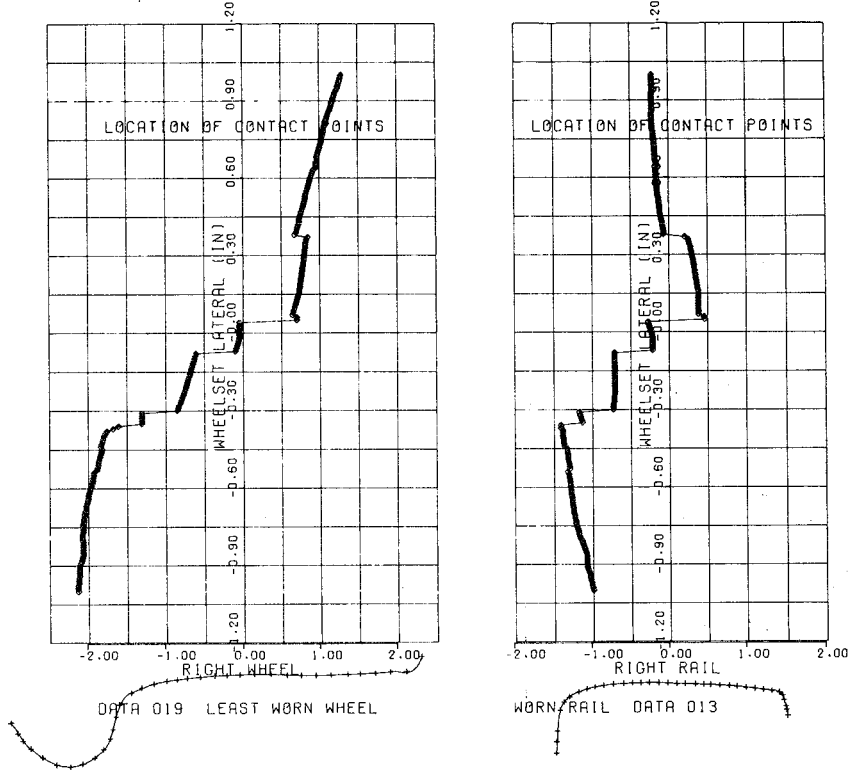
$$\lambda_e = 0.0885$$

$$\Delta_e = 6.9530$$

$$a_e = 0.7870$$

a. WHEEL CONTACT POSITION

b. RAIL CONTACT POSITION



WHEEL GAGE 53.000 IN. RAIL GAGE 56.500 IN.
RAIL CANT .0250

c. WHEELSET ROLL

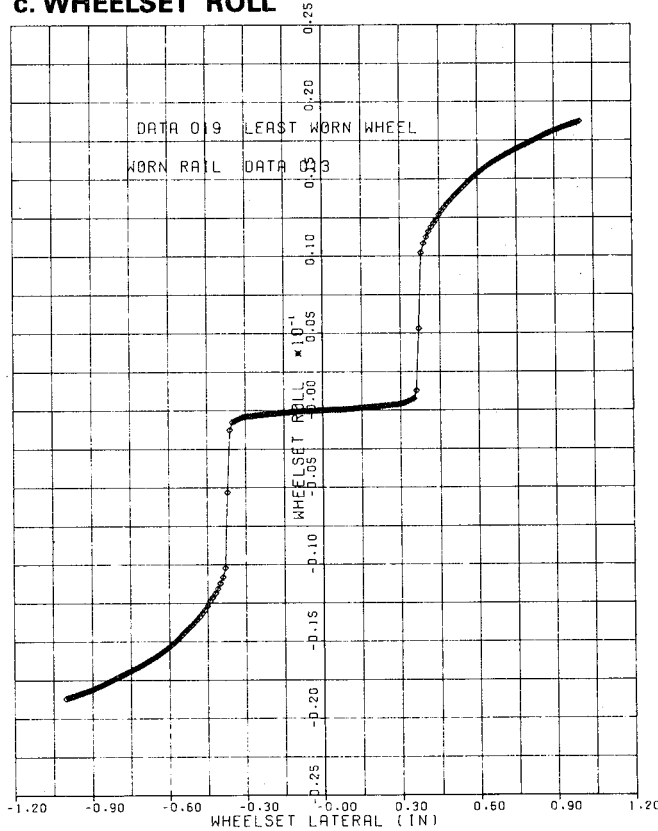
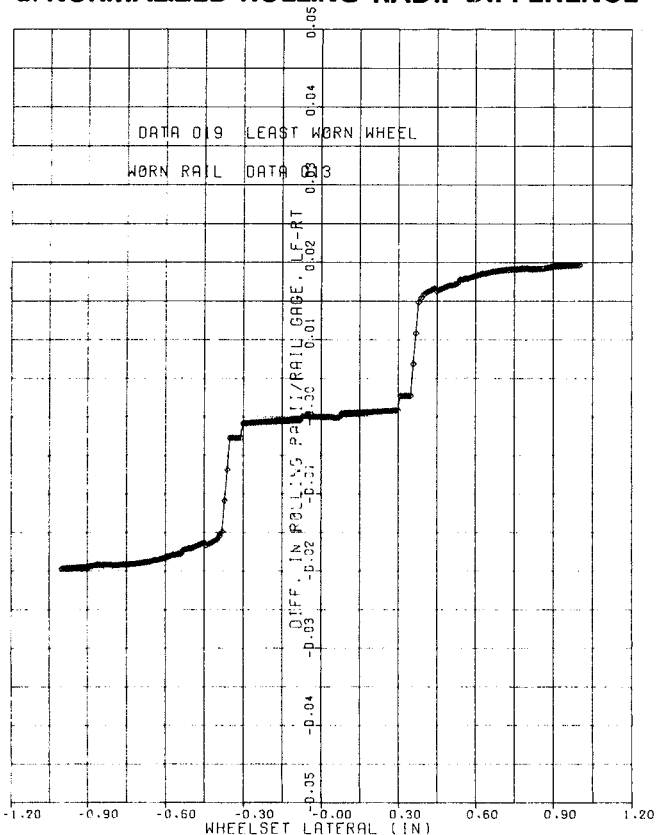
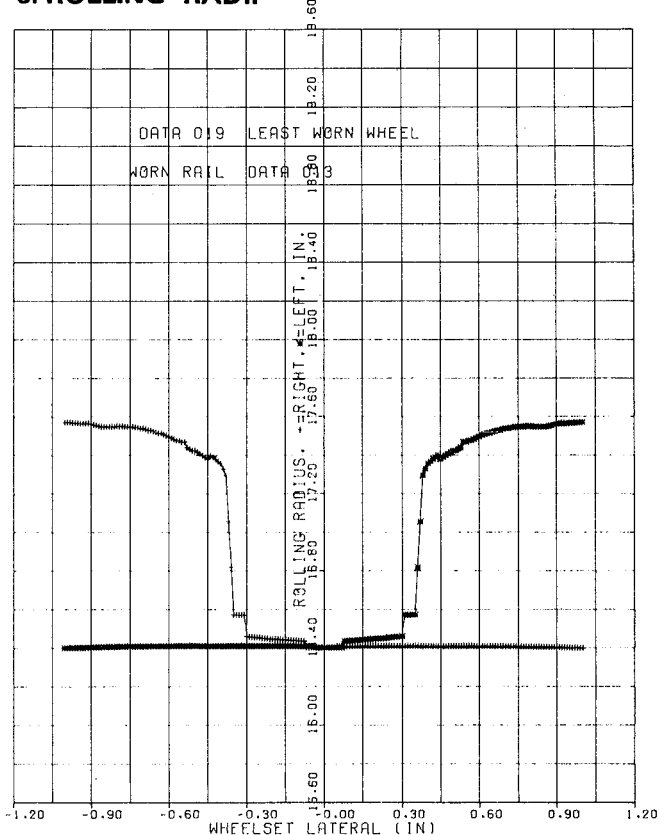


FIGURE 5-2 SLIGHTLY WORN WHEELS, WORN RAILS, AT NOMINAL GAUGE

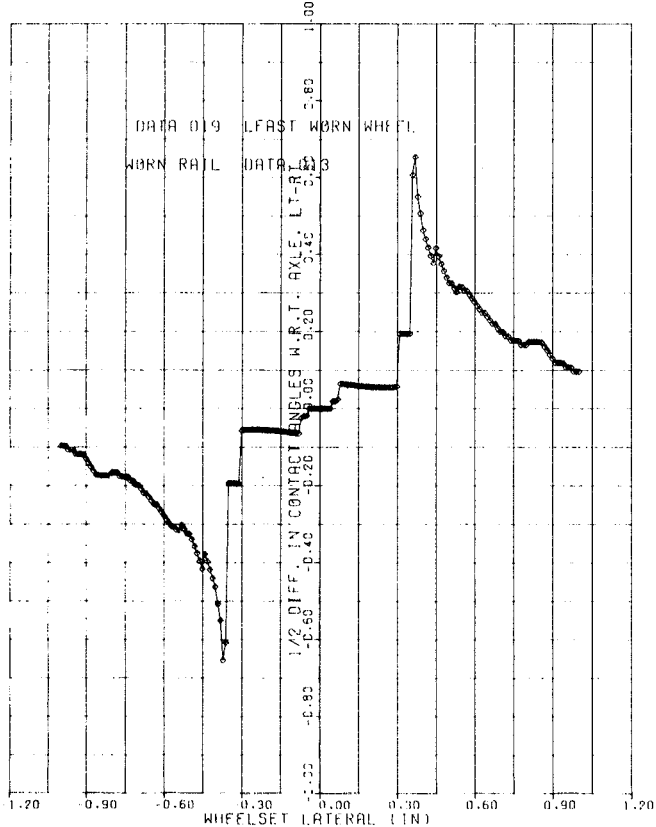
d. NORMALIZED ROLLING RADII DIFFERENCE



e. ROLLING RADII



f. ONE HALF CONTACT ANGLE DIFFERENCE



g. CONTACT ANGLES

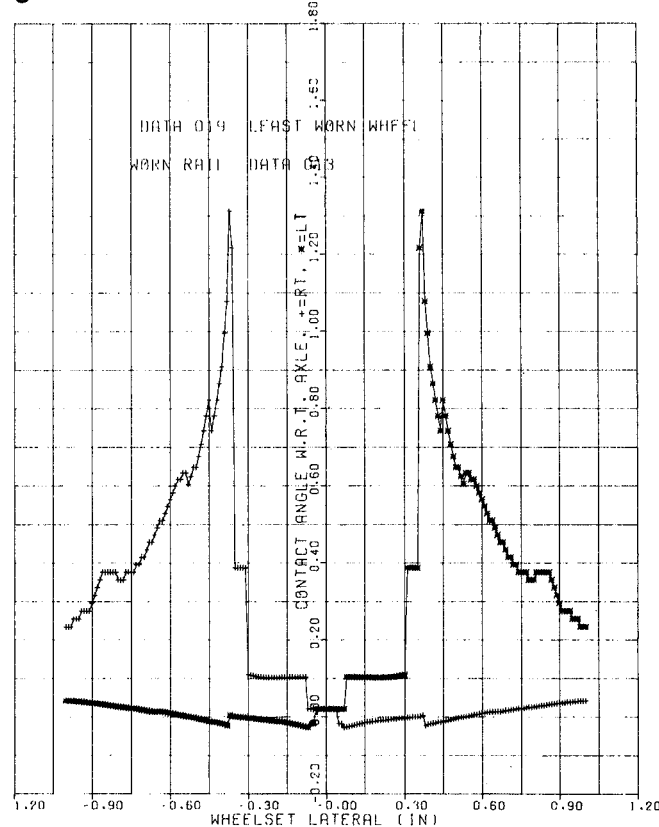


FIGURE 5-2 SLIGHTLY WORN WHEELS, WORN RAILS, AT NOMINAL GAUGE

The roll coefficient has increased from the new wheel value. The conicity increase over the new wheel value is a destabilizing effect. The contact angle difference that contributes to the gravitational stiffness effect is also larger for this wheel. This, together with the increase in the roll coefficient, will be a stabilizing effect when the wheel loads are large.

Flange contact occurs at about the same wheelset lateral position as for the new wheel. The flange is steeper on the worn wheel, increasing the contact angle difference, as seen in figure 5-2f. The rolling radii difference, figure 5-2d, increases faster with the slightly worn wheel than for the new wheel.

Moderately Worn Wheels

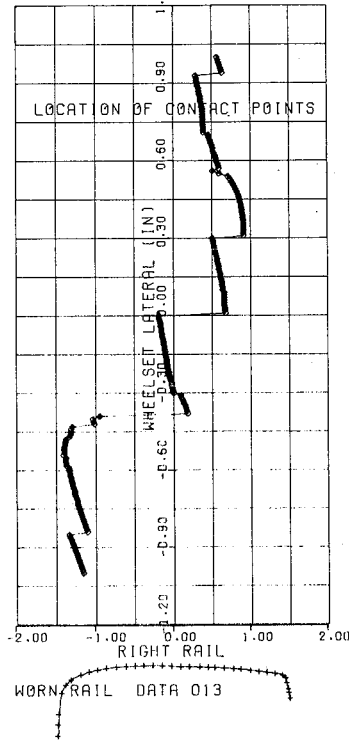
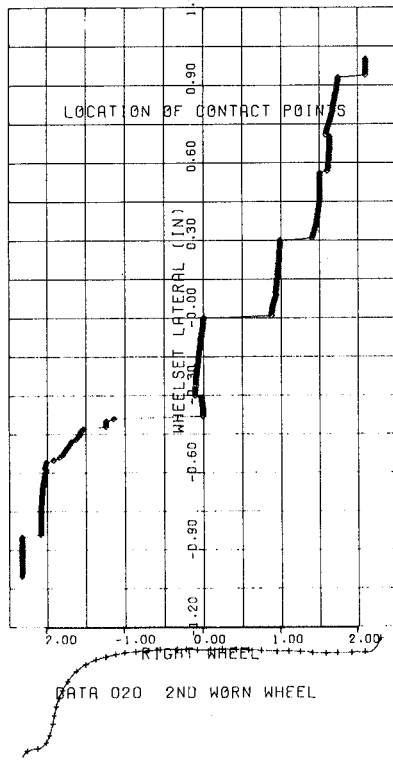
Some dramatic contrasts with less worn wheels may be seen in the wheel/rail geometry results for the moderately worn wheel, profile #2 of figure 2-2. The contact positions on the wheel and rail shown in figures 5-3a and 5-3b now shift to the outside (field side) over much of their range of travel. This moves the contact point to a portion of the wheel profile with negative slope when the wheel moves away from the rail. The contact angle at this position is, of course, negative.

Because the slope of the contact plane is negative over much of the range of wheelset travel, both the difference in rolling radii and the difference in contact angles have negative slopes in this region, as seen in figures 5-3d and 5-3f. Physically, this means that when the wheelset is displaced laterally, the difference in rolling radii will produce a moment that tends to drive the wheelset in the direction of the displacement. Similarly, negative contact angle differences imply lateral components of the normal wheel loads acting in the direction of the displacement, rather than opposing it.

For this moderately worn wheel, in the region about the centered position, the equivalent linear coefficients, λ_e , Δ_e and a_e will be negative. The linear equations of motion with these negative coefficients are unstable at all speeds. Consequently, we expect that a vehicle with this wheel/rail configuration would either seek an equilibrium position displaced from the rail centerline or, experience some sort of limit

a. WHEEL CONTACT POSITION

b. RAIL CONTACT POSITION



WHEEL GAGE 53.000 IN.
RAIL GAGE 56.500 IN.

RAIL CANT .0250

c. WHEELSET ROLL

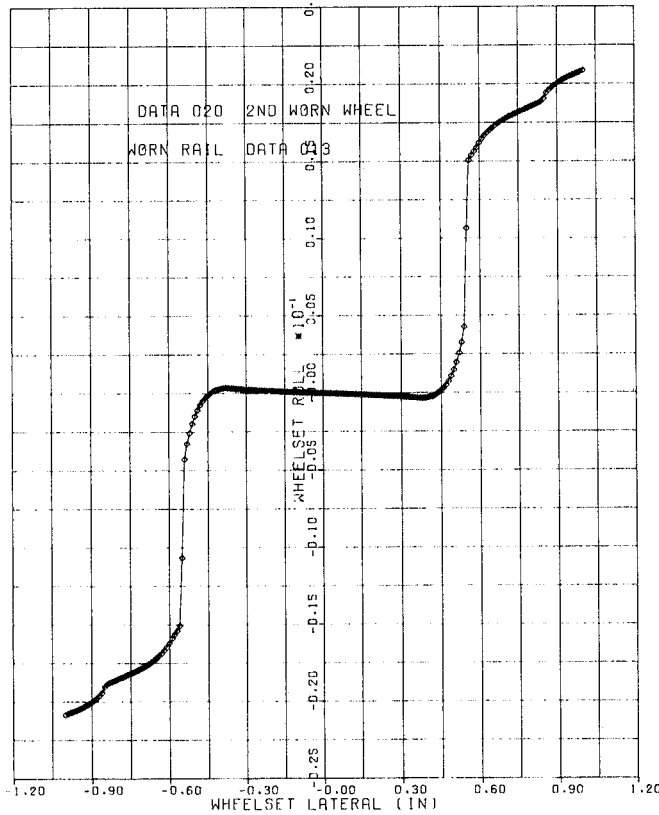
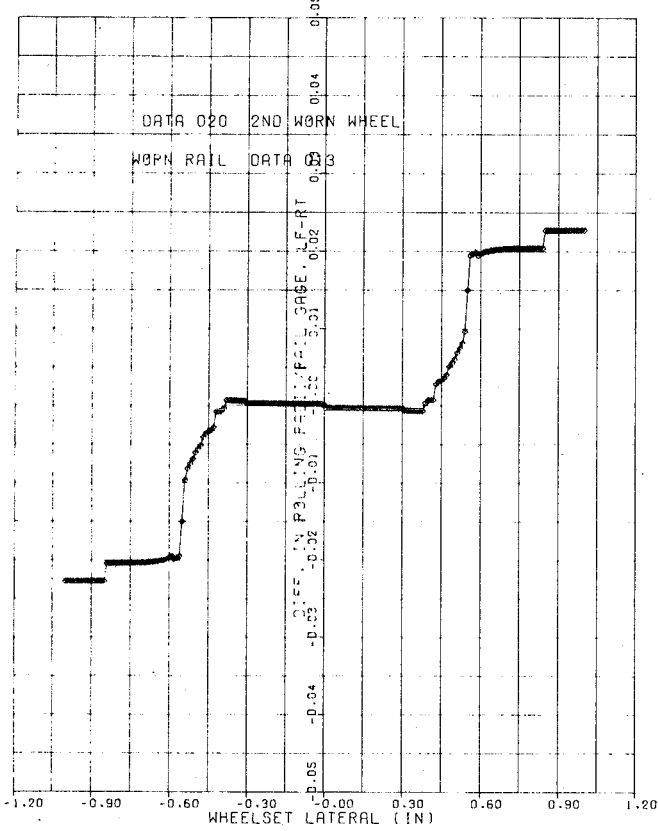
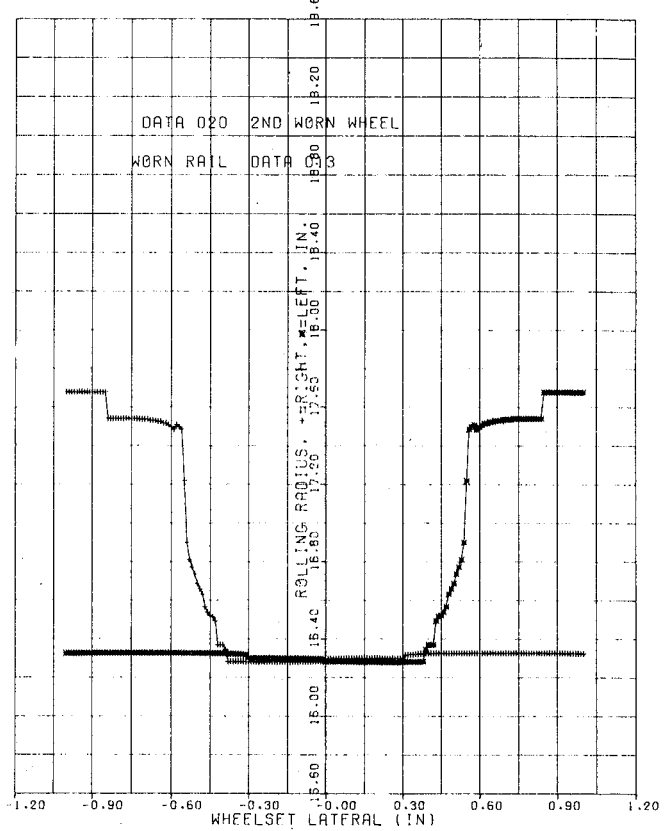


FIGURE 5-3 MODERATELY WORN WHEELS, WORN RAILS AT NOMINAL GAUGE

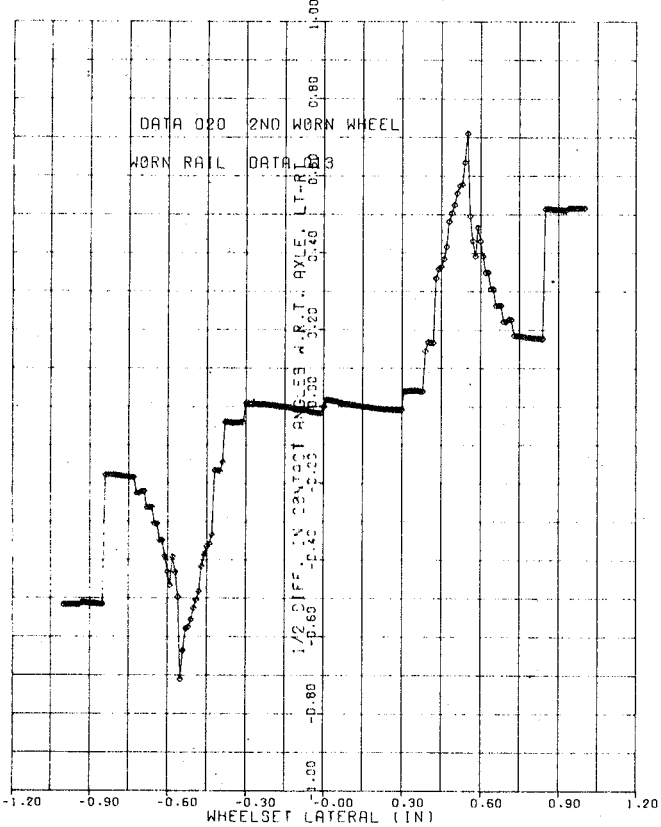
d. NORMALIZED ROLLING RADII DIFFERENCE



e. ROLLING RADII



f. ONE HALF CONTACT ANGLE DIFFERENCE



g. CONTACT ANGLES

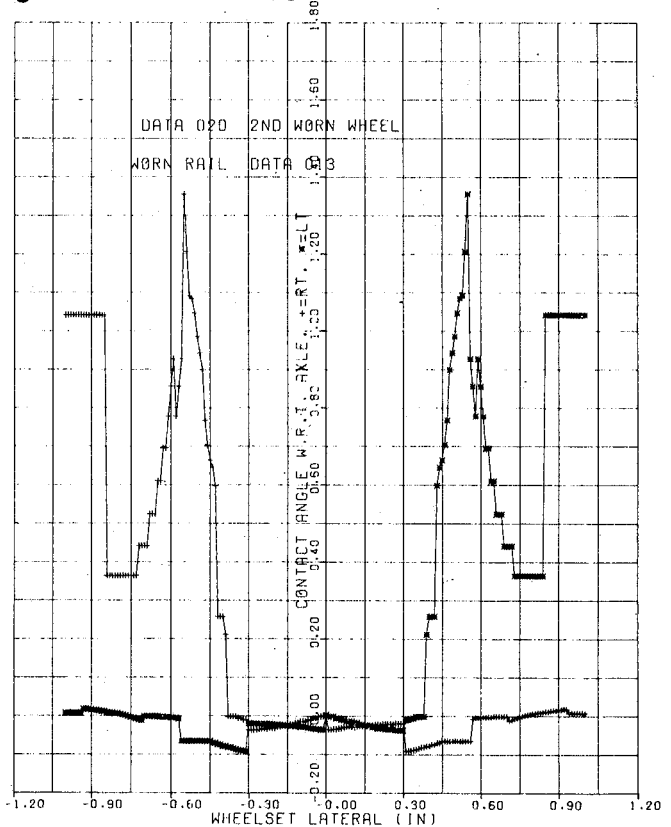


FIGURE 5-3 MODERATELY WORN WHEELS, WORN RAILS AT NOMINAL GAUGE

cycle motion. Recall, however, that many observed freight car wheelsets do not have identical wheel profiles on both wheels, and as a result, may have constraint relationships that differ considerably from those presented here.

Once flange contact occurs, at a lateral displacement of about 0.37 inches, the wheel/rail geometric constraints appear very similar to the preceding case of slightly worn wheels on worn rails. Because the flange is worn thinner on this wheel there is about 0.07 inches more clearance before contact with the flange than there was for the less worn wheel.

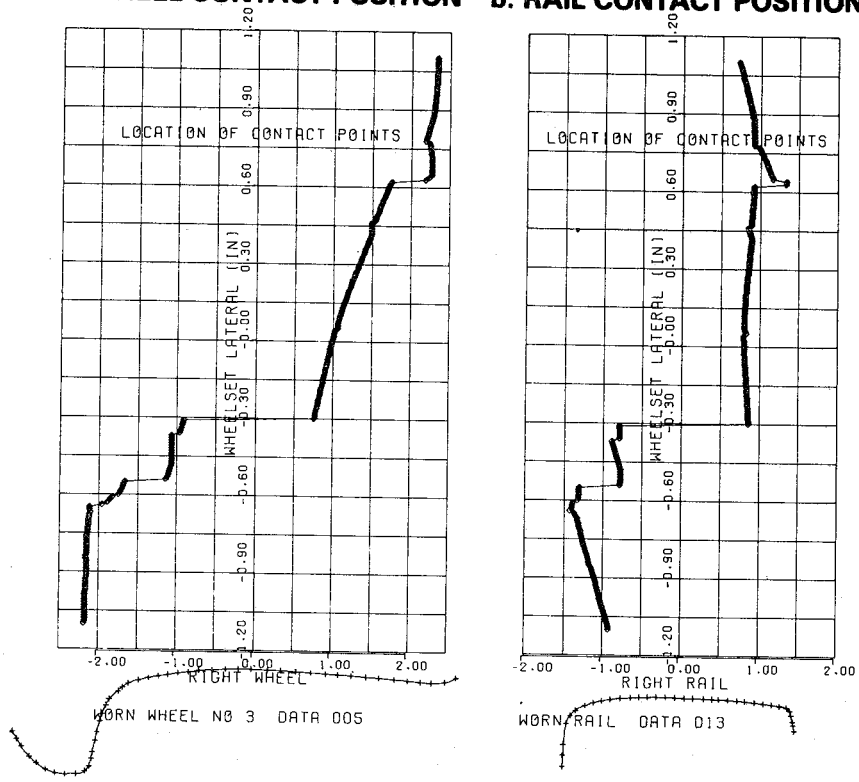
Heavily Worn Wheels

The wheel/rail behavior for the most severely worn wheel, profile #3 of figure 2-2, is quite similar to that found for the moderately worn wheel. The contact positions and constraint relationships for this severely worn wheel on worn rail at nominal gauge are shown in figure 5-4. The contact position remains on the outside of the wheel and rail for the majority of the range of wheelset travel, including the position with the wheelset centered on the rail, as shown in figures 5-4a and b. Again, due to the negative slope on the wheel profile, the contact angle is negative when contact occurs on the outside.

The rolling radii difference, contact angle difference, and wheelset roll constraint relations shown in figures 5-4c, d and f have negative slopes in the region before the flange contacts. The slopes in this region are greater than those for the moderately worn wheel. As in that case, a wheelset with two identical severely worn wheels would either seek a displaced equilibrium position or exhibit limit cycle oscillations.

The lateral wheelset travel before flange contact is quite large with this severely worn profile. The clearance is 0.12 inches more than for the moderately worn wheel, and nearly 0.20 inches more than the new wheel value for a total of almost 0.60 inches of flange clearance. Once flange contact is made, moving in the direction of positive wheelset motion, the geometric constraint relations assume positive values.

a. WHEEL CONTACT POSITION b. RAIL CONTACT POSITION



WHEEL GAGE 53.000 IN. RAIL CANT .0250
 RAIL GAGE 56.500 IN.

c. WHEELSET ROLL

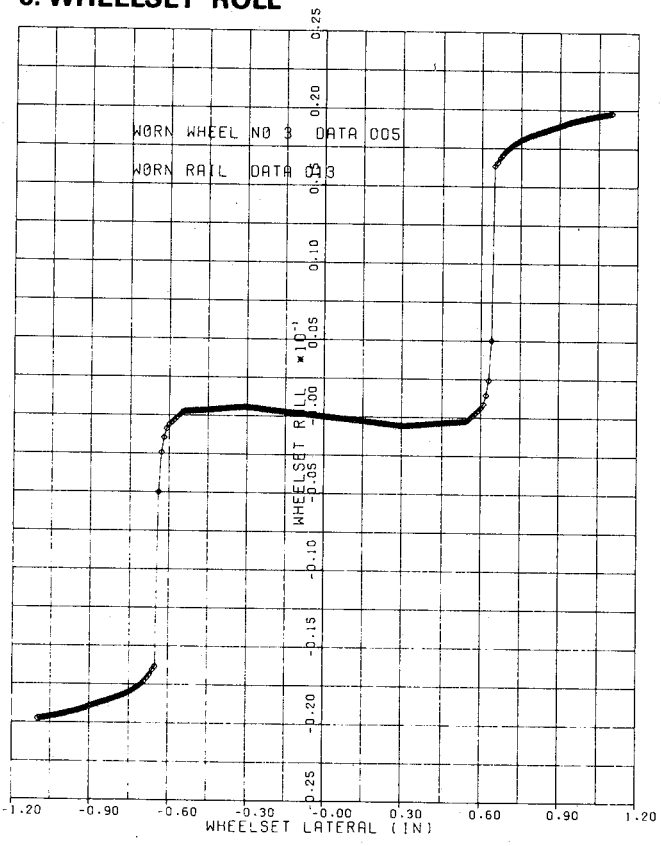
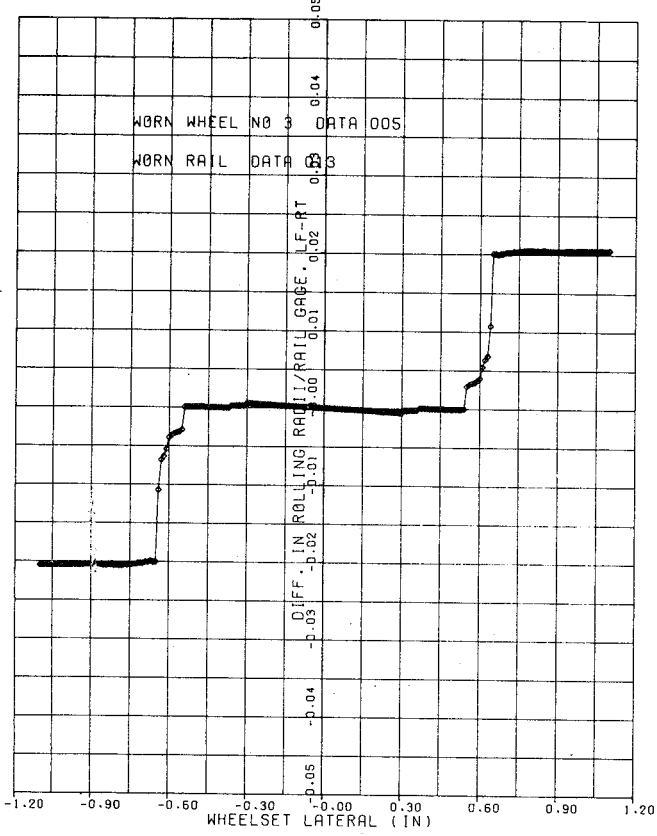
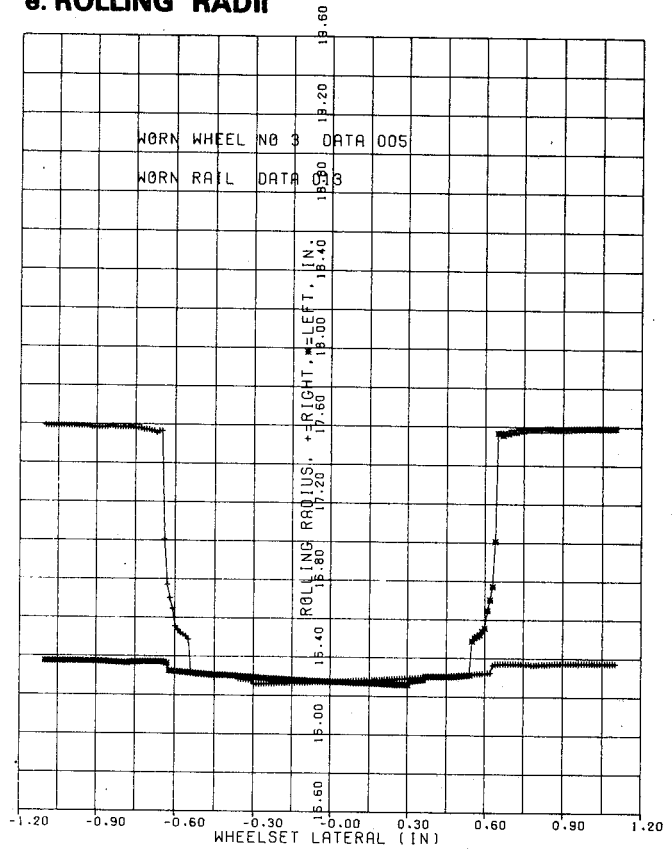


FIGURE 5-4 SEVERELY WORN WHEELS, WORN RAILS AT NOMINAL GAUGE

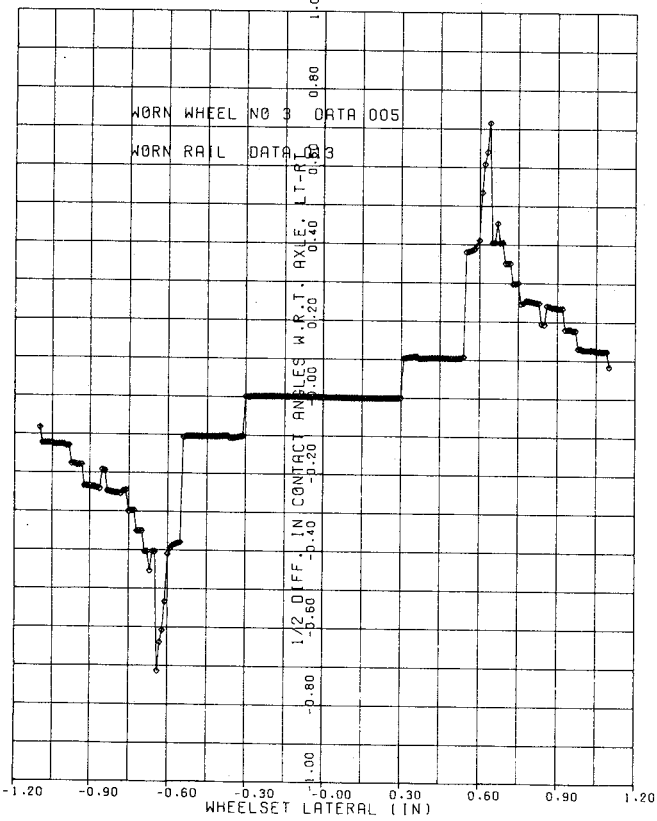
d. NORMALIZED ROLLING RADII DIFFERENCE



e. ROLLING RADII



f. ONE HALF CONTACT ANGLE DIFFERENCE



g. CONTACT ANGLES

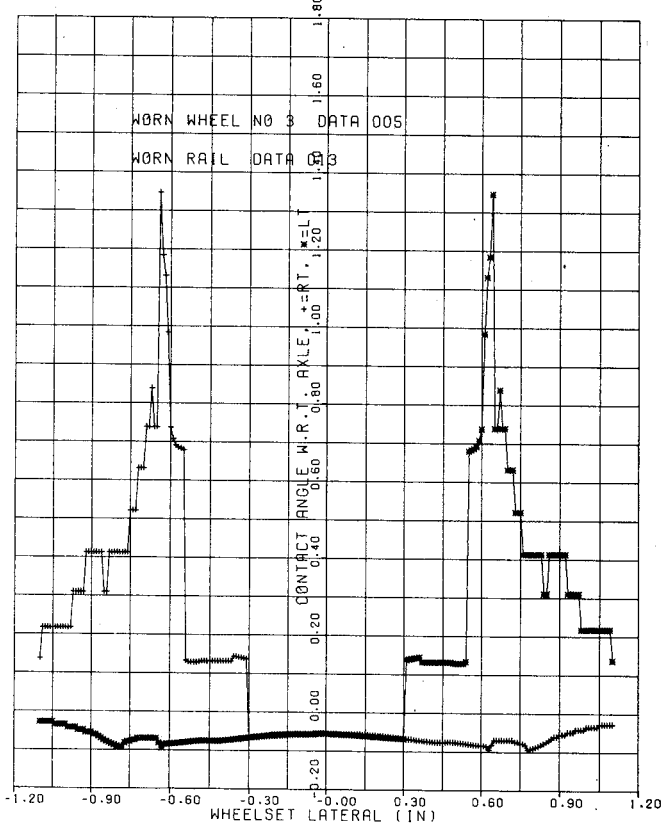


FIGURE 5-4 SEVERELY WORN WHEELS, WORN RAILS AT NOMINAL GAUGE

Heumann Profile

The original Heumann profile was designed with the express intention of obtaining single point contact between the wheel and rail at all wheelset positions. We see in figures 5-5a and 5-5b that the modified Heumann profile of figure 2-3 on our worn rail at nominal gauge closely approximates single point contact. In particular, the transition of the contact point into the flange occurs smoothly. This wide and even contact with the rail should insure that the wheel wears more uniformly than does the standard wheel profile.

The wheel/rail constraint relationships for the modified Heumann profile are also well behaved as seen in figures 5-5c,d,e,f, and g. The difference in rolling radii is approximately linear over a wide range, although the slope of this function is quite steep. Even at small amplitudes, the equivalent conicity is in the range of 0.20 to 0.40. Conicities of this magnitude produce a strongly destabilizing effect. However, the difference in contact angles and wheelset roll angle also have steep slopes. Thus, the gravitational stiffness for a heavily loaded vehicle may offset the destabilizing effect of a high conicity.

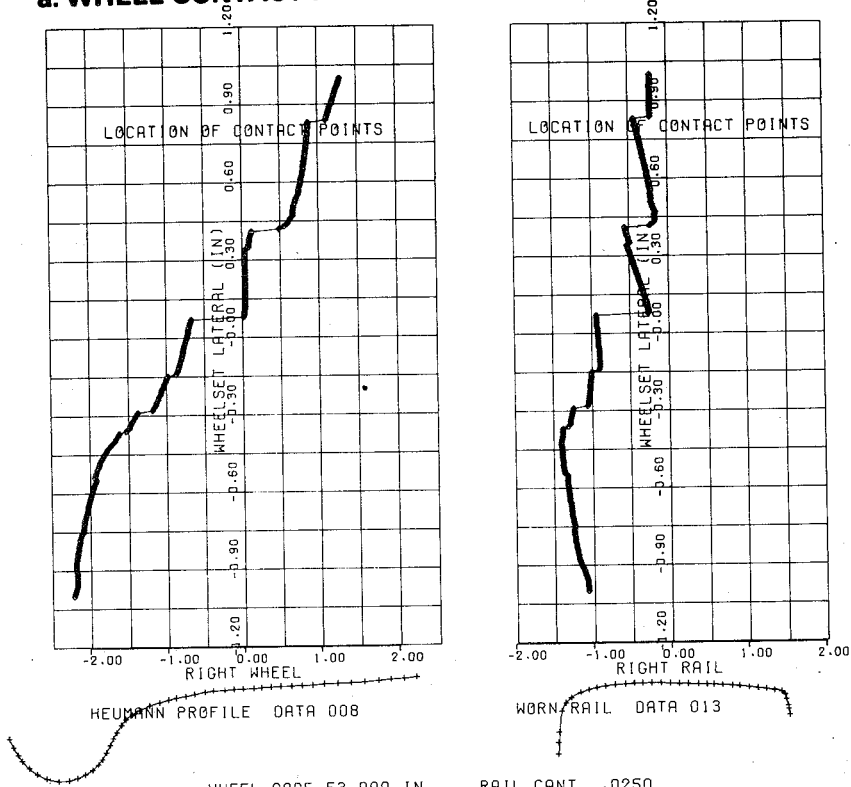
There is no clear transition between tread contact and flange contact with the Heumann profile, although one may see a rapid rise in the contact angles at a lateral displacement of about 0.30 inches. At large wheelset lateral displacements the wheel/rail constraint functions reach levels comparable to those for new, slightly worn and moderately worn wheel profiles.

Summary of Wheel Wear Effects

The influence of the various wheel profiles on rail vehicle dynamics can be summarized by comparing the describing functions of the constraint functions for each wheel profile. Figure 5-6 shows the sinusoidal input describing function of the normalized difference in rolling radii for the five wheels discussed in the preceding sections. Here we see that the describing functions of the effective conicity, in the range before the flange contacts, is largest for the modified Heumann profile, is somewhat smaller for the slightly worn wheel, is small but positive for the new wheel and is negative for the two most worn wheel

a. WHEEL CONTACT POSITION

b. RAIL CONTACT POSITION



RAIL CANT .0250

c. WHEELSET ROLL

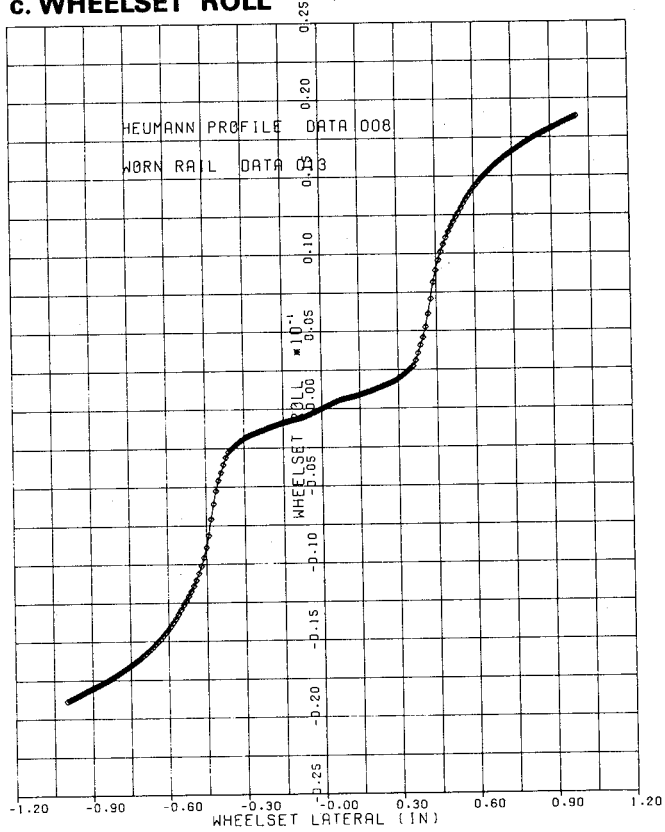
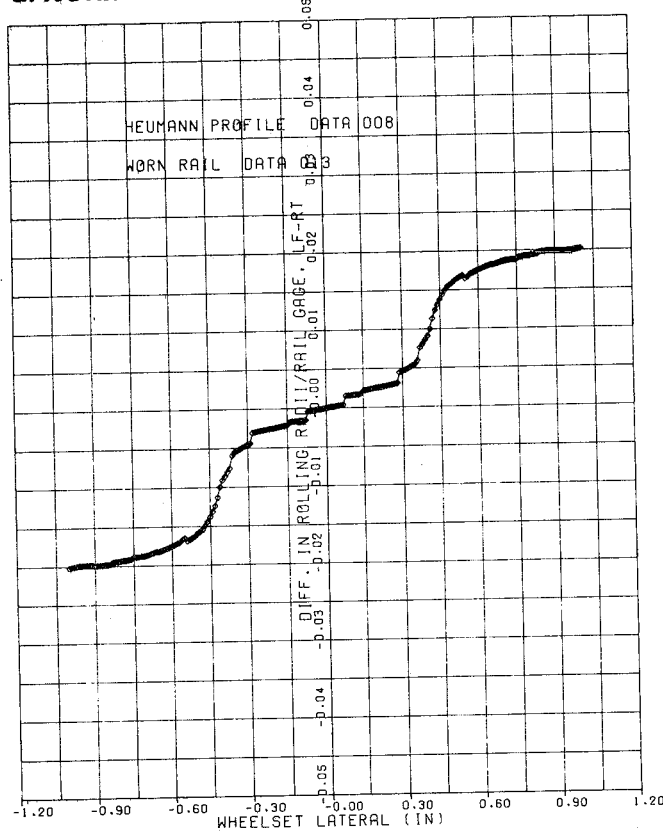
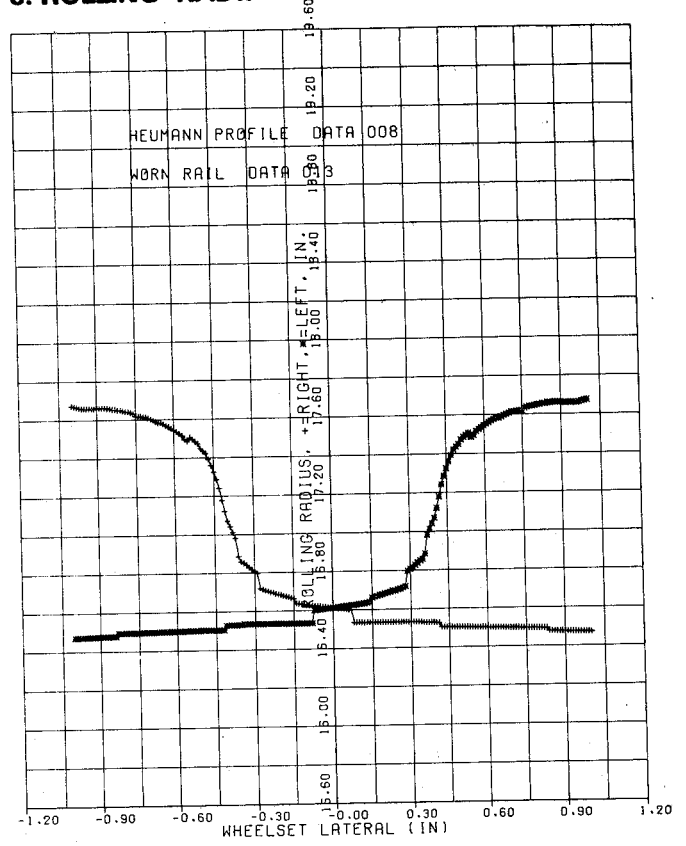


FIGURE 5-5 MODIFIED HEUMANN WHEELS, WORN RAILS AT NOMINAL GAUGE

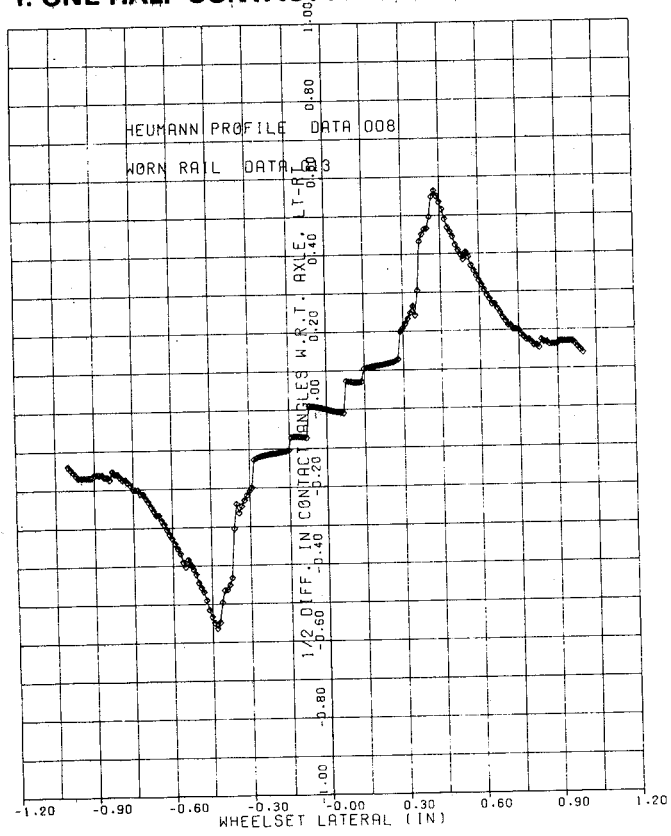
d. NORMALIZED ROLLING RADII DIFFERENCE



e. ROLLING RADII



f. ONE HALF CONTACT ANGLE DIFFERENCE



g. CONTACT ANGLES

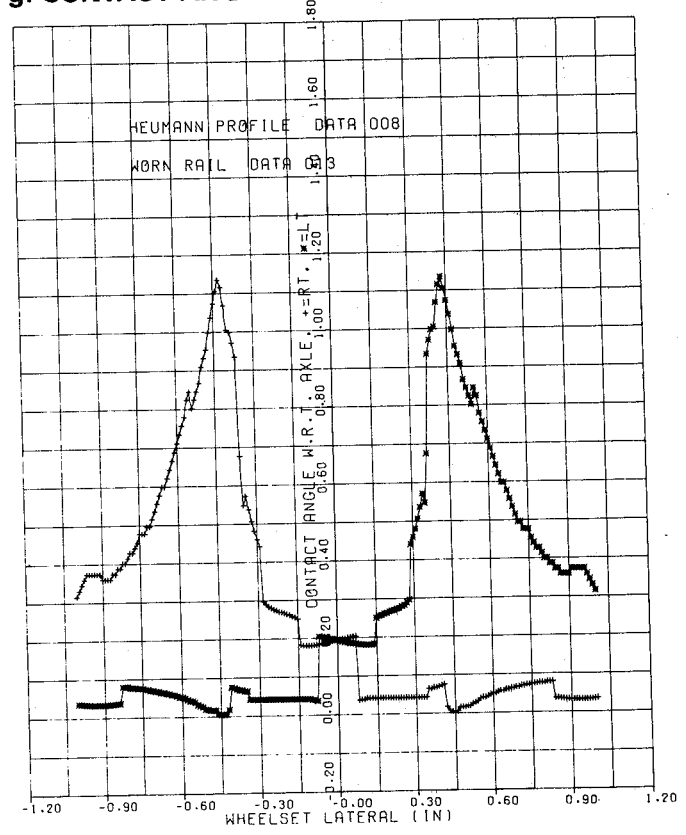


FIGURE 5-5 MODIFIED HEUMANN WHEELS, WORN RAILS AT NOMINAL GAUGE

$$\left(\frac{r_L - r_R}{2a_r}\right) \text{ quasi-linear} = \text{Describing Function} \times \frac{x_w}{a_w}$$

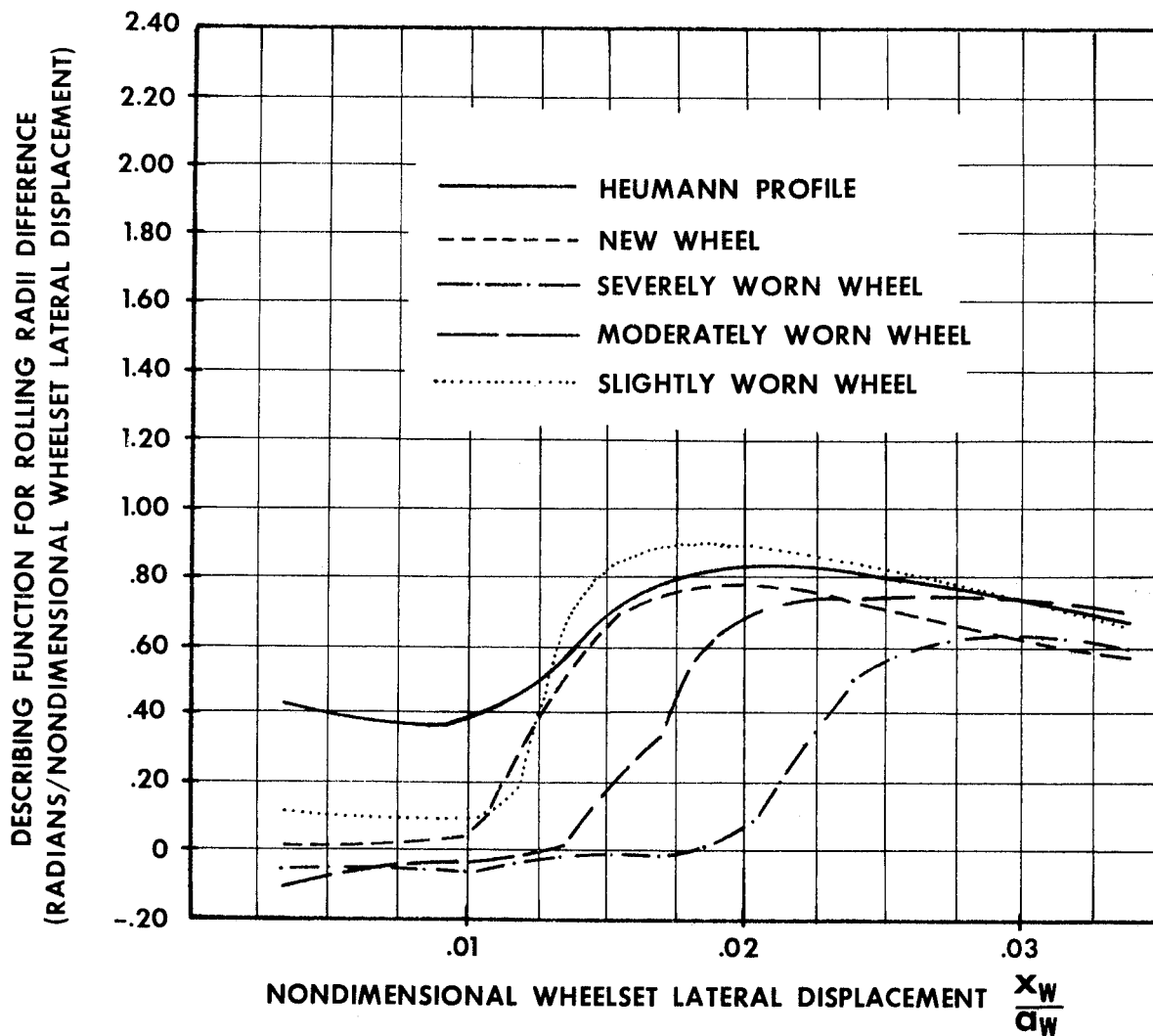


FIGURE 5-6 DESCRIBING FUNCTION FOR ROLLING RADII DIFFERENCE

vs.

NONDIMENSIONAL WHEELSET LATERAL DISPLACEMENT

(WORN RAILS, NOMINAL GAUGE $a_w = 29.562$ in.)

profiles. We see, in these results, that the large conicity of the Heumann profile may cause hunting to begin at a very low speed unless the vehicle is specifically designed to accommodate these characteristics. The slightly worn or new wheels tend to promote more stable behavior. However, the negative conicity exhibited by the two most worn wheels will probably cause vehicles to diverge from the centered position on the rails at all speeds and seek a position or oscillation with one or more flanges contacting the rail.

The sinusoidal input describing functions of one half the difference in contact angles for these same wheel profiles are plotted in figure 5-7. The contact angle difference describing function, at low amplitudes, is greatest for the modified Heumann and slightly worn wheel profiles. The other wheel profiles have relatively small contact angle differences until flange contact occurs. Thus, due to the importance of the contact angle difference in the gravitational stiffness expression, we expect that the gravitational stiffness effect on a heavily loaded Heumann or slightly worn wheel may be large enough to counter the destabilizing effect of the relatively large conicity of these same wheels and allow stable running over a reasonable speed range. For the two worn wheels and the new wheel the gravitational stiffness is not large enough to affect the dynamic behavior during small lateral wheelset excursions. When the wheel/rail contact moves up the flange, the gravitational stiffness is, of course, the primary stabilizing influence.

The describing functions of the wheelset roll function for the various wheel profiles studied here are illustrated in figure 5-8. Here we see that only the Heumann profile has a large describing function value for small wheelset lateral displacements. At larger amplitudes, when the contact position moves up on the wheel flange, the roll coefficient is about the same for all these wheel profiles, although the wheelset lateral position for flange contact differs.

To summarize, we could group the wheel profiles discussed here into three categories. The Heumann and slightly worn wheel belong in a category typified by large conicity and large gravitational stiffness. The new wheel, by comparison, has smaller conicity and very low gravitational

$$\left(\frac{\delta_L - \delta_R}{2}\right) \text{ quasi-linear} = \text{Describing Function} \times \frac{x_w}{a_w}$$

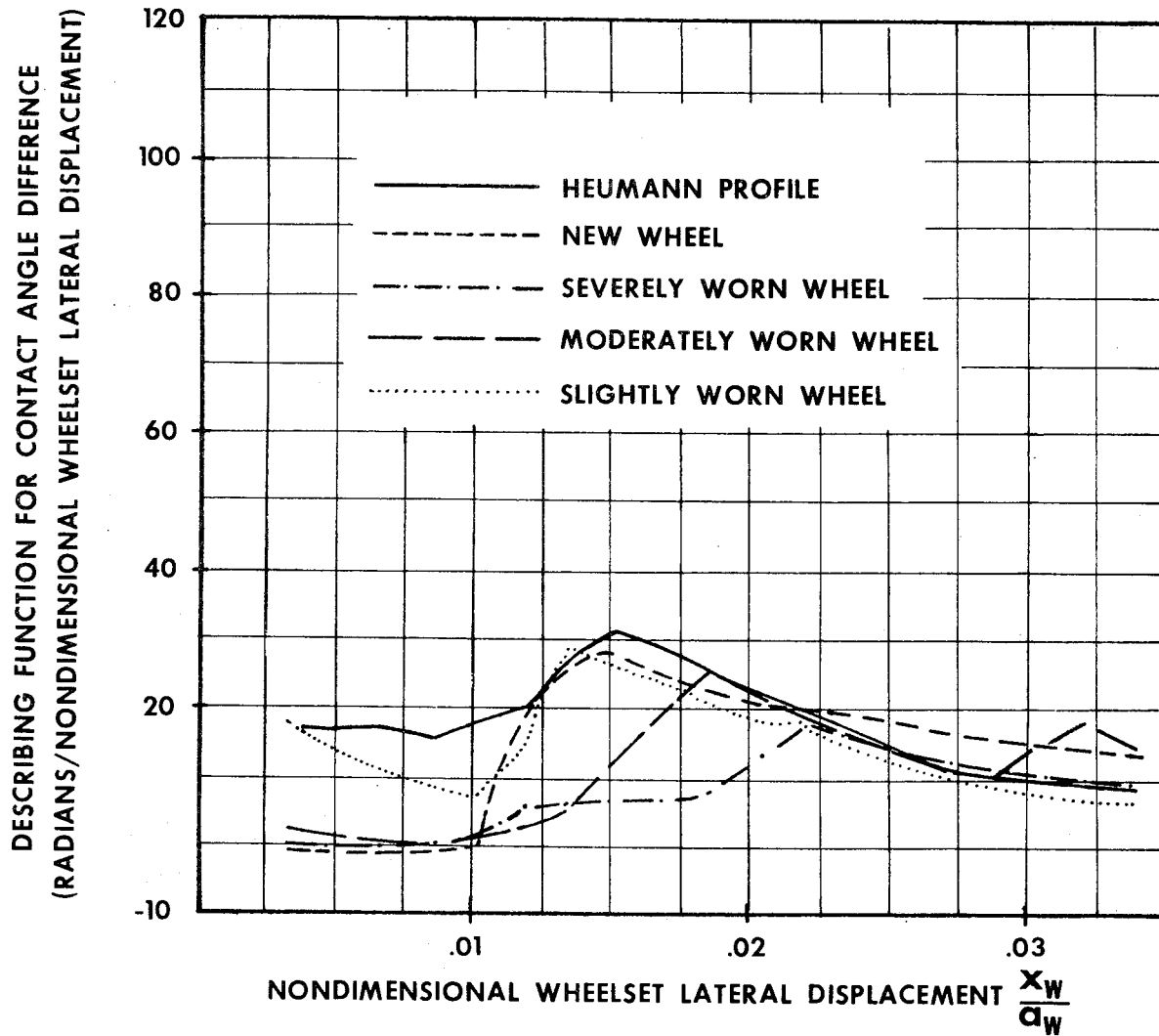


FIGURE 5-7 CONTACT ANGLE DIFFERENCE DESCRIBING FUNCTION

vs.

NONDIMENSIONAL WHEELSET LATERAL DISPLACEMENT

(WORN RAILS, NOMINAL GAUGE, $a_w = 29.562$ in.)

$$(\phi_w)_{\text{quasi-linear}} = \text{Describing Function} \times \frac{x_w}{a_w}$$

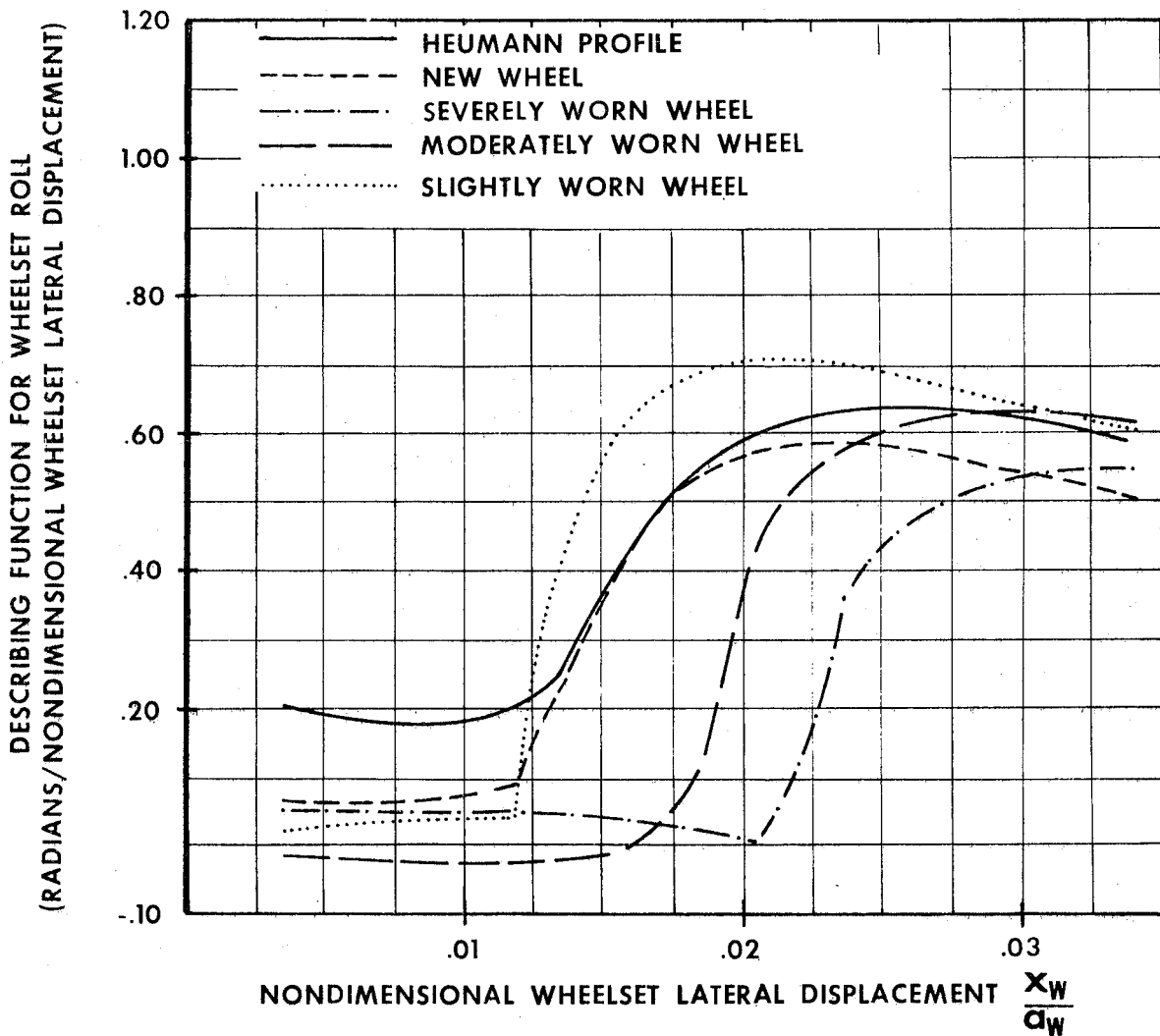


FIGURE 5-8 DESCRIBING FUNCTION FOR WHEELSET ROLL

vs.

NONDIMENSIONAL WHEELSET LATERAL DISPLACEMENT

(WORN RAILS, NOMINAL GAUGE, $a_w=29.562$ in.)

stiffness. The two most worn wheels fall in a group characterized by negative conicity at small wheelset lateral amplitudes. Each of these three groups has a distinct and different influence on vehicle behavior.

RAIL GAUGE EFFECTS

The effect of rail gauge variation on the wheel/rail geometric constant relationships is examined in this section by comparing tight and wide gauge results for new and severely worn wheels on worn rail.

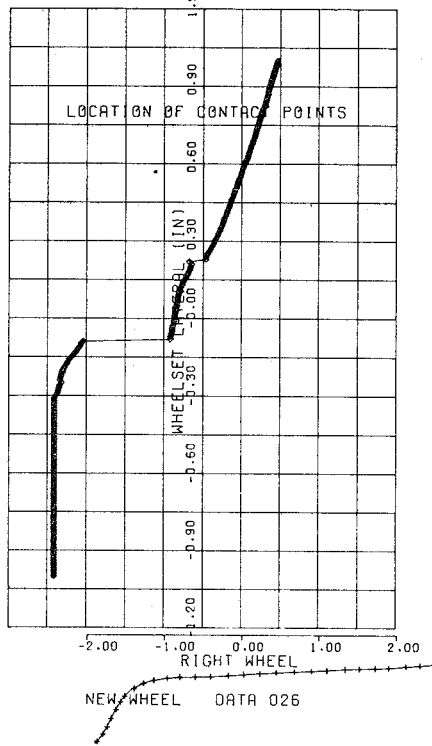
New Wheels

The contact positions and constraint relationships for the new wheel on worn rail at tight gauge are shown in figure 5-9. Figure 5-10 illustrates this information for the same wheel/rail combination at wide gauge. At a "tight" gauge of 56 inches the rail gauge was one-half inch narrower than the nominal value of 56.5 inches. The rail gauge for the "wide" gauge analysis was 57.5 inches, one inch wider than nominal. This range from wide to tight gauge corresponds to the maximum gauge variation permitted on Class 5 track.

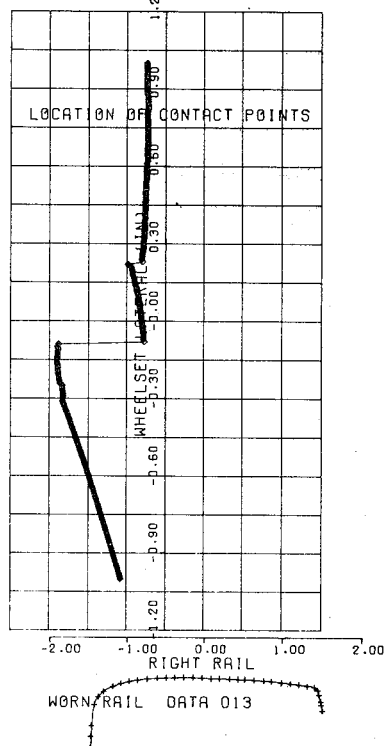
Comparison of the contact position functions in figures 5-1,5-9, and 5-10 reveals that the major effect of rail gauge variation on these functions is to shift the contact curves laterally. The contact position on the rail remains in a narrow band until the wheel flange contacts the rail. The wheelset lateral position at flange contact varies, of course, with rail gauge. As expected, the change in clearance before flange contact is one-half the change in rail gauge.

Not surprisingly, the only effect of rail gauge on the wheel/rail constraint relationships for the new wheel is to shift the position where the flange contact effects dominate these functions. In the rolling radii difference, contact angle difference and roll angle functions shown in figures 5-9 and 5-10 we see that the lateral wheelset position where these quantities begin to increase rapidly shifts by exactly the change in flange clearance. Thus the chief effect of rail gauge on the behavior of vehicles with new wheels is to limit the range of lateral motion before flange contact occurs. The rail gauge change will not affect the dynamic behavior as long as the flange contact does not occur during the wheelset motion.

a. WHEEL CONTACT POSITION



b. RAIL CONTACT POSITION



WHEEL GAGE 53.000 IN.
RAIL GAGE 56.000 IN.

RAIL CANT .0250

c. WHEELSET ROLL

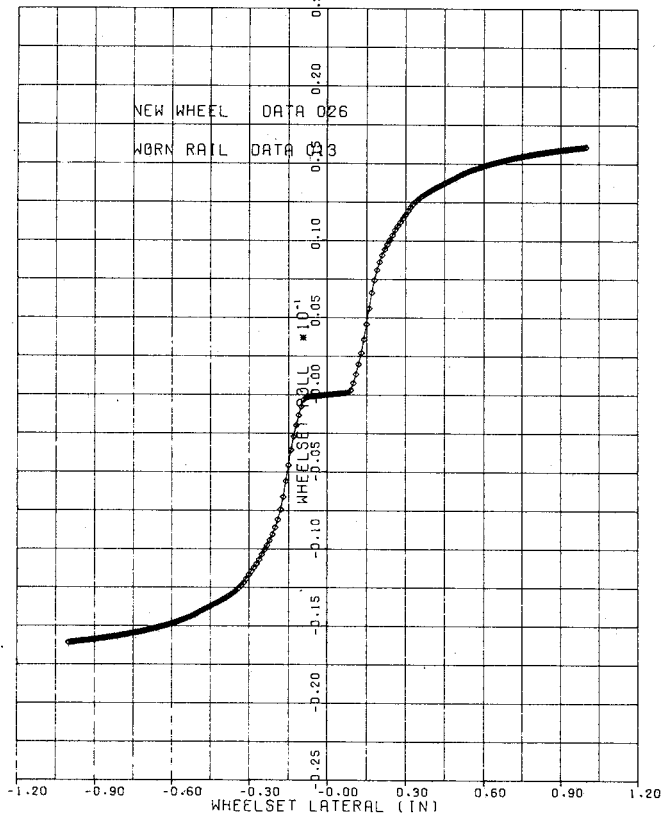
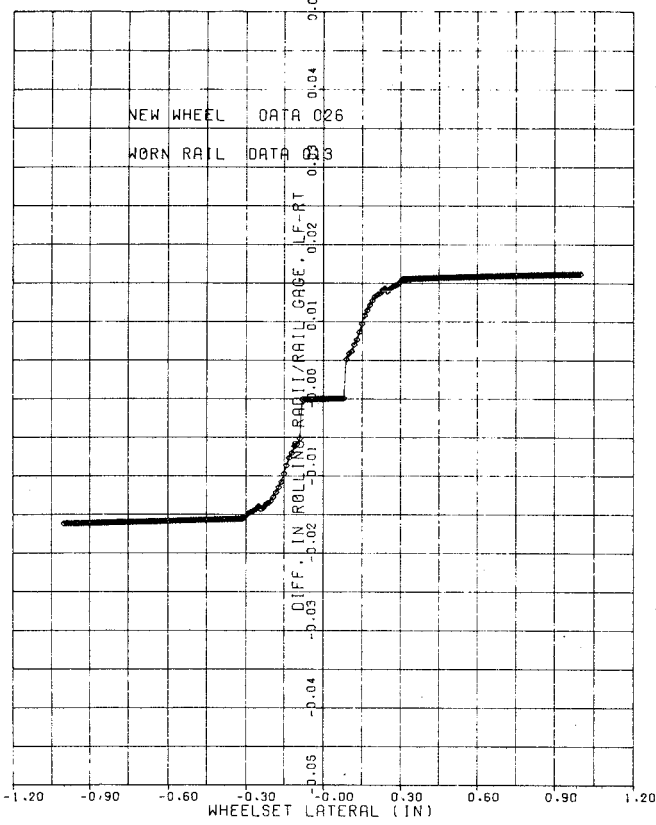
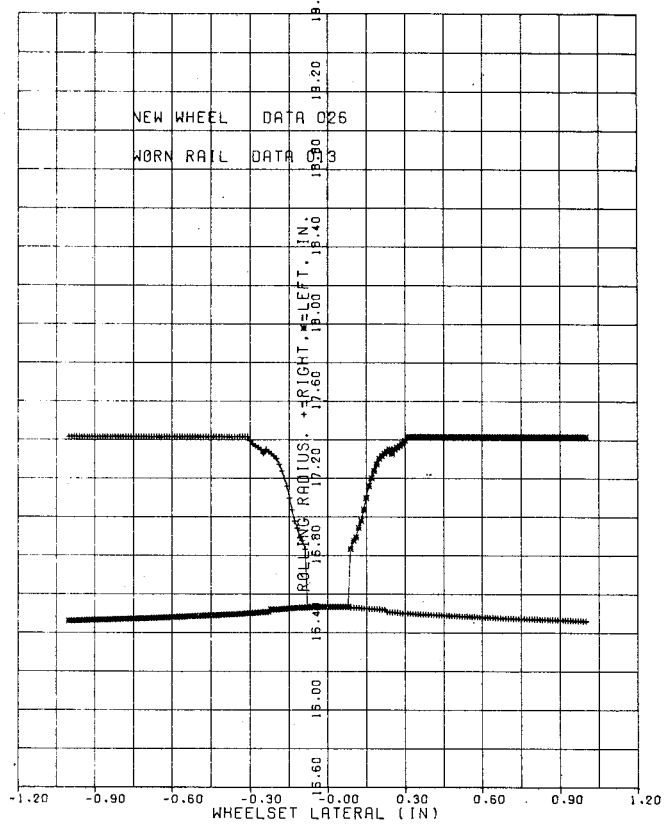


FIGURE 5-9 NEW WHEELS, WORN RAILS AT TIGHT GAUGE

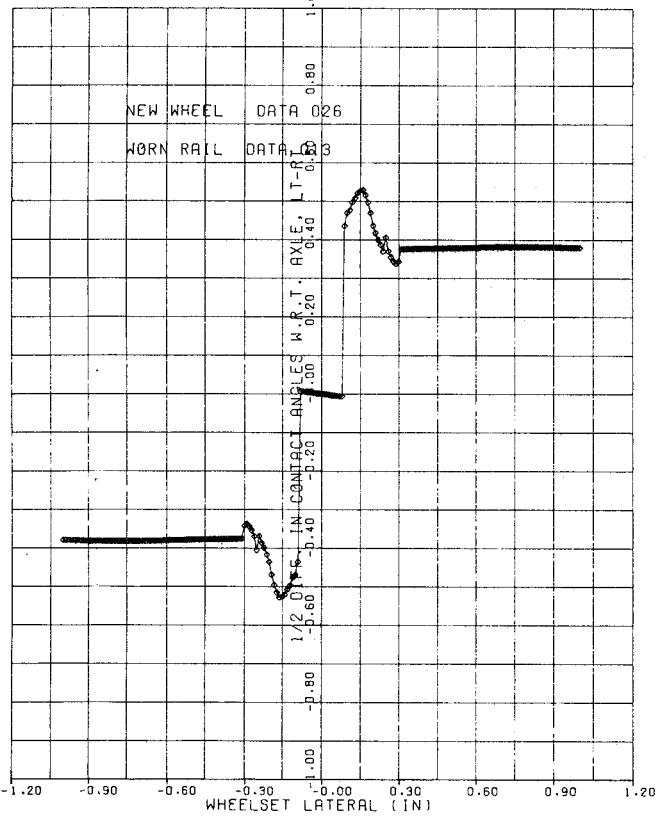
d. NORMALIZED ROLLING RADII DIFFERENCE



e. ROLLING RADII



f. ONE HALF CONTACT ANGLE DIFFERENCE



g. CONTACT ANGLES

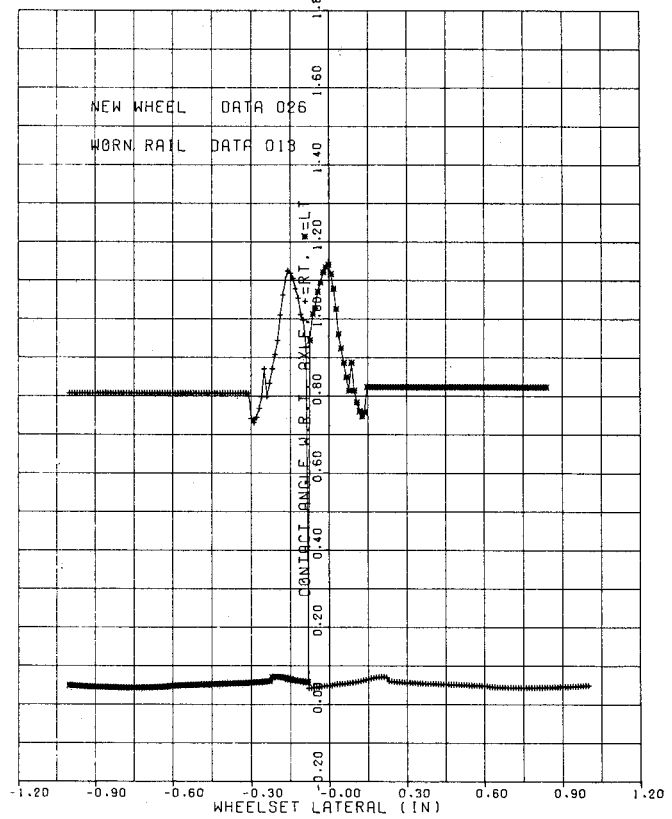
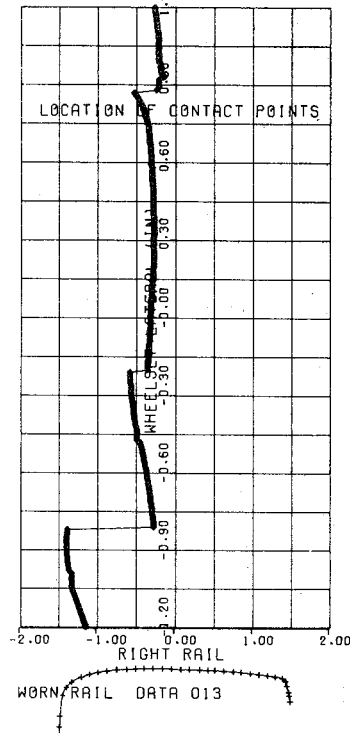
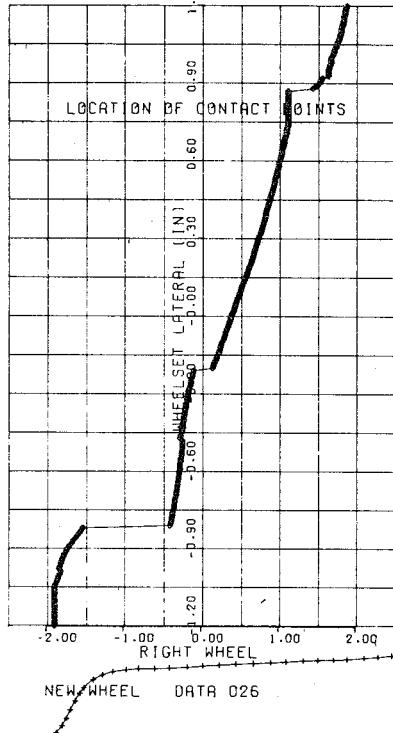


FIGURE 5-9 NEW WHEELS, WORN RAILS AT TIGHT GAUGE

a. WHEEL CONTACT POSITION

b. RAIL CONTACT POSITION



WHEEL GAGE 53.000 IN.
RAIL GAGE 57.500 IN.

RAIL CANT .0250

c. WHEELSET ROLL

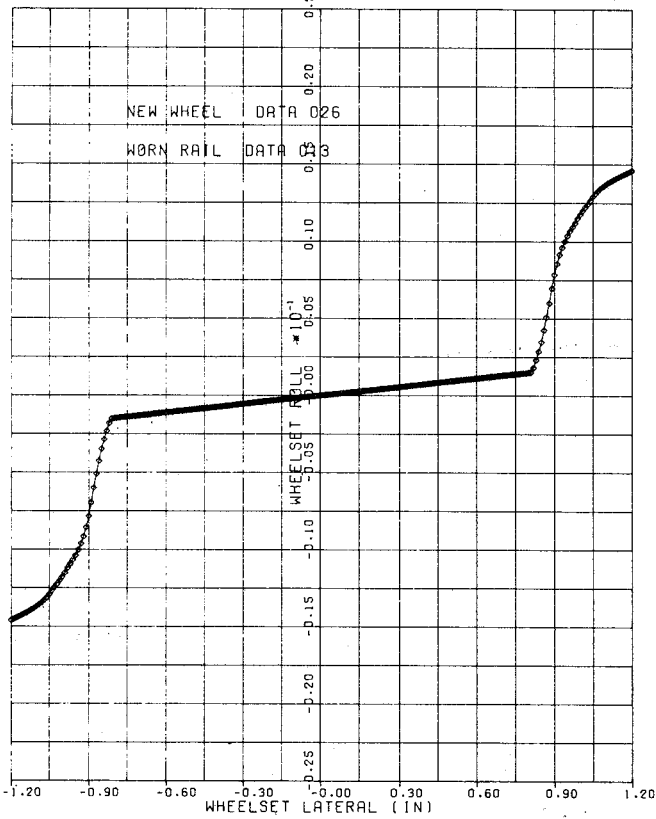
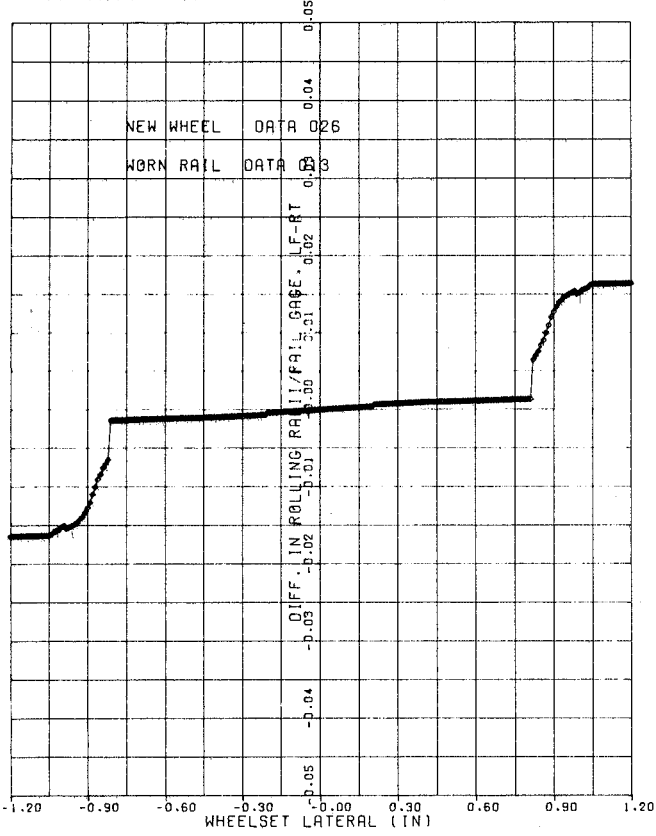
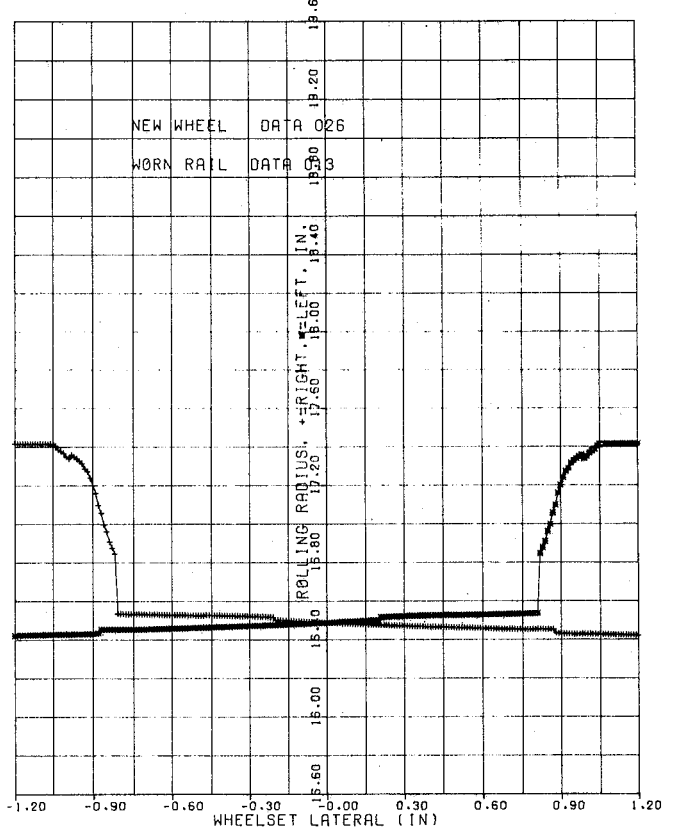


FIGURE 5-10 NEW WHEELS, WORN RAILS AT WIDE GAUGE

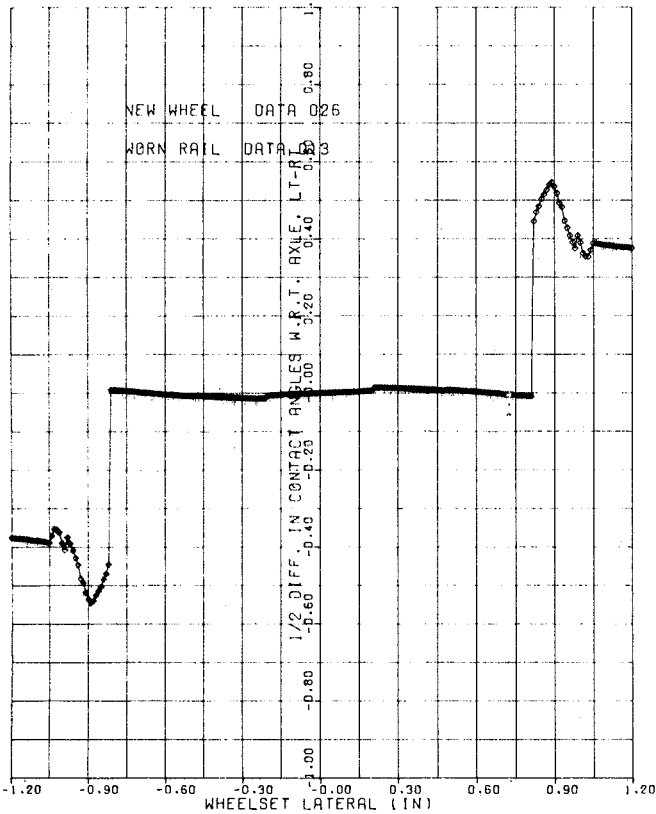
d. NORMALIZED ROLLING RADII DIFFERENCE



e. ROLLING RADII



f. ONE HALF CONTACT ANGLE DIFFERENCE



g. CONTACT ANGLES

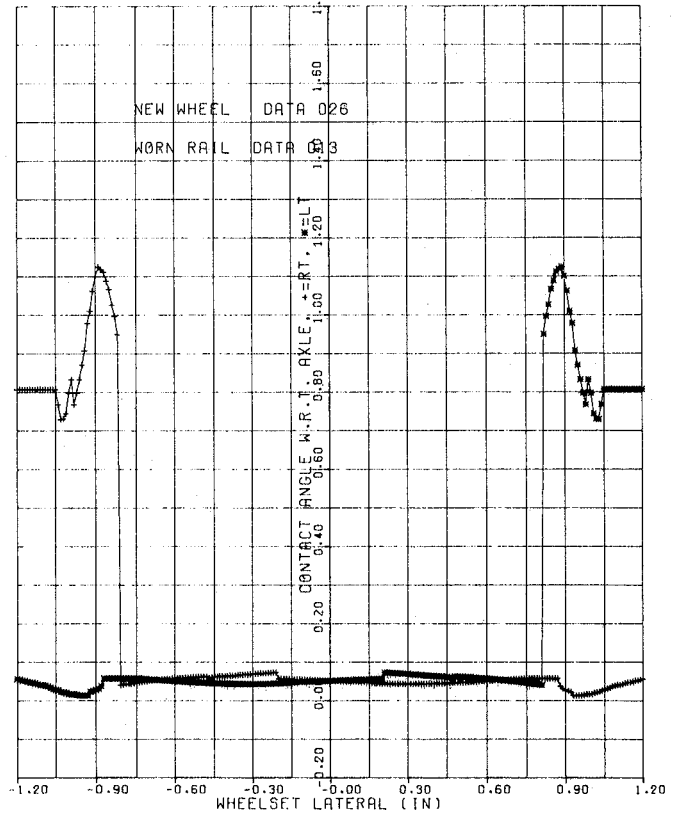


FIGURE 5-10 NEW WHEELS, WORN RAILS AT WIDE GAUGE

Worn Wheels

The contact positions and constraint relationships for the severely worn wheel, profile #3 of figure 2-2, on worn rails, profile A in figure 2-5, at tight and wide gauge conditions are shown in figures 5-11 and 5-12. The geometric constraints for worn wheels, unlike new wheels, change character significantly with gauge variation. The wheel contact position at tight gauge shifts to the inside or gauge side for a greater percentage of the lateral wheelset travel and remains on the field side of the wheel for a majority of the lateral wheelset positions at wide gauge. The shift of the wheel contact position to the outside at wide gauge is expected. However, it is somewhat surprising to note that the contact position on the rail at wide gauge also moves to the field side of the rail. This effect is due to a shift in wheel contact to the downward sloping segment of that profile, where it contacts the rail at the point of equal slope on the field side of the rail.

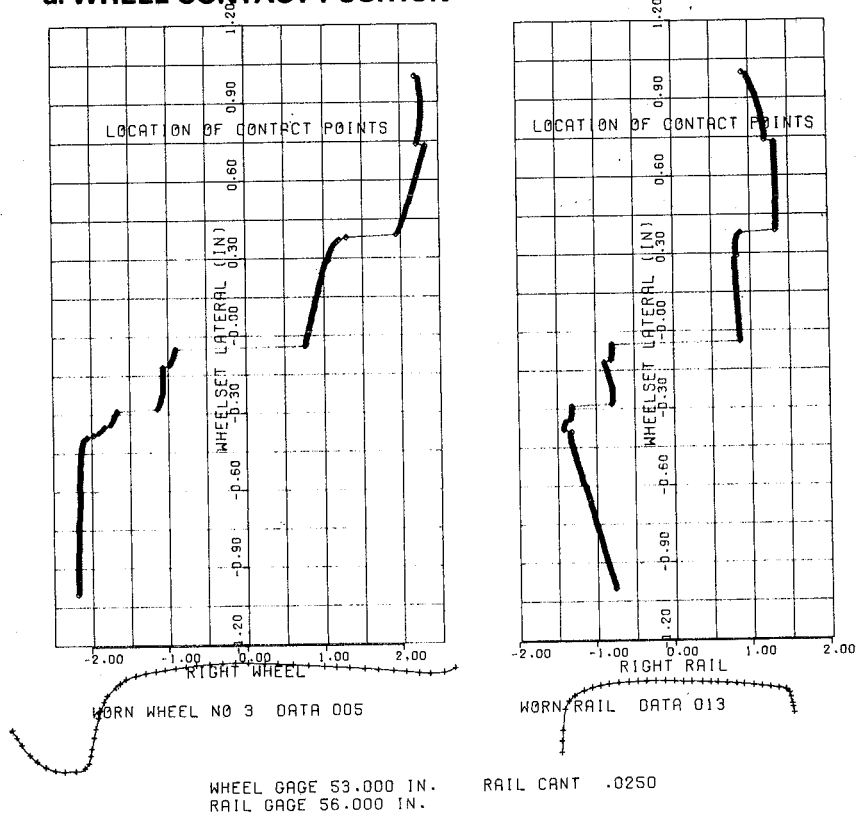
The change in rail gauge, in addition to the obvious direct effect on the clearance before flange climbing begins, strongly influences the difference in rolling radii, difference in contact angle, and roll angle relationships. We see, in figures 5-11 and 5-12, that the slope of these three relationships in the region about the centered position, is positive at tight gauge, but negative at wide gauge. Variations of this magnitude in these slopes will change the vehicle stability significantly. In fact, it is quite likely that the spurts of hunting often observed in rail vehicle operation can be attributed to rail gauge changes that alter the wheel/rail geometric constraint relationships.

Summary of Rail Gauge Effects

The sinusoidal input describing functions for rolling radii difference, contact angle difference and wheelset roll shown in figures 5-13, 5-14, and 5-15 illustrate the overall effects of rail gauge variation on the wheel/rail constraints. The new wheel at tight gauge climbs the flange almost immediately, causing rapid increases in the describing function values for all three quantities. At wide gauge, however, these quantities remain nearly constant for wheelset amplitudes to 0.75 inches, where flange contact occurs. The describing functions increase rapidly

a. WHEEL CONTACT POSITION

b. RAIL CONTACT POSITION



c. WHEELSET ROLL

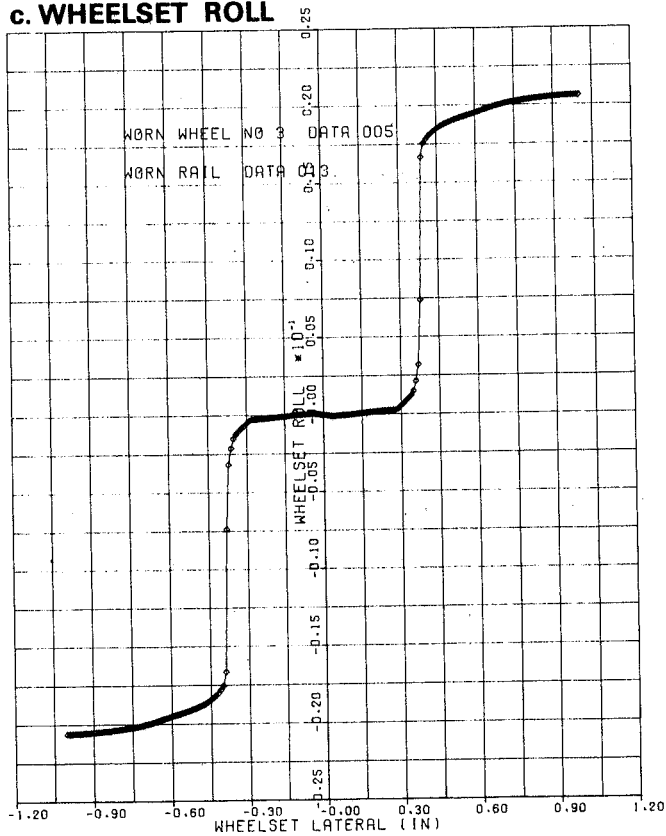
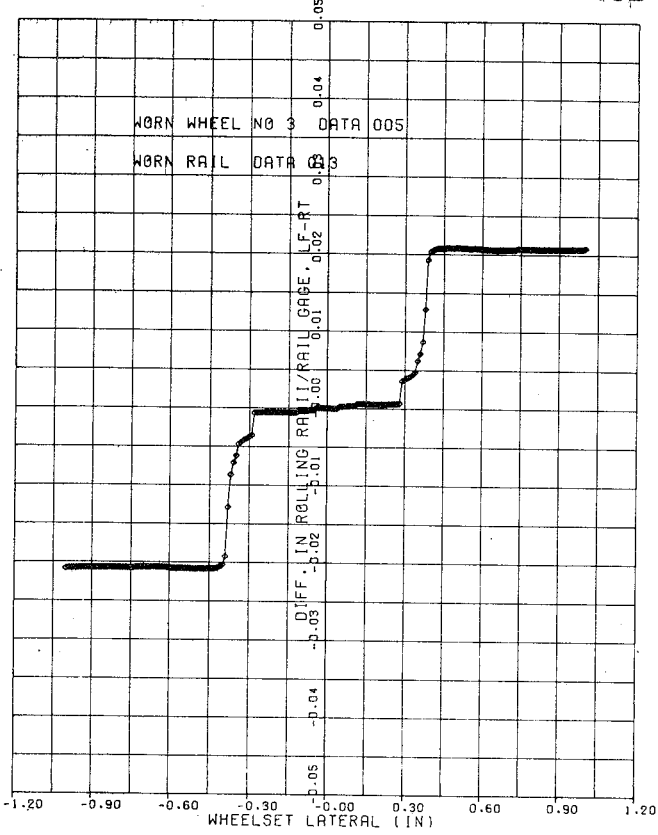
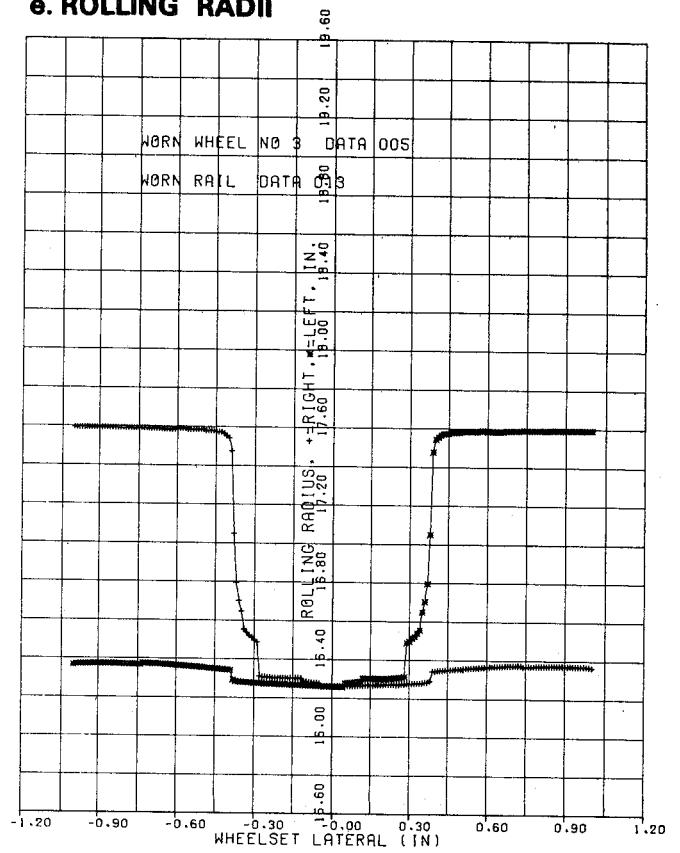


FIGURE 5-11 SEVERELY WORN WHEELS, WORN RAILS AT TIGHT GAUGE

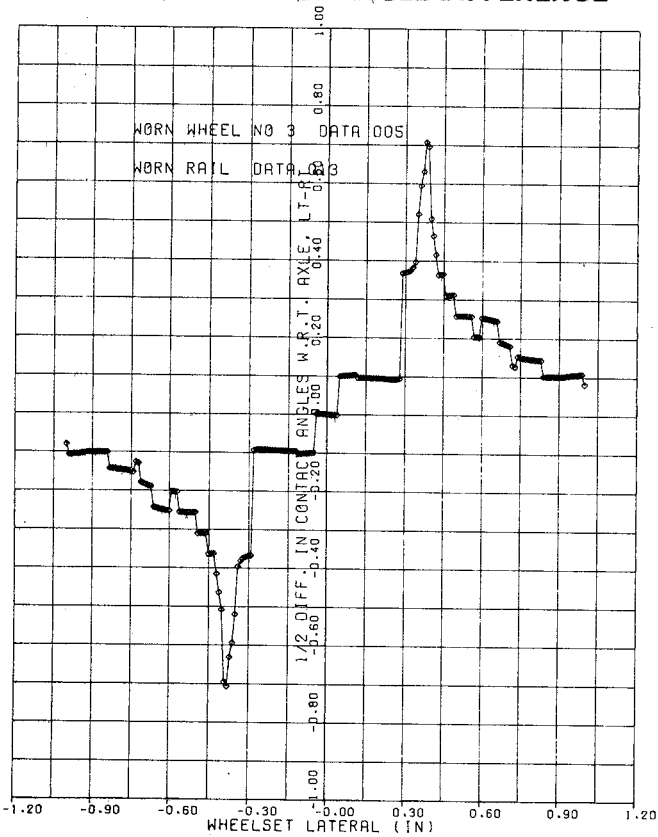
d. NORMALIZED ROLLING RADII DIFFERENCE



e. ROLLING RADII



f. ONE HALF CONTACT ANGLE DIFFERENCE



g. CONTACT ANGLES

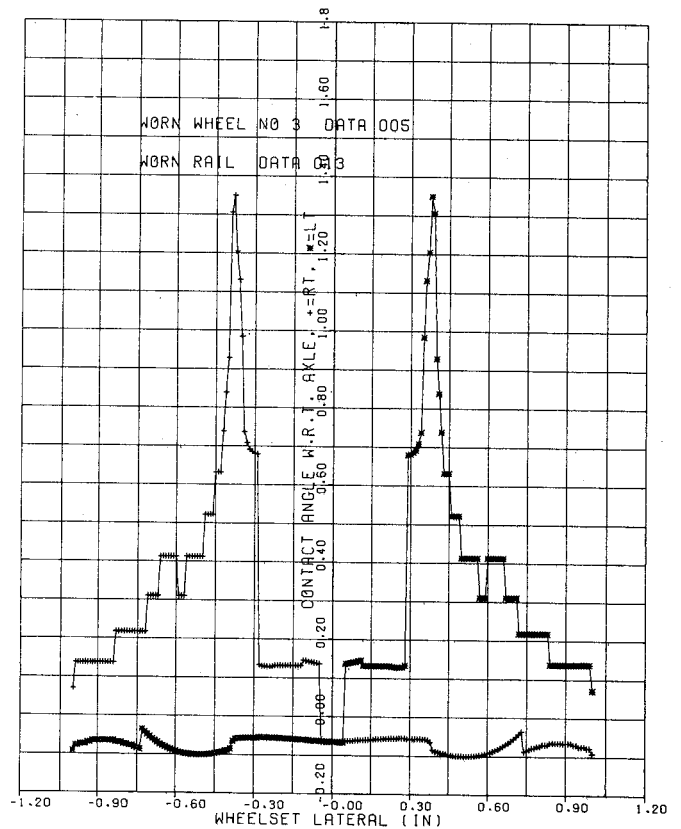
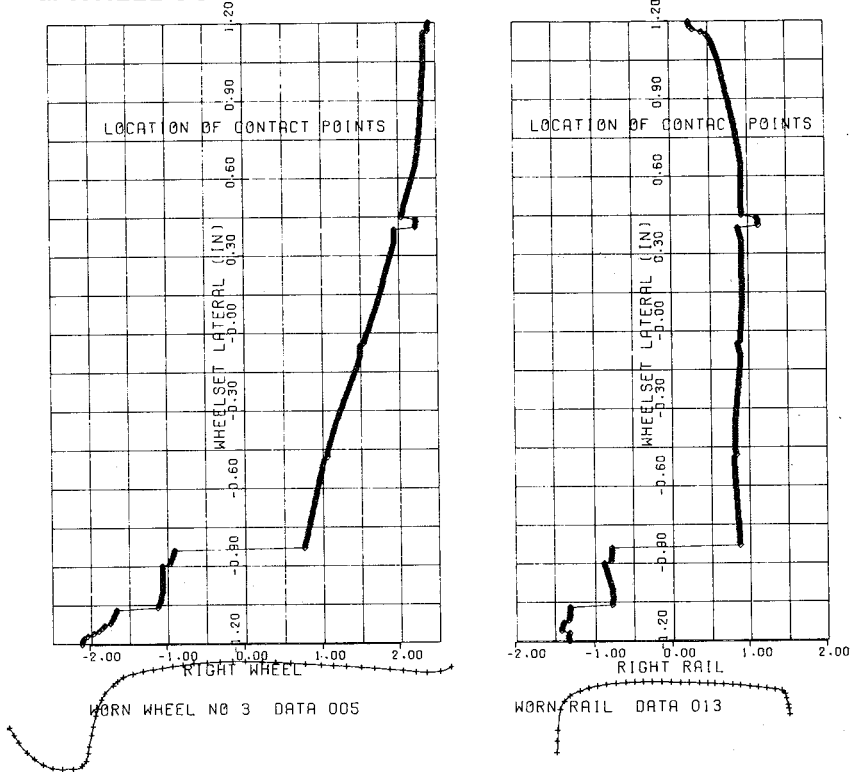


FIGURE 5-11 SEVERELY WORN WHEELS, WORN RAILS AT TIGHT GAUGE

a. WHEEL CONTACT POSITION

b. RAIL CONTACT POSITION



WHEEL GAGE 53.000 IN. RAIL CANT .0250
 RAIL GAGE 57.500 IN.

c. WHEELSET ROLL

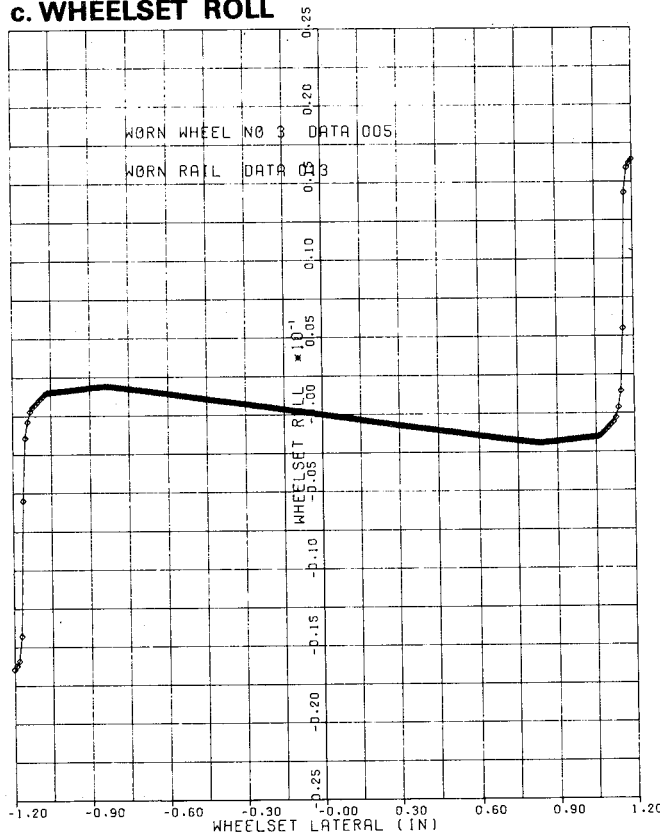
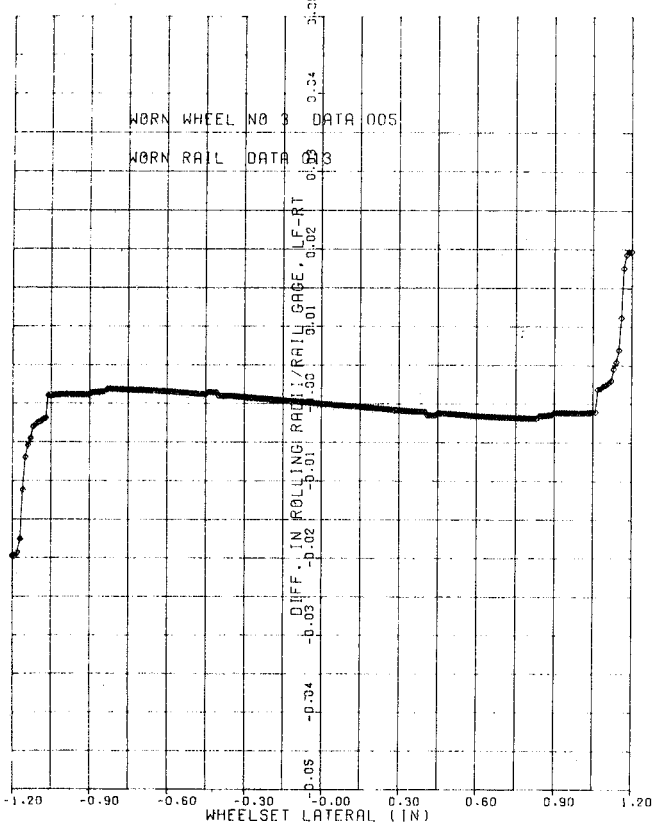
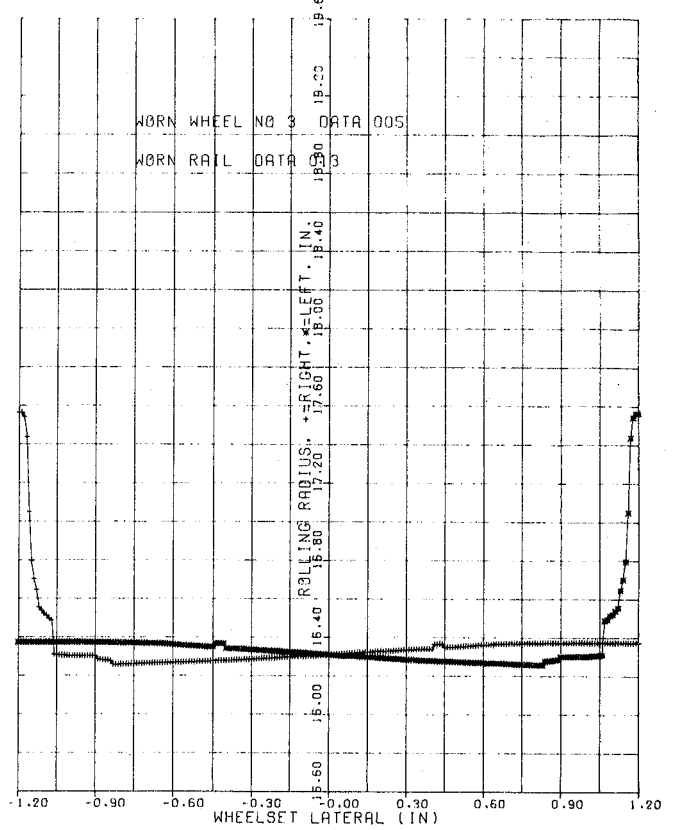


FIGURE 5-12 SEVERELY WORN WHEELS, WORN RAILS AT WIDE GAUGE

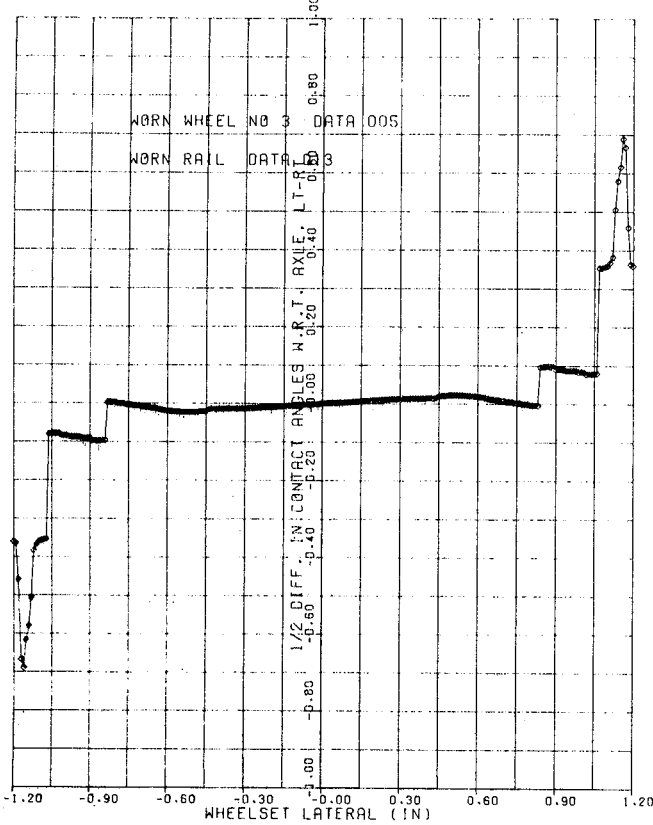
d. NORMALIZED ROLLING RADII DIFFERENCE



e. ROLLING RADII



f. ONE HALF CONTACT ANGLE DIFFERENCE



g. CONTACT ANGLES

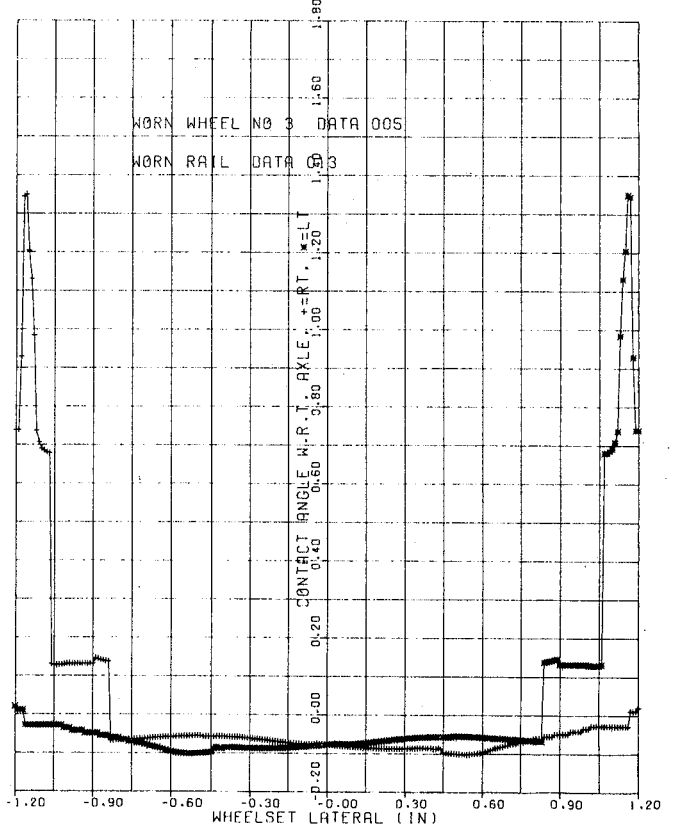


FIGURE 5-12 SEVERELY WORN WHEELS, WORN RAILS AT WIDE GAUGE

$$\left(\frac{r_L - r_R}{2a_r}\right) \text{ quasi-linear} = \text{Describing Function} \times \frac{x_w}{a_w}$$

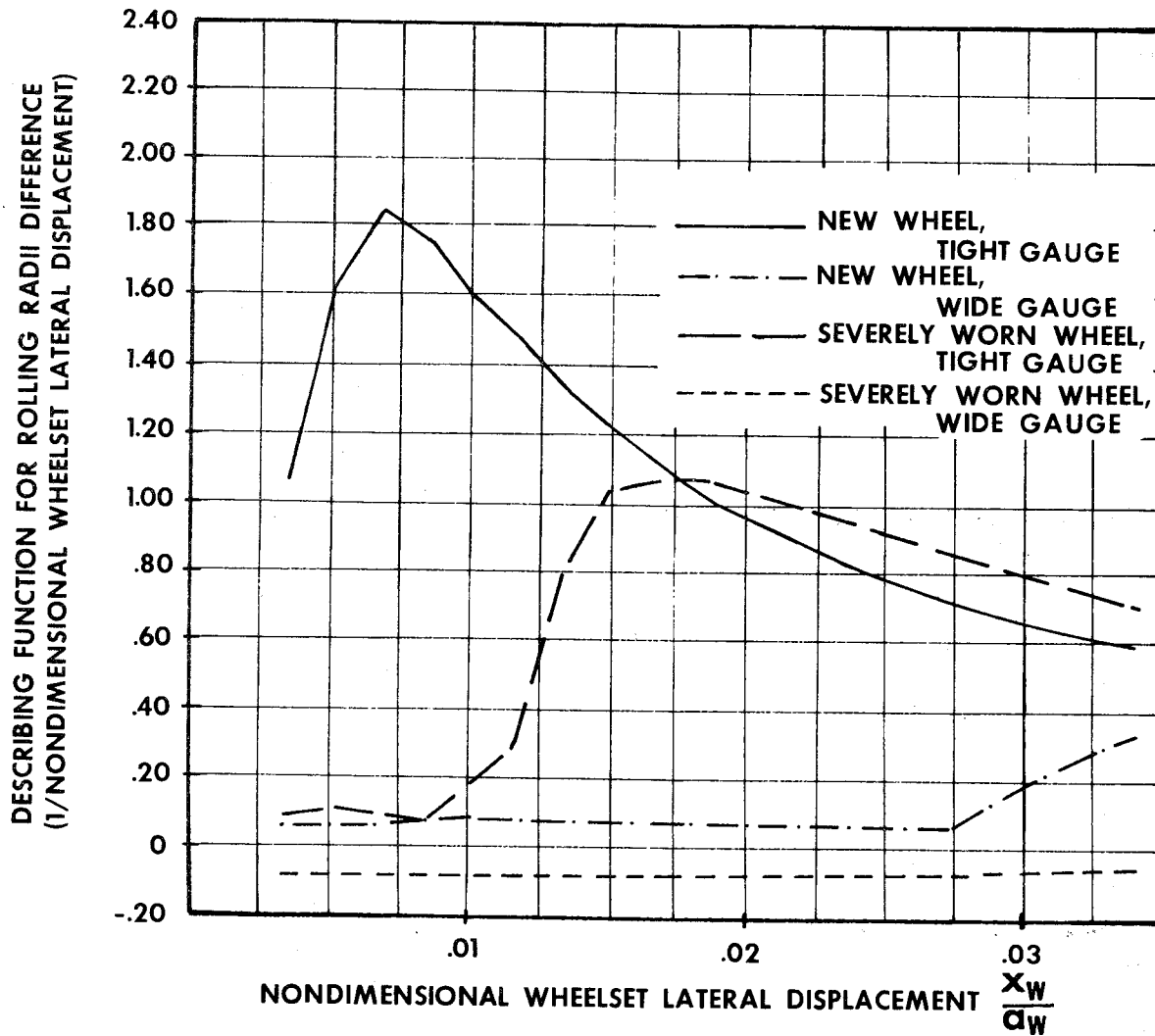


FIGURE 5-13 DESCRIBING FUNCTION FOR ROLLING RADII DIFFERENCE

vs.

NONDIMENSIONAL WHEELSET LATERAL DISPLACEMENT
(WORN RAILS, $a_w = 29.562$ in.)

$$\left(\frac{\delta_L - \delta_R}{2}\right) \text{ quasi-linear} = \text{Describing Function} \times \frac{x_W}{a_W}$$

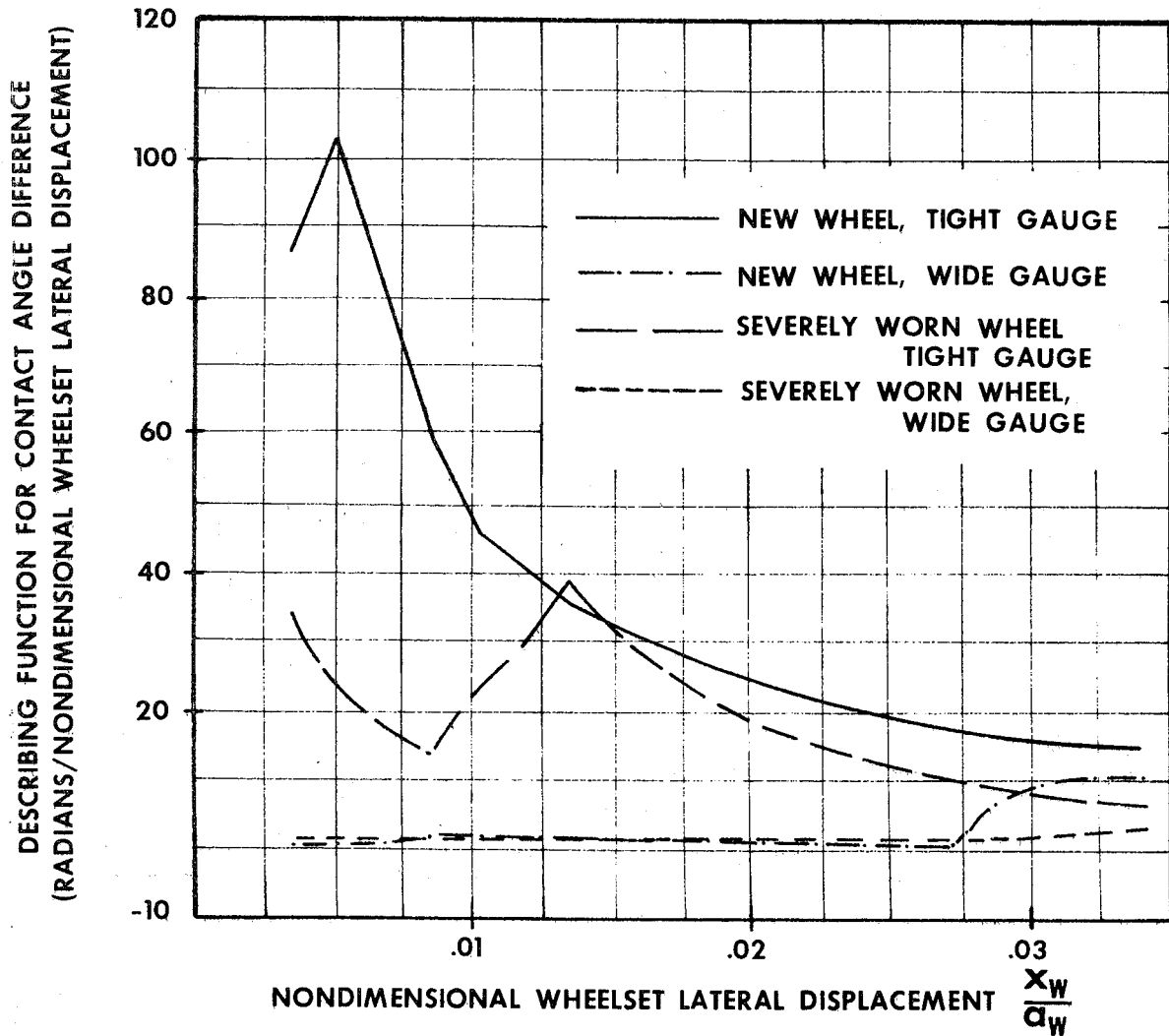


FIGURE 5-14 CONTACT ANGLE DIFFERENCE DESCRIBING FUNCTION

vs.

NONDIMENSIONAL WHEELSET LATERAL DISPLACEMENT

(WORN RAILS, $a_W = 29.562$ in.)

$$(\phi_w)_{\text{quasi-linear}} = \text{Describing Function} \times \frac{x_w}{a_w}$$

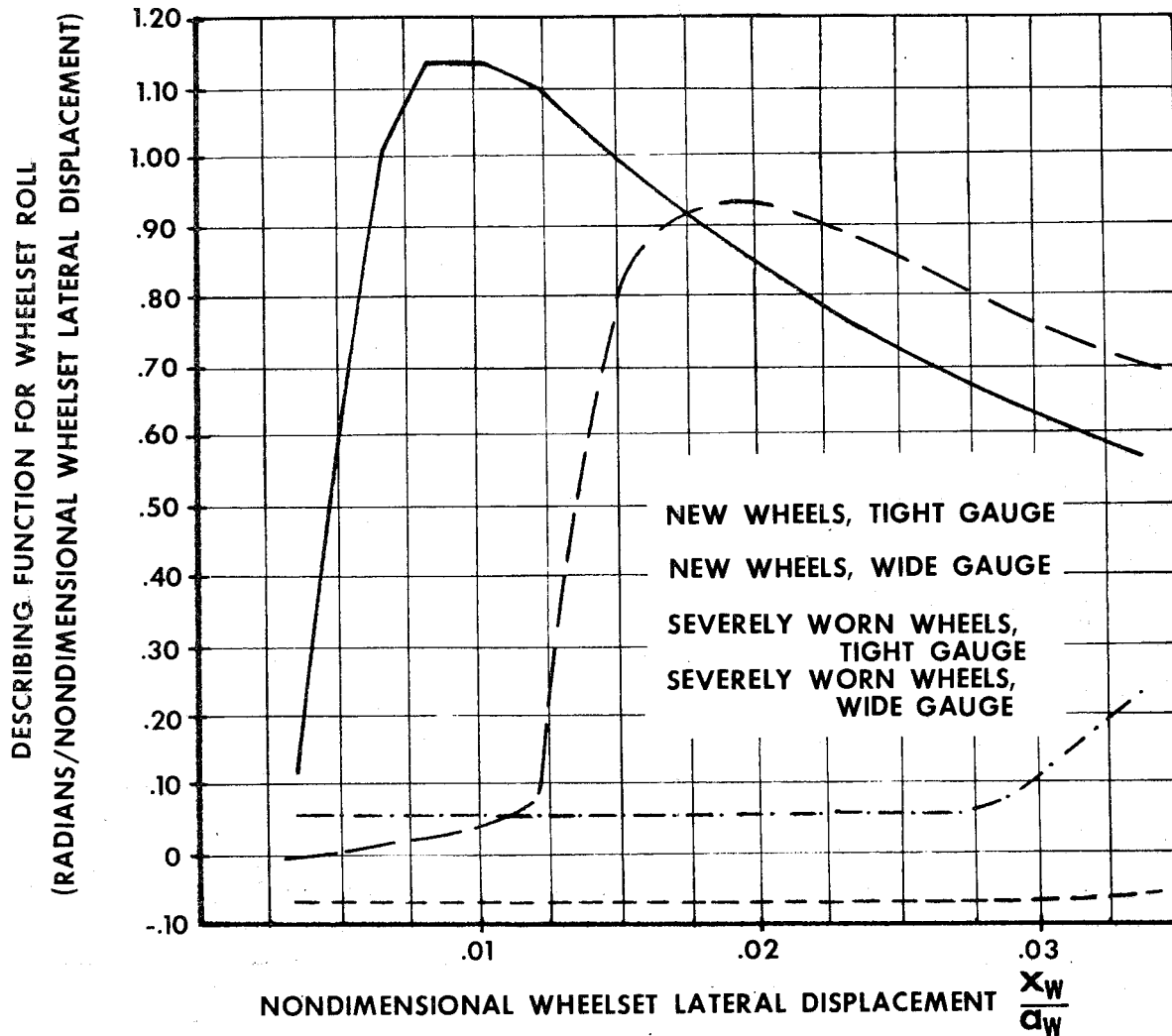


FIGURE 5-15 DESCRIBING FUNCTION FOR WHEELSET ROLL

vs.

NONDIMENSIONAL WHEELSET LATERAL DISPLACEMENT

(WORN RAILS, $a_w = 29.562$ in.)

once the flange contacts the rail. Thus, we expect that a vehicle with new wheels on tight gauge rail may hunt at low speeds due to the large changes in rolling radii that occur for small amplitude lateral wheelset motions. However, the very high gravitational stiffness at these same amplitudes may counter the destabilizing increase in conicity, particularly under heavy wheel loads.

The changes in worn wheel describing functions with rail gauge are similar to those seen with new wheels. The describing function of the rolling radii difference, for example, moves from a nearly constant negative value to a steeply rising curve when the rail gauge changes from wide to tight. The contact angle difference describing function similarly changes from nearly zero to a steeply rising function over this rail gauge range. Such variations dramatically affect vehicle behavior. At tight gauge we expect that the large conicity may cause low speed hunting, particularly if the wheel load is not large enough to counter this effect with a large gravitational stiffness. At wide gauge the negative conicity should cause the vehicle to lay over toward one or the other rail. At a rail gauge value between these two extremes, the effective conicity should be small, providing good stability for small amplitude, lateral motions.

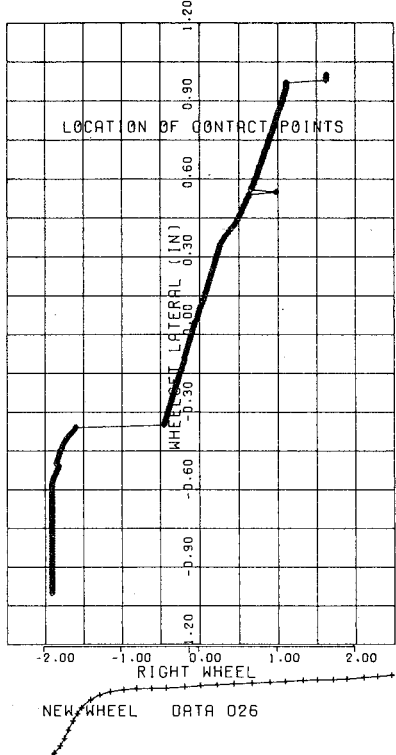
RAIL WEAR EFFECTS

The influence of rail wear on the wheel/rail geometric behavior was the third effect investigated here. The results of this investigation for new, severely worn, and modified Heumann profiles are discussed below.

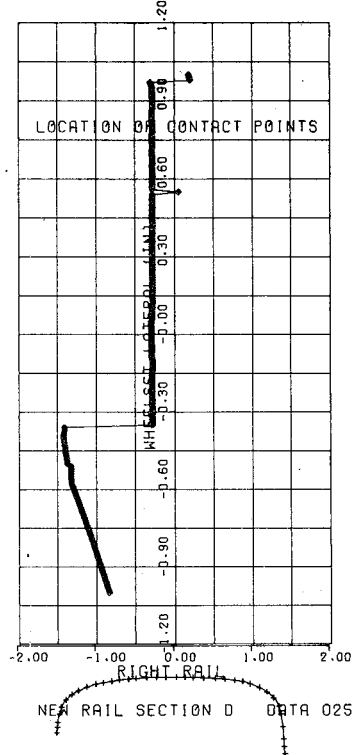
New Wheels

The contact positions and wheel/rail geometric constraints for the new wheel on new rail at nominal gauge are shown in figure 5-16. The chief difference between the contact position functions shown in this figure and those seen in figure 5-1 for the new wheel on worn rail concerns the rail contact position. The contact position on the new rail remains precisely in one spot until the flange contacts while the contact position on the worn rail shifts slightly as the wheelset moves laterally. Thus, small jumps seen in the constraint relations on worn rails, do not occur in

a. WHEEL CONTACT POSITION



b. RAIL CONTACT POSITION



WHEEL GAGE 53.000 IN.
RAIL GAGE 56.500 IN.

RAIL CANT .0250

c. WHEELSET ROLL

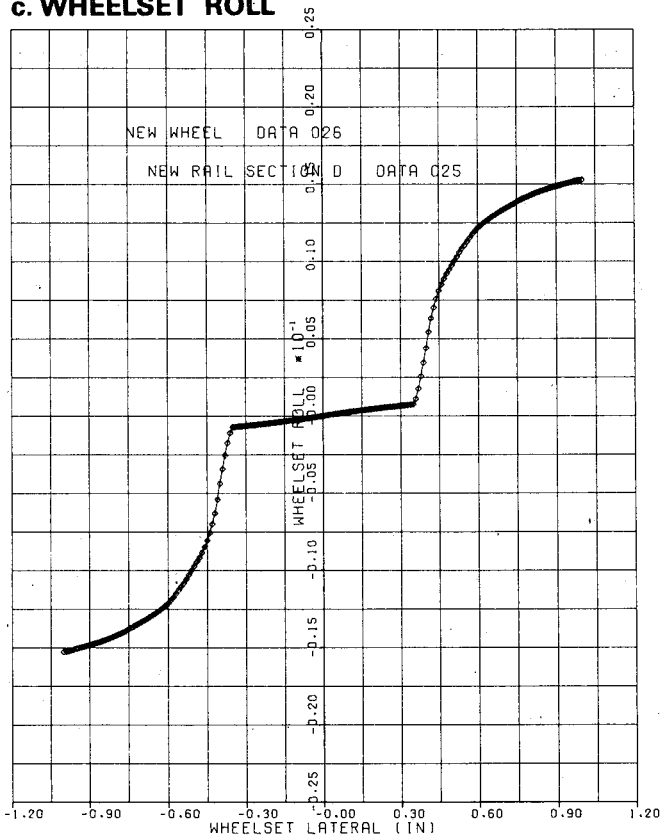
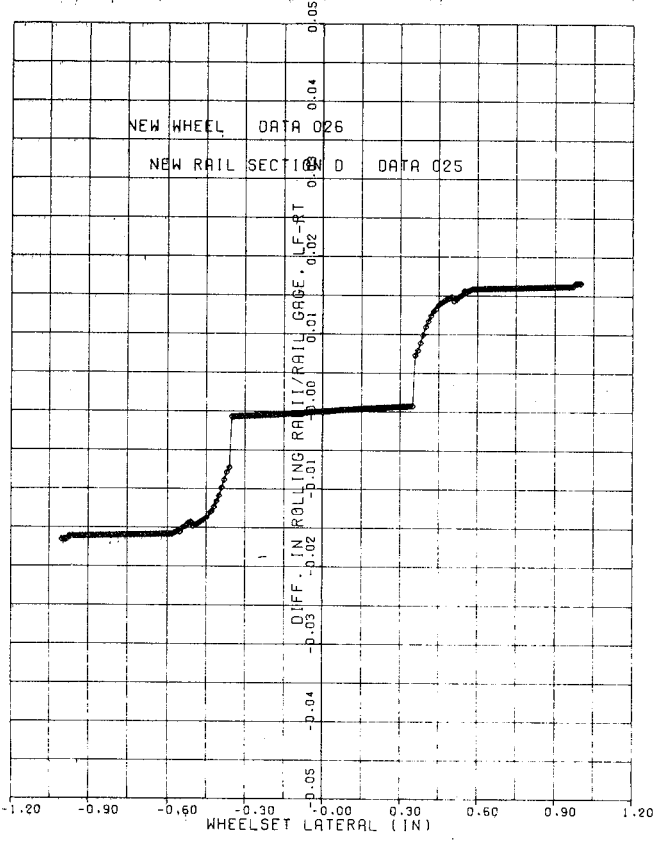
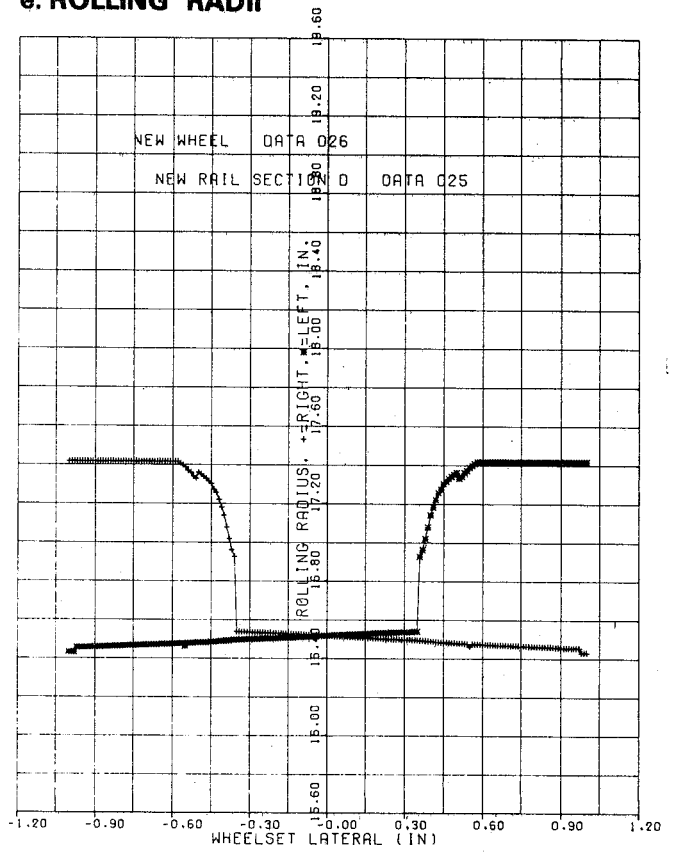


FIGURE 5-16 NEW WHEELS, NEW RAILS AT NOMINAL GAUGE

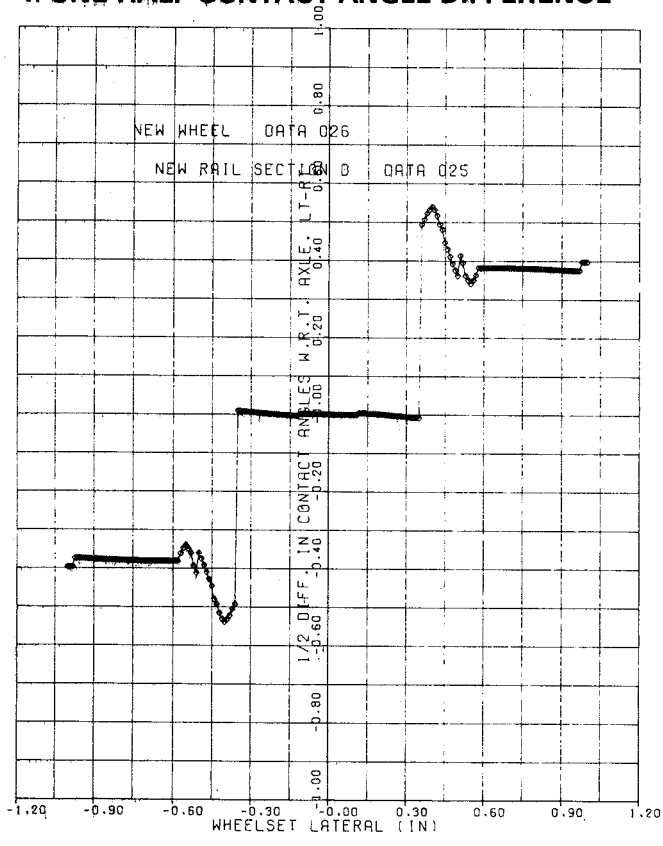
d. NORMALIZED ROLLING RADII DIFFERENCE



e. ROLLING RADII



f. ONE HALF CONTACT ANGLE DIFFERENCE



g. CONTACT ANGLES

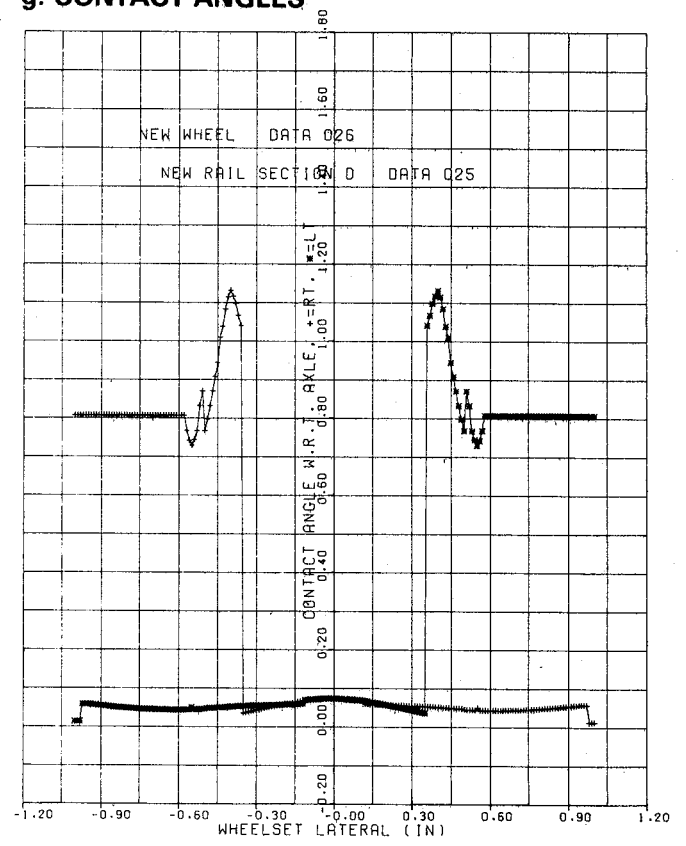


FIGURE 5-16 NEW WHEELS, NEW RAILS AT NOMINAL GAUGE

these functions on new rails. The slope of the rolling radii difference and roll angle functions in the range before flange contact occurs is also somewhat larger in the new rail case.

Severely Worn Wheel

The contact positions and constraint relations for the severely worn wheel profile on new rail at nominal gauge are shown in figure 5-17. Comparison of these results with the corresponding curves in figure 5-4 for the same wheels on worn rail reveals that the contact position on the new rail remains in one position over a wider range of wheelset lateral motion, and that this position is closer to the center of the rail. Although the final jump in contact from the wheel tread to the wheel flange occurs at about the same lateral wheelset position in both cases, the intermediate jump to the inside of the wheel and rail occurs at a larger wheelset displacement on the new rail.

The influence of the difference in rail head profile on the wheel/rail constraints is quite minimal. Figure 5-17 shows that the rolling radii difference, contact angle difference and roll angle functions remain flatter over a wider range on the new rail than on the worn. This effect is small enough that it is doubtful that any difference in vehicle behavior would be noticeable.

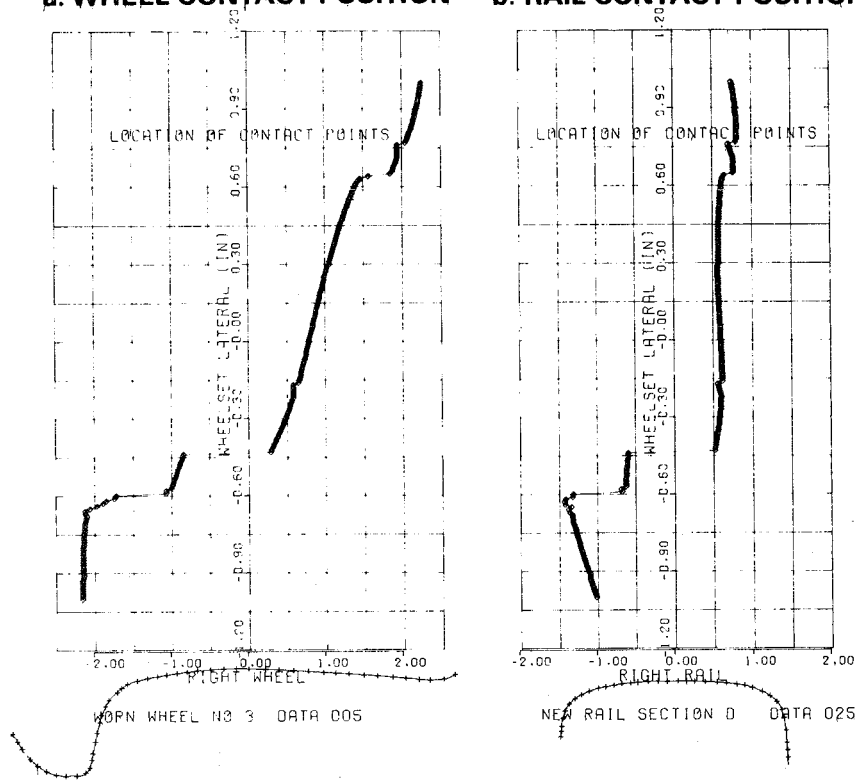
Modified Heumann Profile

The contact positions and constraint relations for the modified Heumann profile on new rail at nominal gauge are shown in figure 5-18. Again, comparison with the contact position functions for this case on worn rails, figure 5-5, indicates that the contact position on the wheel and rail have jumps of about the same magnitude in both cases, although these jumps occur at different wheelset lateral positions. The contact is spread over a wider band on the new rail than on the worn rail, but the contact band on the wheel does not differ in the two situations.

These small contact position differences have a large impact on the constraint relations in the range about the origin. At a lateral wheelset position of 0.30 inches, for example, the rolling radii difference, contact angle difference and roll angle are all about 50% less on the new rail than

a. WHEEL CONTACT POSITION

b. RAIL CONTACT POSITION



WHEEL GAGE 53.000 IN. RAIL CANT .0250
 RAIL GAGE 56.500 IN.

c. WHEELSET ROLL

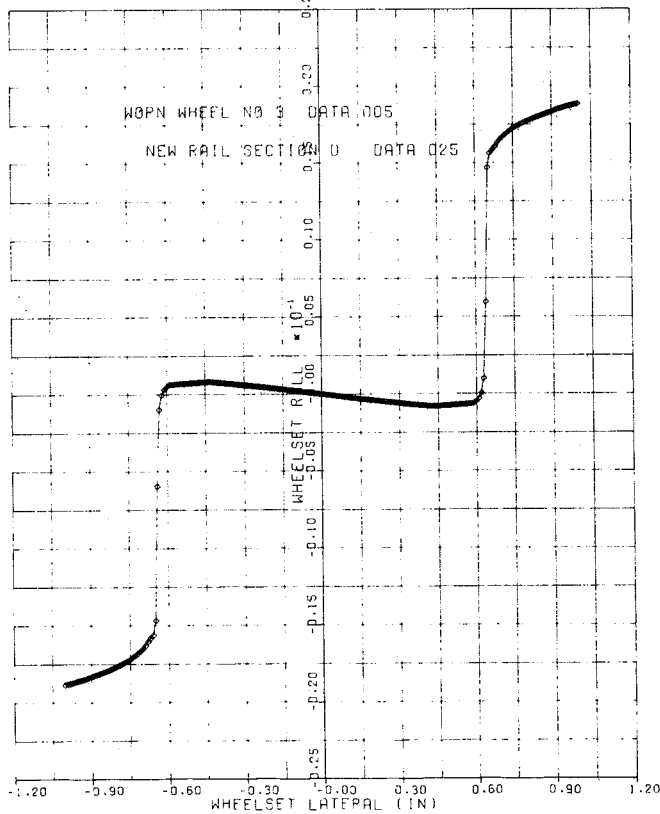
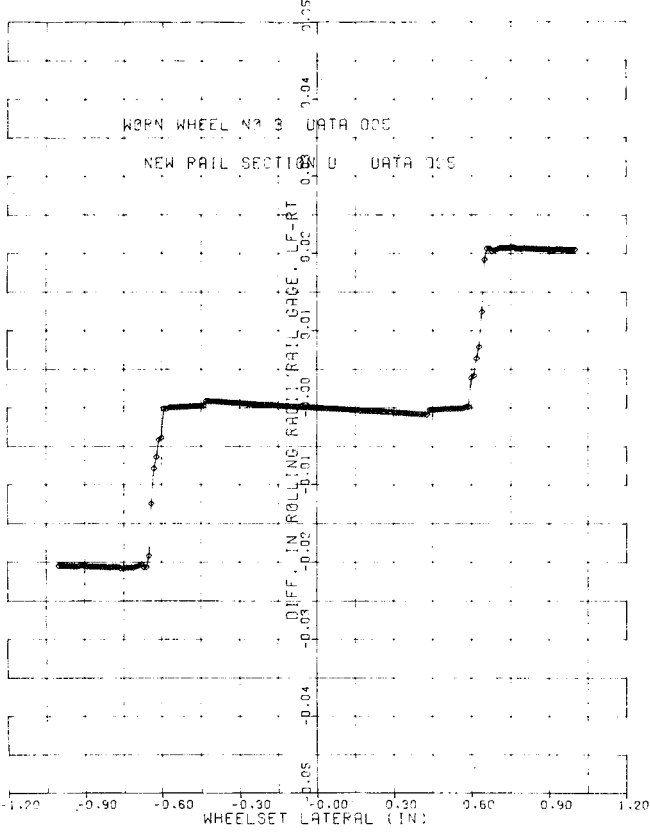
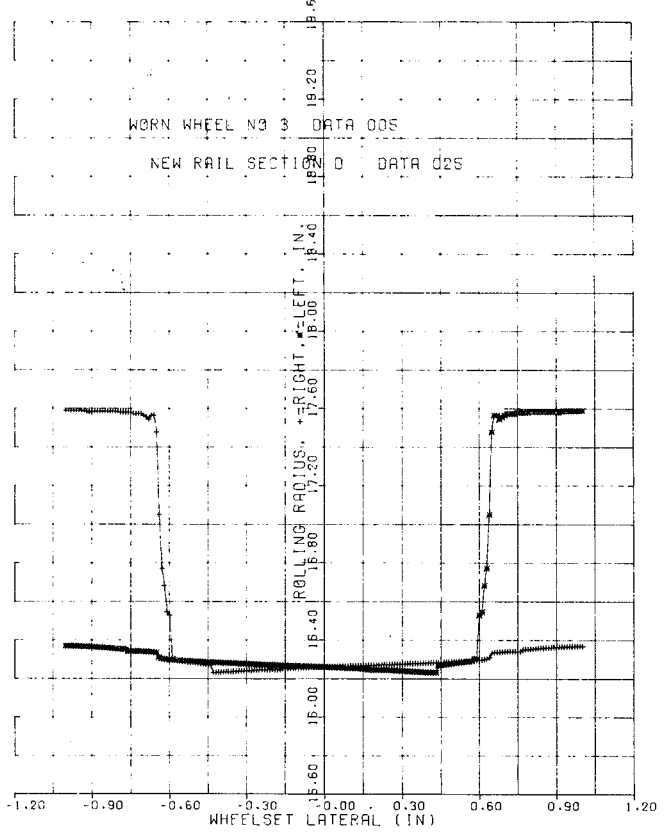


FIGURE 5-17 WORN WHEELS, NEW RAILS AT NOMINAL GAUGE

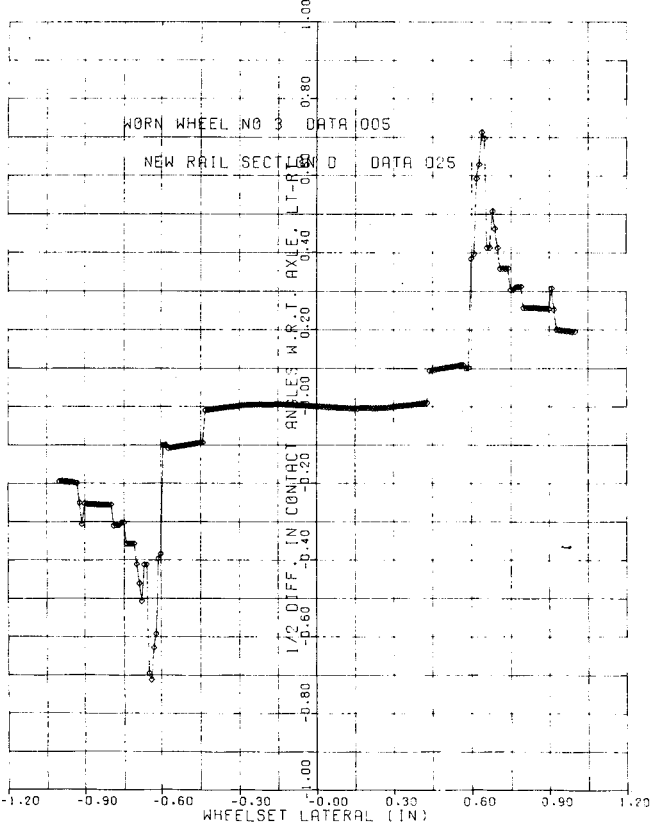
d. NORMALIZED ROLLING RADII DIFFERENCE



e. ROLLING RADII



f. ONE HALF CONTACT ANGLE DIFFERENCE



g. CONTACT ANGLES

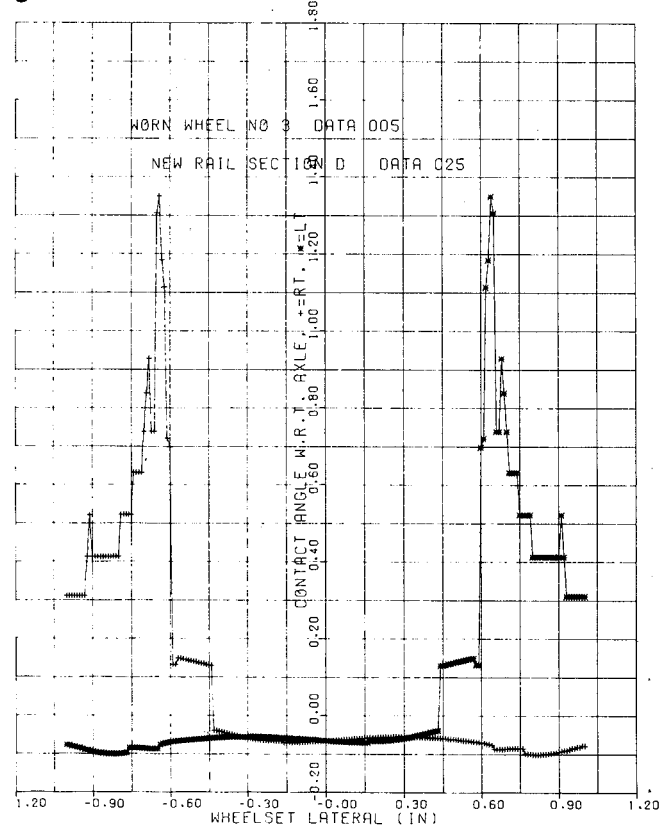
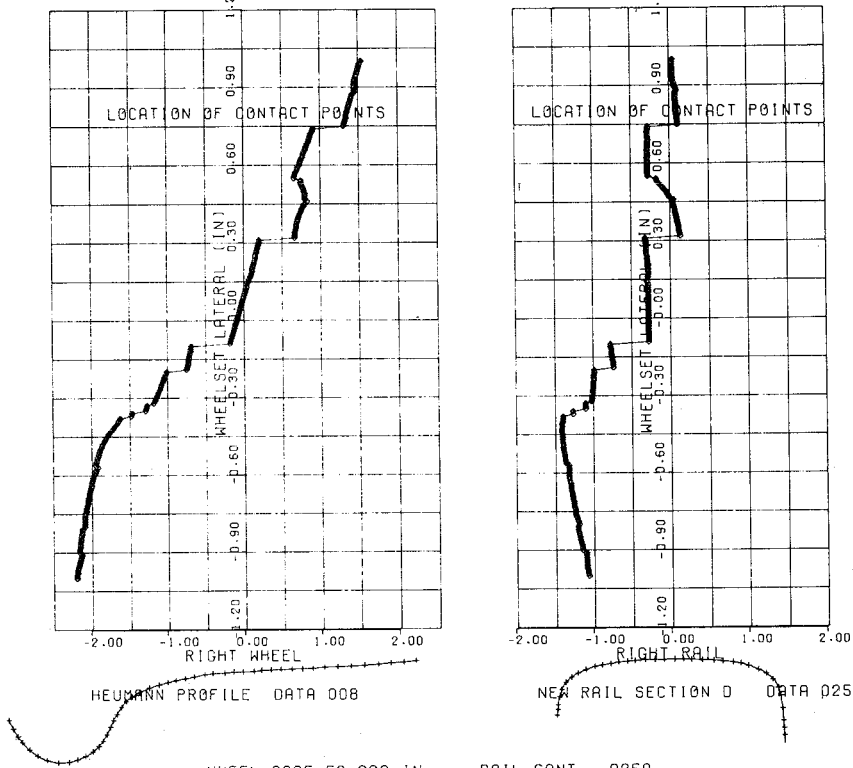


FIGURE 5-17 WORN WHEELS, NEW RAILS AT NOMINAL GAUGE

a. WHEEL CONTACT POSITION b. RAIL CONTACT POSITION



WHEEL GAGE 53.000 IN. RAIL CANT .0250
 RAIL GAGE 56.500 IN.

c. WHEELSET ROLL

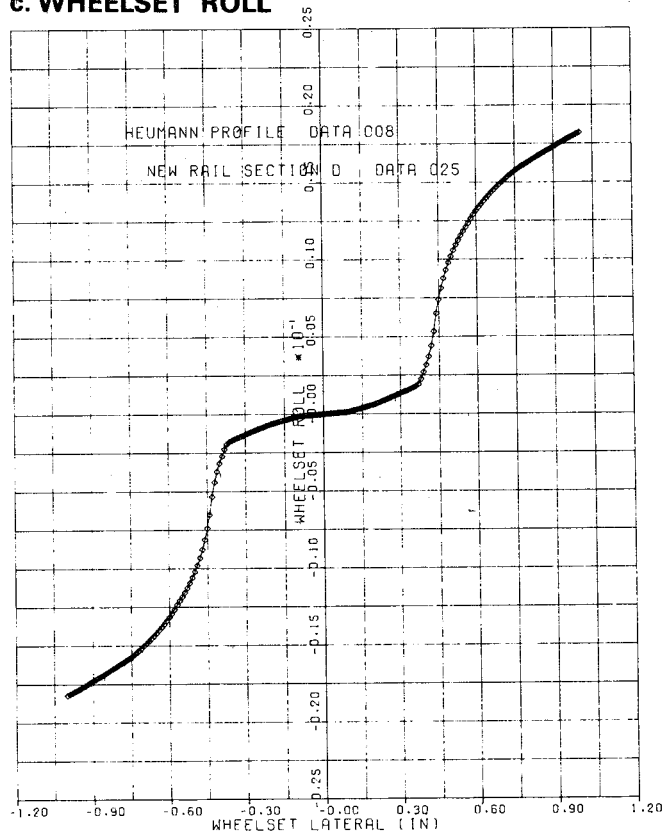
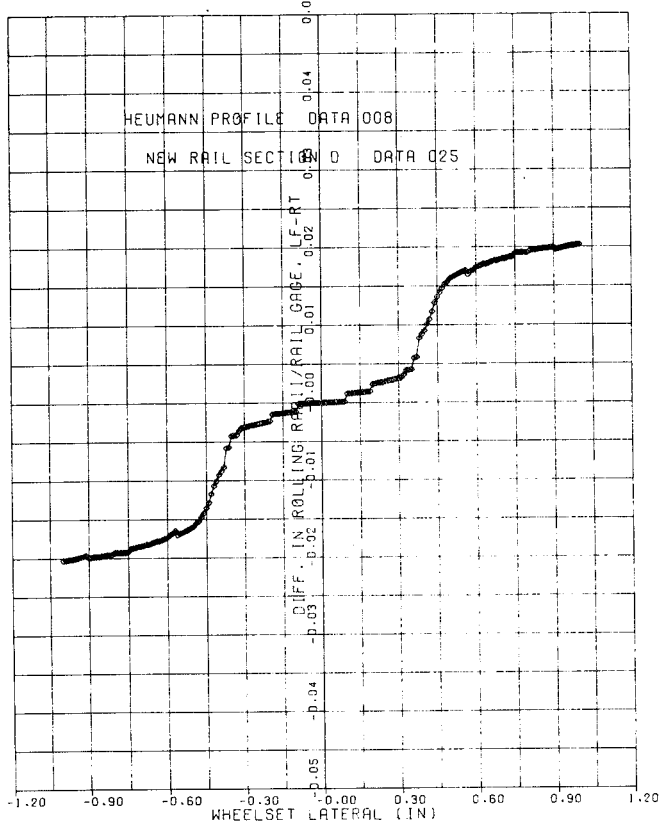
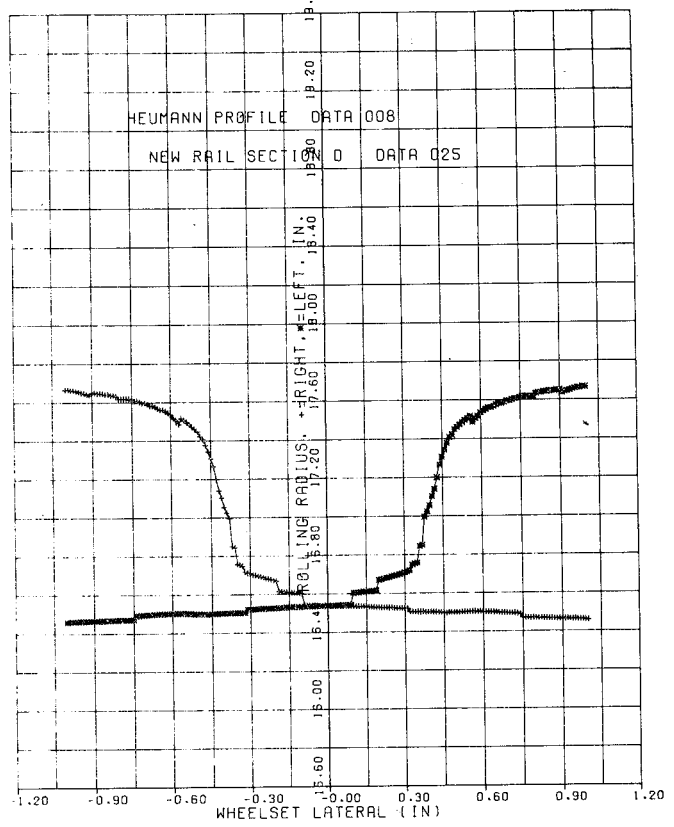


FIGURE 5-18 MODIFIED HEUMANN WHEELS, NEW RAILS AT NOMINAL GAUGE

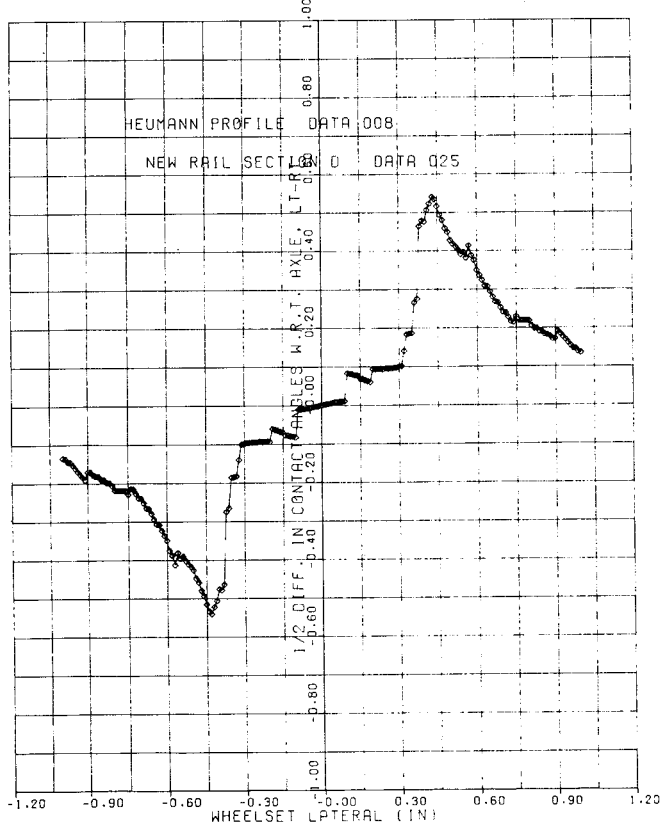
d. NORMALIZED ROLLING RADII DIFFERENCE



e. ROLLING RADII



f. ONE HALF CONTACT ANGLE DIFFERENCE



g. CONTACT ANGLES

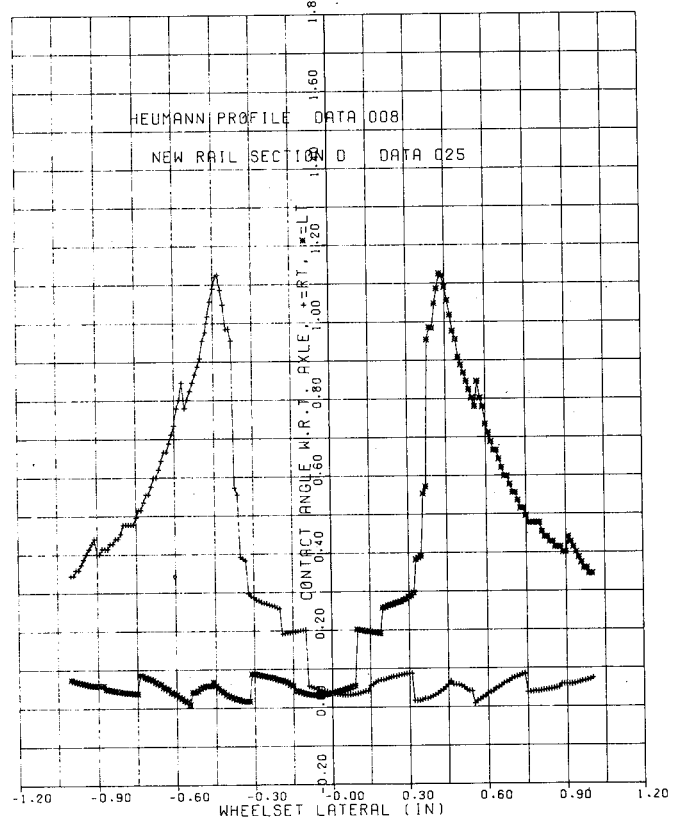


FIGURE 5-18 MODIFIED HEUMANN WHEELS, NEW RAILS AT NOMINAL GAUGE

on the worn rail. At larger displacements, the values of the constrained variables are much closer. At a lateral wheelset displacement of 0.60 inches, for example, the constrained variables are nearly the same for both cases.

These results indicate that vehicles with Heumann profiled wheels may be considerably more stable on new rail than worn rail.

Summary of Rail Wear Effects

The sinusoidal input describing functions of the wheel/rail constraint relationships shown in figures 5-19, 5-20 and 5-21 illustrate graphically the behavior of the new, severely worn and Heumann wheel profiles on new rail. Comparison with the describing functions for the same wheel profiles on worn rails, found in figures 5-6, 5-7 and 5-8, reveals the following differences between wheelset behavior on new and worn rails,

1. New wheel profiles have identical behavior at large amplitudes, but have nearly constant and higher values of conicity on new rail. Thus, the stability of vehicles with new wheels may be slightly better on worn rail.
2. Conicity and roll coefficient values for the Heumann profile are more than 50% larger at small amplitudes on worn rail than on new rail. As a result, vehicles with a modified Heumann profile may be more stable on new rail.

The describing functions of the constraint relationships for the severely worn wheel were substantially unaffected by the differences between new and worn rails. These describing functions at large amplitudes, when the contact point moves onto the flange, were also unaffected by the differences between new and worn rail.

To summarize, rail wear does not affect the wheel/rail geometric constraints as strongly as the other parameters studied here. Some wheel profiles, such as the severely worn wheel profile, profile #3 of figure 2-2, are unaffected by rail wear. The nature of the influence of rail wear can be either stabilizing or destabilizing, depending on the wheel profile characteristics.

$$\left(\frac{r_L - r_R}{2a_r}\right) \text{ quasi-linear} = \text{Describing Function} \times \frac{x_w}{a_w}$$

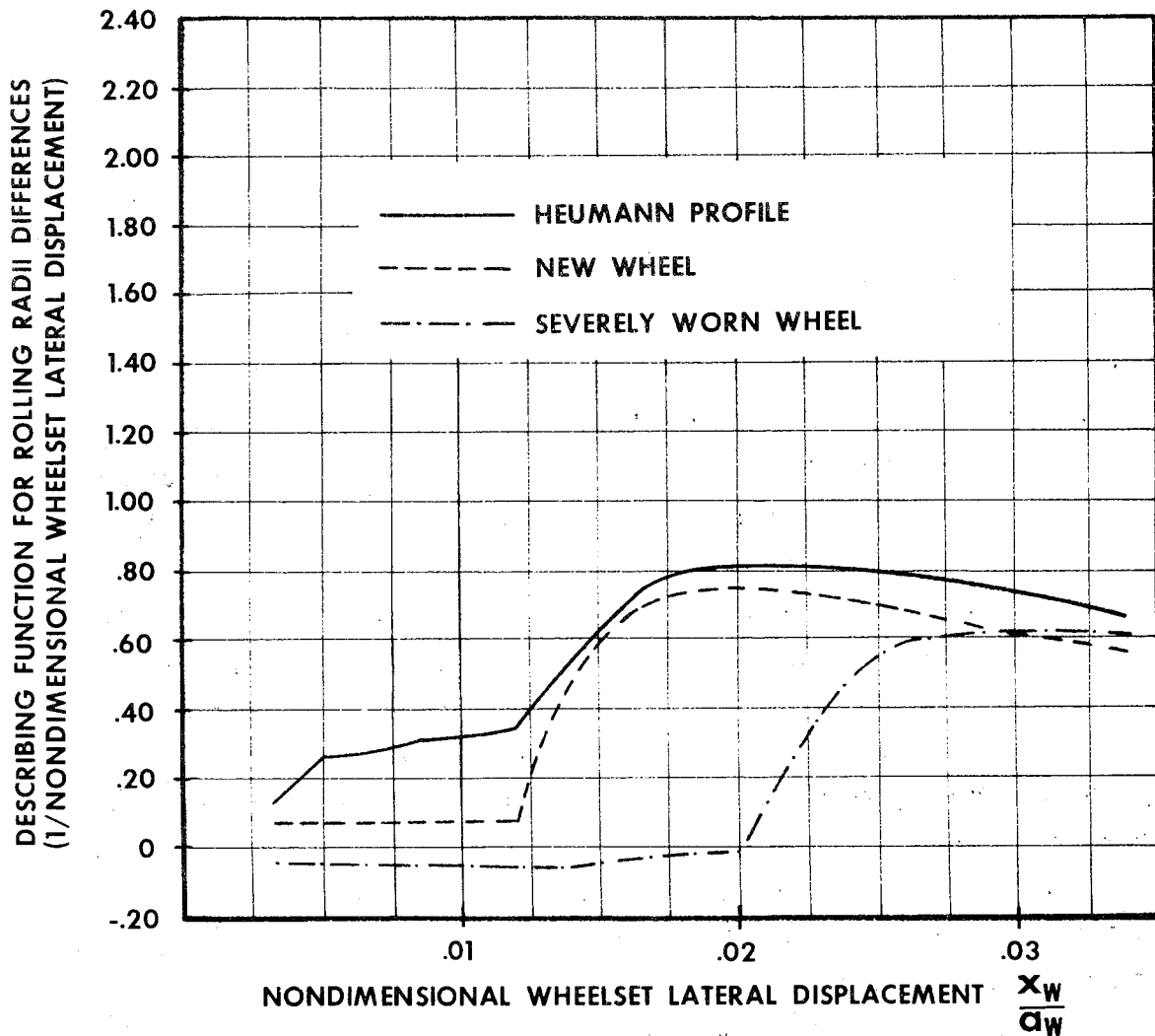


FIGURE 5-19 DESCRIBING FUNCTION FOR ROLLING RADII DIFFERENCE

vs.

NONDIMENSIONAL WHEELSET LATERAL DISPLACEMENT

(NEW RAILS, NOMINAL GAUGE, $a_w = 29.562$ in.)

$$\left(\frac{\delta_L - \delta_R}{2}\right) \text{ quasi-linear} = \text{Describing Function} \times \frac{x_w}{a_w}$$

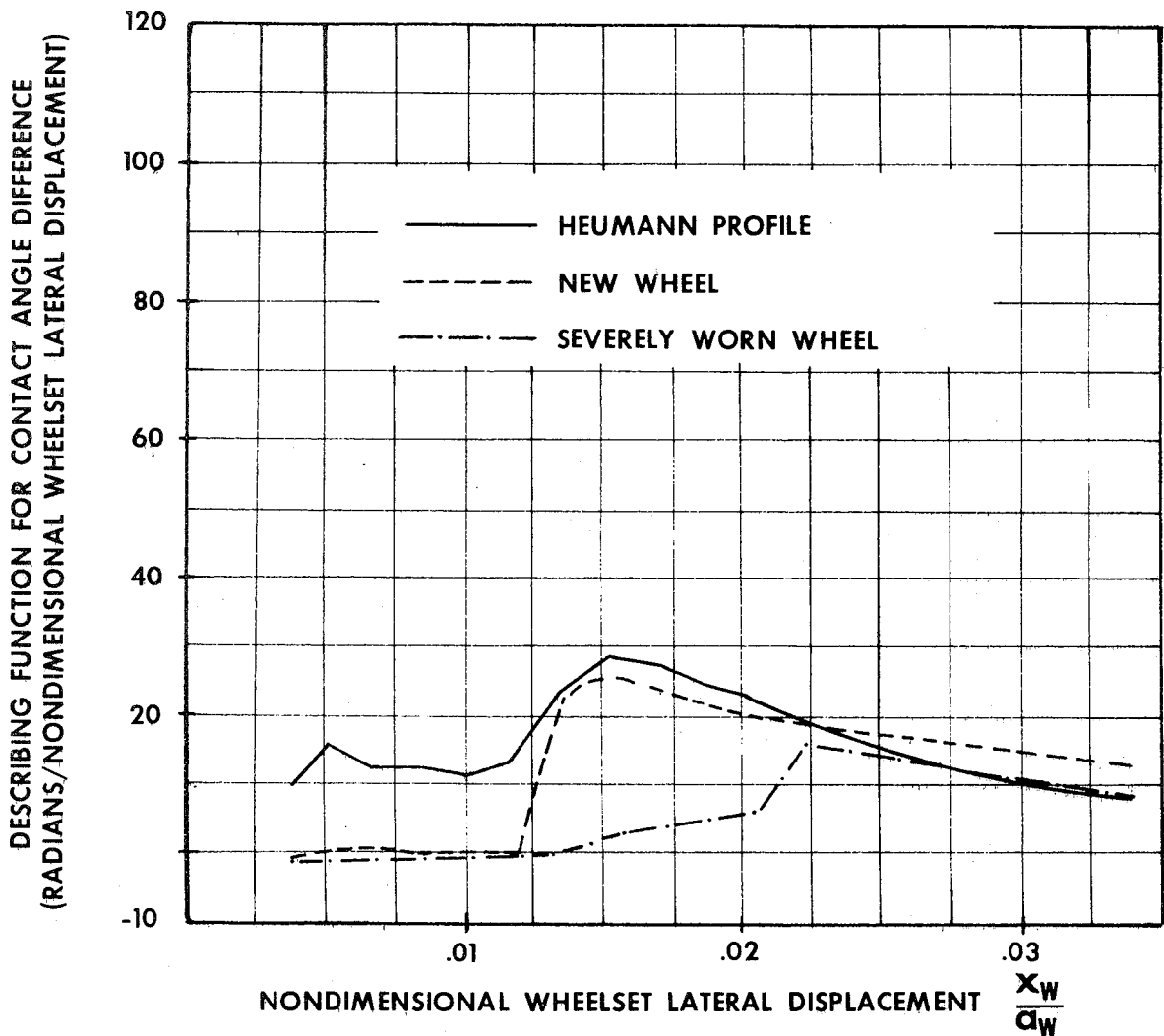


FIGURE 5-20 CONTACT ANGLE DIFFERENCE DESCRIBING FUNCTION

vs.

NONDIMENSIONAL WHEELSET LATERAL DISPLACEMENT

(NEW RAILS, NOMINAL GAUGE, $a_w = 29.562$ in.)

$$(\phi_w)_{\text{quasi-linear}} = \text{Describing Function} \times \frac{x_w}{a_w}$$

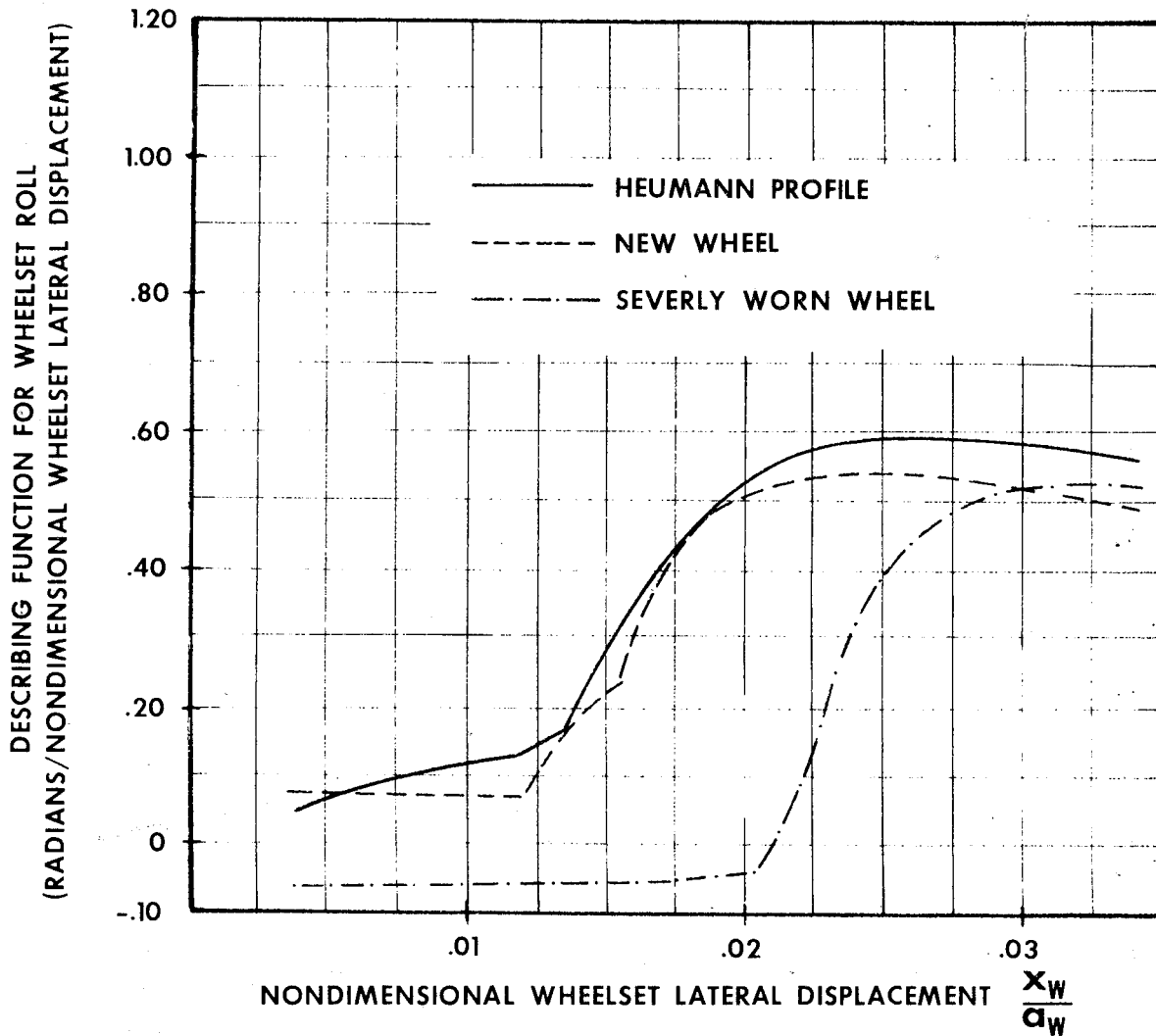


FIGURE 5-21 DESCRIBING FUNCTION FOR WHEELSET ROLL

vs.

NONDIMENSIONAL WHEELSET LATERAL DISPLACEMENT

(NEW RAILS, NOMINAL GAUGE, $a_w = 29.562$ in.)

CONCLUSIONS

Perhaps the most significant accomplishment of this study was to determine the dependence of the wheel/rail geometric constraints on the wheelset lateral amplitudes. In most rail vehicle dynamic studies, the assumption is made that these constraint functions can be represented with linear functions. The results presented in this chapter indicate that this is a poor assumption for all the situations studied except the new wheel on new rail. In most cases, the constraint functions are highly nonlinear, and as a result, we expect that the vehicle behavior will depend strongly on the amplitude of the wheelset motion.

This parametric study revealed that significant changes in the wheel/rail geometric constraint relationships may occur when the wheel, rail and track geometry vary. The wheel profile geometry has the strongest effect of these three parameters. We found that one may be able to classify wheel profiles in three categories, (1) new, (2) hollow with positive slope, and (3) hollow with negative slope. Wheel profiles in the third category when in contact on the negative slope or downturned portion of the profile will cause the wheelset to diverge from a centered position at any speed. The vehicle or wheelset stability at higher speed will be determined by the wheel/rail characteristics and other factors such as the suspension configuration and the vehicle load.

Variations in the rail gauge affect the wheel/rail constraints by shifting the position of the contact point between the wheel and rail. For a uniform wheel profile such as a new, conical wheel, this does not change the constraint relationships until flange contact occurs. On a wheel with downturned profile however, such a shift may move the centered contact point from a stable position with a positive contact angle to an unstable position with a negative slope. Thus, under certain conditions, changes in rail gauge can have dramatic effect on the wheel/rail constraints.

We found that rail wear had very little effect on the geometric constraint relationships for the new and severely worn wheel profiles. The new wheel profile had slightly larger conicity on the new rail. However, effective conicity and the wheelset roll, for a wheelset with modified Heumann profiles were more than 50% larger on new rails than worn at wheelset lateral amplitudes to about 0.30 inches. Thus, we must

conclude that rail wear may strongly affect the behavior of certain classes of wheel profiles.

It should be emphasized that this parametric study dealt with a limited sample of wheel profiles and only with symmetric wheels on a wheelset. We expect that a wide variety of wheel profiles may be found throughout the North American freight car fleet, and that the constraint functions for those may vary considerably from those studied here. It is a fact that wheelsets often have asymmetric wheels. We expect that this, too, will change the constraint functions for the wheelset. These two matters should receive attention in subsequent projects.

CHAPTER 6

CONCLUSIONS

The primary goal of this study was to develop the capability of calculating the wheel/rail geometric constraint relationships for arbitrary wheel and rail profiles, wheel and rail gauges, and rail cant angles. This goal was attained. The equipment and procedures developed to achieve this objective, as well as the results obtained using them have wide applicability to the study of rail vehicle dynamics. Successful completion of this effort has brought us a great deal closer to our ultimate objective of providing the capability to analyze accurately the dynamic behavior of any rail vehicle. The capabilities of the tools developed in this project, the conclusions obtained in a limited application of these tools, and the additional work that is needed to refine the tools and apply them to new problems are discussed below.

STATUS AND ACCOMPLISHMENTS

Laboratory equipment and procedures were developed to achieve the objectives of this project by experimental methods. This effort revealed that experimental measurements would be quite time-consuming, particularly if large numbers of wheel and rail combinations were to be measured. Consequently, an analytical method for determining the desired wheel/rail geometric constraint functions was also developed. The experimental apparatus and procedures were fully developed to provide the following capabilities:

1. Determine the contact position on the wheel and rail and the wheelset roll angle at any lateral wheelset position.
2. Convert wheel and rail profile data from graphical to numerical form suitable for input to digital computer programs.

This experimental process has been thoroughly checked for accuracy and repeatability. Digital data for selected wheel and rail profiles for input to the analytical procedure and experimental contact position measurements for validating that procedure were obtained with the experimental apparatus. This equipment is available for further research, if needed.

The objective of the analytical effort conducted during this project was to develop a more efficient means of determining wheel/rail geometric constraint relationships for arbitrary wheel and rail combinations. This effort resulted in digital computer programs to carry out the following computations:

1. Find the wheel and rail contact positions, wheelset roll angle, contact angles at left and right wheels, and rolling radii at left and right wheels for arbitrary wheel and rail profiles as functions of the wheelset lateral position.
2. Find sinusoidal input describing functions for the odd wheel/rail geometric constraint functions.

These analytical procedures were validated by comparison of computed values with experimental measurements. The computer programs are documented in Appendix A.

A computer program was also developed to compute the wheel/rail constraint relationships from the experimentally determined data for the contact positions on the wheel and rail and tabular data for the wheel and rail profiles. This program was used to reduce the experimental data for comparison with analytical results. The capabilities of this program were incorporated in the programs described above.

Validation of the analytical procedure was accomplished by comparing experimental and analytical values of contact positions, and wheel/rail geometric constraint relationships for the following three cases: (1) new wheels on new rail at a nominal rail gauge, (2) severely worn wheels on worn rail at nominal rail gauge, and (3) severely worn wheels on worn rail at wide gauge. Excellent agreement was obtained between analytical and experimental values for contact positions and rolling radii. In both the analytical and experimented procedures, values for contact angles were obtained by numerically determining the slopes of the wheel and rail profiles at the appropriate contact positions on the wheel and rail profiles for each wheelset lateral position. Although reasonably good agreement was obtained between the solutions obtained by the two processes, further improvement in the method of determining the slopes of the wheel and rail profiles to smooth the contact angle relation-

ships would be worthwhile.

A parametric study utilizing the analytical procedure was undertaken to investigate the effects of wheel wear, rail wear and rail gauge variations on the geometric constraints. Wheel/rail geometric constraint relationships and their describing functions were found for eleven combinations of new, slightly worn, moderately worn, severely worn, and modified Heumann wheel profiles; new and worn rail profiles; and tight, nominal and wide rail gauge. The following conclusions were drawn from this investigation:

1. The wheel/rail constraint relationships are quite nonlinear, even for new wheel profiles on worn rail. Consequently, the frequent assumption that these relationships can be approximated with linear functions in the analysis of rail car dynamics should be taken with extreme caution. A better technique is to use the describing function approach to analyze the behavior of the rail car as a function of the wheelset lateral amplitude. This will reveal directly the dependence of the dynamic behavior on the amplitude of the motion.
2. The wheel profile geometry has the strongest effect of the three parameters studied. Tentative classification of wheel profiles into three classes allowed us to isolate the dominant differences between the wheel profiles studied in this limited investigation.
3. One class of wheel profiles, characterized by a contour with negative slope in a region of the profile, has negative conicity and gravitational stiffness at some wheelset lateral positions. This characteristic will cause the wheelset, when in one of these positions, to diverge from a centered position and either oscillate in a limit cycle or assume a position with one wheel flange in contact with the corresponding rail.
4. Rail gauge variations had very little effect on the constraint relationships for new wheels, but significantly changed these functions for worn wheels. For wheels in the class described in Conclusion 3 above, changes in rail gauge from tight to wide gauge will

cause the conicity and gravitational stiffness at small amplitudes to change from positive to negative values.

5. Rail wear had very little effect on the geometric constraint relationships for all but the modified Heumann profile. The conicity of the wheelset with modified Heumann profiles was more than 50% higher on new rail than on worn rail.
6. The modified Heumann profile had the highest conicity and gravitational stiffness of the wheels studied. As a result, we expect that stability problems will be more severe on lightly loaded, conventional freight cars with Heumann profiled wheels than on the same cars with any of the other wheel profiles studied here. It should be noted that Heumann profiles offer the particular advantage of not changing with mileage to the same degree that standard profiles do. Consequently, Heumann profiles could give good performance if the vehicle were designed for their use.

This parametric study dealt only with a limited number of wheel and rail profiles on wheelsets with identical wheel profiles on left and right wheels. The latter factor, in particular, is not representative of North American rail freight cars. Consequently, the results presented and conclusions discussed here should be regarded as tentative. The asymmetric wheelset and a wider collection of wheel profiles should be studied in the near future.

FUTURE WORK

The future work that is needed to refine the tools developed in this project and to apply them to the problems of the railroad industry can be grouped in the following three categories: (1) efforts to improve or extend the capabilities of the computational procedures for determining wheel/rail constraint relationships, (2) projects to develop the data needed in the computational procedures, and (3) studies to apply these procedures to understand and solve railroad industry problems. Future work in each of these categories is discussed below.

Computational Refinements and Extensions

1. Modify the computer programs to allow computation of contact positions and wheel/rail geometric constraints for asymmetric wheels and rails, i.e. different wheel and rail profiles on the left and right. This modification involves minor programming changes to run through the curve fitting and contact point computations twice. These modifications will be made in the near future.
2. Improve the accuracy of the process of obtaining digital wheel and rail profile data for input to the analytical process. One area for improvement is the digitizing processes used in this study. As discussed in Chapter 3, the method of determining the angular orientation of the profiles during the digitizing process has a larger experimental uncertainty than is desirable. Some ideas for refinement of this process to reduce the uncertainty are discussed in that chapter. Another area for attention is the development of accurate and reliable devices to measure wheel and rail profiles in the field. Ideally, such devices would record the profile measurements on magnetic tape or cards in a form that could be directly used as input to the computational process.
3. Eliminate spurious jumps in the contact position and contact slope functions computed by the analytical procedure. As discussed in Chapter 4, these jumps are caused by slight mismatches of slopes and possibly positions at the junctions between the 4th order polynomials fitted to the profile data. Although these jumps are not large, their elimination is desirable. Refinements such as improving the curve fitting process or averaging the two curve fit values in the overlap region are discussed in Chapter 4.
4. Develop a method of computing the curvature of the wheel and rail profiles. The radii of curvature of the wheel and rail profiles are used in the creep force computations, and in calculations of the contact stresses. Instantaneous values of the curvature at each wheel and rail contact position are needed to determine the

change in creep coefficient as the wheelset displaces laterally. We have tried computing the radius of curvature from the curves fitted to the profile data. However, this computation uses the second derivative of the profile curve, and we found that this value varies a great deal from point to point. Consequently, the values of radii of curvature computed in this way vary wildly, and do not reflect accurately the actual profile curvature. A method of smoothing the data, either before, during or after the curvature computation is needed.

Collection of Wheel and Rail Data

1. Assemble a data bank for all new wheel and rail profiles. This data bank would be available to railroad researchers, designers, and operating personnel to evaluate the expected behavior of rail vehicles.
2. Undertake an effort to make a comprehensive study of worn wheel and rail profiles throughout the country. This project will require development of the instruments and procedures discussed in item 2 of the computational tasks.

Applications of the Analytical Process

1. Assemble a data bank of wheel/rail geometric constraint functions for combinations of the new wheel and new rail profiles assembled in item 1 of the data collection tasks.
2. Develop a scheme for classifying the worn wheel and rail profiles gathered in the second data gathering task described above. This classification method might group profiles or combinations of profiles according to similarities in their geometric constraint functions.
3. Analyze the dynamic behavior of conventional rail vehicles with various combinations of the wheel and rail profiles classified in task 2 above. This study should lead to maintenance standards for wheels and rails that would ensure acceptable dynamic behavior.

When the tasks described above are completed, we should have the information needed to obtain a better understanding of the causes of the poor dynamic performance of conventional rail vehicles, and to design better vehicles.

REFERENCES

- 1-1. Wickens, A. H., "The Dynamic Stability of Railway Vehicle Wheelsets and Bogies Having Profiled Wheels," International Journal of Solids and Structures, Vol. 1, 1965, p. 319-341.
- 1-2. Wickens, A. H., "General Aspects of the Lateral Dynamics of Railway Vehicles," ASME Journal of Engineering for Industry, Vol. 91, Series B. No. 3, August, 1969, p. 869-878.
- 1-3. King, B. L., "An Evaluation of the Contact Conditions Between a Pair of Worn Wheels and Worn Rails in Straight Track", DYN/37, September, 1966, British Railways Research Department, Derby, England.
- 1-4. King, B. L., "An Assessment of the Contact Conditions between Worn Tyres and New Rails in Straight Track," DYN/42, December 1966, British Railways Research Department, Derby, England.
- 1-5. Gilchrist, A. O., "Variation Along the Track of Conicity and Rolling Line Offset," DYN/62, July 1967, British Railways Research Department, Derby, England.
- 1-6. Booton, R. C., "Nonlinear Control Systems with Random Inputs," Inst. of Radio Engineers, Trans. on Circuit Theory, Vol. CT-1, No. 1, 1954.
- 1-7. Anon., "Geometry of the Contact Between Wheelset and Track Part 1: Methods of Measurement and Analysis," Question C116, Interaction Between Vehicles and Track, Report No. 3, October, 1973, Office for Research and Experiments of the International Union of Railways (ORE), Utrecht, The Netherlands.
- 1-8. Anon., "Geometry of the Contact Between Wheelset and Track," Communications of the ORE, Rail International, March 1974, p. 252-256.
- 2-1. Heumann, H. "The Problem of the Tyre Profile," Organ. f.d. Fortschritte des Eisenbahnwesens, Vol. 89, No. 18, Sept. 15, 1934, p. 336-342.
- 2-2. Koffmann, J. L., "Heumann Tyre Profile Tests on British Railways," Railway Gazette, 1965, p. 279
- 2-3. Eck, B.J. and N.W. Berg, "Looking for Tomorrow's Wheel Profile," ASME Winter Annual Meeting, Detroit, Nov. 1973.
- 2-4. Gelb, A., and W. Vander Velde, Multiple-Input Describing Functions and Nonlinear System Design, McGraw-Hill, 1968.
- 2-5. Siljak, D., Nonlinear Systems: The Parameter Analysis and Design, J. Wiley & Sons, 1969.

- 2-6. Cooperrider, N.K., Hedrick, J.K., Law, E.H. and C. W. Malstrom, "The Application of Quasi-Linearization to the Prediction of Nonlinear Railway Vehicle Response," presented at the IUTAM Symposium on Vehicle Mechanics, Delft, August 1975.
- 3-1. Anon, "Wheel and Axle Manual," Tenth Edition, Oct. 1972, Association of American Railroads, Washington, D.C.
- 3-2. Siddall, J. N., Analytical Decision Making in Engineering Design, Prentice-Hall, 1972, p. 43.
- 4-1. MATH-PACK, UP-7542 Rev. 1, Univac Large-Scale Systems, Sperry-Rand Corp., Sec. 13, pp. 24-44.

APPENDIX A. WHEEL/RAIL CONTACT CHARACTERIZATION
PROGRAM

A. PURPOSE

This program and associated subroutines compute the wheel/rail contact positions and geometric constraint functions for any given wheel profile, rail profile, rail cant angle and rail gauge for a symmetric wheelset on symmetric rails.

B. PROGRAM DESCRIPTION

1) Usage: The program consists of a main program and twelve subroutines. The program also uses "canned" subroutines in the Univac MATHPAC. Input is coordinated by the main program WHRAIL and subroutine PRFLE. Output is from the main program and subroutine DCRFCN. The bulk of the communication is in COMMON storage.

The main program, WHRAIL, coordinates the input and calculations. Subroutine PRFLE reads in the digitized profiles and fits a series of 4th order polynomials to the data using subroutine CRVFT. Subroutine PLOT1 plots the profile data points and the curve-fits using subroutine GTPTS to calculate the fitted points and the plotting routines associated with the CALCOMP 770/763 plotter. Subroutine EQSOLV, coordinates subroutines CHECK, CHOOSE, and RADII, to find the contact point locations. Subroutine EQSUB2, using subroutine RADII, calculates values of the constraint parameters which are plotted by subroutine PLOT2, using the CALCOMP plotter routines. The main program, WHRAIL, outputs the results and calls subroutine DCRFCN to compute describing functions for certain of the results. The describing function results are output from within DCRFCN.

2) Subroutines Required: SUBROUTINE PRFLE (NW, XW, YX, NC, RR, XB, F1, F2, F3, SS, INC) profile fitting routine reads in data points describing a profile, divides each profile into a series of regions, and fits a 4th order polynomial to each region. Uses subroutine CRVFT.

SUBROUTINE CRVFT (N, L, X, Y, W, A) finds the coefficients of the fourth order polynomial that best fits an array of data points. Uses subroutines ORTHLS and COEFS from the Univac MATHPAC.

SUBROUTINE PLOT1 (NW, XW1, YW1, NY, XW2, YW2, ICT, IWG, IRG) plots the wheel and rail profiles with a symbol at every other data point and draws a line representing the curve-fit. Uses subroutine GTPTS and the CALCOMP plotter routines.

SUBROUTINE GTPTS (XMAX, XMIN, RR, B, NC, AXW, AR1, S1, NU) calculates an array of points on the curves fitted to a profile.

SUBROUTINE EQSOLV (NUMBR, XOLD, XMIN, XMAX, XMAXW, XMINW) coordinates the search for the contact points. It also transposes the results to get values for negative wheelset lateral displacement. Uses subroutine CHECK.

SUBROUTINE CHECK (XW, DXW, XOLD, XMIN, XMAX, XMAXW, XMINW, WR) uses a search procedure to find the contact point locations. Uses subroutines CHOOSE and RADII.

SUBROUTINE CHOOSE (X1, X2, X3, X4) chooses the curves which represent the wheel and rail profiles at the instantaneous points of interest.

SUBROUTINE RADII (RR, YR, RL, YL, X1, X2, X3, X4, R1, R2, R3, R4) finds the functions of four fourth order polynomials for four inputs.

SUBROUTINE EQSUB2 (NUMBR, W) calculates the geometric constraint relations by substituting the contact point locations into the defining equations. Uses subroutines RADII and CHOOSE.

SUBROUTINE PLOT2 (NUMBR, ITODAY, ITIM) plots the results. Uses the CALCOMP plotter and associated routines.

SUBROUTINE DCRFCN (N, AXW, AR5, AM3, AW1, AR) performs quasi-linearizations using describing function techniques for a sinusoidal input.

3) Description of Parameters:

Main Program WHRAIL -- Input parameters

NUMB	Number of points to be calculated, ≤ 121 . The amplitude of wheel-set lateral displacement = $\frac{\text{NUMB}-1}{100}$ inches
INC	Number of data points per curve-fit zone, $3 \leq \text{INC} \leq M/3$, where M = number of data points
WG	Wheel gauge measured from flangeback to flangeback, inches
RG	Rail gauge measured from inside one rail at a point 5/8" from the top of the rail to the corresponding point on the other rail, inches
BR	Cant of right rail, radians (positive cant to the inside)
BL	Cant of left rail, radians, (positive cant to the inside)
IWHEEL	Label for wheel, alphanumeric
DTF	Distance from tapeline to flangeback, inches
NW	Number of wheel profile data points, $9 \leq \text{NW} \leq 200$
XW,YW	Arrays of data points for wheel profile, dimension NW XW(I) = distance from tape line, positive out, inches YW(I) = wheel radius at XW(I), inches
IRAIL	Label for rail, alphanumeric
DRW	Distance from rail head centerline to a point on the inside of the rail 5/8" down from the top of the rail, inches
XW1, YW1	Arrays of data points for rail profile, dimension NW XW1(I) = distance from centerline of rail, positive out, inches YW1(I) = height of rail at XW1(I), inches

4) Input Formats:

A sample deck set up is listed in section E of this appendix. The program requires the wheel and rail profile data, rail cant, rail gauge, wheel gauge and certain program control information in the following format:

Card #	Col. #	Contents	Format
1	1-3	NUMB	(2I3)
"	4-6	INC	
2	X	WG	()-unspecified
"	X	RG	
"	X	BR	
"	X	BL	
3	1-72	IWHEEL	(13A6)
4	X	DTF	()
5	1-3	NW	(I3)
6 to NW+5	11-25 26-40	XW(I) (data must be in order starting with largest XW) YW(I)	(10X,2E15.7)
NW+6	1-72	IRAIL	(13A6)
NW+7	X	DRW	()
NW+8	1-3	NY	(I3)
NW+9 to NY+NW+8	11-25 26-40	XW1(I) (data must be in order start- ing with largest XW1) YW1(I)	(10X,2E15.7)

5) Output: For a sample output, see section D of this appendix.

The main program prints out the first section which contains wheel and rail descriptions and the coefficients of the fourth order polynomials used to fit the profiles. Describing functions of certain of the results are printed by the DCRFCN subroutine. Finally, a table is printed by the main program that contains all the results in tabular form. The input profiles and results are plotted by subroutines PLOT1 and PLOT2.

The Fortran names used in the program output are the following:

AMP	Amplitude of wheelset lateral motion, inches
ALAM	Describing function of the nondimensional difference in rolling radii, $(r_L - r_R)/2a$, as a function of nondimensional wheelset lateral position, x_W/a_W .
DELM	Describing function of one half the difference in contact angles as a function of nondimensional wheelset lateral position, x_W/a_W .
WSRL	Describing function of the wheelset roll angle as a function of nondimensional wheelset lateral position, x_W/a_W .
XW	Wheelset lateral displacement, positive to the left, inches
X1, X3	Contact locations on the right and left wheels, positive out from tapeline, inches
X2, X4	Contact locations on the right and left rails, positive out from centerline, inches
RR, RL	Rolling radii, right and left wheels, inches

YR, YL Rail head profile height, right and left rails, inches
 MR, ML Contact angles on the right and left wheel with respect to the axle, radians
 WR Wheelset roll angle with respect to the horizontal (positive up on left), radians
 YCG Vertical displacement of wheelset centroid from nominal position, inches
 R1, R2 Profile radii of curvature on right wheel and right rail, inches

6) Summary of User Requirements and Recommendations:

All input data is on cards with the formats shown. To pick a value for NUMB, the number of points to be calculated, note that NUMB determines the range of the wheelset lateral positions, i.e., the maximum wheelset amplitude = $\frac{\text{NUMB} - 1}{100}$ inches. If calculations are made for too large a wheelset lateral displacement then the plotted results may extend past the borders of the graphs. Suggested values for NUMB are (1) for wide gauge take NUMB = 121 (the maximum allowed), (2) normal gauge take NUMB = 101, and (3) narrow gauge take NUMB = 81. INC determines the data points per curve-fit zone. If INC is small then the fitted curve will fit the points more closely. If INC is larger, more numerical smoothing will be done. Take INC = 6 for a start. If the curves do not fit the profiles well enough (this is determined from the plot where the profile data points and curve-fits are plotted together) then decrease INC. Remember to input the profile data points (wheel and rail) in a sequence that starts with the largest "X" value and moves toward the smallest. This is necessary because the program separates the profiles into zones assuming this order. There are a few error messages in the program which are self-explanatory. There is also a warning printed when the wheelset roll angle iteration does not converge.

C. METHOD

The computations carried out in this program can be divided into four sections:

- (1) Mathematical Description of Rail and Wheel Profiles
- (2) Calculation of Contact Point Locations

(3) Quantitative Description of Geometric Constraint Relations

(4) Quasi-linearization

The computational procedures and mathematical representations used in these four sections, respectively, are described below. A program listing for each subroutine may be found in section E of the appendix.

1) Mathematical Description of Rail and Wheel: The inputs to the program are:

- (a) parameters specifying the size of regions to be curve-fit and the amplitude of wheelset lateral displacement allowed
- (b) wheel and rail gauges
- (c) tabular wheel and rail profile data
- (d) tapeline to flange-back distance and one-half head rail width.

The rail and wheel profiles are described by fourth order polynomials fitted to sub-intervals of the profiles. The sub-intervals consist of a specified number of data points with an overlap of three data points on each adjoining interval. The tabular profile data is read into a subroutine, PRFLE, that separates the data into the regions and then calls another subroutine, CRVFT, to fit a fourth order polynomial to each region. The curve-fitting is accomplished in subroutines ORTHLS and COEFS [A-1] that use an orthogonal polynomial, least-squares curve fitting approach.

The output of the profile subroutine for each profile is:

- (1) a set of fourth order polynomials with each polynomial fitting a certain interval of the profile and (2) the limits defining each interval of the profile.

2) Calculation of Contact Point Locations: The theory behind the contact point calculations is described in Chapter 4. The iteration and sweeping procedures described there are performed in subroutine CHECK. Subroutine EQSOLV increment increases the wheelset lateral displacement and calls on the CHECK subroutine to find the contact points. Several geometric relations are used in subroutine CHECK. The first is the equation describing the correspondence between points on the wheel and points on the rail. The equations that express the requirement that the wheel and rail contact at the same lateral positions are, on the right

A-1. Math-Pack, UP-7542 Rev. 1, Univac Large Scale Systems, Sperry Rand Corporation, Sec. 13, pp. 24-44.

$$a_r + x_{r_R} = -x_w + (a_w + x_{w_R}) \cos \phi_w - r_R \sin \phi_w \quad (A-1)$$

and, on the left

$$a_r + x_{r_L} = x_w + (a_w + x_{w_L}) \cos \phi_w + r_L \sin \phi_w \quad (A-2)$$

The variables in these equations are shown in figures 2-6 and 2-7. The equations equate the lateral distance of corresponding wheel and rail points from the track centerline. They are used in subroutine CHECK to find corresponding points on the wheel and rail to check for the minimum separation distance. Recall that the minimum separation distance indicates a contact point.

The heights that are required in calculating the minimum separation distance are computed from the following four equations, one set for the wheels and one set for the rails.

$$h_{\text{right wheel}} = -r_R \cos \phi_w - (a_w + x_{w_R}) \sin \phi_w \quad (A-3)$$

$$h_{\text{left wheel}} = -r_L \cos \phi_w + (a_w + x_{w_L}) \sin \phi_w \quad (A-4)$$

$$h_{\text{right rail}} = Y_R + X_{r_R} \sin \beta_R \quad (A-5)$$

$$h_{\text{left rail}} = Y_L + X_{r_L} \sin \beta_L \quad (A-6)$$

The datum used for the wheel heights is a horizontal line through the wheelset centroid. Distances above the line are positive. The datum used for rail heights is the horizontal line through the base of the rails. Rail cant is assumed to tilt only the top of the rail head about its midpoint, in accordance with the standard practice of measuring the rail gauge after the rail has been canted. The actual datums used for the wheel or rail are arbitrary, as we are only interested in the minimum separation.

Wheelset roll angle is calculated from

$$\phi_w = \frac{(Y_L - Y_R) + X_{r_L} \sin \beta_L - X_{r_R} \sin \beta_R + (r_L - r_R) \cos \phi_w}{(2 a_w + x_{w_R} + x_{w_L}) \cos \phi_w} \quad (A-7)$$

where the variables are again shown in figures 2-6 and 2-7. Note that ϕ_w is defined in terms of itself. In the program an iterative scheme was used to solve this equation.

3) Quantitative Description of Geometric Constraint Relations. The defining equations used to calculate the geometric constraint relations are evaluated in subroutine EQSUB2. EQSUB2 calls subroutines CHOOSE and RADII to choose the applicable curve-fits and to evaluate them at the contact locations determined from the value of wheelset lateral position under consideration. The defining equations for these constraint relations follow below. See figure 2-6 for an illustration of the variables appearing in the equations.

1. Rolling radii and rail heights

r_R, Y_R, r_L, Y_L - evaluated from curve-fits

2. Contact angles

$$\delta_R = \text{arc tan} \left[\frac{d}{dx_{wR}} (r_R) \right] \quad (\text{A-8})$$

$$\delta_L = \text{arc tan} \left[\frac{d}{dx_{wL}} (r_L) \right]$$

3. Normalized difference in rolling radii

$$\Delta r = \frac{r_L - r_R}{2 a_r} \quad (\text{A-9})$$

4. Normalized difference in contact angles

$$\Delta \delta = \frac{\delta_L - \delta_R}{2} \quad (\text{A-10})$$

5. Roll angle

$$\phi_w = \text{arc tan} \frac{(Y_L + r_L \sin \beta_L + r_L \cos \phi_w) - (Y_R + X_{rR} \sin \beta_R + r_R \cos \phi_w)}{(2 a_w + X_{wR} + X_{wL}) \cos \phi_w} \quad (\text{A-11})$$

6. Vertical displacement of wheelset c.g.

$$y_{cg} = \begin{bmatrix} \frac{Y_L + Y_R + x_{r_L} \sin \beta_L + x_{r_R} \sin \beta_R + (r_L + r_R) \cos \phi_w}{2} \\ \frac{Y_L + Y_R + x_{r_L} \sin \beta_L + x_{r_R} \sin \beta_R + (r_L + r_R) \cos \phi_w}{2} \end{bmatrix}_{x_w = 0} \quad (A-12)$$

7. Radii of curvature of profiles

$$R_{Wheel} = \frac{\left[1 + \left(\frac{d}{dx_{w_R}} (r_R) \right)^2 \right]^{3/2}}{\frac{d^2}{dx_{w_R}^2} (r_R)}$$

$$R_{Rail} = - \frac{\left[1 + \left(\frac{d}{dx_{r_L}} (Y_r) \right)^2 \right]^{3/2}}{\frac{d^2}{dx_{r_L}^2} (Y_L)} \quad (A-13)$$

Although the radii of curvature calculation is included in this program, there are problems associated with the calculation of the second derivatives of the wheel and rail profiles that are required in the equation for the radius of curvature. The second derivatives of the curves fitted to the profiles are not continuous. Thus, the computed radii of curvature do not vary in a reasonable manner between sub-intervals. Further work is needed to find a better method of evaluating these derivatives. Perhaps interpolation and differentiation directly from the data points would provide smoother results for the first and second derivatives of the curves.

4) Quasi-linearization. The sinusoidal input describing function was defined in Chapter 2 by the following equation:

$$Y_q = \frac{1}{\pi A^2} \int_0^{2\pi} F(A \sin \phi) A \sin \phi d \phi. \quad (A-14)$$

The relations we wished to quasi-linearize were the following:

$$\Delta r \equiv \frac{r_L - r_R}{2a_r}, \quad \Delta \delta \equiv \frac{\delta_L - \delta_R}{2}, \quad \text{and} \quad \phi_w.$$

These are non-dimensional and non-hysteretic. Also, due to the symmetry of the wheel and rail profiles, they are odd functions of the wheelset lateral position, i.e. $\Delta r(x_w) = -\Delta r(-x_w)$. If these properties are applied, the describing function can be re-written as:

$$Y_q = \frac{4}{\pi A^2} \int_0^{\pi/2} F(A \sin \phi) A \sin \phi d \phi. \quad (A-15)$$

This equation is numerically integrated in the program. To do this, the integration increment, $d\phi$, was expressed as a function of x , because the functions to be quasi-linearized were tabulated as functions of x . The substitution was made by letting

$$x = A \sin \phi \quad (A-16)$$

or

$$\phi = \sin^{-1} \frac{x}{A}, \quad 0 \leq \phi \leq \pi/2 \quad (A-17)$$

and thus

$$\begin{aligned} \Delta \phi_n &= \phi_n - \phi_{n-1} \\ &= \sin^{-1} \left(\frac{x_n}{A} \right) - \sin^{-1} \left(\frac{x_{n-1}}{A} \right) \end{aligned} \quad (A-18)$$

Substitution of this result into the describing function equation gives

$$Y_q = \frac{4}{\pi A^2} \int_0^{\pi/2} F(x) x d \phi(x) \quad (A-19)$$

When we let $f(x) = F(x) x$ and numerically integrate using the trapezoidal rule, we obtain

$$Y_q \cong \frac{4}{\pi A^2} \frac{f(x_1) + f(x_2)}{2} \left(\sin^{-1} \frac{x_2}{A} - \sin^{-1} \frac{x_1}{A} \right) + \frac{f(x_2) + f(x_3)}{2} \left(\sin^{-1} \frac{x_3}{A} - \sin^{-1} \frac{x_2}{A} \right) + \dots + \frac{f(x_{n-1}) + f(x_n)}{2} \left(\sin^{-1} \frac{x_n}{A} - \sin^{-1} \frac{x_{n-1}}{A} \right)$$

where $x_1 = 0$ and $x_n = A$.

(A-20)

This equation was programmed in subroutine DCRFCN. It was multiplied, in the subroutine, by a_r to non-dimensionalize the describing function for the parameters considered.

D. TEST PROBLEM

The following test problem is given to demonstrate the program. The calculations were performed on a Univac 1110 computer.

Profiles: New Wheel
 New Rail
 Gauges: Rail gauge - nominal, 4' 8 1/2"
 Wheel gauge - nominal, 4' 8"

Maximum Allowed Wheelset Lateral Displacement: One Inch

The program listing, input, and output for this problem are contained in the following section.

E. PROGRAM LISTINGS WITH EXAMPLE INPUT AND OUTPUT

- 1) Listings
- 2) Sample Input
- 3) Sample Output

MAIN PROGRAM WHRAIL

```

COMMON /COMA/ AW,AK,BR,FL,RR(70,5),YR(70,5),RL(70,5),YL(70,5),
1 B1(70,2),B2(70,2),B3(70,2),B4(70,2),S1(5),S2(5),S3(5),S4(5),
1 AXW(244),AX1(244),AX2(244),AX3(244),AX4(244),AR1(244),AR2(244),
1 AR3(244),AR4(244),AR5(244),AM1(244),AM2(244),AM3(244),AW1(244),
1 AY1(244),I,HEEL(13),IRAIL(13),NC1,NC2,NC3,NC4,R1(244),R2(244)

COMMON /COMB/ X1(402),Y1(402),W3(402),C(5),ALPHA(4),RETA(4),
1 T1(402),T2(402),T3(402),YF(402)

DIMENSION XW1(200),YW1(200),          XW2(200),YW2(200),
1 XOLF(4),W(402),F1(200),F2(200),F3(200),ITODAY(2),ITIM(2)

REAL NR,NL

C INPUT DATE AND TIME OF THIS RUN
CALL DATE(ITODAY)
CALL TIME(ITIM)
30 FORMAT(3I3)
READ 30,NUMB,INC
NUMBR=2.*NUMB

C NUMBR=NO OF PTS TO BE CALCULATED
C * NO OF PTS TO BE CALCULATED MUST BE LT 400, XW IS + OR - NUMBR*.01/2.
C * FIT A CURVE EVERY INC DATA PTS (SUGGEST INC=5)
C WG=WHEEL GAGE, RG=RAIL GAGE, BR=BL=CANT OF RAILS
READ 20,WG,RG,BR,BL
C *** READ A ONE LINE LABEL FOR THE TYPE OF WHEEL
READ 10,(IWHEEL(I),I=1,13)
10 FORMAT(13A6)
READ 20,DTE
C DTE=DIST FROM TAPELINE TO FLANGEBACK ON WHEEL
AW=WG/2.+DTE
C *** AW=SEMI WHEEL GAGE=1/2 DIST BETWEEN TAPE LINES
20 FORMAT( )
CALL PRFL(NW,XW1,YW1,NC1,RR,B1,F1,F2,F3,S1,INC)
C *** READ A ONE LINE LABEL FOR TYPE OF RAIL
READ 10,(IRAIL(I),I=1,13)
READ 20,DRW
C *** DRW=1/2 RAIL WIDTH AT 5/8 IN DOWN
AK=RG/2+DRW
C *** AK=1/2 DIST FROM CENTER OF ONE RAIL TO CENTER OF THE OTHER
CALL PRFL(NY,XW2,YW2,NC2,YR,B2,F1,F2,F3,S1,INC)
C RECORD THE LIMITS OF THE RAIL AND WHEEL PROFILES
XMIN=XW2(NY)
XMAX=XW2(1)
XMAXW=XW1(1)
XMINW=XW1(NW)
C USE THE SAME WHEEL PROFILE ON EITHER END OF THE WHEELSET
NC3=NC1
DO 60 I=1,NC1
DO 50 J=1,5
RL(I,J)=RK(1,J)
50 CONTINUE
B3(I,1)=B1(I,1)
B3(I,2)=B1(I,2)
60 CONTINUE
C USE THE SAME RAIL PROFILE ON EITHER SIDE OF THE TRACK
NC4=NC2
DO 80 I=1,NC2
DO 70 J=1,5
YL(I,J)=YR(I,J)
70 CONTINUE
B4(I,1)=B2(I,1)
B4(I,2)=B2(I,2)
80 CONTINUE
C ENCODE THE CANT, WHEEL GAGE, AND RAIL GAGE FOR USE ON OUTPUTTING
C THEM IN THE PLOTTING ROUTINES
ENCODE(6,98,ICT)PK
ENCODE(6,99,IWG)WG
ENCODE(6,99,IRG)RG
98 FORMAT(F6.4)
99 FORMAT(F6.3)
CALL PLOTS(0,0,0)

```

```

C PLOTTER CONTROL CARD, VARIES WITH COMPUTER
  CALL LATEND(32.)
  CALL PLOT1(IW,XW1,YW1,NY,XW2,YW2,ICT,IWG,IRG)
C PLOT TABULAR WHEEL AND RAIL DATA AND FITTED CURVES
  CALL EQSOLV(NUMBR,XOLD,XMIN,XMAX,XMAXW,XMINW)
C FINDS THE CONTACT PT LOCATIONS
  CALL EQSUB2(NUMBR,W)
C FINDS THE GEOMETRIC CONSTRAINT RELATIONS
  CALL PLOT2(NUMBR,ITODAY,ITIM)
C PLOT THE C.P. LOCATIONS AND THE GEOMETRIC CONSTRAINT RELATIONS
  CALL PLOT(0.,0.,999)
C PLOTTER CONTROL CARD, VARIES WITH COMPUTER
  IREQ=0.
  NL=0.
  PRINT 199
190 FORMAT(1H1///2X,'***** RESULTS ***** '////)
C PRINT MATHEMATICAL DESCRIPTIONS OF WHEELSET AND TRACK
  PRINT 200,IWHEEL,WG,AW,INC
200  FORMAT(12X,'WHEEL/RAIL CONTACT CHARACTERIZATION'///9X,13A6/
1 2X,'WHEEL GAGE=' ,F6.3/2X,'1/2 DIST BETWEEN TAPE LINES=' ,F6.3//
1 5X,'CURVE FITS',3X,I2,' PTS/CURVE FIT ZONE'/12X,'0TH',10X,'1ST',
1 10X,'2ND',10X,'3RD',10X,'4TH')
C
  DO 210 I=1,NC1
  PRINT 205,I,(RR(I,J),J=1,5),B1(I,1),B1(I,2)
205  FORMAT(2X,I3,3X,5(E11.6,2X),3X,'FROM ',F7.4,' TO ',F7.4)
210  CONTINUE
C
  PRINT 220,IRAIL,RG,AR,BR,BL,NR,NL,INC
220  FORMAT(//79X,13,6/2X,'RAIL GAGE=' ,F6.3/2X,'1/2 DIST BETWEEN RAIL CE
1 INTERS=' ,F6.3/ 2X,'3R=' ,F6.3,2X,'PL=' ,F6.3,2X,'NR=' ,F6.3,2X,'NL=' ,
1 F6.3//5X,'CURVE FITS',3X,I2,' PTS/CURVE FIT ZONE'/12X,'0TH',
1 10X,'1ST',10X,'2ND',10X,'3RD',10X,'4TH')
C
  DO 230 I=1,NC2
  PRINT 205,I,(YR(I,J),J=1,5),B2(I,1),B2(I,2)
230  CONTINUE
C
C PRINT A TABLE OF MOST OF THE RESULTS
  PRINT 240
240  FORMAT(1H1///2X,'***** DATA POINTS *****'/ )
  PRINT 245
245  FORMAT(//4X,'XW',7X,'X1',6X,'X2',6X,'X3',6X,'X4',7X,'RR',7X,'YR',
1 7X,'RL',7X,'YL',9X,'MR',8X,'ML'//)
  PRINT 250,(AXW(I),AX1(I),AX2(I),AX3(I),AX4(I),AR1(I),AR2(I),
1 AR3(I),AR4(I),AM1(I),AM2(I),I=1,NUMBR)
250  FORMAT(2X,F6.3,2X,F7.4,1X,F7.4,1X,F7.4,1X,F7.4,2X,F8.5,1X,F8.5,
1 1X,F8.5,1X,F8.5,2X,F9.6,1X,F9.6)
  PRINT 255
255  FORMAT(//4X,'XW',4X,'(RL-RR)/2A',1X,'(ML-MR)/2',
1 6X,'WR',8X,'YCG',9X,'R1',9X,'R2'//)
  PRINT 260,(AXW(I),AR5(I),AM3(I),AW1(I),AY1(I),R1(I),R2(I),I=1,
1 NUMBR)
260  FORMAT(2X,F6.3,2X,F9.6,2X,F9.6,2X,F9.6,2X,F9.6,2X,F8.3,2X,F8.3)
C QUASI-LINEARISE SOME OF THE RELATIONS AND PRINT OUT RESULTS
  CALL DCREFCN(NUMBR,AXW,AR5,AM3,AW1,AR)
310  FORMAT(8E10.5)
C OUTPUT RESULTS ON CARDS
  PUNCH 320,ITODAY,ITIM
320  FORMAT(2A6,2A6)
  PUNCH 10,(IWHEEL(I),I=1,13)
  PUNCH 335,WG,AW,NC1
  DO 322 I=1,NC1
  PUNCH 340,I,(RR(I,J),J=1,5),B1(I,1),B1(I,2)
322  CONTINUE
  PUNCH 10,(IRAIL(I),I=1,13)
  PUNCH 345,RG,AR,BR,BL,NR,NL,NC2
  DO 328 I=1,NC2
  PUNCH 340,I,(YR(I,J),J=1,5),B2(I,1),B2(I,2)
328  CONTINUE
  PUNCH 30,NUMBR,INC

```

```
PUNCH 330, (, XW(I), AX1(I), AX2(I), AX3(I), AX4(I), AR1(I), AR2(I),  
1 AR3(I), AR4(I), AM1(I), AM2(I), AR5(I), AM3(I), AW1(I), AY1(I), R1(I),  
IR2(I), I=1, NIMBR)  
330 FORMAT(7E11.6/7E11.6/3E11.6)  
335 FORMAT(2E10.5, I3)  
340 FORMAT(I3, 5E11.6, 2E11.6)  
345 FORMAT(6E10.5, I3)  
400 CONTINUE  
END
```

```

SUBROUTINE PRFILE(NW,XW,YW,NC,RR,XB,F1,F2,F3,SS,INC)
DIMENSION XW(1),YW(1),RR(70,1),XB(70,1),F1(1),F2(1),F3(1),SS(1)
C INPUT
C NW=NO OF DATA PTS
C DATA MUST BE IN ORDER STARTING WITH POSITIVE XW
10 FORMAT(3I3)
15 FORMAT(10X,2E15.7)
READ 10,NW
READ 15,XW
C DECIDE THE NO OF CURVE FITS, NC, TO USE
C FIT A CURVE EVERY INC DATA PTS
NC=NW/INC
IF((NW-INC*NC).GE.3)NC=NC+1
IF(NC.LT.3) PRINT 18
18 FORMAT(2X,'*** ERROR *** TOO LARGE AN INCREMENT OR NOT ENOUGH DATA
1 PTS')
C FIT FIRST CURVE
C XB(1,1)=UPPER LIMIT OF CURVEFIT
C XB(1,2)=LOWER LIMIT
XB(1,1)=200.
XB(1,2)=XW(INC)
J=INC+1
DO 20 I=1,J
F1(I)=XW(I)
F2(I)=YW(I)
20 CONTINUE
CALL CRVFT(J,0,F1,F2,F3,SS)
DO 25 I=1,5
RR(1,I)=SS(I)
25 CONTINUE
C FIT OTHER CURVES
NC1=NC-1
DO 100 II=2,NC1
J=II-1
XB(II,1)=XB(J,2)
J=INC*II
XB(II,2)=XW(J)
J=(II-1)*INC-2
K=II*INC+3
L=0
DO 40 I=J,K
L=L+1
F1(L)=XW(I)
F2(L)=YW(I)
40 CONTINUE
CALL CRVFT(L,0,F1,F2,F3,SS)
DO 45 I=1,5
RR(II,I)=SS(I)
45 CONTINUE
100 CONTINUE
C FIT LAST CURVE
XB(NC,1)=XB(NC1,2)
XB(NC,2)=XW(NW)
K=NW
J=NC1*INC-2
DO 150 I=J,NW
K=K+1
F1(K)=XW(I)
F2(K)=YW(I)
150 CONTINUE
CALL CRVFT(K,0,F1,F2,F3,SS)
DO 155 I=1,5
RR(NC,I)=SS(I)
155 CONTINUE
RETURN
END

```

```

SUBROUTINE CRVFT(N,L,X,Y,W,A)
COMMON /COMB/ X1(402),Y1(402),W1(402),C(5),ALPHA(4),BETA(4),
1 T1(402),T2(402),T3(402),YF(402)
DIMENSION X(1),Y(1),W(1),A(1)
J=0
K=4
DO 10 I=1,N
C STORE X AND Y VALUES
X1(I)=X(I)
Y1(I)=Y(I)
W1(I)=W(I)
10 CONTINUE
C FIT CURVE
CALL ORTHLS(X1,Y1,W1,N,L,J,C,ALPHA,BETA,K,T1,T2,T3,IND1)
C GET COEFFICIENTS OF THE CURVE
CALL COEFS(J,C,ALPHA,BETA,K,A,T1,T2,T3,IND2)
RETURN
END

```

```

SUBROUTINE PLOT1(NW,XW1,YW1,NY,XW2,YW2,ICT,IWG,IRG)
COMMON /COMA/ AW,AR,BR,BL,RR(70,5),YR(70,5),RL(70,5),YL(70,5),
1 B1(70,2),B2(70,2),B3(70,2),B4(70,2),S1(5),S2(5),S3(5),S4(5),
1 AXW(244),AX1(244),AX2(244),AX3(244),AX4(244),AR1(244),AR2(244),
1 AR3(244),AR4(244),AR5(244),AM1(244),AM2(244),AM3(244),AW1(244),
1 AY1(244),IWHEEL(13),IRAIL(13),NC1,NC2,NC3,NC4,ZZ(488)
DIMENSION XW1(1),YW1(1),XW2(1),YW2(1)
C CALCULATE AN ARRAY OF PTS FROM POLYNOMIALS FIT TO WHEEL PROFILE
CALL GTPTS(XW1(1),XW1(NW),RR,B1,NC1,AXW,AR1,S1,NU)
C CALCULATE AN ARRAY OF PTS FROM POLYNOMIALS FIT TO RAIL PROFILE
CALL GTPTS(XW2(1),XW2(NY),YR,B2,NC2,AX1,AR3,S2,NB)
C DEFINE SCALING FACTORS FOR PLOTS
NW1=NW+1
NW2=NW+2
NY1=NY+1
NY2=NY+2
XW1(NW1)=0.
YW1(NW1)=0.
XW2(NY1)=0.
YW2(NY1)=0.
XW1(NW2)=1.
YW1(NW2)=1.
XW2(NY2)=1.
YW2(NY2)=1.
NU1=NU+1
NU2=NU+2
NB1=NB+1
NB2=NB+2
AXW(NU1)=0.
AR1(NU1)=0.
AR3(NB1)=0.
AX1(NB1)=0.
AXW(NU2)=1.
AR1(NU2)=-1.
AR3(NB2)=1.
AX1(NB2)=1.
C SUBTRACT CONSTANT TERMS FROM DATA POINTS TO REDUCE MAGNITUDES
DO 10 I=1,NU
AK1(I)=AR1(I)-16.5
10 CONTINUE
DO 15 I=1,NB
AK3(I)=AR3(I)-7.
15 CONTINUE
DO 20 I=1,NW
YW1(I)=-YW1(I)+16.5
20 CONTINUE
DO 30 I=1,NY
YW2(I)=YW2(I)-7.
30 CONTINUE
C PLOT THE PROFILES AND LABEL THEM
CALL PLOT(23.,17.5,-3)
CALL AXIS(-2.,.5,11,RIGHT WHEEL,-11,4.,0.,-2.,1.)
CALL LINE(AXW,AR1,NU,1,0,3)
CALL LINE(XW1,YW1,NW,1,-2,3)
CALL SYMBOL(-2.,-.4,.14,IWHEEL,0.,78)
CALL PLOT(5.5,0.,-3)
CALL AXIS(-2.,.5,10,RIGHT RAIL,-10,4.,0.,-2.,1.)
CALL LINE(AX1,AR3,NB,1,0,3)
CALL LINE(XW2,YW2,NY,1,-2,3)
CALL SYMBOL(-2.,-.4,.14,IRAIL,0.,78)
CALL SYMBOL(-6.,-1.4,.14,11HWHEEL GAGE ,0.,11)
CALL SYMBOL(-4.46,-1.4,.14,IWG,0.,6)
CALL SYMBOL(-3.48,-1.4,.14,3HIN.,0.,3)
CALL SYMBOL(-6.,-1.63,.14,10HRAIL GAGE ,0.,10)
CALL SYMBOL(-4.6,-1.63,.14,IRG,0.,6)
CALL SYMBOL(-3.62,-1.63,.14,3HIN.,0.,3)
CALL SYMBOL(-2.48,-1.4,.14,10HRAIL CANT ,0.,10)
CALL SYMBOL(-1.08,-1.4,.14,ICT,0.,6)
CALL PLOT(-28.5,-17.5,-3)
RETURN
END

```

```

SUBROUTINE GTPTS(XMAX,XMIN,RR,B,NC,AXW,AR1,S1,NU)
DIMENSION AXW(1),AR1(1),S1(1),RR(70,1),B(70,1)
C DEFINE STARTING VALUES
X=XMAX
IJ=1
C LOOP TO FIND EACH PT.
DO 6 I=1,400
  NU=I
C CHOOSE THE POLYNOMIAL VALID FOR THE SPECIFIC X
  DO 2 J=IJ,NC
    IF(B(J,2).LE.X.AND.B(J,1).GT.X) GO TO 3
  2 CONTINUE
  3 IJ=J
C STORE THE POLY COEFS
  DO 4 K=1,5
    S1(K)=RR(J,K)
  4 CONTINUE
  AXW(I)=X
C CALCULATE THE Y VALUE
  AR1(I)=S1(1)+S1(2)*X+S1(3)*X**2+S1(4)*X**3+S1(5)*X**4
C INCREMENT X BY -.025 INCHES
  X=X-.025
C CHECK FOR END OF PROFILE
  IF(X.LT.XMIN) GO TO 7
  6 CONTINUE
  7 CONTINUE
  RETURN
END

```



```

SUBROUTINE EQSOLV(NUMBR,XOLD,XMIN,XMAX,XMAXW,XMINW)
COMMON /COMA/ AW,AR,BR,BL,RR(70,5),YR(70,5),RL(70,5),YL(70,5),
1 B1(70,2),B2(70,2),B3(70,2),B4(70,2),S1(5),S2(5),S3(5),S4(5),
1 AXW(244),AX1(244),AX2(244),AX3(244),AX4(244),AR1(244),AR2(244),
1 AR3(244),AR4(244),AR5(244),AM1(244),AM2(244),AM3(244),AW1(244),
1 AY1(244),I_WHEEL(13),IRAIL(13),NC1,NC2,NC3,NC4,ZZ(488)
C
C DIMENSION XOLD(1)
C INITIALIZE WHEELSET DISPLACEMENT, INCREMENTS OF DISPLACEMENT, AND ROLL
XW=0.
XWI=0.
WR=0.
C COMPUTE 1/2 THE NUMBER OF DATA PTS DESIRED
NHALF=NUMBR/2
C COMPUTE C.P. LOCATIONS AS WHEELSET IS LATERALED INCREMENTALLY IN THE
C POSITIVE DIRECTION
DO 250 NUMB=1,NHALF
C ROUTINE THAT FINDS CONTACT PT LOCATIONS
CALL CHECK(XW,XWI,XOLD,XMIN,XMAX,
1 XMAXW,XMINW,WR)
C XW IS INCREMENTED WITHIN CHECK
C STORE CONTACT PTS AND WHEELSET LATERAL
50 AXW(NUMB)=XW
AX1(NUMB)=XOLD(1)
AX2(NUMB)=XOLD(2)
AX3(NUMB)=XOLD(3)
AX4(NUMB)=XOLD(4)
C XWI=SIZE OF WHEELSET LATERAL INCREMENTS
XWI=.01
250 CONTINUE
C TRANSPOSE RESULTS TO GET RESULTS FOR WHEELSET LATERALED IN NEGATIVE DIR
DO 220 J=1,NHALF
I=J+NHALF
AXW(I)=-AXW(J)
AX1(I)=AX3(J)
AX2(I)=AX4(J)
AX3(I)=AX1(J)
AX4(I)=AX2(J)
220 CONTINUE
C STORE ALL THE RESULTS
DO 400 I=1,NUMBR
AR1(I)=AXW(I)
AR2(I)=AX1(I)
AR3(I)=AX2(I)
AR4(I)=AX3(I)
AR5(I)=AX4(I)
400 CONTINUE
C REARRANGE THE RESULTS SO THEY GO FROM NEGATIVE TO POSITIVE
DO 405 I=1,NHALF
J=I+NHALF
K=NUMBR-I+1
AXW(J)=AR1(I)
AX1(J)=AR2(I)
AX2(J)=AR3(I)
AX3(J)=AR4(I)
AX4(J)=AR5(I)
AXW(I)=AR1(K)
AX1(I)=AR2(K)
AX2(I)=AR3(K)
AX3(I)=AR4(K)
AX4(I)=AR5(K)
405 CONTINUE
RTURN
END

```

```

SUBROUTINE CHECK(XW,DXW,XOLD,XMIN,
1 XMAX,XMAXW,XMINW,WR)
COMMON /COMA/ AW,AR,BR,BL,RR(70,5),YR(70,5),RL(70,5),YL(70,5),
1 B1(70,2),B2(70,2),B3(70,2),B4(70,2),S1(5),S2(5),S3(5),S4(5),
1 Z(3660),I,WHEEL(13),IRAIL(13),NC1,NC2,NC3,NC4,ZZ(488)
C
C DIMENSION XOLD(1)
C INCREMENT WHEELSET LATERAL
XW=XW+DXW
C ITERATION LOOP ON WHEELSET ROLL ANGLE
A1=XMINW
A3=XMINW
DO 120 IJK=1,8
C CHOOSE PTS, ON INSIDE EDGES, FROM WHICH TO START SEARCH
AX1=I1
AX3=A3
C=COS(BR)
S=SIN(WR)
DO 30 I=1,600
CALL CHOOSE(AX1,0.,AX3,0.)
CALL RADII(S1,S2,S3,S4,AX1,0.,AX3,0.,R1,R2,R3,R4)
AX2=-XW-AR+(AW+AX1)*C -R1*S
AX4=XW-AR+(AW+AX3)*C +R3*S
IF(AX2.GE.XMIN) GO TO 10
A1=AX1+.01
10 IF(AX4.GE.XMIN) GO TO 20
A3=AX3+.01
20 IF(AX2.GE.XMIN.AND.AX4.GE.XMIN) GO TO 40
30 CONTINUE
C INITIALIZE DIFFERENCES IN HEIGHTS
40 DL1=100.
DL3=100.
A1=AX1
A3=AX3
C LOOP TO SEARCH PROFILES FOR CONTACT PTS
DO 100 I100=1,500
C CALCULATE HTS OF PTS
CALL CHOOSE(AX1,AX2,AX3,AX4)
CALL RADII(S1,S2,S3,S4,AX1,AX2,AX3,AX4,R1,R2,R3,R4)
H2=AR2+AX2*SIN(BR)
H4=AR4+AX4*SIN(BL)
H1=-AR1*C -(AW+AX1)*S
H3=-AR3*C +(AW+AX3)*S
C CALCULATE SEPARATION DIST
DH1=H1-H2
DH3=H3-H4
C CHECK FOR MIN SEP ON RT
IF(DH1.GE.DL1) GO TO 50
BX1=AX1
BX2=AX2
DL1=DH1
C CHECK FOR MIN SEP ON LT
50 IF(DH3.GE.DL3) GO TO 60
BX3=AX3
BX4=AX4
DL3=DH3
C GET NEXT PTS TO CHECK
60 X1=AX1+.01
X3=AX3+.01
CALL CHOOSE(X1,0.,X3,0.)
CALL RADII(S1,S2,S3,S4,X1,0.,X3,0.,R1,R2,R3,R4)
X2=-XW-AR+(AW+X1)*C -R1*S
X4=XW-AR+(AW+X3)*C +R3*S
C CHECK FOR END OF PROFILE
IF(X1.GE.XMAXW.OR.X2.GE.XMAX) GO TO 70
AX1=X1
AX2=X2
70 IF(X3.GE.XMAXW.OR.X4.GE.XMAX) GO TO 80
AX3=X3
AX4=X4
80 IF((X1.GE.XMAXW.OR.X2.GE.XMAX).AND.(X3.GE.XMAXW.OR.X4.GE.XMAX))
1 GO TO 110

```

```

100 CONTINUE
C KEEP PREVIOUS ROLL ANGLE
110 WR2=WR
    C=COS(WR2)
C COMPUTE NEW ROLL ANGLE
    X1=BX1
    X2=BX2
    X3=BX3
    X4=BY4
    CALL CHOOSE(X1,X2,X3,X4)
    CALL RADII(S1,S2,S3,S4,X1,X2,X3,X4,R1,R2,R3,R4)
    WR=(R4-R2+X4*SIN(BL)-X2*SIN(BR)+(R3-R1)*C )/
    1 ((2.*AW+X1+X3)*C )
C CHECK FOR CONVERGENCE BY COMPAIRING ROLL ANGLES
    IF(ABS(WR-WR2).LE..00001 ) GO TO 125
120 CONTINUE
125 CONTINUE
C ERROR CHECK
    ER=WR-WR2
    IF(IJK.GE.8) PRINT 130,ER,XW
130 FORMAT( 4X,'*** WARNING *** WHEELSET ROLL ANGLE CONVERGED ONLY WI
    1THIN WR(NEW)-WR(OLD)=',F9.5,' AT XW=',F6.3)
C STORE THE CONTACT PT LOCATIONS
    XOLD(1)=BX1
    XOLD(2)=BX2
    XOLD(3)=BX3
    XOLD(4)=BX4
    RETURN
    END

```

```

SUBROUTINE CHOOSE(X1,X2,X3,X4)
COMMON /COMA/ AW,AR,BR,BL,RR(70,5),YR(70,5),RL(70,5),YL(70,5),
1 B1(70,2),B2(70,2),B3(70,2),B4(70,2),S1(5),S2(5),S3(5),S4(5),
1 AXW(244),AX1(244),AX2(244),AX3(244),AX4(244),AR1(244),AR2(244),
1 AR3(244),AR4(244),AR5(244),AM1(244),AM2(244),AM3(244),AW1(244),
1 AY1(244),IWHEEL(13),IRAIL(13),NC1,NC2,NC3,NC4,R1(244),R2(244)

```

```

C CHOOSE THE CURVEFIT VALID FOR PT X1 ON THE RT WHEEL

```

```

DO 20 I=1,NC1
  IF(B1(I,2).LE.X1.AND.B1(I,1).GT.X1) GO TO 25
20 CONTINUE
25 DO 30 J=1,5
  S1(J)=RR(I,J)
30 CONTINUE

```

```

C CHOOSE THE CURVEFIT VALID FOR PT X2 ON THE RT RAIL

```

```

DO 40 I=1,NC2
  IF(B2(I,2).LE.X2.AND.B2(I,1).GT.X2) GO TO 45
40 CONTINUE
45 DO 50 J=1,5
  S2(J)=YR(I,J)
50 CONTINUE

```

```

C CHOOSE THE CURVEFIT VALID FOR PT X3 ON THE LEFT WHEEL

```

```

DO 60 I=1,NC3
  IF(B3(I,2).LE.X3.AND.B3(I,1).GT.X3) GO TO 65
60 CONTINUE
65 DO 70 J=1,5
  S3(J)=RL(I,J)
70 CONTINUE

```

```

C CHOOSE THE CURVEFIT VALID FOR PT X4 ON THE LEFT RAIL

```

```

DO 80 I=1,NC4
  IF(B4(I,2).LE.X4.AND.B4(I,1).GT.X4) GO TO 85
80 CONTINUE
85 DO 90 J=1,5
  S4(J)=YL(I,J)
90 CONTINUE
RETURN
END

```

```

SUBROUTINE RADII(RR,YR,RL,YL,X1,X2,X3,X4,R1,R2,R3,R4)
DIMENSION RR(1),YR(1),RL(1),YL(1)
C COMPUTES THE VALUES OF FOUR 4TH ORDER POLYNOMIALS AT THE GIVEN
C PTS, RESPECTIVELY
R1=RR(1)+X1*(RR(2)+X1*(RR(3)+X1*(RR(4)+X1*RR(5))))
R2=YR(1)+X2*(YR(2)+X2*(YR(3)+X2*(YR(4)+X2*YR(5))))
R3=RL(1)+X3*(RL(2)+X3*(RL(3)+X3*(RL(4)+X3*RL(5))))
R4=YL(1)+X4*(YL(2)+X4*(YL(3)+X4*(YL(4)+X4*YL(5))))
RETURN
END

```

```

SUBROUTINE EQSUB2(NUMBR,W)
COMMON /COMA/ AW,AR,BR,BL,RR(70,5),YR(70,5),RL(70,5),YL(70,5),
1 B1(70,2),B2(70,2),B3(70,2),B4(70,2),S1(5),S2(5),S3(5),S4(5),
1 AXW(244),AX1(244),AX2(244),AX3(244),AX4(244),AR1(244),AR2(244),
1 AR3(244),AR4(244),AR5(244),AM1(244),AM2(244),AM3(244),AW1(244),
1 AY1(244),WHEEL(13),IRAIL(13),NC1,NC2,NC3,NC4,R1(244),R2(244)
C
C DIMENSION W(1)
C CALCULATE THE CONSTRAINT RELATIONS AT EACH OF THE INCREMENTS OF
C WHEELSET LATERAL
DO 100 I=1,NUMBR
C CHOOSE THE CURVE FITS VALID AT THE POINTS
CALL CHOOSE(AX1(I),AX2(I),AX3(I),AX4(I))
C CALCULATE THE ROLLING RADII AND HEIGHT OF THE RAIL AT THE POINTS
CALL RADII(S1,S2,S3,S4,AX1(I),AX2(I),AX3(I),AX4(I),AR1(I),
1 AR2(I),AR3(I),AR4(I))
C CALCULATE WHEELSET ROLL ANGLE
AW1(I)=(AR4(I)-AR2(I)+AX4(I)*SIN(BL)-AX2(I)*SIN(BR)+AR3(I)
1 -AR1(I))/(2.*AW+AX1(I)+AX3(I))
AW1(I)=ATAN(AW1(I))
AW1(I)=(AR4(I)-AR2(I)+AX4(I)*SIN(BL)-AX2(I)*SIN(BR)+(AR3(I)-
1 AR1(I))*COS(AW1(I)))/((2.*AW+AX1(I)+AX3(I))*COS(AW1(I)))
AW1(I)=ATAN(AW1(I))
C CALCULATE RIGHT CONTACT ANGLE
AM1(I)=-(S1(2)+2.*S1(3)*AX1(I)+3.*S1(4)*AX1(I)**2.+4.*S1(5)*
1 AX1(I)**3.)
AM1(I)=ATAN(AM1(I))
C CALCULATE LEFT CONTACT ANGLE
AM2(I)=-(S3(2)+2.*S3(3)*AX3(I)+3.*S3(4)*AX3(I)**2.+4.*S3(5)*
1 AX3(I)**3.)
AM2(I)=ATAN(AM2(I))
C CALCULATE NORMALIZED DIFFERENCE IN CONTACT ANGLES
AM3(I)=(AM2(I)-AM1(I))/2.
C CALCULATE NORMALIZED DIFFERENCE IN ROLLING RADII
AR5(I)=(AR3(I)-AR1(I))/(2.*AR)
C CALCULATE RADII OF CURVATURE, RT AND LT
FPP1=2.*S1(3)+6.*S1(4)*AX1(I)+12.*S1(5)*AX1(I)**2.
FPP2=2.*S2(3)+6.*S2(4)*AX2(I)+12.*S2(5)*AX2(I)**2.
FP1=S1(2)+2.*S1(3)*AX1(I)+3.*S1(4)*AX1(I)**2.+4.*S1(5)*AX1(I)**3.
FP2=S2(2)+2.*S2(3)*AX2(I)+3.*S2(4)*AX2(I)**2.+4.*S2(5)*AX2(I)**3.
FP1=FP1*FP1
FP2=FP2*FP2
R1(I)=(1.+FP1)**1.5/FPP1
R2(I)=(1.+FP2)**1.5/FPP2
C CALCULATE VERTICAL DISPLACEMENT OF WHEELSET
AY1(I)=(AR4(I)+AR2(I)+AX4(I)*SIN(BL)+AX2(I)*SIN(BR)+(AR3(I)
1 +AR1(I))*COS(AW1(I)))/2.
100 CONTINUE
C NORMALIZE VERTICAL DISPLACEMENT TO ZERO AT XW=0
N=NUMBR/2
Y=AY1(N)
DO 110 I=1,NUMBR
AY1(I)=AY1(I)-Y
110 CONTINUE
RETURN
END

```

```

SUBROUTINE PLOT2(NUMBR,ITODAY,ITIM)
COMMON /COMA/ AW,AR,BR,BL,RR(70,5),YR(70,5),RL(70,5),YL(70,5),
1 B1(70,2),B2(70,2),B3(70,2),B4(70,2),S1(5),S2(5),S3(5),S4(5),
1 AXW(244),AX1(244),AX2(244),AX3(244),AX4(244),AR1(244),AR2(244),
1 AR3(244),AR4(244),AR5(244),AM1(244),AM2(244),AM3(244),AW1(244),
1 AY1(244),IWHEEL(13),IRAIL(13),NC1,NC2,NC3,NC4,ZZ(488)

C
C DIMENSION ITODAY(2),ITIM(2)
C COMPUTE SCALING FACTORS
AN=NUMBR
XW=-AN*.005+.01
NI=-XW/.01+1.
N1=NUMBR+1
N2=NUMBR+2
N11=N1+1
N12=N1+2
AXW(N1)=-1.2
AXW(N2)=.3
AR1(N1)=15.6
AR1(N2)=.4
AR3(N1)=AR1(N1)
AR3(N2)=AR1(N2)
AR5(N1)=-.05
AR5(N2)=.01

C
C AW1(N1)=-.025
C AW1(N2)=.005

C
C AM1(N1)=-.2
C AM1(N2)=.2
C AM2(N1)=AM1(N1)
C AM2(N2)=AM1(N2)
C AM3(N1)=-1.
C AM3(N2)=.2

C
C PLOT DIFF IN CONTACT ANGLES
CALL PLOT(.5,5.,-3)
CALL GRID(0.,0.,.5,.5,16,20)
CALL AXIS(0.,0.,21HWHEELSET LATERAL (IN),-21,0.,0.,AXW(N1),
1 AXW(N2))
CALL LINE(AXW,AM3,NUMBR,1,+1,5)
CALL AXIS(4.0,0.,46H1/2 DIFF. IN CONTACT ANGLES W.R.T. AXLE, LT-RT
1 46,10.,90.,AM3(N1),AM3(N2))
CALL SYMBOL(1.5,8.6,.14,IWHEEL,0.,78)
CALL SYMBOL(1.5,8.1,.14,IRAIL,0.,78)

C
C PLOT DIFF IN ROLLING RADII
CALL PLOT(0.,11.5,-3)
CALL GRID(0.,0.,.5,.5,16,20)
CALL AXIS(0.,0.,21HWHEELSET LATERAL (IN),-21,0.,0.,AXW(N1),
1 AXW(N2))
CALL LINE(AXW,AR5,NUMBR,1,+1,5)
CALL AXIS(4.0,0.,39HDIFF. IN ROLLING RADII/RAIL GAGE, LF-RT,
1 39,10.,90.,AR5(N1),AR5(N2))
CALL SYMBOL(1.5,8.6,.14,IWHEEL,0.,78)
CALL SYMBOL(1.5,8.1,.14,IRAIL,0.,78)

C
C PLOT ROLLING RADII
CALL PLOT(9.,0.,-3)
CALL GRID(0.,0.,.5,.5,16,20)
CALL AXIS(0.,0.,21HWHEELSET LATERAL (IN),-21,0.,0.,AXW(N1),
1 AXW(N2))
CALL AXIS(4.0,0.,35HROLLING RADIUS, +=RIGHT,*=LEFT, IN.,35,10.,
1 90.,AR1(N1),AR1(N2))
CALL LINE(AXW,AR1,NUMBR,1,+1,3)
CALL LINE(AXW,AR3,NUMBR,1,+1,11)
CALL SYMBOL(1.5,8.1,.14,IRAIL,0.,78)
CALL SYMBOL(1.5,8.6,.14,IWHEEL,0.,78)

C
C PLOT CONTACT ANGLES
CALL PLOT(0.,-11.5,-3)

```

```

CALL GRID(0.,0.,.5,.5,16,20)
CALL AXIS(0.,0.,21HWHEELSET LATERAL (IN),-21,8.,0.,AXW(N1),
1 AXW(N2))
CALL AXIS(4.0,0.,.57HCONTACT ANGLE W.R.T. AXLE, +=RT, *=LT,37,
1 10.,90.,AM1(N1),AM1(N2))
CALL LINE(AXW,AM1,NUMBR,1,+1,3)
CALL LINE(AXW,AM2,NUMBR,1,+1,11)
CALL SYMBOL(1.5,8.6,.14,IWHEEL,0.,78)
CALL SYMBOL(1.5,8.1,.14,IRAIL,0.,78)

```

```

C
C PLOT WHEELSET ROLL ANGLES
CALL PLOT(12.,0.,-3)
CALL GRID(0.,0.,.5,.5,16,20)
CALL AXIS(0.,0.,21HWHEELSET LATERAL (IN),-21,8.,0.,AXW(N1),
1 AXW(N2))
CALL AXIS(4.0,0.,.13HWHEELSET ROLL,13,10.,90.,AW1(N1),AW1(N2))
CALL LINE(AXW,AW1,NUMBR,1,+1,5)
CALL SYMBOL(1.5,8.6,.14,IWHEEL,0.,78)
CALL SYMBOL(1.5,8.1,.14,IRAIL,0.,78)

```

```

C
C SCALING FACTORS
AX1(N1)=0.
AX1(N2)=1.
AX2(N1)=0.
AX2(N2)=1.

```

```

C PLOT WHEEL CONTACT PTS
CALL PLOT(1.5,13.0,-3)
CALL AXIS(0.,0.,21HWHEELSET LATERAL (IN),21,8.,90.,-1.2,.3)
CALL SYMBOL(-1.75,6.6,.14,26HLOCATION OF CONTACT POINTS,0.,26)
CALL GRID(-2.5,0.,.5,.5,10,16)
CALL LINE(AX1,AXW,NUMBR,1,+1,5)

```

```

C PLOT RAIL CONTACT PTS
CALL PLOT(5.5,0.,-3)
CALL AXIS(0.,0.,21HWHEELSET LATERAL (IN),21,8.,90.,-1.2,.3)
CALL SYMBOL(-1.75,6.6,.14,26HLOCATION OF CONTACT POINTS,0.,26)
CALL GRID(-2.,0.,.5,.5,8,16)
CALL LINE(AX2,AXW,NUMBR,1,+1,5)
CALL SYMBOL(0.,-15.,.07,ITODAY,0.,12)
CALL SYMBOL(1.,-15.,.07,ITIM,0.,12)
RETURN
END

```



```

SUBROUTINE DCRFCN(N,AXW,AR5,AM3,AW1,AR)
  DIMENSION AXW(1),AR5(1),AM3(1),AW1(1)
C LINEARIZATION USING DESCRIBING FUNCTIONS WITH A SINUSIODAL INPUT
C AMP=AMP OF MOTION=A
C ALAM=SLOPE OF (RL-RR)/2AR=AN2
C DELM=SLOPE OF (ML-MR)/2=AN1
C WSRL=SLOPE OF WHEELSET ROLL ANGLE DATA =AN3
  PRINT 10
  10 FORMAT(////2X,'LINEARIZATION USING DESCRIBING FCNS'/3X,'AMP',
    1 5X,'ALAM',5X,'DELM',5X,'WSRL'/)
C COMPUTE POINT IN ARRAYS CORRESPONDING TO START OF XW GT 0
  N2=N/2+2
C COMPUTE FOR EACH AMPLITUDE
  DO 100 IJK=1,30
    AI=IJK
    A=.05*AI
C CHECK LIMIT OF ARRAY
    IF(A.GT.AXW(N)+.002) GO TO 200
C DEFINE OR INITIALIZE PARAMETERS
    AK=4./(3.14159*A**2.)
    AN1=0
    AN2=0
    AN3=0
C USE TRAPAZOIDAL RULE TO NUMERICALLY INTEGRATE EQUATIONS
    DO 40 I=N2,402
      I1=I-1
      S1=ASIN(AXW(I)/A)-ASIN(AXW(I1)/A)
      AN1=AN1+(AM3(I)*AXW(I)+AM3(I1)*AXW(I1))*S1/2.
      AN2=AN2+(AR5(I)*AXW(I)+AR5(I1)*AXW(I1))*S1/2.
      AN3=AN3+(AW1(I)*AXW(I)+AW1(I1)*AXW(I1))*S1/2.
C CHECK TO SEE IF AMPLITUDE REACHED
      IF((AXW(I)-A).GE.-.002) GO TO 50
    40 CONTINUE
C COMBINE TERMS AND NORMALIZE
    50 AN1=AN1*AK*AR
      AN2=AN2*AK*AR
      AN3=AN3*AK*AR
C OUTPUT
    PRINT 60,AXW(I),AN2,AN1,AN3
    60 FORMAT(2X,F5.3,3(2X,F7.4))
    100 CONTINUE
    200 RETURN
  END

```

DATA USED IN SAMPLE RUN

101005
 52.56.5.025, 025
 NEW WHEEL DATA 026
 2.0625
 056

•2482374+01	•1637062+02
•2279514+01	•1638278+02
•2298308+01	•1638788+02
•2210096+01	•1639655+02
•2121566+01	•1640149+02
•2004057+01	•1641267+02
•1900559+01	•1642101+02
•1819672+01	•1642586+02
•1724455+01	•1642905+02
•1621276+01	•1642966+02
•1518735+01	•1643260+02
•1423199+01	•1643344+02
•1334998+01	•1643835+02
•1224484+01	•1644620+02
•1106657+01	•1645422+02
•1003794+01	•1645920+02
•9082612+00	•1646426+02
•8050820+00	•1646925+02
•6802480+00	•1647444+02
•5627390+00	•1647919+02
•4522360+00	•1648421+02
•3493760+00	•1649142+02
•2388720+00	•1649667+02
•1286880+00	•1650182+02
•2582800-01	•1650694+02
- 7735097-01	•1651505+02
- 1732060+00	•1652180+02
- 2980390+00	•1652998+02
- 4085420+00	•1653506+02
- 5040790+00	•1654015+02
- 5996140+00	•1654073+02
- 7094800+00	•1654124+02
- 7976910+00	•1654204+02
- 8859020+00	•1655125+02
- 9601020+00	•1655791+02
- 1062962+01	•1657082+02
- 1136845+01	•1658423+02
- 1204040+01	•1660268+02
- 1270916+01	•1662659+02
- 1338110+01	•1665821+02
- 1391294+01	•1668880+02
- 1459127+01	•1674220+02
- 1512948+01	•1679153+02
- 1536196+01	•1681941+02
- 1567407+01	•1686523+02
- 1599255+01	•1691809+02
- 1623141+01	•1696322+02
- 1647346+01	•1700259+02
- 1686200+01	•1707988+02
- 1703718+01	•1711224+02
- 1735567+01	•1718874+02
- 1760090+01	•1722028+02
- 1790982+01	•1728251+02
- 1822830+01	•1732202+02
- 1868690+01	•1737601+02
- 1914549+01	•1741570+02

NEW PATI SECTION D DATA 025

1.5
 072

•1432941+01	•6106113+01
•1429108+01	•6159716+01
•1425682+01	•6202402+01
•1422167+01	•6255852+01

SAMPLE RUN OUTPUT

```

*** WARNING *** WHEELSET ROLL ANGLE CONVERGED ONLY WITHIN WR(NEW)-R(OLD)= .00001 AT XW= .380
*** WARNING *** WHEELSET ROLL ANGLE CONVERGED ONLY WITHIN WR(NEW)-R(OLD)= .00001 AT XW= .390
*** WARNING *** WHEELSET ROLL ANGLE CONVERGED ONLY WITHIN WR(NEW)-R(OLD)= .00002 AT XW= .400
*** WARNING *** WHEELSET ROLL ANGLE CONVERGED ONLY WITHIN WR(NEW)-R(OLD)= .00002 AT XW= .410
*** WARNING *** WHEELSET ROLL ANGLE CONVERGED ONLY WITHIN WR(NEW)-R(OLD)= .00000 AT XW= .420
  
```

***** RESULT *****

WHEEL/RAIL CONTACT CHARACTERIZATION

NEW WHEEL DATA 026
 WHEEL GAGE=33.000
 1/2 DIST BETWEEN TAPP LINES=29.500

CURVE FILE	5 PTS/CURVE FILE ZONE					FROM	*****	TO
	0TH	1ST	2ND	3RD	4TH			
1	.402497+01	-225244+02	-.159851+02	-.509786+01	-.586468+00	FROM	*****	TO 2.1216
2	.190019+00	-.590395+01	-.05286+01	-.180847+01	-.253462+00	FROM	2.1216	TO 1.6213
3	.161332+00	-.18324+01	-.145259+01	-.726376+00	-.130137+00	FROM	1.6213	TO 1.1067
4	.165153+02	-.89981-01	-.603534-01	-.234207-01	-.295671-02	FROM	1.1067	TO .5627
5	.105090+00	-.600057-01	.192552-01	-.205300-01	.159524-01	FROM	.5627	TO .0258
6	.105093+00	-.700068-01	.457987-01	.162197+00	-.875416-01	FROM	.0258	TO -.5041
7	.164715+02	-.307266+00	-.69123+00	-.393252+00	-.513671-01	FROM	-.5041	TO -.9601
8	.161009+02	-.910023+00	-.590055+00	.159610+00	.215398+00	FROM	-.9601	TO -1.3381
9	.131775+00	-.630538+01	-.270224+01	.109666+01	.757565+00	FROM	-1.3381	TO -1.5674
10	-.204115+00	-.700132+03	-.603883+03	-.277318+03	-.432634+02	FROM	-1.5674	TO -1.7037
11	.113033+04	.251536+04	.211795+04	.790131+03	.110264+03	FROM	-1.7037	TO -1.9145

NEW RAIL SECTION D DATA 025
 RAIL GAGE=50.500
 1/2 DIST BETWEEN RAIL CENTERS=29.750
 UN= .025 DL= .025 WK= .000 HI= .000

CURVE FILE	5 PTS/CURVE FILE ZONE					FROM	*****	TO
	0TH	1ST	2ND	3RD	4TH			
1	-.124239+07	.350124+07	-.770009+07	.173780+07	-.306001+06	FROM	*****	TO 1.4189
2	-.223598+05	.607642+05	-.747934+05	.372382+05	-.695153+04	FROM	1.4189	TO 1.3773
3	-.218787+03	.709970+03	-.902220+03	.555805+03	-.117813+03	FROM	1.3773	TO 1.2032
4	-.268976-01	.207106+02	-.431239+02	.265850+02	-.714411+01	FROM	1.2032	TO .9313
5	.070912+01	-.200253+01	-.543864+01	.531423+01	-.196454+01	FROM	.9313	TO .6537
6	.711551+01	-.207796+00	-.637569+00	-.910246+00	.386839+00	FROM	.6537	TO .3192
7	.709479+01	.209459-01	-.656303-01	-.479297+00	.975510+00	FROM	.3192	TO -.0367
8	.709451+01	.209713-01	.405690-02	-.473650+00	-.110873+01	FROM	-.0367	TO -.2704
9	.703009+01	-.615082+00	-.230525+01	-.337383+01	-.181877+01	FROM	-.2704	TO -.5725
10	.086775+01	-.100022+01	-.103331+01	-.854616+00	-.120705+00	FROM	-.5725	TO -.8299
11	.977233+01	.100490+02	.101115+02	.104977+02	.246707+01	FROM	-.8299	TO -1.1093
12	-.145228+02	-.104407+02	-.101140+03	-.592892+02	-.130626+02	FROM	-1.1093	TO -1.3332
13	-.103275+04	-.491243+04	-.551630+04	-.275217+04	-.514826+03	FROM	-1.3332	TO -1.4586
14	.178044+06	.469093+06	.501502+06	.228499+06	.390335+05	FROM	-1.4586	TO -1.5932

***** DATA POINTS *****

AW	AL	AP	AS	A4	RR	YR	RL	YL	MR	ML
-1.0000	-1.9145	-1.8390	1.0254	.1834	17.41621	7.03332	16.43060	7.09466	.807289	.013083
-.9900	-1.9145	-1.8490	1.0254	.1939	17.41621	7.03170	16.43069	7.09431	.807289	.013083
-.9800	-1.9145	-1.8590	1.0254	.2044	17.41621	7.03009	16.43060	7.09391	.807289	.013083
-.9700	-1.9145	-1.8690	1.1054	-.0051	17.41621	7.02843	16.45435	7.09183	.807289	.057859
-.9600	-1.9145	-1.8719	1.1054	-.2943	17.41621	7.02674	16.45435	7.09241	.807289	.057859
-.9500	-1.9145	-1.8842	1.1054	-.2835	17.41621	7.02503	16.45435	7.09292	.807289	.057859
-.9400	-1.9145	-1.8933	1.0954	-.2828	17.41621	7.02327	16.45435	7.09295	.807289	.057092
-.9300	-1.9145	-1.9042	1.0854	-.2820	17.41621	7.02146	16.45519	7.09298	.807289	.055634
-.9200	-1.9145	-1.9150	1.0754	-.2813	17.41621	7.01957	16.45575	7.09301	.807289	.055623
-.9100	-1.9145	-1.9250	1.0654	-.2805	17.41621	7.01759	16.45631	7.09305	.807289	.054921
-.9000	-1.9145	-1.9350	1.0554	-.2797	17.41621	7.01552	16.45685	7.09308	.807289	.054241
-.8900	-1.9145	-1.9450	1.0454	-.2789	17.41621	7.01333	16.45739	7.09312	.807289	.053582
-.8800	-1.9145	-1.9550	1.0354	-.2780	17.41621	7.01103	16.45792	7.09315	.807289	.052944
-.8700	-1.9145	-1.9650	1.0254	-.2772	17.41621	7.00863	16.45845	7.09319	.807289	.052326
-.8600	-1.9145	-1.9701	1.0054	-.2862	17.41621	7.00606	16.45949	7.09280	.807289	.051158
-.8500	-1.9145	-1.0011	.9954	-.2852	17.41621	7.00335	16.46000	7.09284	.807289	.050606
-.8400	-1.9145	-1.0122	.9854	-.2842	17.41621	7.00049	16.46050	7.09289	.807289	.050074
-.8300	-1.9145	-1.0233	.9754	-.2831	17.41621	6.99746	16.46100	7.09294	.807289	.049563
-.8200	-1.9145	-1.0344	.9654	-.2820	17.41621	6.99428	16.46149	7.09299	.807289	.049073
-.8100	-1.9145	-1.0455	.9554	-.2808	17.41621	6.99092	16.46198	7.09304	.807289	.048604
-.8000	-1.9145	-1.0566	.9454	-.2796	17.41621	6.98738	16.46246	7.09309	.807289	.048155
-.7900	-1.9145	-1.0682	.9354	-.2783	17.41621	6.98367	16.46294	7.09314	.807289	.047728
-.7800	-1.9145	-1.0794	.9254	-.2770	17.41621	6.97981	16.46342	7.09319	.807289	.047321
-.7700	-1.9145	-1.0906	.9154	-.2858	17.41621	6.97579	16.46386	7.09281	.807289	.046568
-.7600	-1.9145	-1.1021	.9054	-.2844	17.41621	6.97153	16.46432	7.09285	.807289	.046223
-.7500	-1.9145	-1.1141	.8954	-.2824	17.41621	6.96541	16.46478	7.09297	.807289	.045898
-.7400	-1.9145	-1.1257	.8854	-.2808	17.41621	6.96006	16.46524	7.09304	.807289	.045593
-.7300	-1.9145	-1.1373	.8754	-.2792	17.41621	6.95596	16.46562	7.09310	.807289	.045308
-.7200	-1.9145	-1.1490	.8654	-.2775	17.41621	6.95109	16.46605	7.09317	.807289	.045043
-.7100	-1.9145	-1.1605	.8554	-.2861	17.41621	6.94628	16.46655	7.09280	.807289	.044575
-.7000	-1.9145	-1.1722	.8454	-.2845	17.41621	6.94128	16.46709	7.09285	.807289	.044370
-.6900	-1.9145	-1.1839	.8354	-.2828	17.41621	6.93619	16.46763	7.09295	.807289	.044185
-.6800	-1.9145	-1.1955	.8254	-.2810	17.41621	6.93095	16.46818	7.09303	.807289	.044021
-.6700	-1.9145	-1.2074	.8154	-.2793	17.41621	6.92556	16.46873	7.09310	.807289	.043875
-.6600	-1.9145	-1.2194	.8054	-.2773	17.41621	6.91988	16.46925	7.09316	.807289	.043750
-.6500	-1.9145	-1.2311	.7954	-.2856	17.41621	6.91414	16.47063	7.09282	.807289	.043558
-.6400	-1.9145	-1.2432	.7854	-.2836	17.41621	6.90794	16.47106	7.09291	.807289	.043491
-.6300	-1.9145	-1.2553	.7754	-.2815	17.41621	6.90135	16.47150	7.09301	.807289	.043443
-.6200	-1.9145	-1.2677	.7654	-.2792	17.41621	6.89425	16.47193	7.09310	.807289	.043415
-.6100	-1.9145	-1.2800	.7554	-.2768	17.41621	6.88663	16.47237	7.09320	.807289	.043406
-.6000	-1.9145	-1.2925	.7454	-.2841	17.41621	6.87817	16.47324	7.09289	.807289	.043446
-.5900	-1.9145	-1.3050	.7354	-.2811	17.41621	6.86878	16.47367	7.09302	.807289	.043494
-.5800	-1.9145	-1.3171	.7254	-.2779	17.41621	6.85840	16.47411	7.09315	.807289	.043562
-.5700	-1.9145	-1.3293	.7154	-.2838	17.40613	6.84800	16.47498	7.09296	.767823	.043753
-.5600	-1.8945	-1.3415	.7054	-.2798	17.39676	6.83722	16.47542	7.09306	.741627	.043876
-.5500	-1.8845	-1.3537	.6954	-.2854	17.38774	6.82772	16.47610	7.09290	.729446	.043956
-.5400	-1.8745	-1.3659	.6854	-.2821	17.36969	6.81823	16.47674	7.09298	.744291	.044359
-.5300	-1.8645	-1.3784	.6754	-.2781	17.36035	6.80914	16.47719	7.09315	.767492	.044557

520	-1.0545	-1.3250	5954	-2833	17.33976	85339	16.47808	7.09293	.832943	.045008
510	-1.0645	-1.3301	5854	-2784	17.32834	84895	16.47853	7.09314	.870270	.045261
500	-1.0745	-1.3345	5754	-2838	17.36036	80223	16.47945	7.09291	.767492	.045822
490	-1.0845	-1.3379	5654	-2792	17.35037	79744	16.47991	7.09310	.797889	.047534
480	-1.0945	-1.3445	5554	-2844	17.33976	79205	16.48087	7.09288	.832943	.048097
470	-1.1045	-1.3498	5254	-2791	17.32834	78584	16.48135	7.09311	.870270	.048367
460	-1.1145	-1.3591	5054	-2830	17.31599	77817	16.48232	7.09294	.907859	.048883
450	-1.1245	-1.4131	4854	-2862	17.30284	78519	16.48331	7.09280	.944263	.049371
440	-1.1345	-1.4120	4754	-2777	17.27306	77017	16.48380	7.09316	1.009694	.049605
430	-1.1445	-1.4119	4554	-2782	17.25659	75476	16.48480	7.09315	1.037628	.050057
420	-1.1545	-1.4147	4354	-2765	17.22075	75093	16.48581	7.09321	1.083040	.050488
410	-1.1645	-1.4195	4054	-2817	17.18144	74084	16.48733	7.09300	1.114355	.051103
400	-1.1745	-1.4275	3754	-2843	17.13972	72377	16.48867	7.09286	1.131495	.051689
390	-1.1845	-1.4308	3554	-2788	17.07827	73232	16.48991	7.09312	1.116091	.052069
380	-1.1945	-1.4388	3254	-2841	17.01811	74226	16.49148	7.09289	1.097685	.052630
370	-1.2045	-1.4484	3054	-2810	16.96152	75406	16.49254	7.09303	1.066734	.053003
360	-1.2145	-1.4587	2854	-2799	16.92632	75174	16.49361	7.09307	1.040619	.053378
350	-1.2245	-1.4700	2654	-2841	16.53741	769507	16.49468	7.09299	.035745	.053759
340	-1.2345	-1.2000	2554	-2838	16.53704	769306	16.49522	7.09290	.037279	.053953
330	-1.2445	-1.2000	2454	-2836	16.53666	769305	16.49576	7.09292	.038809	.054149
320	-1.2545	-1.2000	2354	-2833	16.53626	769304	16.49630	7.09293	.040332	.054348
310	-1.2645	-1.2111	2254	-2830	16.53585	769302	16.49685	7.09294	.041858	.054550
300	-1.2745	-1.2114	2154	-2827	16.53543	769301	16.49739	7.09295	.043353	.054756
290	-1.2845	-1.2217	2054	-2824	16.53499	769300	16.49794	7.09297	.044845	.054966
280	-1.2945	-1.2320	1954	-2821	16.53453	769299	16.49849	7.09298	.046323	.055180
270	-1.3045	-1.2423	1854	-2818	16.53406	769297	16.49905	7.09299	.047784	.055399
260	-1.3145	-1.2526	1754	-2815	16.53357	769296	16.49960	7.09300	.049226	.055624
250	-1.3245	-1.2629	1654	-2812	16.53307	769295	16.50016	7.09302	.050647	.055854
240	-1.3345	-1.2732	1554	-2809	16.53256	769293	16.50072	7.09303	.052046	.056090
230	-1.3445	-1.2835	1454	-2806	16.53203	769292	16.50128	7.09304	.053419	.056332
220	-1.3545	-1.2938	1354	-2803	16.53149	769290	16.50185	7.09306	.054766	.056581
210	-1.3645	-1.3041	1254	-2800	16.53094	769289	16.50242	7.09307	.056083	.056837
200	-1.3745	-1.3144	1154	-2796	16.53037	769287	16.50299	7.09309	.057369	.057101
190	-1.3845	-1.3247	1054	-2793	16.52979	769286	16.50356	7.09310	.058621	.057372
180	-1.3945	-1.3350	954	-2789	16.52919	769284	16.50414	7.09311	.059837	.057652
170	-1.4045	-1.3453	854	-2786	16.52859	769283	16.50471	7.09313	.061017	.057940
160	-1.4145	-1.3556	754	-2782	16.52797	769281	16.50530	7.09314	.062156	.058237
150	-1.4245	-1.3659	654	-2779	16.52734	769280	16.50588	7.09316	.063254	.058544
140	-1.4345	-1.3762	554	-2775	16.52666	769321	16.50647	7.09317	.064316	.058861
130	-1.4445	-1.3865	454	-2772	16.52594	769320	16.50706	7.09319	.065316	.059187
120	-1.4545	-1.3968	354	-2767	16.52473	769318	16.50765	7.09321	.066276	.059525
110	-1.4645	-1.4071	254	-2867	16.52405	769317	16.50821	7.09321	.067186	.059853
100	-1.4745	-1.4174	154	-2862	16.52337	769316	16.50881	7.09321	.068044	.060181
90	-1.4845	-1.4277	54	-2858	16.52269	769315	16.50941	7.09321	.068848	.060510
80	-1.4945	-1.4380	146	-2854	16.52201	769268	16.51003	7.09283	.069596	.071684
70	-1.5045	-1.4483	246	-2850	16.52133	769266	16.51065	7.09285	.070285	.072211
60	-1.5145	-1.4586	346	-2846	16.52065	769264	16.51127	7.09287	.070914	.072646
50	-1.5245	-1.4689	446	-2842	16.52005	769262	16.51189	7.09289	.071480	.073050
40	-1.5345	-1.4792	546	-2837	16.51943	769260	16.51251	7.09291	.072024	.073423
30	-1.5445	-1.4895	646	-2833	16.51881	769258	16.51313	7.09293	.072541	.073732
20	-1.5545	-1.4998	746	-2829	16.51819	769256	16.51375	7.09295	.073027	.074012
10	-1.5645	-1.5101	846	-2825	16.51756	769254	16.51437	7.09297	.073484	.074251
0	-1.5745	-1.5204	946	-2820	16.51692	769252	16.51499	7.09299	.073902	.074450
0	-1.5845	-1.5307	1046	-2816	16.51628	769250	16.51561	7.09301	.074280	.074609
0	-1.5945	-1.5410	1146	-2812	16.51564	769248	16.51623	7.09303	.074618	.074738
0	-1.6045	-1.5513	1246	-2808	16.51500	769246	16.51685	7.09305	.074916	.074827

.030	.0746	.2933	.1346	.2908	16.51471	7.09245	16.51911	7.09258	.073512	.072417
.040	.0646	.2937	.1446	.2904	16.51398	7.09243	16.51983	7.09260	.073423	.071982
.050	.0546	.2942	.1546	.2899	16.51324	7.09241	16.52055	7.09262	.073250	.071480
.060	.0446	.2948	.1646	.2894	16.51250	7.09239	16.52127	7.09264	.073077	.070974
.070	.0346	.2950	.1746	.2889	16.51176	7.09237	16.52199	7.09266	.072904	.070468
.080	.0246	.2955	.1846	.2884	16.51102	7.09235	16.52271	7.09268	.072731	.069962
.090	.0146	.2958	.1946	.2879	16.51028	7.09233	16.52343	7.09270	.072558	.069456
.100	.0046	.2961	.2046	.2874	16.50954	7.09231	16.52415	7.09272	.072385	.068950
.110	.0000	.2963	.2146	.2869	16.50880	7.09229	16.52487	7.09274	.072212	.068444
.120	.0000	.2965	.2246	.2864	16.50806	7.09227	16.52559	7.09276	.072039	.067938
.130	.0000	.2967	.2346	.2859	16.50732	7.09225	16.52631	7.09278	.071866	.067432
.140	.0000	.2969	.2446	.2854	16.50658	7.09223	16.52703	7.09280	.071693	.066926
.150	.0000	.2971	.2546	.2849	16.50584	7.09221	16.52775	7.09282	.071520	.066420
.160	.0000	.2973	.2646	.2844	16.50510	7.09219	16.52847	7.09284	.071347	.065914
.170	.0000	.2975	.2746	.2839	16.50436	7.09217	16.52919	7.09286	.071174	.065408
.180	.0000	.2977	.2846	.2834	16.50362	7.09215	16.52991	7.09288	.071001	.064902
.190	.0000	.2979	.2946	.2829	16.50288	7.09213	16.53063	7.09290	.070828	.064396
.200	.0000	.2981	.3046	.2824	16.50214	7.09211	16.53135	7.09292	.070655	.063890
.210	.0000	.2983	.3146	.2819	16.50140	7.09209	16.53207	7.09294	.070482	.063384
.220	.0000	.2985	.3246	.2814	16.50066	7.09207	16.53279	7.09296	.070309	.062878
.230	.0000	.2987	.3346	.2809	16.50000	7.09205	16.53351	7.09298	.070136	.062372
.240	.0000	.2989	.3446	.2804	16.49936	7.09203	16.53423	7.09300	.069963	.061866
.250	.0000	.2991	.3546	.2800	16.49872	7.09201	16.53495	7.09302	.069790	.061360
.260	.0000	.2993	.3646	.2795	16.49808	7.09199	16.53567	7.09304	.069617	.060854
.270	.0000	.2995	.3746	.2790	16.49744	7.09197	16.53639	7.09306	.069444	.060348
.280	.0000	.2997	.3846	.2785	16.49680	7.09195	16.53711	7.09308	.069271	.059842
.290	.0000	.2999	.3946	.2780	16.49616	7.09193	16.53783	7.09310	.069098	.059336
.300	.0000	.3001	.4046	.2775	16.49552	7.09191	16.53855	7.09312	.068925	.058830
.310	.0000	.3003	.4146	.2770	16.49488	7.09189	16.53927	7.09314	.068752	.058324
.320	.0000	.3005	.4246	.2765	16.49424	7.09187	16.53999	7.09316	.068579	.057818
.330	.0000	.3007	.4346	.2760	16.49360	7.09185	16.54071	7.09318	.068406	.057312
.340	.0000	.3009	.4446	.2755	16.49296	7.09183	16.54143	7.09320	.068233	.056806
.350	.0000	.3011	.4546	.2750	16.49232	7.09181	16.54215	7.09322	.068060	.056300
.360	.0000	.3013	.4646	.2745	16.49168	7.09179	16.54287	7.09324	.067887	.055794
.370	.0000	.3015	.4746	.2740	16.49104	7.09177	16.54359	7.09326	.067714	.055288
.380	.0000	.3017	.4846	.2735	16.49040	7.09175	16.54431	7.09328	.067541	.054782
.390	.0000	.3019	.4946	.2730	16.48976	7.09173	16.54503	7.09330	.067368	.054276
.400	.0000	.3021	.5046	.2725	16.48912	7.09171	16.54575	7.09332	.067195	.053770
.410	.0000	.3023	.5146	.2720	16.48848	7.09169	16.54647	7.09334	.067022	.053264
.420	.0000	.3025	.5246	.2715	16.48784	7.09167	16.54719	7.09336	.066849	.052758
.430	.0000	.3027	.5346	.2710	16.48720	7.09165	16.54791	7.09338	.066676	.052252
.440	.0000	.3029	.5446	.2705	16.48656	7.09163	16.54863	7.09340	.066503	.051746
.450	.0000	.3031	.5546	.2700	16.48592	7.09161	16.54935	7.09342	.066330	.051240
.460	.0000	.3033	.5646	.2695	16.48528	7.09159	16.55007	7.09344	.066157	.050734
.470	.0000	.3035	.5746	.2690	16.48464	7.09157	16.55079	7.09346	.065984	.050228
.480	.0000	.3037	.5846	.2685	16.48400	7.09155	16.55151	7.09348	.065811	.049722
.490	.0000	.3039	.5946	.2680	16.48336	7.09153	16.55223	7.09350	.065638	.049216
.500	.0000	.3041	.6046	.2675	16.48272	7.09151	16.55295	7.09352	.065465	.048710
.510	.0000	.3043	.6146	.2670	16.48208	7.09149	16.55367	7.09354	.065292	.048204
.520	.0000	.3045	.6246	.2665	16.48144	7.09147	16.55439	7.09356	.065119	.047698
.530	.0000	.3047	.6346	.2660	16.48080	7.09145	16.55511	7.09358	.064946	.047192
.540	.0000	.3049	.6446	.2655	16.48016	7.09143	16.55583	7.09360	.064773	.046686
.550	.0000	.3051	.6546	.2650	16.47952	7.09141	16.55655	7.09362	.064600	.046180
.560	.0000	.3053	.6646	.2645	16.47888	7.09139	16.55727	7.09364	.064427	.045674
.570	.0000	.3055	.6746	.2640	16.47824	7.09137	16.55799	7.09366	.064254	.045168
.580	.0000	.3057	.6846	.2635	16.47760	7.09135	16.55871	7.09368	.064081	.044662
.590	.0000	.3059	.6946	.2630	16.47696	7.09133	16.55943	7.09370	.063908	.044156
.600	.0000	.3061	.7046	.2625	16.47632	7.09131	16.56015	7.09372	.063735	.043650
.610	.0000	.3063	.7146	.2620	16.47568	7.09129	16.56087	7.09374	.063562	.043144
.620	.0000	.3065	.7246	.2615	16.47504	7.09127	16.56159	7.09376	.063389	.042638
.630	.0000	.3067	.7346	.2610	16.47440	7.09125	16.56231	7.09378	.063216	.042132
.640	.0000	.3069	.7446	.2605	16.47376	7.09123	16.56303	7.09380	.063043	.041626
.650	.0000	.3071	.7546	.2600	16.47312	7.09121	16.56375	7.09382	.062870	.041120
.660	.0000	.3073	.7646	.2595	16.47248	7.09119	16.56447	7.09384	.062697	.040614
.670	.0000	.3075	.7746	.2590	16.47184	7.09117	16.56519	7.09386	.062524	.040108
.680	.0000	.3077	.7846	.2585	16.47120	7.09115	16.56591	7.09388	.062351	.039602
.690	.0000	.3079	.7946	.2580	16.47056	7.09113	16.56663	7.09390	.062178	.039096
.700	.0000	.3081	.8046	.2575	16.46992	7.09111	16.56735	7.09392	.062005	.038590
.710	.0000	.3083	.8146	.2570	16.46928	7.09109	16.56807	7.09394	.061832	.038084
.720	.0000	.3085	.8246	.2565	16.46864	7.09107	16.56879	7.09396	.061659	.037578
.730	.0000	.3087	.8346	.2560	16.46800	7.09105	16.56951	7.09398	.061486	.037072
.740	.0000	.3089	.8446	.2555	16.46736	7.09103	16.57023	7.09400	.061313	.036566
.750	.0000	.3091	.8546	.2550	16.46672	7.09101	16.57095	7.09402	.061140	.036060
.760	.0000	.3093	.8646	.2545	16.46608	7.09099	16.57167	7.09404	.060967	.035554
.770	.0000	.3095	.8746	.2540	16.46544	7.09097	16.57239	7.09406	.060794	.035048
.780	.0000	.3097	.8846	.2535	16.46480	7.09095	16.57311	7.09408	.060621	.034542
.790	.0000	.3099	.8946	.2530	16.46416	7.09093	16.57383	7.09410	.060448	.034036
.800	.0000	.3101	.9046	.2525	16.46352	7.09091	16.57455	7.09412	.060275	.033530
.810	.0000	.3103	.9146	.2520	16.46288	7.09089	16.57527	7.09414	.060102	.033024
.820	.0000	.3105	.9246	.2515	16.46224	7.09087	16.57599	7.09416	.059929	.032518
.830	.0000	.3107	.9346	.2510	16.46160	7.09085	16.57671	7.09418	.059756	.032012
.840	.0000	.3109	.9446	.2505	16.46096	7.09083	16.57743	7.09420	.059583	.031506
.850	.0000	.3111	.9546	.2500	16.46032	7.09081	16.57815	7.09422	.059410	.031000
.860	.0000	.3113	.9646	.2495	16.45968	7.09079	16.57887	7.09424	.059237	.030494
.870	.0000	.3115	.9746	.2490	16.45904	7.09077	16.57959	7.09426	.059064	.030000
.880	.0000	.3117	.9846	.2485	16.45840	7.09075	16.58031	7.09428	.058891	.029494
.890	.0000	.3119	.9946	.2480	16.45776	7.09073	16.58103	7.09430	.058718	.029000
.900	.0000	.3121	.0046	.2475	16.45712	7.09071	16.58175	7.09432	.058545	.028494
.910	.0000	.3123	.0146	.2470	16.45648	7.09069	16.58247	7.09434	.058372	.028000
.920	.0000	.3125	.0246	.2465	16.45584	7.09067	16.58319	7.09436	.058199	.027494
.930	.0000	.3127	.0346	.2460	16.45520	7.09065	16.58391	7.09438	.058026	.027000
.940	.0000	.3129	.0446	.2455	16.45456	7.09063	16.58463	7.09440	.057853	.026494
.950	.0000	.3131	.0546	.2450	16.45392	7.09061	16.58535	7.09442	.057680	.026000
.960	.0000	.3133	.0646	.2445	16.45328	7.09059	16.58607	7.09444	.057507	.025494
.970	.0000	.3135	.0746	.2440	16.45264	7.09057	16.58679	7.09446	.057334	.025000
.980	.0000	.3137	.0846	.2435	16.45200	7.09055	16.58751	7.09448	.057161	.024494
.990	.0000	.3139	.0946	.2430	16.45136	7.09053	16.58823	7.09450	.056988	.024000
1.000	.0000	.3141	.1046	.2425	16.45072	7.09051	16.58895	7.09452	.056815	.023494

.590	.6954	-1.2141	-1.9145	-1.3059	16.47367	7.09302	17.41621	6.86876	.043494	.807289
.600	.7054	-1.2141	-1.9145	-1.2928	16.47324	7.09289	17.41621	6.87817	.043446	.807289
.610	.7154	-1.2141	-1.9145	-1.2800	16.47237	7.09320	17.41621	6.88665	.043406	.807289
.620	.7254	-1.2141	-1.9145	-1.2677	16.47193	7.09316	17.41621	6.89425	.043415	.807289
.630	.7354	-1.2141	-1.9145	-1.2553	16.47150	7.09301	17.41621	6.90135	.043443	.807289
.640	.7454	-1.2141	-1.9145	-1.2432	16.47106	7.09291	17.41621	6.90794	.043491	.807289
.650	.7554	-1.2141	-1.9145	-1.2311	16.47063	7.09282	17.41621	6.91414	.043558	.807289
.660	.7654	-1.2141	-1.9145	-1.2194	16.46975	7.09316	17.41621	6.91988	.043750	.807289
.670	.7754	-1.2141	-1.9145	-1.2074	16.46832	7.09310	17.41621	6.92558	.043875	.807289
.680	.7854	-1.2141	-1.9145	-1.1956	16.46688	7.09303	17.41621	6.93095	.044021	.807289
.690	.7954	-1.2141	-1.9145	-1.1839	16.46543	7.09295	17.41621	6.93519	.044185	.807289
.700	.8054	-1.2141	-1.9145	-1.1722	16.46399	7.09288	17.41621	6.94128	.044370	.807289
.710	.8154	-1.2141	-1.9145	-1.1605	16.46255	7.09280	17.41621	6.94628	.044575	.807289
.720	.8254	-1.2141	-1.9145	-1.1490	16.46110	7.09317	17.41621	6.95109	.044804	.807289
.730	.8354	-1.2141	-1.9145	-1.1373	16.46065	7.09310	17.41621	6.95596	.045030	.807289
.740	.8454	-1.2141	-1.9145	-1.1257	16.46020	7.09304	17.41621	6.96072	.045293	.807289
.750	.8554	-1.2141	-1.9145	-1.1141	16.46028	7.09297	17.41621	6.96541	.045598	.807289
.760	.8654	-1.2141	-1.9145	-1.1021	16.46082	7.09288	17.41621	6.97153	.045898	.807289
.770	.8754	-1.2141	-1.9145	-1.0906	16.46436	7.09281	17.41621	6.97579	.046568	.807289
.780	.8854	-1.2141	-1.9145	-1.0794	16.46342	7.09319	17.41621	6.97981	.047321	.807289
.790	.8954	-1.2141	-1.9145	-1.0682	16.46294	7.09309	17.41621	6.98367	.047728	.807289
.800	.9054	-1.2141	-1.9145	-1.0569	16.46246	7.09309	17.41621	6.98738	.048155	.807289
.810	.9154	-1.2141	-1.9145	-1.0456	16.46198	7.09304	17.41621	6.99092	.048604	.807289
.820	.9254	-1.2141	-1.9145	-1.0344	16.46149	7.09299	17.41621	6.99426	.049073	.807289
.830	.9354	-1.2141	-1.9145	-1.0233	16.46100	7.09294	17.41621	6.99746	.049563	.807289
.840	.9454	-1.2141	-1.9145	-1.0122	16.46050	7.09286	17.41621	7.00049	.050074	.807289
.850	.9554	-1.2141	-1.9145	-1.0011	16.46000	7.09284	17.41621	7.00335	.050606	.807289
.860	1.0054	-1.2141	-1.9145	-0.9901	16.45949	7.09286	17.41621	7.00606	.051158	.807289
.870	1.0154	-1.2141	-1.9145	-0.9791	16.45898	7.09319	17.41621	7.00863	.051732	.807289
.880	1.0254	-1.2141	-1.9145	-0.9683	16.45845	7.09315	17.41621	7.01103	.052328	.807289
.890	1.0354	-1.2141	-1.9145	-0.9574	16.45792	7.09312	17.41621	7.01333	.052944	.807289
.900	1.0454	-1.2141	-1.9145	-0.9466	16.45739	7.09312	17.41621	7.01552	.053582	.807289
.910	1.0554	-1.2141	-1.9145	-0.9358	16.45685	7.09308	17.41621	7.01759	.054241	.807289
.920	1.0654	-1.2141	-1.9145	-0.9250	16.45631	7.09305	17.41621	7.01957	.054921	.807289
.930	1.0754	-1.2141	-1.9145	-0.9142	16.45575	7.09301	17.41621	7.02146	.055623	.807289
.940	1.0854	-1.2141	-1.9145	-0.9035	16.45519	7.09298	17.41621	7.02327	.056347	.807289
.950	1.0954	-1.2141	-1.9145	-0.8927	16.45462	7.09295	17.41621	7.02503	.057092	.807289
.960	1.1054	-1.2141	-1.9145	-0.8819	16.45405	7.09292	17.41621	7.02674	.057859	.807289
.970	1.1154	-1.2141	-1.9145	-0.8711	16.45348	7.09241	17.41621	7.02843	.058659	.807289
.980	1.1254	-1.2141	-1.9145	-0.8603	16.45291	7.09183	17.41621	7.03009	.059483	.807289
.990	1.1354	-1.2141	-1.9145	-0.8498	16.45234	7.09391	17.41621	7.03170	.060333	.807289
1.000	1.1454	-1.2141	-1.9145	-0.8393	16.45177	7.09436	17.41621	7.03332	.061203	.807289

λ_w	$(R_L - R_R) / \lambda_w$	$(R_L - R_R) / \lambda_c$	WR	YCG	R1	R2
-1.000	-.016565	-.397103	-.015273	.375063	.316	-4.852
-.990	-.016565	-.397103	-.015243	.374107	.318	-13.438
-.980	-.016565	-.397103	-.015213	.373151	.318	19.374
-.970	-.016171	-.374715	-.015168	.376473	.318	5.772
-.960	-.016171	-.374715	-.015120	.375932	.316	3.464
-.950	-.016171	-.374715	-.015073	.375342	.316	2.521
-.940	-.016161	-.375099	-.015030	.374655	.318	2.013
-.930	-.016152	-.375471	-.014986	.373933	.318	1.096
-.920	-.016142	-.375833	-.014941	.373171	.318	1.461
-.910	-.016133	-.376184	-.014895	.372362	.318	1.327

-.900	-.010124	-.070524	-.074847	.371502	.318	1.214
-.890	-.010115	-.070854	-.074797	.370585	.318	1.121
-.880	-.010106	-.071173	-.074745	.369607	.318	1.062
-.870	-.010097	-.071481	-.074692	.368571	.310	1.012
-.860	-.010079	-.071805	-.074641	.367373	.310	.973
-.850	-.010071	-.072342	-.074582	.366185	.318	.944
-.840	-.010052	-.072686	-.074521	.364919	.318	.923
-.830	-.010054	-.073086	-.074457	.363572	.318	.910
-.820	-.010046	-.073490	-.074390	.362140	.318	.903
-.810	-.010038	-.073934	-.074320	.360622	.318	.902
-.800	-.010029	-.074356	-.074247	.359113	.318	.907
-.790	-.010021	-.074781	-.074171	.357317	.313	.919
-.780	-.010013	-.075224	-.074093	.355345	.318	.936
-.770	-.015998	-.075686	-.074018	.353385	.318	.959
-.760	-.015990	-.076163	-.073932	.351615	.318	.990
-.750	-.015982	-.076650	-.073814	.349728	.318	.414
-.740	-.015974	-.077146	-.073721	.348543	.318	2.709
-.730	-.015967	-.077651	-.073626	.347321	.318	.794
-.720	-.015959	-.078173	-.073530	.346204	.318	6.306
-.710	-.015944	-.078715	-.073442	.342040	.318	2.305
-.700	-.015937	-.079276	-.073343	.339971	.318	1.923
-.690	-.015929	-.079856	-.073243	.337332	.318	1.570
-.680	-.015922	-.080454	-.073140	.334939	.318	1.277
-.670	-.015914	-.081070	-.073035	.332479	.318	1.047
-.660	-.015907	-.081707	-.072924	.329936	.318	.867
-.650	-.015892	-.082366	-.072819	.327255	.318	.734
-.640	-.015885	-.083049	-.072700	.324416	.318	.629
-.630	-.015876	-.083756	-.072573	.321481	.318	.549
-.620	-.015870	-.084487	-.072437	.318348	.318	.469
-.610	-.015863	-.085241	-.072292	.314969	.318	.443
-.600	-.015848	-.086019	-.072138	.311328	.318	.410
-.590	-.015841	-.086822	-.071961	.307160	.318	.388
-.580	-.015834	-.087649	-.071767	.302659	.318	.375
-.570	-.015830	-.088500	-.071523	.297665	.318	.373
-.560	-.015825	-.089375	-.071285	.291053	.420	.374
-.550	-.015820	-.090284	-.071060	.284931	.706	.373
-.540	-.015805	-.091226	-.070826	.277044	2.	.373
-.530	-.014843	-.092203	-.070587	.272893	-.726	.373
-.520	-.014482	-.093216	-.070328	.266729	-.510	.373
-.510	-.014282	-.094264	-.070007	.258956	-.407	.373
-.500	-.014085	-.095346	-.069733	.251391	-.411	.373
-.490	-.014030	-.096461	-.069462	.243803	-.510	.390
-.480	-.014035	-.097611	-.069175	.236789	-.432	.311
-.470	-.014035	-.098796	-.068853	.229086	-.407	.261
-.460	-.014011	-.099996	-.068493	.220662	-.411	.229
-.450	-.013774	-.101211	-.068085	.210979	-.437	.216
-.440	-.013205	-.102440	-.067578	.199960	-.481	.210
-.430	-.012971	-.103786	-.067007	.186480	-.634	.209
-.420	-.012352	-.105270	-.066301	.170979	-.750	.209
-.410	-.011066	-.106820	-.065425	.151747	-1.113	.209
-.400	-.010934	-.108490	-.064381	.127660	-1.869	.206
-.390	-.009800	-.110201	-.063442	.093392	-4.799	.335
-.380	-.008851	-.112027	-.062554	.073297	6.073	.209
-.370	-.007817	-.114086	-.061760	.049893	2.621	.264
-.360	-.007275	-.116362	-.061090	.027247	1.711	.232
-.350	-.000718	-.118907	-.060730	.009653	1.422	.237
				-.000168	-6.516	1.524

340	.000703	.000337	.000714	.000080	-6.531	1.539
350	.000637	.000767	.000698	.000000	-6.554	1.544
320	.000672	.000700	.000681	.000074	-6.585	1.550
310	.000650	.000351	.000664	.000141	-6.627	1.555
300	.000639	.000570	.000647	.000202	-6.670	1.560
290	.000623	.000506	.000629	.000256	-6.713	1.566
280	.000606	.000442	.000612	.000304	-6.756	1.572
270	.000588	.000380	.000594	.000345	-6.800	1.578
260	.000571	.000319	.000575	.000381	-6.843	1.584
250	.000555	.000260	.000557	.000416	-6.887	1.590
240	.000535	.000202	.000538	.000453	-6.930	1.596
230	.000517	.000145	.000518	.000490	-6.974	1.603
220	.000498	.000090	.000499	.000462	-7.019	1.609
210	.000479	.000377	.000479	.000468	-7.064	1.616
200	.000460	.000134	.000459	.000469	-7.109	1.623
190	.000441	.000624	.000439	.000465	-7.154	1.630
180	.000421	.000100	.000418	.000456	-7.200	1.637
170	.000401	.000153	.000397	.000442	-7.245	1.644
160	.000381	.000195	.000376	.000424	-7.291	1.652
150	.000361	.000235	.000355	.000401	-7.336	1.659
140	.000329	.000322	.000333	.000390	-7.382	1.667
130	.000308	.000354	.000311	.000356	-7.427	1.674
120	.000287	.000383	.000289	.000310	-7.473	1.682
110	.000266	.000411	.000280	.000262	-7.518	1.690
100	.000245	.000439	.000255	.000216	-7.564	1.698
090	.000224	.000467	.000230	.000170	-7.609	1.706
080	.000203	.000495	.000206	.000124	-7.655	1.714
070	.000184	.000523	.000180	.000078	-7.700	1.723
060	.000164	.000551	.000155	.000032	-7.746	1.731
050	.000143	.000579	.000129	.000000	-7.791	1.740
040	.000123	.000607	.000104	.000000	-7.837	1.749
030	.000104	.000635	.000078	.000000	-7.882	1.758
020	.000084	.000663	.000052	.000000	-7.928	1.767
010	.000065	.000691	.000026	.000000	-7.973	1.776
000	.000045	.000719	.000000	.000000	-8.019	1.785
000	.000025	.000747	.000000	.000000	-8.064	1.794
000	.000005	.000775	.000000	.000000	-8.110	1.803
000	.000000	.000803	.000000	.000000	-8.155	1.812
000	.000000	.000831	.000000	.000000	-8.201	1.821
000	.000000	.000859	.000000	.000000	-8.246	1.830
000	.000000	.000887	.000000	.000000	-8.292	1.839
000	.000000	.000915	.000000	.000000	-8.337	1.848
000	.000000	.000943	.000000	.000000	-8.383	1.857
000	.000000	.000971	.000000	.000000	-8.428	1.866
000	.000000	.001000	.000000	.000000	-8.474	1.875
000	.000000	.001028	.000000	.000000	-8.519	1.884
000	.000000	.001056	.000000	.000000	-8.565	1.893
000	.000000	.001084	.000000	.000000	-8.610	1.902
000	.000000	.001112	.000000	.000000	-8.656	1.911
000	.000000	.001140	.000000	.000000	-8.701	1.920
000	.000000	.001168	.000000	.000000	-8.747	1.929
000	.000000	.001196	.000000	.000000	-8.792	1.938
000	.000000	.001224	.000000	.000000	-8.838	1.947
000	.000000	.001252	.000000	.000000	-8.883	1.956
000	.000000	.001280	.000000	.000000	-8.929	1.965
000	.000000	.001308	.000000	.000000	-8.974	1.974
000	.000000	.001336	.000000	.000000	-9.020	1.983
000	.000000	.001364	.000000	.000000	-9.065	1.992
000	.000000	.001392	.000000	.000000	-9.111	1.999
000	.000000	.001420	.000000	.000000	-9.156	2.006
000	.000000	.001448	.000000	.000000	-9.202	2.013
000	.000000	.001476	.000000	.000000	-9.247	2.020
000	.000000	.001504	.000000	.000000	-9.293	2.027
000	.000000	.001532	.000000	.000000	-9.338	2.034
000	.000000	.001560	.000000	.000000	-9.384	2.041
000	.000000	.001588	.000000	.000000	-9.429	2.048
000	.000000	.001616	.000000	.000000	-9.475	2.055
000	.000000	.001644	.000000	.000000	-9.520	2.062
000	.000000	.001672	.000000	.000000	-9.566	2.069
000	.000000	.001700	.000000	.000000	-9.611	2.076
000	.000000	.001728	.000000	.000000	-9.657	2.083
000	.000000	.001756	.000000	.000000	-9.702	2.090
000	.000000	.001784	.000000	.000000	-9.748	2.097
000	.000000	.001812	.000000	.000000	-9.793	2.104
000	.000000	.001840	.000000	.000000	-9.839	2.111
000	.000000	.001868	.000000	.000000	-9.884	2.118
000	.000000	.001896	.000000	.000000	-9.930	2.125
000	.000000	.001924	.000000	.000000	-9.975	2.132
000	.000000	.001952	.000000	.000000	-10.021	2.139
000	.000000	.001980	.000000	.000000	-10.066	2.146
000	.000000	.002008	.000000	.000000	-10.112	2.153
000	.000000	.002036	.000000	.000000	-10.157	2.160
000	.000000	.002064	.000000	.000000	-10.203	2.167
000	.000000	.002092	.000000	.000000	-10.248	2.174
000	.000000	.002120	.000000	.000000	-10.294	2.181
000	.000000	.002148	.000000	.000000	-10.339	2.188
000	.000000	.002176	.000000	.000000	-10.385	2.195
000	.000000	.002204	.000000	.000000	-10.430	2.202
000	.000000	.002232	.000000	.000000	-10.476	2.209
000	.000000	.002260	.000000	.000000	-10.521	2.216
000	.000000	.002288	.000000	.000000	-10.567	2.223
000	.000000	.002316	.000000	.000000	-10.612	2.230
000	.000000	.002344	.000000	.000000	-10.658	2.237
000	.000000	.002372	.000000	.000000	-10.703	2.244
000	.000000	.002400	.000000	.000000	-10.749	2.251
000	.000000	.002428	.000000	.000000	-10.794	2.258
000	.000000	.002456	.000000	.000000	-10.840	2.265
000	.000000	.002484	.000000	.000000	-10.885	2.272
000	.000000	.002512	.000000	.000000	-10.931	2.279
000	.000000	.002540	.000000	.000000	-10.976	2.286
000	.000000	.002568	.000000	.000000	-11.022	2.293
000	.000000	.002596	.000000	.000000	-11.067	2.300
000	.000000	.002624	.000000	.000000	-11.113	2.307
000	.000000	.002652	.000000	.000000	-11.158	2.314
000	.000000	.002680	.000000	.000000	-11.204	2.321
000	.000000	.002708	.000000	.000000	-11.249	2.328
000	.000000	.002736	.000000	.000000	-11.295	2.335
000	.000000	.002764	.000000	.000000	-11.340	2.342
000	.000000	.002792	.000000	.000000	-11.386	2.349
000	.000000	.002820	.000000	.000000	-11.431	2.356
000	.000000	.002848	.000000	.000000	-11.477	2.363
000	.000000	.002876	.000000	.000000	-11.522	2.370
000	.000000	.002904	.000000	.000000	-11.568	2.377
000	.000000	.002932	.000000	.000000	-11.613	2.384
000	.000000	.002960	.000000	.000000	-11.659	2.391
000	.000000	.002988	.000000	.000000	-11.704	2.398
000	.000000	.003016	.000000	.000000	-11.750	2.405
000	.000000	.003044	.000000	.000000	-11.795	2.412
000	.000000	.003072	.000000	.000000	-11.841	2.419
000	.000000	.003100	.000000	.000000	-11.886	2.426
000	.000000	.003128	.000000	.000000	-11.932	2.433
000	.000000	.003156	.000000	.000000	-11.977	2.440
000	.000000	.003184	.000000	.000000	-12.023	2.447
000	.000000	.003212	.000000	.000000	-12.068	2.454
000	.000000	.003240	.000000	.000000	-12.114	2.461
000	.000000	.003268	.000000	.000000	-12.159	2.468
000	.000000	.003296	.000000	.000000	-12.205	2.475
000	.000000	.003324	.000000	.000000	-12.250	2.482
000	.000000	.003352	.000000	.000000	-12.296	2.489
000	.000000	.003380	.000000	.000000	-12.341	2.496
000	.000000	.003408	.000000	.000000	-12.387	2.503
000	.000000	.003436	.000000	.000000	-12.432	2.510
000	.000000	.003464	.000000	.000000	-12.478	2.517
000	.000000	.003492	.000000	.000000	-12.523	2.524
000	.000000	.003520	.000000	.000000	-12.569	2.531
000	.000000	.003548	.000000	.000000	-12.614	2.538
000	.000000	.003576	.000000	.000000	-12.660	2.545
000	.000000	.003604	.000000	.000000	-12.705	2.552
000	.000000	.003632	.000000	.000000	-12.751	2.559
000	.000000	.003660	.000000	.000000	-12.796	2.566
000	.000000	.003688	.000000	.000000	-12.842	2.573
000	.000000	.003716	.000000	.000000	-12.887	2.580
000	.000000	.003744	.000000	.000000	-12.933	2.587
000	.000000	.003772	.000000	.000000	-12.978	2.594
000	.000000	.003800	.000000	.000000	-13.024	2.601
000	.000000	.003828	.000000	.000000	-13.069	2.608
000	.000000	.003856	.000000	.000000	-13.115	2.615
000	.000000	.003884	.000000	.000000	-13.160	2.622
000	.000000	.003912	.000000	.000000	-13.206	2.629
000	.000000	.003940	.000000	.000000	-13.251	2.636
000	.000000	.003968	.000000	.000000	-13.297	2.643
000	.000000	.003996	.000000	.000000	-13.342	2.650
000	.000000	.004024	.000000	.000000	-13.388	2.657
000	.000000	.004052	.000000	.000000	-13.433	2.664
000	.000000	.004080	.000000	.000000	-13.479	2.671
000	.000000	.004108	.000000	.000000	-13.524	2.678
000	.000000	.004136	.000000	.000000	-13.570	2.685
000	.000000	.004164	.000000	.000000	-13.615	2.692
000	.000000	.004192	.000000	.000000	-13.661	2.699
000	.000000					

•210	•000479	-•000377	•000479	•000468	38.553	1.533
•220	•000498	-•000900	•000499	•000462	39.667	1.539
•230	•000517	-•001450	•000518	•000451	40.784	1.545
•240	•000535	-•002022	•000538	•000433	41.898	1.552
•250	•000553	-•002603	•000557	•000410	43.009	1.558
•260	•000571	-•003199	•000575	•000381	44.097	1.564
•270	•000588	-•003808	•000594	•000345	45.169	1.570
•280	•000606	-•004429	•000612	•000304	46.213	1.575
•290	•000623	-•005060	•000629	•000256	47.221	1.581
•300	•000639	-•005702	•000647	•000202	48.185	1.587
•310	•000655	-•006351	•000664	•000141	49.098	1.593
•320	•000672	-•007000	•000681	•000074	49.951	1.598
•330	•000687	-•007670	•000698	•000000	50.736	1.604
•340	•000703	-•008337	•000714	-•000000	51.445	1.609
•350	•000718	-•009007	•000730	-•000168	52.070	1.615
•360	•000727	•493620	•001090	•009053	53.045	1.621
•370	•000732	•500865	•001760	•027247	53.614	1.627
•380	•000851	•522527	•002554	•048894	53.752	1.633
•390	•000908	•532011	•003342	•073294	53.140	1.639
•400	•010939	•539900	•004381	•098932	52.215	1.645
•410	•011606	•531620	•005425	•127668	50.155	1.651
•420	•012352	•510270	•006301	•151747	47.435	1.657
•430	•012971	•493780	•007007	•170973	45.430	1.663
•440	•013205	•480045	•007578	•186480	43.273	1.669
•450	•013774	•447446	•008085	•199960	42.168	1.675
•460	•014011	•429480	•008493	•210979	39.935	1.681
•470	•014235	•410951	•008853	•220662	37.708	1.687
•480	•014436	•392420	•009175	•229086	36.608	1.693
•490	•014630	•375170	•009462	•236789	34.453	1.699
•500	•014805	•360835	•009733	•243803	33.570	1.705
•510	•014972	•342504	•010007	•251391	38.206	1.711
•520	•014472	•393967	•010298	•258950	41.058	1.717
•530	•014843	•301467	•010587	•266729	48.314	1.723
•540	•015008	•349960	•010826	•272893	53.028	1.729
•550	•015170	•339942	•011060	•277044	-20.009	3.200
•560	•015345	•340875	•011285	•284931	75.216	1.531
•570	•015500	•302035	•011523	•291054	87.517	1.010
•580	•015634	•301864	•011767	•297065	130.419	1.456
•590	•015841	•301897	•011961	•302659	173.086	1.555
•600	•015848	•301922	•012138	•307180	257.716	1.615
•610	•015803	•301941	•012292	•311328	311928	1.476
•620	•015870	•301937	•012437	•314909	***	1.519
•630	•015878	•301923	•012573	•318348	-264.578	1.502
•640	•015885	•301899	•012700	•321481	-175.063	1.605
•650	•015892	•301860	•012819	•324416	-130.687	1.647
•660	•015907	•301770	•012924	•327255	-86.564	1.484
•670	•015914	•301707	•013035	•329935	-74.004	1.520
•680	•015922	•301634	•013140	•332472	-64.598	1.554
•690	•015929	•301552	•013243	•334939	-57.290	1.588
•700	•015937	•301460	•013343	•337332	-51.449	1.622
•710	•015944	•301357	•013442	•339671	-40.674	1.657
•720	•015959	•301120	•013530	•342040	-39.335	1.489
•730	•015967	•300991	•013626	•344321	-30.454	1.520
•740	•015974	•300840	•013721	•346543	-33.959	1.550
•750	•015982	•300690	•013814	•348728	-31.776	1.580
•760	•015990	•300530	•013932	•351615	-29.651	1.621

.770	.015978	.380360	.014018	.353585	-28.140	1.651
.780	.016015	.379984	.014093	.355545	-25.234	1.480
.790	.016021	.379781	.014171	.357317	-23.989	1.562
.800	.016029	.379567	.014247	.359015	-22.855	1.526
.810	.016038	.379345	.014320	.360622	-21.825	1.549
.820	.016048	.379118	.014390	.362147	-20.879	1.572
.830	.016054	.378885	.014457	.363572	-20.009	1.595
.840	.016071	.378608	.014521	.364910	-19.206	1.617
.850	.016071	.378342	.014582	.366185	-18.462	1.639
.860	.016079	.378065	.014641	.367373	-17.773	1.660
.870	.016097	.377781	.014692	.368571	-16.531	1.482
.880	.016102	.377481	.014745	.369607	-15.971	1.497
.890	.016115	.377054	.014797	.370585	-15.446	1.528
.900	.016124	.376524	.014847	.371502	-14.953	1.513
.910	.016135	.376184	.014895	.372362	-14.489	1.544
.920	.016142	.375835	.014941	.373171	-14.052	1.559
.930	.016152	.375471	.014986	.373933	-13.639	1.574
.940	.016161	.375059	.015030	.374655	-13.249	1.588
.950	.016171	.374715	.015073	.375342	-12.880	1.603
.960	.016171	.374415	.015120	.375932	-12.530	1.647
.970	.016171	.374115	.015168	.376473	-12.206	2.156
.980	.016165	.373718	.015213	.373113	-12.479	3.456
.990	.016165	.373718	.015243	.374167	-12.479	3.245
1.000	.016155	.373718	.015273	.375088	-12.479	3.062

LINEARIZATION USING DESCRIBING FUNCS.

AMP	ALAM	FREQ	WSRL
.050	.0704	-3.120	.0741
.100	.0741	-3.342	.0750
.150	.0769	-4.255	.0714
.200	.0895	-1.420	.0694
.250	.0874	-0.841	.0670
.300	.0854	-3.199	.0659
.350	.0834	-5.189	.0641
.400	.4305	22.6049	.1590
.450	.6315	25.4735	.3224
.500	.7153	23.0304	.4184
.550	.7307	21.2005	.4754
.600	.7450	20.3413	.5160
.650	.7504	19.3630	.5282
.700	.7070	18.3081	.5330
.750	.6819	17.4183	.5325
.800	.6555	16.5259	.5279
.850	.6296	15.6950	.5202
.900	.6040	14.9210	.5103
.950	.5812	14.2027	.4992
1.000	.5610	13.7381	.4875

10-114